INTERNATIONAL COLLOQUIUM

STABILITY OF STEEL STRUCTURES

HUNGARY, BUDAPEST 1990

PRELIMINARY REPORT

VOLUME I.

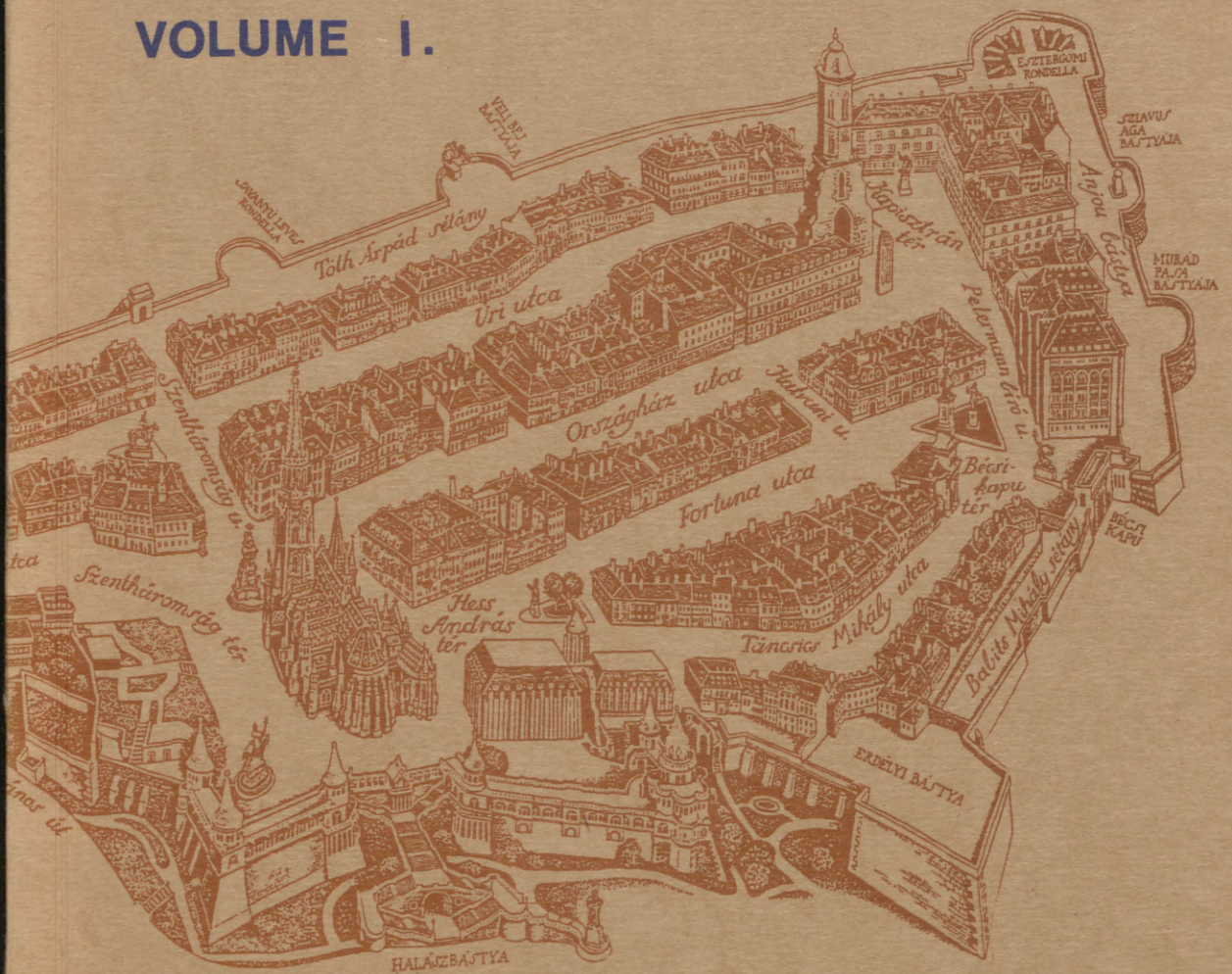

TECHNICAL UNIVERSITY OF BUDAPEST

HUNGARIAN ACADEMY OF SCIENCES

STRUCTURAL STABILITY RESEARCH COUNCIL

INTERNATIONAL ASSOCIATION FOR BRIDGE
AND STRUCTURAL ENGINEERING

INTERNATIONAL COLLOQUIUM
EAST-EUROPEAN SESSION

STABILITY OF STEEL STRUCTURES

PRELIMINARY REPORT

VOLUME I.

EDITED BY
M. IVÁNYI
B. VERŐCI

HUNGARY, BUDAPEST
APRIL 25-27, 1990

Címlap
részlet Somogyi Győző
rajzából

Cover
a piece of Győző Somogyi's
drawing

ISBN 963-421-487-8 Ö.

R 2

ISBN 963 420 218 7 T.

MC 109 788/1

ORSZ. SZÉCHÉNYI KÖNYVTÁR

1990

Felelős szerkesztők: Dr. Iványi Miklós
Dr. Verőci Béla
Kiadja: a Budapesti Műszaki Egyetem
Acélszerkezetek Tanszék
A kiadásért felelős: az Acélszerkezetek
Tanszék vezetője
Készült: a Budapesti Műszaki Egyetem
Sokszorosító Üzemében
Felelős vezető: Miszori Sándor
Példányszám: 350, Méret: B/5

FOREWORD

This Colloquium is the third international conference organized on the Hungarian territory with the view to deal with problems of structural stability, the first of them having been held at Balatonfüred in 1977 and the second at Tihany in 1986.

The objectives of the 1990 Colloquium are very similar to those of the previous two stability conferences, viz. to summarize the progress in theoretical and experimental research in the field of stability of steel (and other metal) structures, special emphasis being given to new concepts of analysis, design rules and recommendations in recent national and international Design Specifications and Codes.

Of course, the success of our striving to a great extent depends on the support the Colloquium receives from specialists from various countries of the globe. And we are happy to say that the support the 1990 Colloquium has to date been given, with 139 contributions (from 23 countries of 4 continents) being submitted, has even surpassed that which was granted to the two preceding stability conferences. All of these contributions are published in the Preliminary Report, while general reports and contributions to the Free Discussion will then appear in the Final Report of the Colloquium.

Besides the significant financial and other support by the Technical University, Budapest and the Hungarian Academy of Sciences, the Colloquium is fortunate to enjoy the important sponsorship of (i) the International Association for Bridge and Structural Engineering (IABSE) and (ii) the Structural Stability Research Council (SSRC). Therefore, the program of the Colloquium has been fixed up so as to aid these organizations in their continuous striving to achieve further headway in the field of constructional steelwork. Let us here mention, for instance, the important project "Stability of Metal Structures - A World View" sponsored by SSRC, in this respect our Colloquium desires to follow the same aims as the 1989 New York session, 1989 Beijing session and the Istanbul and Western Europe conferences to come in the near future.

To conclude, we wish you a most rewarding and agreeable stay in Hungary and at the same time the Colloquium may provide possibility to establish new contacts and strengthen the old ones, thus giving new impetus to international cooperation in research and preparation of Recommendations for Design of Steel Structures.

On behalf of the Scientific Committee

Prof. Miklós IVÁNYI, DSc.
Chairman

SESSION 1

GENERAL DESIGN CONCEPTS

(1)
GLAS, Hans-Dieter (1)
LUTTEROTH, Ascan (2)

NEW GDR CODES FOR STEEL STRUCTURES ESPECIALLY CONCERNING STABILITY

INTERNATIONAL COLLOQUIUM
STABILITY OF STEEL STRUCTURES
BUDAPEST, HUNGARY, 1990
PRELIMINARY REPORT

Summary: There are presented the recently introduced codes for limit states design using partial safety factors. The stability checks are based on calculation models proved in practice. For compressed members, an initial deflection is set up in place of the imperfection, and calculations are performed according to second-order theory. For combined compression and bending, this imperfection and the bending moment are superposed. There are differentiated four groups of members as it is also the case with torsional buckling. For buckling, the post-critical behaviour is taken into account.

1. Introduction

In 1989, in the GDR the codes for steel structures concerning the fields of civil engineering changed to partial safety factor design. With that, the previous conception of the allowable stresses was left and the international trend is followed. The modular conception for the structure of codes having proved successful for years has been maintained. It comprises:

a) basic standard TGL 13 500 which includes the checks to be performed, strength values to be observed as well as rules for bolted, riveted and welded structural members;

b) universally valid standards, as for instance TGL 13 503 "Stability of steel supporting structures" or TGL 13 510 "Manufacture of steel supporting structures";

c) specific standards, as for instance TGL 13 450 "Steel supporting structures in building construction", TGL 13 460

(1) Professor Dr. sc. techn., Technische Hochschule Leipzig
(2) Dr.-Ing., VEB Metalleichtbaukombinat Leipzig

(2)
"Steel road bridges" or TGL 13 471 "Steel supporting structures for craneways".

The standards are binding for everybody, i.e. they are law. Variations are allowed, provided they were proved reasonably by theory and tests, and the competent inspection office has approved them. Competent inspection offices, among others, are: State Building Supervision Authority, Acceptance Office of the Deutsche Reichsbahn or the Supreme Mining Office.

2. Form of checking in ultimate limit state

Generally, it can be written:

$$\bar{S}\left[\gamma_n \Sigma \left(F^n \cdot \gamma_f \cdot \psi\right)\right] \leq \frac{\bar{R}^n \cdot \gamma_d}{\gamma_m} \qquad (1)$$

where:

$\bar{S}[\ldots]$ - loading (stress or internal force) due to ...

γ_n - importance factor for taking into account social and economic consequences resulting from failure of the structural member

F^n - standard load

γ_f - load factor

ψ - combination factor

$\bar{R}^n$ - standard load-carrying capacity, general; the same dimension as with $\bar{S}$

γ_m - material factor

γ_d - modifying factor for taking into account special influences.

This form of checking applies to such cases which have to be treated according to first-order theory as well as for those according to second-order theory, because the deformation influences the internal force. In the case of checking according to second-order theory, the modulus of elasticity has to be substituted with its calculation value, i.e. E/γ_m /1/.

The regulations concerning the importance factor γ_n according to specification 207/88 of the State Building Supervision Authority are shown in table 1.

It should be emphasized that it is allowed to classify structural members in the next lower reliability category if in case of their failure the consequences will be locally restricted. This is the case, for instance, with purlins, wall cross members, wall posts, stairs, railings and so on.

Standard loads F^n, load factors γ_f and combination factors ψ are defined uniformly for all building systems in TGL 32 274 "Design loads for buildings".

(3)
Table 1: Reliability categories and importance factor

Reliability category	Consequences in failure case	importance factor
I	- very severe dangers to the population - catastrophic conditions - very severe economic consequences	≥ 1.1
II	- severe dangers to gatherings of people - severe economic losses - severe cultural losses	1.05
III	- dangers to groups of persons - essential economic consequences	1.0
IV	- slight danger to persons - slight economic consequences	0.95
V	- very slight danger to persons - very slight economic consequences	0.90

It should be noted that, depending on the probability with which the respective standard load may still be exceeded during the service life of the structure, the value of the load factors is differentiated. So, the dead loads of structural members of steel or normal reinforced concrete show only little scattering, and for that reason, it is allowed to take γ_f = = 1.1 in this case. Members of light concrete with a thickness $\leq$ 50 mm or insulating materials, however, are to be calculated with γ_f = 1.3. A second example: floors, the service load of which is < 3 kN/m^2, are calculated with a load factor γ_f = = 1.4, for 3 up to < 5 kN/m^2 γ_f = 1.3 and for $\geq$ 5 kN/m^2 γ_f = 1.2. These regulations are entirely in accordance with progressive safety conceptions. The present definitions concerning the combination factor ψ, however, are conservative, for which reason they are under revision at present.

For steel building construction, a material factor γ_m = 1.15 has been defined. It takes into account the variations in strength as well as those in the dimensions of cross section and, furthermore, it includes a correction factor which, in connection with the importance factors and design loads defined for the whole civil engineering, ensures the required level of reliability. In other branches may be defined another value. In bridge construction will probably be calculated with γ_m = 1.1, but with importance factors which are, on average, above those of civil engineering.
In contrast with the other partial safety factors, the modifying factors are defined in a deterministic way. They take into account the accuracy of the calculation model and systematic influences which were compensated up to now by safety

(4)
factors deviating from the common ones and by the allowable stresses, respectively.
Flexural stresses may be calculated taking into account partial plastification with the section modulus

$$W_T = \frac{W_{el} + W_{pl}}{2} \leq 1.2\, W_{el} \qquad (2)$$

unless a progressive plastification due to movable load is to be expected. Here, reference should be made to TGL 13 450/02 which regularizes the plastic design of steel supporting structures in building construction. In section 2.1, it says: "By the design loads (i.e. $\gamma_n \cdot \gamma_f \cdot \psi$ -fold standard loads), a statically admissible and safe moment distribution in the frame structure has to be checked. In places where the calculation value of the fully plastic moment (M_{pl} / γ_m) is reached, plastic hinges are to be assumed... The calculated plastic load is reached when in that place of the decisive statically indeterminate system where in case of further load increase a plastic hinge would be formed, the internal moment reaches the quantity M_T^n / γ_m."

Here is $M_T^n = W_T \cdot R_Z^n$

R_Z^n - standard yield point longitudinally to the structural member.

3. Stability checks

The tradition to regularize the stability checks in a special standard was followed by TGL 13 503 "Stability of steel supporting structures". This standard is divided into a Part 1 "Bases of limit states design using partial safety factors" and a Part 2 "Methods of limit states design using partial safety factors". Part 1 is binding, Part 2 is recommended for application; the project engineer is allowed to use other approved design methods, too. With the stability specification TGL 13 503, a high degree of uniformity in the treatment of the different stability cases is reached. This applies to the form of checking, the definition of the calculated safety, the use of plastic design results and a uniform measure for the sensitivity to loss of stability. /2/
In principle, for all stability cases can be performed a stress check according to second-order theory (exceptions are made with interaction relations). The quantities of the standard values for strength, of partial safety factors and of assumed imperfections were defined so, that there are formed continuous transitions to the associated stress problems according to first-order theory.
The check for a member of constant cross section subjected to compression and to bending in one of the two principal axes,

(5)
for instance, may be performed on the basis of the edge stress which is determined according to the following relations:

$$\sigma = \frac{N}{A}(1 + \mu_N f_N) + \frac{M}{W_d} f_M \qquad (3)$$

$$\sigma = \frac{N}{A}(-1 + \mu_N f_N) + \frac{M}{W_z} f_M \qquad (4)$$

where:

N = absolute value of compressive force

M = absolute value of bending moment

W_d = section modulus referred to the compression edge

W_z = section modulus referred to the tension edge

For W_d and W_z may be substituted W_T according to equation (2).

f_N, f_M = factor expressing the increase of the bending moments according to second-order theory compared with those according to first-order theory. For f_N, a sinusoidal initial deflection is specified.

$\mu_N = (93\,\bar{\lambda} - c_1)/c_2$ = imperfection

For comparison, Eurocode and ISO:

$$\mu_N = \alpha(\bar{\lambda} - \lambda_0)$$

$$\bar{\lambda} = \frac{\lambda}{\lambda_s} = \frac{\lambda}{\pi}\sqrt{\frac{R_z^N}{E}} \qquad \text{relative slenderness}$$

	TGL		(TGL)		EC, ISO	
buckling curve	c_1	c_2	α	λ_0	α	λ_0
a	15	500	0,186	0.161	0.21	0.2
b	10	320	0.290	0.108	0.34	0.2
c	10	220	0.422	0.108	0.49	0.2
d	10	160	0.581	0.108	0.76	0.2

The variations in the buckling factor φ (χ resp.) which result from the different imperfections specified in TGL and EC and ISO, resp., are below 2 % with the buckling curves a, b and c. For buckling curve d, TGL gives values being higher up to 6.5 %. This variation was introduced intentionally in order to provide a more uniform graduation. For very small slenderness, the buckling factor of the buckling curves a to d according to

(6)
TGL is lower by 1 to 5 % than according to EC and ISO:

Equation (3) applies to the compression edge, equation (4) to the tension edge of the compressed member.
Substituting M = 0 into equation (3), we have the relation for the centrically compressed member

$$\sigma = \frac{N}{A}\left(1 + \mu_N f_N\right) \tag{5}$$

In place of the check according to equation (5), it can also be written

$$\frac{N}{A} \leq \sigma_{kr} / \gamma_m = R_z^N \cdot \varphi / \gamma_m \tag{6}$$

which gives the same result. φ is the buckling factor which, in accordance with buckling curves a...d, depends on the shape of the cross section and on the level of residual stresses as well as on the relative slenderness $\bar{\lambda}$, and which can be taken from a table. It can be determined as well according to the following relation:

$$\varphi = \frac{1}{2}\left(\frac{1+\mu_N}{\bar{\lambda}^2} + 1\right) - \sqrt{\left[\frac{1}{2}\left(\frac{1+\mu_N}{\bar{\lambda}^2} + 1\right)\right]^2 - \frac{1}{\bar{\lambda}^2}} \tag{7}$$

The calculation having proved successful for years provides a sufficiently uniform reliability in the whole range of slenderness, as was demonstrated by calculations using several assumptions of loading, imperfection, yield point and modulus of elasticity as stochastic variables. /3/

A girder subjected to bending may be checked for lateral torsional buckling according to

$$\frac{M}{W_d} \leq \sigma_{kr} / \gamma_m = R_z^N \cdot \varphi_M / \gamma_m \tag{8}$$

Relation (8) is similar to relation (6). The torsional buckling factor φ_M depends on

- torsional buckling curve a...d into which the member has to be classified, and
- the relative slenderness $\bar{\lambda} = \sqrt{M_T^n / M_{ki}}$

M_{ki} is the ideal torsional buckling moment which, for instance, can be given for the single-span girder of constant double symmetrical cross section:

$$M_{ki} = \zeta \frac{\pi^2 E I_y}{(\beta l)^2}\left[\sqrt{(0.5\beta^2 v)^2 + c^2} - 0.5\beta^2 v\right] \tag{9}$$

where:

ζ = coefficient taking into account the development of the bending moment over the girder length

E = modulus of elasticity (210 000 N/mm^2)

(7)

I_y = moment of inertia about the axis exposed to torsional buckling

β = value taking into account the degree of elastic restraint at right angles to web plane

l = girder span

v = distance of the points of application of the transverse loading from the girder axis, to be introduced positively in direction of the zone of combined compression and bending

$$c = \sqrt{\frac{C_M \left(\frac{\beta l}{\beta_o l_o}\right)^2 + 0.039 (\beta l)^2 I_D}{I_y}}$$ = radius of rotation

C_M = warping constant

β_o = parameter for the degree of warping restraint at supports

l_o i.e. equal to l

I_D = torsional constant

The standard makes it also possible

- to determine the relative slenderness by a simplified relation (flexural member analogy)
- to perform the lateral torsional buckling check as a stress check according to second-order theory.

The buckling check takes into account the post-critical behaviour in case of compression by the effective width and in case of shear by the tension field model. The safety factors which, according to the previous regulations, are lower in some cases, are taken into account by modifying factors >1. In accordance with the residual stresses to be expected due to welds and with the initial deflections, four buckling curves are differentiated. Proceeding from the ideal buckling stress, a real critical stress is calculated which in case of static loading may be above the ideal buckling stress. These regulations were also proved by tests with structural members.

4. Summary

New codes for steel structures are presented which are now valid in the GDR. They are based on the conception of limit states and checks using partial safety factors.
Concerning the stability check, it is emphasized that a high degree of uniformity in the treatment of the different stability cases has been reached and that to the checks according to second-order theory was given the place being due to them in accordance with the present state of engineering theory.

(8)

References

/1/ Lutteroth, A.: Einführung der Bemessung mit Teilsicherheitsfaktoren im Stahlbau, Bauplanung-Bautechnik 42 (1988) 10, p. 437 - 439

/2/ Einführung in die neue Stabilitätsvorschrift TGL 13 503/01 und /02, Wissenschaftliche Berichte der TH Leipzig (1982) 18, 19

/3/ Lutteroth, A.: Theoretische Zuverlässigkeit von Stahlbauteilen, Bauplanung-Bautechnik. Will be published soon.

(1)
Iffland, Jerome S.B. (1)

World View General Provisions

INTERNATIONAL COLLOQUIUM
STABILITY OF STEEL STRUCTURES
BUDAPEST, HUNGARY, 1990
PRELIMINARY REPORT

Summary

The General Provisions of the 2nd edition of "Stability of Metal Structures-A World View" are necessarily limited in length. Decisions had to be made on what topics to include and how extensive the coverage should be. The World View document cover 78 specifications from six regions of the world. This total number indicated material would have to be limited. It was decided to provide quantitative information in the General Provisions rather than extensive philosophical discussions. This will enhance the use of the document. Summaries of the North American Region General Provisions are provided for Limits of Applicability, Materials and Design Basis.

Introduction

Early in the development of the outline for the 2nd edition of "Stability of Metal Structures - A World View," common sense suggested that comparisons of differences and the reasons for these differences between design provisions for various structural components and systems might be meaningless because of philosophical differences about loads, combinations of loads, use of materials and design bases. Accordingly, a section of the document covering these differences was included and designated General Provisions.

While the 1st edition of "Stability of Metal Structures - A World View," also recognized the need for some general discussion by providing a section of "Philosophical Background and Safety Concepts," no quantitative data was given. In addition, there was not a consistent approach to the discussion between the various world regions. It has been attempted to overcome these shortcomings in the 2nd edition.

The first section of the General Provisions in the 2nd edition was designated "Limits of Applicability." The initial concept was to provide verbatim extracts from each specification being covered to define the limits of applicability in the exact words of the specification writers. This would eliminate misinterpretation and possible unintentional expansion of areas not intended. This approach was attempted for the North American Region covering

(1) President, Iffland Kavanagh Waterbury, P.C. New York, New York

(2)

some 17 specifications. The result was an 18 page document. If this were expanded to cover all regions, totaling some 78 specifications, the section on "Limits of Applicability" alone would be completely out of proportion to the rest of the document. Since much of the philosophical statements on "Limits of Applicability" in the individual specifications could be covered quantitatively in other sections of the General Provisions, it was decided to limit this section to a simple matrix covering types of structural members and structural systems covered by each of the specifications.

The second section of the General Provisions was designated "Material." It was decided to provide quantitative data on the materials covered by each specification. It was agreed that this would be of value and so, for each specification, for each steel material covered, the thickness limitations, the minimum yield stress and the minimum tensile strength are tabulated. The comparison, in matrix form, provides information on the specification requirements for other material properties. A similar coverage is provided for steel-concrete composite materials.

A third section of the General Provisions was planned designated "Loads and Load Combinations." Again, this approach revealed itself to be over ambitious, but also not even possible. Specifications for design of highway and railway structural members provided a voluminous amount of information on dead, live, wind, earthquake, temperature and other loads while those specifications that addressed building structures provided almost nothing and covered the topic by reference to other standards which in turn were also voluminous. It was decided that the actual design loads themselves and the philosophy behind their derivations was a subject to vast to be covered in this document. The important issue was the load combinations. Accordingly, it was decided to eliminate the section in the General Provisions on loads and include the subject of load combinations together with the section on design basis with which they were intricately linked to factors of safety or member factored resistances.

The third and last section of the General Provisions was designated "Design Basis" which includes load combinations. In this section, quantitative information is provided for each specification on factors of safety, load factors, load combinations. resistance factors, load combination factors, importance factors and other parameters used in the design basis for each specification. It is noted that some specifications provide more than one design basis and most have specific serviceability checks. Thus, by providing this quantitative information, the specification philosophical approach is presented.

Historical Highlights

The 1st edition of "Stability of Metal Structures' A World View," provided historical information for four world regions. These were Japan, North America, West Europe, and East Europe. Some of the following information was adapted from this publication. It is important to note that code and specification development is directly related to the particular social-political nature of each country. Centralization of a government and a structured social-political system is reflected in development of individual specifications and in building, bridge and other structure design codes. The 2nd edition of the World View covers the following number of specifications by region:

(3)

Australia	-	7
China	-	5
East Europe	-	18
Japan	-	10
North America	-	17
West Europe	-	21
Total		78

In addition, if a particular country had the wisdom, motivation, leadership and necessary consensus to establish a national standards association organization responsible for specification development, this status obviously is reflected in their code and specification development. There are two extremes represented by China (one country) reporting on 5 specifications and North America (two countries) reporting on 17 specifications. The former specifications reflects a minimum number of specifications and a consistent philosophical approach as well as in format while the latter covers many specifications, diverse philosophies of design bases and there is little consistency in format. Following are some generalized comments about specifications development in the several regions of the world covered by the World View document.

Australia. Except for a specification covering structural design of steel bins for bulk solids, all of the Australian specifications are developed by the Standards Association of Australia (SAA). This fact, and because only one country is being covered, results in only 7 specifications treated in the World View document. In addition, there is the obvious consistency in philosophy of design bases and format that can be expected. While Australia has a limit state specification for design of building structures, all of the other specifications are based on allowable stress design.

China. This region also covers only one country and has the further advantage of all specifications being developed by one organization, the China Technical Committee for Standards of Steel Structures. The result is that only 5 specifications are needed for full representation in the World View document. Four of these specifications follow the instruction of the Unified Code for the Design of Building Structures which has adopted the limit state design approach based on probabilities theory. The specification for design of highway and railway structural members utilizes the allowable stress approach.

East Europe. Because of the number of countries covered by the region designated as East Europe, the number of specifications is large, totaling 18. While progress is slow there is an effort in progress aimed at unification of national codes and specifications. This was initialed in the 1970's under the framework of the Council of Mutual Economic Aid (CMEA). This organization has adopted and approved two unified specifications, one covering steel structures which is included in the list of 18 for the region. At present, those specifications within each country are those most commonly used. However, because of the existence of two approved regional standards (with more underway) there is a definite trend for consistency and unification. Most of the East European countries

(4)

covered have national Boards of Standardization so that, at least in an individual country, there is consistency in philosophy of the design bases and format between the several national specifications. While there are some exceptions for specific types of members and structures, in general, most of the East Europeans specifications adopt some form of limit state design approach based on a probabilistic theory. Use of divided safety factors to express uncertainties due to loads and uncertainties due to resistance is common.

Japan. All of the Japanese specifications reflect the dominating load effect caused by earthquakes and accordingly both ultimate limit states permitting significant damage without collapse and serviceability limit states restricting damage are addressed for extreme earthquakes of low probability and moderate earthquake of reasonable probability respectively. All of the Japanese building specifications are developed by the Architectural Institute of Japan (AIJ) while the railway bridge specifications are developed by the Japan Society of Civil Engineers (JSCE) and the highway bridge specifications are developed by the Japan Road Association (JRA). This involvement by is minimum number of specification bodies helps in formulating consistent specifications. While limit state specifications are available for building design, the allowable stress approach is still most commonly used.

North America. Specifications in the U.S.A, except for bridges, are generally industry initiated, while in Canada they are developed by the Canadian Standards Association (CSA). In the U.S.A., highway bridge specifications are developed by the American Association of State Highway and Transportation Officials (AASHTO) while railway bridge specifications are developed by a users group, the American Railway Engineering Association (AREA). Highway bridge specifications in Canada are developed by both the CSA and the Provincial governments. However, the U.S.A. is characterized by the local autonomy that modifies specifications for building structures for adaptation into city building codes and modifies specifications for highway bridge structures for adaptation into state highway bridge specifications. While these modifications are not necessarily substantial, every city and every state make enough modifications to express their local independence and an engineer has to keep up with all the local variations in the areas he practices. The situation in Canada is similar. The U.S.A. situation is further complicated by the existence of private organizations that develop model building codes which are often adapted by smaller municipalities. The model building code groups, of course, first modify any industry developed specifications if they incorporate them into their model codes to demonstrate and establish their expertize over the industry groups. In establishing the 17 specifications reviewed in the World View document for North American, a list of 47 specifications was culled. Except for one Canadian Provincial highway bridge specifications, no local autonomous building codes or specifications were considered. However, one model code for earthquake design was included. Both building and bridge design specifications in Canada are limit state based while specifications in the U.S.A. are a mixture of allowable stress design and limit state design for buildings and a mixture of allowable stress design and load factor design

(5)

for bridge structures.

West Europe. The region designated as West Europe has the largest number of specifications, 21, covered in the World View document. However, because this group makes up the Common Market Community, the future of unification and reduction in the number of design specifications looks good. Several of the Eurocode specifications are included in the total of 21 although most of the specifications represent national codes of the counties covered by this region. While the prospects for unification look good, the date is still in the future and the specifications for each country will be continued to be used for some time after the Eurocodes become official. The Eurocodes will be mandatory for common market activities but each country can continue to use their own design specifications within their country although charges are frozen and eventually these specifications will be outdated. In general all West Europe specifications adopt limit state design concepts based on probabilistic theory although there ar still some allowable stress design specifications in use.

Limits of Applicability

Table 1 indicates the specification applications covered by the 2nd edition of "Stability of Metal Structures - A World View" by region. Lack of indicated coverage does not imply there is no specification on a subject, only that because of space limitations, nothing was included in the World View document.

TABLE 1

APPLICATION	REGION					
	AUSTRALIA	CHINA	EAST EUROPE	JAPAN	NORTH AMERICA	WEST EUROPE
Steel						
Building	X	X	X	X	X	X
Bridges	X	X		X	X	X
Transmission Towers	-	-	-	X	-	-
Shells/Tub. Mem.	X	-	X	X	X	X
Aluminum						
Buildings	X	-	-	-	X	-
Bridges	-	-	-	-	X	-
Cold-Formed Steel						
Buildings	X	X	X	X	X	X
Composite-Steel/Conc. Col.						
Buildings	X	X	X	X	X	X
Seismic						
Buildings	-	X	X	X	X	-
Bridges	-	X	X	X	X	-

(6)

(7)

Materials

The material section in the World View document is lengthy. For the purpose of providing an example of the information provided, a summary has been prepared of the maximum strength of materials covered by the North American Specifications. This summary is provided in Table 2. Summaries for other regions would be similar.

TABLE 2

STEEL PRODUCT	MAX. OBTAINABLE YIELD STRESS (MPA)
Shapes-Groups 1 & 2	480
Shapes-Group 3	400
Shapes-Group 4	350
Shapes-Group 5	320
Bars-Up To 65 mm Thick	690
Bars-Up To 100 mm Thick	620
Bars-Up To 200 mm Thick	290
Bars-Up To 300 mm Thick	230
Plates-Up To 65 mm Thick	690
Plates-Up To 100 mm Thick	620
Plates-Up To 200 mm Thick	290
Plates-Up To 300 mm Thick	230
Plates-Up To 800 mm Thick	270
Pipe-Up To 25.4 mm Thick	360
Pipe-Up To 63.5 mm Thick	240
Tubing-Up To 38.1 mm Thick	345
Round Tubing-Up To 15.88 mm Thick	317
Shaped Tubing-Up To 15.88 mm Thick	345
Sheet and Strip-Up To 6 mm Thick	550
Coated Sheet-Up To 6 mm Thick	550
Hollow Sections-Up To 16 mm Thick	380

Design Basis

Summary tables have been prepared for the North American Region specifications to compare the design bases utilized. Tables 3 and 4 compare Factors of Safety for Allowable Stress Design of buildings and bridges respectively. Tables 5 and 6 compare Member Resistance Factors and Load Factors for Limit State Design or Load Factor Design for buildings and bridges respectively.

(7)

TABLE 3

BUILDINGS

ALLOWABLE STRESS DESIGN

MEMBER TYPE	SPECIFICATION	FACTOR OF SAFETY ON YIELD STRENGTH
Tension	AA - 1986	1.65
	AISC-ASD - 1989	1.52
	AISI - 76	1.52
	AISI - 86	1.67
	API RP2A - 1989	1.52
Compression (Buckling)	AA - 1986	1.95
	AISC-ASD - 1989	1.67 To 1.92
	AISI - 76	
	AISI - 86	1.92
	API RP2A - 1989	
Flexure	AA - 1986	1.65
	AISC-ASD - 1989	1.67
	AISI - 76	
	AISI - 86	1.67
	API RP2A - 1989	

TABLE 4

BRIDGES

ALLOWABLE STRESS DESIGN

MEMBER TYPE	SPECIFICATION	FACTOR OF SAFETY ON YIELD STRENGTH
Tension	AA - 1986	1.85
	AASHTO - 1989	1.82
	AREA - 1989	1.82
Compression (Buckling)	AA - 1986	2.20
	AASHTO - 1989	2.17
	AREA - 1989	1.82
Flexure	AA - 1986	1.85
	AASHTO - 1989	1.82
	AREA - 1989	1.82

(8)

TABLE 5

BUILDINGS

LIMIT STATES DESIGN

PARAMETER	SPECIFICATION		
	AISC-LRFD-1986	CSA S16.1 M89	CSA S136 M89
MEMBER RESISTANCE FACTOR			
Tension	0.90	0.90	0.90
Compression	0.85	0.90	0.90
Flexure (Sym)	0.90	0.90	0.90
LOAD FACTOR			
Dead Load	1.20	1.25	1.25
Live Load	1.60	1.50	1.50

TABLE 6

BRIDGES

LIMIT STATES DESIGN (OR LOAD FACTOR DESIGN)

PARAMETER	SPECIFICATION			
	AASHTO-1989	CSA S6-M89	OHBDC-1983	
MEMBER RESISTANCE POLICY			FABRICATED SHAPES	ALL OTHER
Tension	1.00	1.00	0.95	0.90
Compression	1.00	1.00	0.95	0.90
Flexure (Sym)	1.00	1.00	0.95	0.90
LOAD FACTOR				
Dead Load	1.30	1.30	1.20	
Live Load	1.67	2.17	1.40	

IVÁNYI, Miklós (1)

DESIGN CONCEPTS OF NEW HUNGARIAN CODES

INTERNATIONAL COLLOQUIUM
STABILITY OF STEEL STRUCTURES
BUDAPEST, HUNGARY, 1990
PRELIMINARY REPORT

Summary: A brief account is given of the philosophical background, safety concepts and formulae used in the new Hungarian specifications (MSZ) for the analysis of stability phenomena of steel structures.

Part A. PHILOSOPHICAL BACKGROUND AND SAFETY CONCEPTS (HALÁSZ 1979)

A1. Historical remarks

The Safety Concept, as adopted by most East European countries, was originally worked out and formulated mostly by Soviet experts in the 30's and 40's of this century (see BALDIN 1951). It was officially introduced first by the Soviet Building Code in 1946 and afterwards by all Soviet specifications. Similar concepts were adopted in Hungary and Poland around 1950. These initiatives had great influence on the work of other international organizations (ISO, CEB) in their standardizing activity as well.

The background, development and details of this process are summarized in several monographs (GVOZDEV 1949, BALDIN 1951, BROUDE 1953, STRELECKIJ 1952, KORÁNYI 1952, BOLOTIN 1965, MURZEWSKI 1970, HALÁSZ 1979).

The Safety Concept - called by different names as "limit states approach", "method of divided safety factors", "semi-probabilistic method" and lately as "level I. method in probabilistic approach", indicating thus the different stages of its development - was originally offered as an alternative instead of the previously generally adopted "allowable stress approach" and was motivated by its criticism. Based on contemporary comments (BALDIN 1951) this can be summarized as follows.

(1) Professor of Structural Engineering
Department for Steel Structures
Technical University, Budapest, Hungary

(2)

A2. Limit states

With broadening knowledge about performance of steel structures in the elastic range and reinforced concrete elements in their different working stages, it seemed necessary to re-interpret the original and newly accumulated ideas hidden behind the desing formulae of the allowable stress approach:

$$\sigma(F_K) \leq \sigma_v \qquad e(F_K) \leq e_v \qquad \text{(A1)}$$

$$\text{(a) } \sigma_v = \sigma_y/n_1 \quad \text{(b) } \sigma_v = \sigma_{cr}/n_2 \quad \text{(c) } \sigma_v = \sigma_f/n_3 \qquad \text{(A2)}$$

expressing comparision of the stresses (and deflections) due to code-specified loads F_K to their allowable values σ_v (and e_v), but the former one derived from yield stress σ_y, critical stress σ_{cr} and fatigue strength σ_F by safety factors n_1, n_2, n_3 respectively. First of all Eq. A2 (b) proved to be problematic, as it represents *in some cases* the requirements of elastic behaviour under normative loads - giving thus but an indirect and often irrelevant information about margin of safety (KAZINCZY 1914) and bearing little relevance upon actual behaviour of reinforced concrete elements (GVOZDEV 1949) - *in other cases* (bearing in mind the design practice of trusses, connections and alike) it includes at least quantitatively the consequences of ductile behaviour and refers directly to failure. To avoid ambiguities and unreasonable differences in actual safety it was suggested

- to take systematically into account all known phenomena rendering the structure unsuitable to satisfy anticipated design requirements, bringing it thus to a "limit state",
- to select parameters ϕ (loads, load-effects, stresses, deflections and so on), suitable for quantitative description of the limit states by their values ϕ_L^i depending on geometrical, strength and stiffness characteristics of the structure,
- to adopt adequate computational methods to monitor the changing values of ϕ_F^i of this parameters in the loading process, and
- to judge safety by comparison of the most infavourable value of ϕ_F^i during erection and life-time to ϕ_L^i, considering the consequences of reaching the limit state.

Two categories of limit states were suggested (for steel)

Group I. Ultimate limit states (rendering the structure unfit for further use), follow:

a.) strength limit states

- excessive yielding, slip in connections, residual strains, if structure can not be used as designated

(3)

any more;
- unrestrained flow (collapse mechanism formation);
- accumulation of residual deflections;
- plastic fracture.

b.) stability limit states
- instability if loads to lose load bearing capacity or change of shape of structure;
- loss of equilibrium as a whole (overturning, sliding, etc.);

c.) brittle fracture;
d.) fatigue.

Group II. Serviceability limit states (restricting regular use of the structure) follow:

a.) deflections, rotations, swings and vibrations causing difficulties in designated use of structure;
b.) buckling of plate element (local buckling) if does not occur simultaneously with losing load bearing capacity.

Most attention was paid to group I., where in general the load F and carrying capacity R can be regarded as parameter ϕ_F^i and ϕ_L^i respectively.

A3. Divided safety factors

Progress in understanding structural behaviour and in reliability of material was manifested by a successive increase of allowable stresses (as for instance the raise of σ_v for mild steel from 140 Mpa to 160 Mpa during the Second World War in the Sovietunion). It was of common opinion that further general increase would jeopardize safety and further progress can be achieved by differentiating among structures and loading cases only. As main view-point of differentiation (within a certain class of structures and materials) differences in variability of loads offered themselves; reflecting the general experience, that structures with high proportion of (unchanging) self-weight are less vulnerable and superior in longevity, that light structures with high proportion of strongly varying live or climatic loads. This motivated the early Soviet specifications for reinforced concrete (OST 90003/38, SACHNOVSKIJ 1951) to apply different safety factors depending on the ratio of dead load to live loads, and subsequently to the splitting up the general safety factors in Eqs A2. into two parts:

$$n = \gamma_F \cdot \gamma_m \qquad (A3)$$

the first one expressing uncertainties due to loads, the second one those due to resistance.

A4. Semi-probabilistic approach

In this relation it was necessary to clear up the actual meaning of traditional terms as "characteristic" (normative, code-specified, nominal, guaranteed) values of load (F_K) and

(4)

resistence (R_K). This brought about the concept (MAYER 1926, CHOCIALOV 1929, STRELECKIJ 1935, WIERZBICKI 1936), that they can be interpreted by regarding load and resistence as random values, characterised by a probability density function, mean values $(F_{max})_m$, R_m; standard deviation s_F, s_R; and coefficient of variation δ_F, δ_R respectively (Fig. A1).

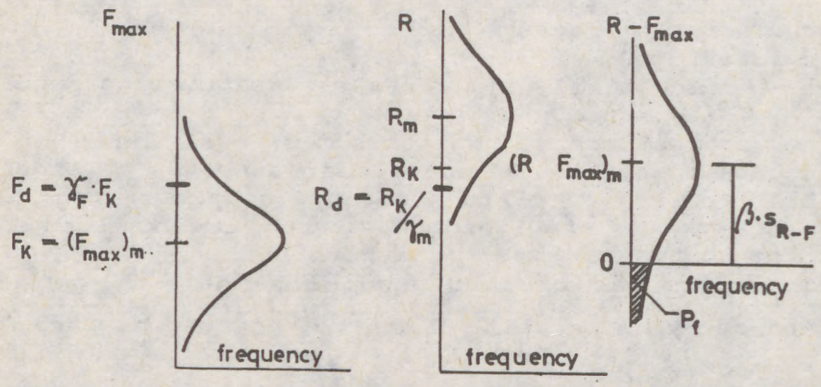

Fig. A1

Following the interpretation of RZANICIN 1947, 1949, 1954, the risk of failure P_f can be expressed by the probability

$$P\,(R - S < 0) = P_f \qquad (A4)$$

(shadowed area in Fig. A1b), which - in case of Gaussian distribution - depens on safety index:

$$\beta = \frac{(R - F_{max})_m}{s_{R-F}} = \frac{R_m - (F_{max})_m}{([R_m \cdot \delta]^2 + [(F_{max})_m \cdot \delta_F]^2)^{1/2}} \qquad (A5)$$

allowing to establish correlation between risk of failure and "central" safety factor n_c

$$n_c = \frac{R}{(F_{max})_m} = \frac{1 + (\beta^2(\delta_R^2 + \delta_F^2) + \beta^4 \delta_R^2 \delta_F^2)^{1/2}}{1 - \beta^2 \delta_R^2} \qquad (A6)$$

This can be - somewhat arbitrarily and approximately - split up:

$$n_c \sim n_F \cdot n_R \; ; \; n_F = 1 + \bar{\beta} \cdot \delta_F \; ; \; n_R = \frac{1}{1 - \bar{\beta}\,\delta_R} \qquad (A7)$$

and thus - in case of arbitrarily chosen characteristic values - by

$$\gamma_F = n_F \frac{(F_{max})_m}{F_K} \quad ; \quad \gamma_m = n_r \frac{R_K}{R_m} \qquad (A8)$$

(5)
the basic design formula can be established:

$$\gamma_F F_K \leq \frac{R_K}{\gamma_m} \quad \text{or} \quad \gamma_F F_K = F_d \; ; \; \frac{R_K}{\gamma_m} = R_d \; ; \; F_d \leq R_d \qquad (A9)$$

In case of combined loading - adopting different γ_{Fj} values according to different coefficients of variation of the components

$$\sum_j \gamma_{Fj} \cdot F_{Kj} \leq \frac{R_K}{\gamma_m} \qquad (A10)$$

or more generally:

$$\phi_F^i (\gamma_{Fj} F_{Kj}) \leq m \, \phi_L^i (\sigma_y / \gamma_m , A) \qquad (A11)$$

where m represents correction factor for special circumstances in fabrication, tolerances, structural behaviour and A stands for geometrical quantities.

A5. Resistance factors

Originally (BALDIN 1951) $\bar{\beta} = 3$ was suggested. For characteristic value of yield stress usually

$$(\sigma_y)_K = (\sigma_y)_m - 2 s_\sigma \qquad (A12)$$

is chosen, equal approximately to traditional "guaranteed" minimum value. Thus for most steel grades

$$\gamma_m = \frac{(\sigma_y)_m - 2s_\sigma}{(\sigma_y)_m - 3s_\sigma} \sim 1.1 - 1.2 \qquad (A13)$$

For ultimate tensile stress $\gamma_m \sim 1.45 - 1.6$.

A6. Load factors

The characteristic value of loads is chosen as the mean value of maxima:

$$F_K = (F_{max})_m \qquad (A14)$$

F_{max} being the greatest load on individual structures of the population or similar structures, or the maximum load within certain characteristic time interval (for instance one year for snow-load). Having very few data about δ_F, load factors were mainly estimated using as measure data of previous specifications and existing structures. Recently most specifications adopt

$$\gamma_F = 1 + 1.65 \, \delta_F , \qquad (A15)$$

in case of non-Gaussian distribution the value $F_d = \gamma_F . F_K$ characterized by being surpassed with probability less than 5%. Examples for γ_F values

For limit states group I.:
- Dead load $\gamma_F = 1.1$ (0.9)
exceptionally 1.2,

(6)

- Live load, distributed:

  if intensity q [kN/m^2]: $q \leq 2$; $\gamma_F=1.4$,

  $2 < q \leq 5$; $\gamma_F=1.3$,

  $q > 5$; $\gamma_F=1.2$,

- Live load, concentrated: $\gamma_F=1.2$.
- Snow load $\gamma_F=1.4$
- Wind load $\gamma_F=1.2$

For limit states group II. $\gamma_F=1.0$

A7. Load combinations

To express the reduced probability of coincidence of maxima of more components in a loading process, loads are categorized as

- Permanent loads (self-weight, earth pressure),
- Variable loads and actions (live, climatic loads, imposed deformations), subdivided wholly are partially to
  - sustained (long-term) loads or load-parts,
  - instantaneous (short-term) loads or load-parts.
- Catastrophe loads (seismic loads and alike).

The combination factor γ_c expresses the reduced probability of coincidence of high values of loads. Having more variable loads

- to the one causing the highest load effect $\gamma_c=1$;
- to the other long-term loads $\gamma_c=0.8$;
- to short-term loads $\gamma_c=0.6$ is applied.

Part B. GENERAL RULES FOR STEEL STRUCTURE DESIGN

B1. Analysis of load bearing capacity for static loads

General case: elastic design of frameworks

(a) Calculation of frameworks with spatial model (statical skeleton) (Fig. B1)

When applying spatial statical skeleton, internal forces must be calculated either by second-order analysis or such succesive approximation process, where internal forces and displacements are determined by first order analysis, but during repeated calculations displacements from previous steps modify the shape of considered bar.

If statical skeleton contains initial imperfectness besides strength analyses only plate buckling analysis of elements should be carried out.

This method can be applied if designer proves with detailed analysis attached to the calculation, that the estimated magnitude and distribution of initial imperfectness gives reliable basis for judging the proper load bearing capacity of structure.

Applying spatial model makes stability analysis unnecessary, so there is no need to determine slenderness ratios of bars. On the other hand spatial model requires computer for

(7)
performing voluminous calculation and extra analysis for taking the values of the initial imperfectness.

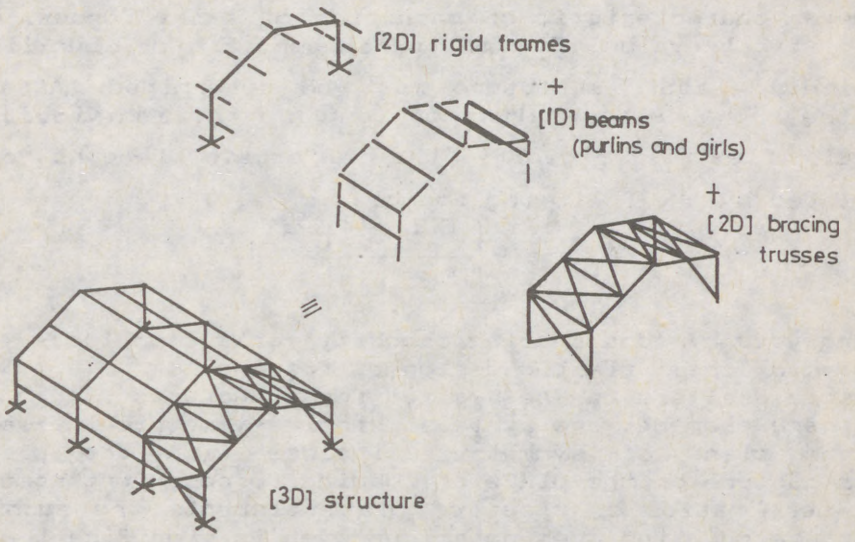

Fig. B1

(b) Calculation of plane frameworks (statical skeleton)
Spatial structures can be analyzed dividing the frame to structures loaded in their planes assumming planar statical skeletons.(Fig. B1)

If initial imperfectness is considered at planar statical skeletons; beside second order strength analyses only the buckling of plate elements and those stability limit states must be checked, which are in connection with displacements perpendicular to the plane of structure and twist of axis of bar.

(c) Calculation of frameworks by disassemble to elements (to beams, columns, etc.) (Fig. B1)

The originally spatial or planar frameworks can be analyzed by disassembling to separate elements (columns, beams). In these cases at individual bars such supports should be assumed, that they satisfactory reflect - occasionally with approximation for the safety - the supporting effect of connecting elements (columns, beams, bracings, foundations).

If structure includes eccentrically loaded elements in compression, the effect of deformations on internal forces must be taken into consideration. For this purpose either internal forces should be calculated by second order analysis or bending moments calculated by first order analysis should be modified.

The effective length $l_o = v.l$ can be determined from insta-

(8)

bility of the whole structure loaded with axial forcess only. Writing the axial forces of individual elements in the form of

$$N_i = m_i F \qquad (B1)$$

(where m_i is the ratio of axial forces, F is a common parameter characteristic of magnitude of axial forces), first the critical value F_{cr} of parameter F for buckling of infinitely elastic structure must be determined. Afterwards with the known design values of length l_i of individual beams and EI_i flexural rigidity the effective lengths can be calculated by the following formula:

$$v_i . l_i = \pi . \left\{ \frac{E I_i}{m_i F_{cr}} \right\}^{1/2} \qquad (B2)$$

B2. Analysis of load bearing capacity for static loads

Special case: plastic design of frameworks

Plastic analysis can be applied for structures

- where elements are at least single symmetrical I-sections and plane of symmetry coincides with the plane of structure or the plane of loading forces; furthermore
- where ratios of sizes of plate elements are such, that plate buckling does not occur even in significant plastic deformation. These conditions are fulfilled if limits of plate slendernesses in MSZ 15024/1-85 are satisfied;
- not sensitive for instability, such as
  - continious beams,
  - one- or two-storey frames,
  - multi-storey frames with rigid connections, where internal displacements of connections in plane of structure are restrained by shear wall or bracing with efficient stiffness;
- whose connections (splices and connecting) are of uniform load bearing capacity, despite if it is obvious that platic hinge can not be formed in connection;
- where the whole structure is stiff enough that internal forces can be determined by first order analysis.

In case of planar frameworks having bars with straight axis this condition is satisfied if all elements of structure fulfill the requirement

$$\frac{N}{A \sigma_H} \leq 0.1 \left[\frac{\lambda_E}{\lambda_x} \right]^2 \qquad (B3)$$

where N is the axial force in the member

A is the cross sectional area

σ_H is the ultimate strength

$\lambda_E = 93.01$ (strength group "37")

λ_x is the slenderness ratio for buckling in plane of structure.

If these requirements are slightly (with a maximum of 25%

(9)
exceeding) not satisfied than at calculation of ultimate internal forces of cross sections, ultimate stress must be reduced to

$$\sigma_H' = \sigma_H \frac{1}{0.9 + \frac{N}{A.\sigma_H}\left(\frac{\lambda_x}{\lambda_E}\right)^2} \qquad (B4)$$

- whose elements are supported continuously or at sufficient locations against displacements perpendicular to the plane of structure and against twist such a way that buckling of bars perpendicular to the plane of structure or their lateral-torsional buckling can not occur until the computed load carrying limit.

Equations (B3) and (B4) correspond to the modified Rankine-Merchant formula.

The compression flange of I-sections bent about the major axis should be supported laterally in the assumed plastic hinge cross section and in a distance to both direction of

$$c \leq \beta_p \cdot i_y \cdot \lambda_E \qquad (B5)$$

In this formula i_y is the radius of gyration of I-section in the plane of bending;

$$\beta_p = 0.45, \qquad \text{if } 0.5 \leq \frac{M_{min}}{M_{max}} \leq 1.0$$

$$\beta_p = 0.675 - 0.45 \frac{M_{min}}{M_{max}}, \qquad \text{if } -1 \leq \frac{M_{min}}{M_{max}} \leq 0.5 \qquad (B6)$$

where M_{max} is the moment at the plastic hinge, M_{min} is the moment at the next lateral support. M_{max} should be substituted with positive sign, while M_{min} is positive if its sense is identical to the one of M_{max} and negative if the opposite.

Part C. APPROACHES AND DESIGN PROCEDURES FOR STRUCTURAL COMPONENTS

For the preparation of design codes and for the verification of new theoretical approaches for predicting the resistence of structure, test data relating to the behaviour of steel structures and structural components throughout the entire range of loading up to ultimate load are an essential requirement.

According to the semi-probabilistic concept adopted by the specifications σ_c is to be design value defined by a given probability of not being surpassed, taking into account the various random imperfections (including eccentricity, initial curvature, residual stresses, scatter in mechanical and geometrical properties, etc.) a "real" column exhibits compared to an ideal one. As - compared to the multitude required for a statistical analysis - only a limited number of domestic tests were available, experimental results published in the literature were relied upon, first of all

(10)
those collected by FUKUMOTO 1982.

For the interpretation of the results it seemed to be more advantageous - instead of following the traditional way of prescribing fictitious or equivalent initial curvature - to use interaction formulae which can be fitted better to test results influenced by considerable residual stresses.

C1. Centrally compressed steel members

The limit load N_c of a centrally compressed steel member of uniform cross section governed by flexural buckling is given in the form

$$N_c = A \cdot \varphi \cdot \frac{\sigma_y}{\gamma_m} \qquad (C1)$$

A denoting the gross cross sectional area, φ buckling factor for column and σ_y / γ_m the specified yield stress.

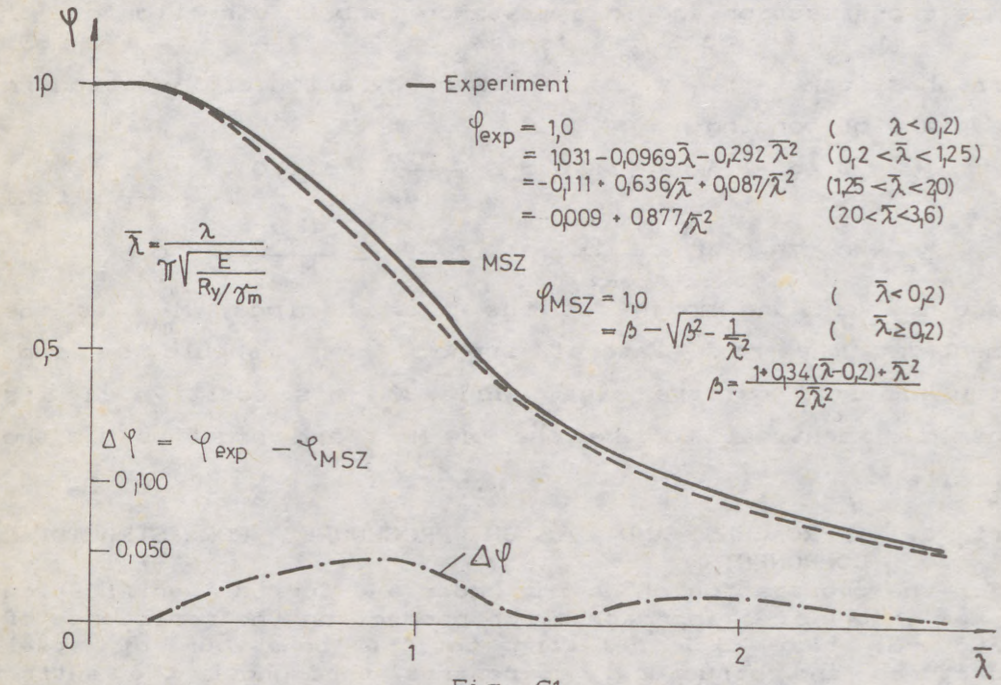

Fig. C1

The basic column strength formula in the new Hungarian code (MSZ 15024/1-85) is compared graphically with the experimental curve (M) which was determined through statistical manipulation of NDSS test data (FUKUMOTO, ITOH 1983/a) (Fig. C1)

C2. Lateral buckling of beams

The aim of the specifications was to follow the same concept as outlined in par. *C1* and to include into the computation the effect of various imperfections. The problem is much more

(11)

complex, than that of a compression member, as cases differ not only in the end restrains, but in the shape of moment diagram, level of application of loads; and imperfections may have different importance depending on the actual features of the problem. Lacking the satisfactory number of experimental evidence - enough for statistical evaluation - different cases are supposed to be represented by a simple parameter, the fictitious slenderness ratio λ_i defined by the equation

$$\frac{\pi^2 E}{\lambda_i^2} = \frac{M_{cr}}{W} \qquad \lambda_i = \pi \cdot \left[\frac{E \cdot W}{M_{cr}} \right]^{1/2} \qquad (C2)$$

M_{cr} denoting the theoretical value of maximum bending moment causing bifurcation of an ideal, elastic beam computed with due regard to end restrains and loading conditions - inclusive the level of application of loads - (for which in different cases formulae are offered in the specifications).

The limit value of the bending moment is given by

$$M_c = W \cdot \varphi_K \cdot \frac{\sigma_y}{\gamma_m}$$

φ_K buckling factor for beams and σ_y/γ_m the specified yield stress.

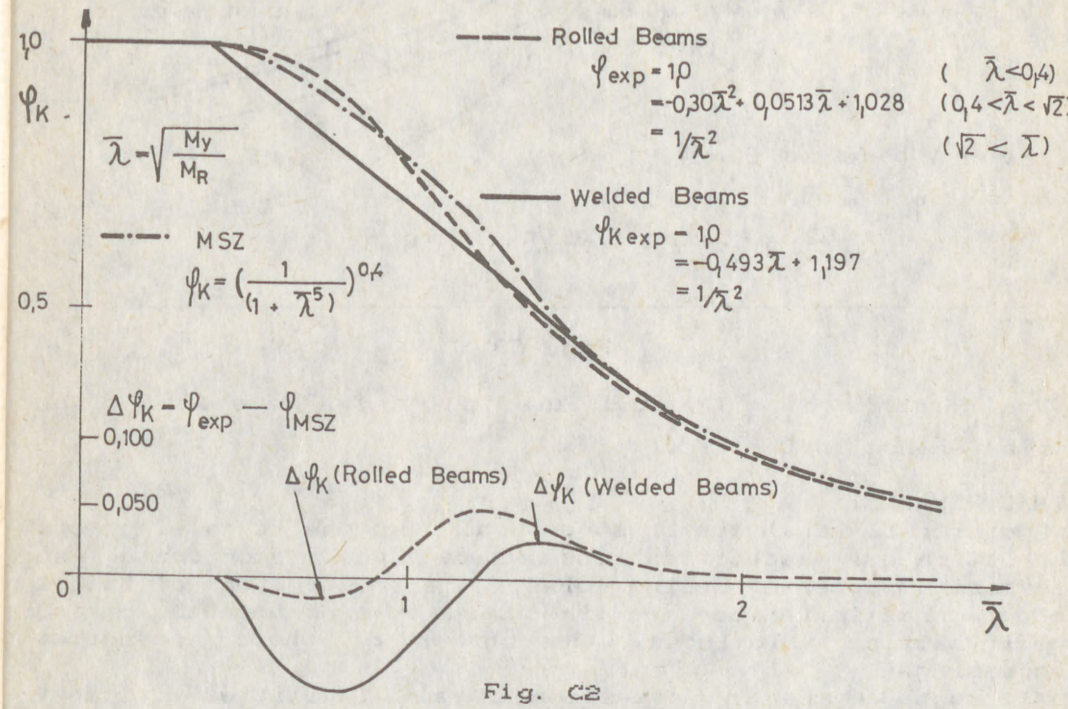

Fig. C2

The basic beam strength formula in the new Hungarian code is compared graphically with the experimental mean curve (M) which was determined through statistical manipulation of NDSS test data (FUKUMOTO, ITOH 1983/b). (Fig. C2)

(12)

C3. Plate buckling

The specification generally still contains formulae based on the concept of linear buckling stresses, but this gives way in special cases to different methods as well. The critical stress is defined by the traditional critical value $\sigma_{e,cr}$ of the equivalent stress $\sigma_{eq.}$, using the classical interaction curves in case of different combinations of stresses originated by compression, bending and shear.

The φ_b buckling factor for plate in the new Hungarian code is compared graphically with the experimental mean curve (M) which was determined by FUKUMOTO 1984. (Fig. C3)

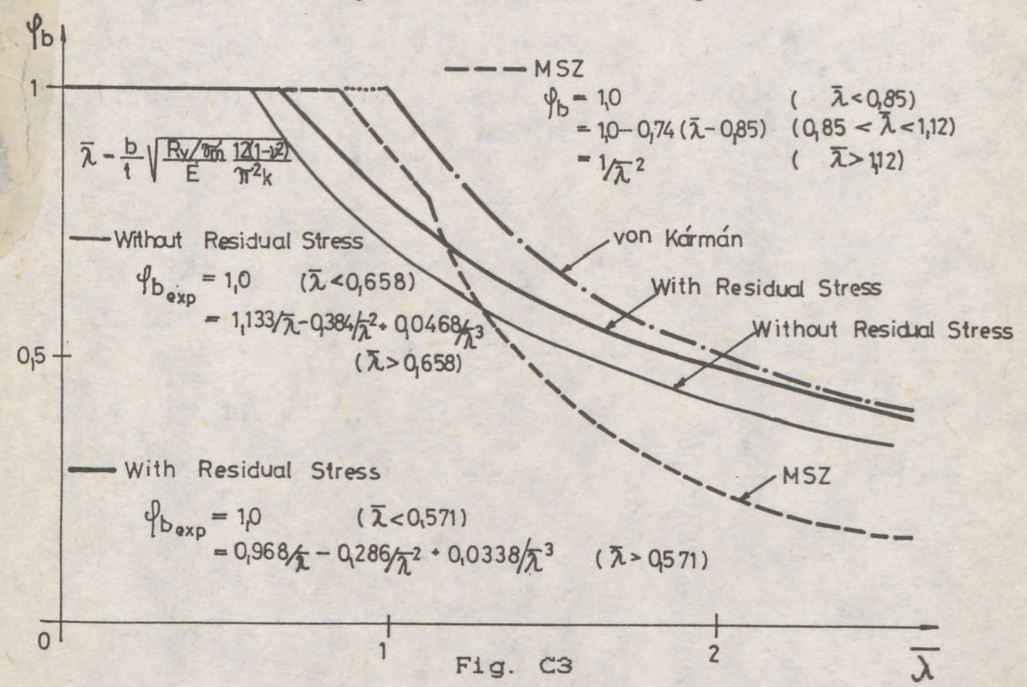

Fig. C3

Von Kármán's $\varphi_b = 1/\bar{\lambda}$ and Euler's $\varphi_b = 1/\bar{\lambda}^2$ are also given for reference in the figure.

FINAL REMARKS

Additionally analysis of structural response is growing more sophisticated: specifications have to incorporate an increasing number of design rules, sometimes in form of tables and diagrams (often derived directly from experiments), making specifications voluminous, the number of their appendices increasing.

Although we are in possession of all facilities to carry through any complicated calculations, it seems necessary to regard them mainly as a tool for research and to find a good balance between the real needs of a safe and economic everyday design praxis and the way of feeding back the accumulating information gained by research.

(13)

REFERENCES

BALDIN, V.A., GOLDENBLAT, V.M., KOCHENOV, V.M., PILDISH, M.I. and TALJ, K.E. (Ed. Keldish, V.M.) 1951.
Design of structures by the method of limit states (in Russian), Gosstrojizdat, Moscow-Leningrad

BOLOTIN, V.V., 1965.
Statistical methods in structural mechanics (in Russian), Izdat.Lit.Stroit., Moscow

BOLOTIN, V.V., 1972.
Reliability theory and stochastic stability. University of Waterloo, Study No.6. Stability. Ed. Leipholz, pp. 385-422.

BROUDE, B.M., 1953.
Limit states of steel girders (in Russian). Gossrojizdat, Moscow-Leningrad

CHOCIALOV, N.F., 1929.
Strength reserves (in Russian).
Strojitelnaja Promishlennost, No.10.

FUKUMOTO, Y. 1982.
Numerical data bank for the ultimate strength of steel structures. Der Stahlbau 1/1982. pp. 21-27.

FUKUMOTO, Y., ITOH, Y. 1983/a.
Evaluation of multiple column curves using the experimental data-base approach. J. of Constructional Steel Research Vol.3, No.3 , pp. 2-19.

FUKUMOTO, Y., ITOH, Y. 1983/b.
Evaluation of beam strength from the experimental data-base approach. Third International Colloquium, "Stability of Metal Structures" May 1983.,Canada, pp. 133-149.

FUKUMOTO, Y. 1984.
Experimental data base for stability of columns, beams and plates. "Verba volent, Scripta monent". Dedicated to Prof. Ch. Massonnet, Liege, Belgium, pp. 171-197.

GVOZDEV, A.A., 1949.
Ultimate load analysis of structures (in Russian). Gosstrojizdat, Moscow

HALÁSZ, O., 1979.
Philosophical background and safety concepts. "Stability of Steel Structures", Summary, Budapest

KORANYI, I., 1952.
New aspects in Hungarian codes for bridges (in Hungarian), MTI, Budapest

(1)
MENDERA, Zbigniew (1)

UNIFORM APPROACH TO METAL STRUCTURES STABILITY DESIGN

INTERNATIONAL COLLOQUIUM
STABILITY OF STEEL STRUCTURES
BUDAPEST, HUNGARY, 1990
PRELIMINARY REPORT

SUMMARY: Uniform approach to the buckling design of several metal structures has been proposed. The limit states method is prefered. Semi-empirical interaction formula of elastic and plastic load-carrying capacities has been used. Universal character of the derived limit strength formulas has been stressed, taking into consideration various forms of instability of bars, plates and shells. Design examples have been shown in a general form. Nomenclature and terms are conformable to the International Standards [ISO 3898, 1987 and ISO/DIS 8930, 1986].

1. INTRODUCTION

In order to compare and assess various approaches to providing a certain degree of design reliability of structures it is necessary to adopt a number of uniform assuptions and hypotheses which have sound theoretical bases and have been proved experimentally with satisfactory results. The aim is to reduce the comparison to a common denominator. Only then will it be possible to draw both qualitative and quantitative comparisons. It is not an easy task because of various safety factors, especially

(1) Professor of Civil Engineering, Cracow Technical University

(2)

when formulating stability conditions in which non-linear formulas appear and which cover both elastic and elastic-plastic instabilities.

In the elastic range critical load-carrying capacity N_{cr} depends on the geometry of structural element and elastic moduli of the material (E,v); in the plastic range plastic load-carrying capacity N_{pl} depends mainly on the cross-section characteristics and yield point of steel (f_y), while in the elastic-plastic range ultimate load-carrying capacity N_u depends on all these parameters combined in the interaction formula. Thus, these parameters should be determined at the same probability level (due to statistic character of mechanical properties of material, geometric conditions and load-effects). They may be central (mean) or extreme values, e.g. characteristic or design values. In the presented comparative analysis we shall consistently use design values in the sense of limit states method (method of devided safety factors). The essence of this approach is a comparison, in the condition of safety, of loads-effect design value with load-carrying capacity design value:

$$F_u \leq N_u \quad , \tag{1}$$

where:

$$F_u = \sum_i \gamma_{fi} \cdot G_{ki} + \sum_j \Psi_{oj} \cdot \gamma_{fj} \cdot Q_{kj} \quad ,$$

$$N_u = A \frac{f_y}{\gamma_m} \varphi = A \cdot f_d \cdot \varphi \quad ,$$

G_k - dead load and permanent actions-effect (characteristic v.)
Q_k - live load and variable actions-effect (characteristic v.),
γ_f - load factors (γ_f = 1,1 - 1,4) ,
Ψ_o - load combination coefficients (Ψ_o = 1,0 - 0,7) ,
A - geometric characteristics of cross-section ,
f_y - yield point of steel (characteristic value) ,
γ_m - material factor (γ_m = 1,1 - 1,25) ,
φ - factor of stability (buckling factor),

$f_d = \frac{f_y}{\gamma_m}$ - design strength of steel.

(3)

Characteristic values are determined at the probability level ca. 0,980 and design values at the probability level ca. 0.999 (assuming the existence of control systems).

2. INTERACTION FORMULA OF ELASTIC AND PLASTIC RESISTANCES FOR STRUCTURES UNDER COMPRESSION

The plastic load-carrying capacity (at the level of design value) of an element can be determined:

$$N_{pl} \equiv N_d = A.f_d \quad , . \tag{2}$$

The critical load-carrying capacity (at the level of design value) of a compressed element in elastic range can be generally presented in the form:

$$N_{cr} \equiv N_e = A.f^i_{cr}.k_\lambda = A.f_e = A\,\frac{c\,E}{\lambda^m} \leq A.f_d \quad , \tag{3}$$

where:

f^i_{cr} - elastic critical stress of an ideal structure (it is determined at the mean value level),

k_λ - parameter of imperfection sensitivity of the structure in the elastic range (partial factor of safety in the elastic range); for structures of lower imperfection sensitivity in pure elastic range $k_\lambda < 1$ and it is accepted as a constant; for structures of high imperfection sensitivity $k_\lambda = f(\lambda) \neq \text{const.}$

$f_e = f^i_{cr}.k_\lambda = \frac{c\,E}{\lambda^m}$ - elastic critical stress of an actual (real) structure (at the design value level),

E - modulus of elasticity (at the mean value level),

λ - an adequately defined slenderness ratio for a given form of structure instability,

m - exponent corresponding to the critical stress function power for an actual structure,

c - constant (or parametrically variable) factor corresponding to an adequate value in the function of critical stress (it includes the k_λ parameter on the whole or partially together with exponent m).

For $f_e = f_d$, i.e. $\frac{c\,E}{\lambda^m} = f_d$, the so-called transient slenderness can be determined:

$$\lambda_k = \left(\frac{c\,E}{f_d}\right)^{1/m} \quad , \tag{4}$$

(4)

Also, the so-called relative slenderness (slenderness parameter) can be defined:

$$\lambda = \frac{\lambda}{\lambda_k} = \left(\frac{f_d}{f_e}\right)^{1/m} \equiv \left(\frac{N_d}{N_e}\right)^{1/m} . \qquad (5)$$

In order to derive a uniform formula of limit load-cyrrying capacity N_u, valid for the whole elastic and elastic-plastic range, we shall use the nonlinear interaction Rankine-Merchant formula, theoretically generalized by Murzewski [Murzewski 1974, Allen 1978]. The structure load-carrying capacity is treated here as an alternative of two independent random events (of Weibull distribution function): plastic resistance and elastic critical resistance. This formula can also be interpreted as semi-empirical interaction formula of elastic and plastic load-carrying capacities, namely:

$$N_u^{-1/u} = N_d^{-1/u} + N_e^{-1/u} , \qquad (6)$$

in which:

$N_u = A\, f_d\, \varphi = A\, f_u$ -design load-carrying capacity of an element,

$N_d = A\, f_d$ - plastic load-carrying capacity,

$N_e = A\, f_e$ - elastic (critical) load-carrying capacity,

u - Weibull's generalized coefficient of variation, treated as empirical index of elastic-plastic (technological) imperfections ($u \equiv 1/n = 0{,}25 - 1{,}0$),

φ - factor of stability.

Substituting values (2) and (3) in formula (6) we obtain:

$$(A\, f_d\, \varphi)^{-1/u} = (A\, f_d)^{-1/u} + (A\, f_e)^{-1/u} ,$$

and after the reduction and using dependence (5) we finally obtain a dimensionless uniform formula [Mendera, 1988]:

$$\frac{N_u}{N_d} \equiv \frac{f_u}{f_d} = \varphi = \left[\, 1 + \left(\frac{f_d}{f_e}\right)^{1/u} \,\right]^{-u} = \left(1 + \lambda^{m/u} \right)^{-u} , \qquad (7)$$

in which λ and m are characteristic of the given form of instability and its quantitative evaluation in structural elements in the elastic range. The index u is an evaluation of the effect

(5)

of technological imperfections and their interaction character in the elastic-plastic range. It is therefore a general formula and profitable since important empirical information can be used with it.

These considerations and results are explained in Fig.1.

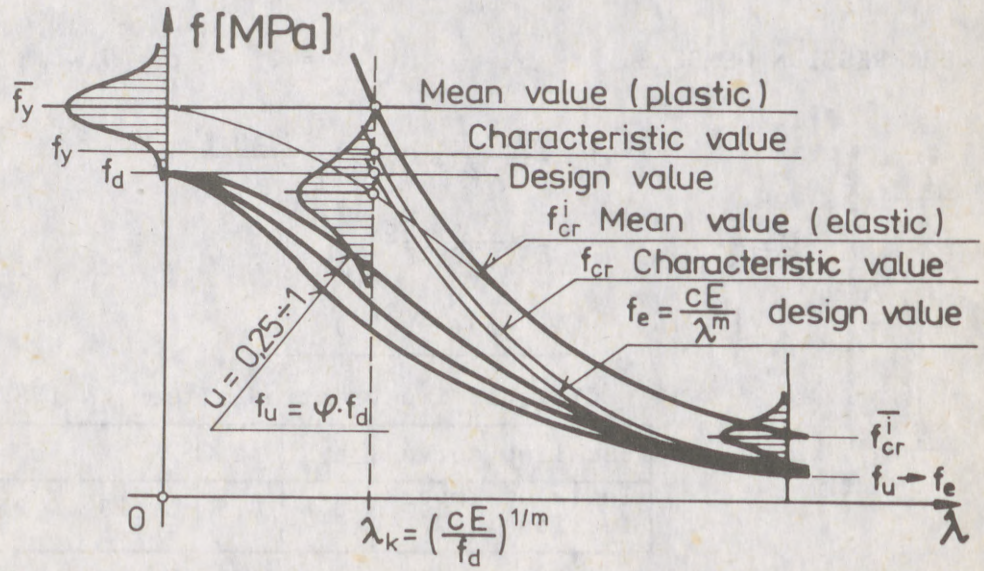

a) Dimensional way to present design strength f_u

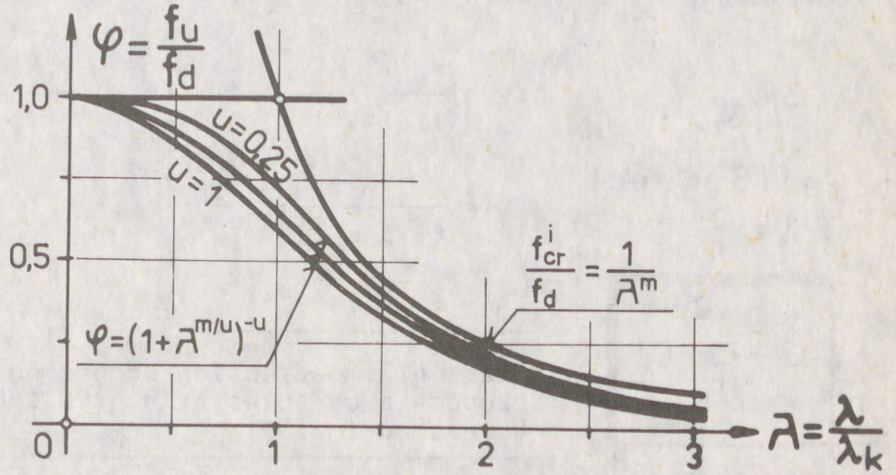

b) Nondimensional way to present factor of stability φ

Fig.1.

3. DESIGN EXAMPLES IN GENERAL FORM

$$\sigma(F_u) \le f_u = f_d \cdot \varphi \; ;$$

$$f_d = \frac{f_y}{\gamma_m} \; ; \qquad \varphi = (1 + \bar{\lambda}^{m/u})^{-u} \; ; \qquad \bar{\lambda} = \frac{\lambda}{\lambda_k} = \left(\frac{f_d}{f_e}\right)^{1/m} \; ;$$

$$f_e = f_{cr}^{i}\, k_\lambda = \frac{c\,E}{\lambda^m} \; ; \qquad \lambda_k = \left(\frac{c\,E}{f_d}\right)^{1/m} \; ;$$

3.1. COMPRESSION MEMBERS

$\lambda = \frac{l}{i}$; $m = 2$; $c = 7{,}40$;

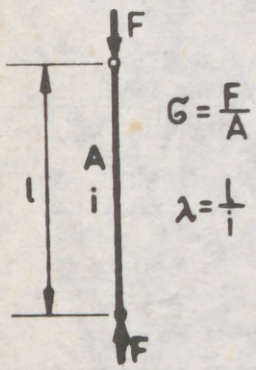

$$f_e = \frac{\pi^2 E}{\lambda^2} \cdot 0{,}75 = \frac{7{,}40\,E}{\lambda^2} \; ;$$

$$\bar{\lambda} = \frac{\lambda}{2{,}72} \left(\frac{f_d}{E}\right)^{1/2} \; ;$$

$$\varphi = (1 + \bar{\lambda}^{2/u})^{-u}$$

Class of imperfection after [PN 1989]

Buckling curve	a_o	a	b	c
Index of imperfection u	0,4	0,5	0,625	0,833

3.2. LOCAL BUCKLING OF PLATES

$\lambda = \frac{b}{t}$; $m = 2$; $c = 0{,}9\, k_c$;

$\sigma_1, \sigma_2,$

$k_c = f(\sigma, \alpha, e.c.)$

$\lambda = \frac{b}{t}$

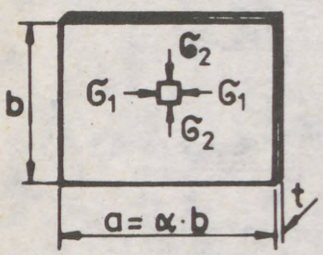

$$f_e = \frac{k_c \pi^2 E}{12(1-\nu^2)\,\lambda^2}(1{,}1 \cdot 0{,}9) = \frac{0{,}9\,k_c\,E}{\lambda^2} \; ;$$

$$\bar{\lambda} = \frac{\lambda}{0{,}95\,k_c^{1/2}} \left(\frac{f_d}{E}\right)^{1/2} \; ;$$

$$\varphi = (1 + \bar{\lambda}^{2/u})^{-u}$$

Class of imperfection according to new proposals by autor after [PN 1989 and Bornscheuer 1985]

Local buckling curve	a
Index of imperfection u	0,5

(7)

3.3. CYLINDRICAL SHELLS UNDER AXIAL COMPRESSION

$\lambda = \frac{r}{t}$;

$m = 3/2$; $c = 2$;

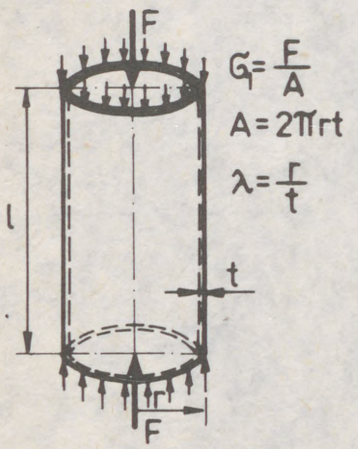

$\sigma = \frac{F}{A}$

$A = 2\pi rt$

$\lambda = \frac{r}{t}$

$$f_e = \frac{E}{[3(1-\nu^2)]^{1/2}.\lambda} \frac{3,3}{\lambda^{1/2}} = \frac{2\,E}{\lambda^{3/2}} ;$$

$$\bar{\lambda} \equiv \bar{\lambda}_1 = \frac{\lambda}{1,59} \left(\frac{f_d}{E}\right)^{2/3} ;$$

$$\varphi \equiv \varphi_1 = (1 + \bar{\lambda}_1^{3/2u})^{-u}$$

Class of imperfection after [Mendera a) 1986]

Buckling curve	a_o	a	b	c
Index u	0,25	0,50	0,75	1,00

3.4. CIRCULAR TUBES UNDER COMPRESSION

$\lambda = \frac{l}{i}$; $\lambda_1 = \frac{r}{t}$;

$$\frac{l}{r} > \sqrt{\frac{r}{t}}$$

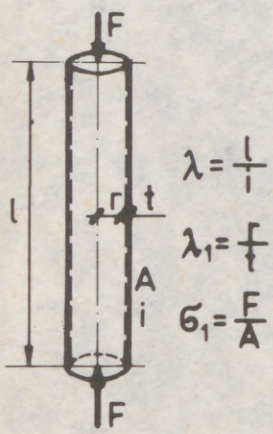

$\lambda = \frac{l}{i}$

$\lambda_1 = \frac{r}{t}$

$\sigma_1 = \frac{F}{A}$

$\bar{\lambda}$ - according to 3.1.

$\bar{\lambda}_1$ - according to 3.3.

Interaction formula after [Mendera 1989]

$$\varphi = (1 + \bar{\lambda}^{2/u} + \bar{\lambda}_1^{3/2u})^{-u}$$

Class of imperfection [as above]

Interaction buckling curve	a
Index of imperfection u	0,5

(8)

3.5. CYLINDRICAL SHELLS UNDER EXTERNAL PRESSURE $\lambda = \frac{r}{t}$;

After [SNIP 1982, ČSN 1978, DASt 013, 1980]

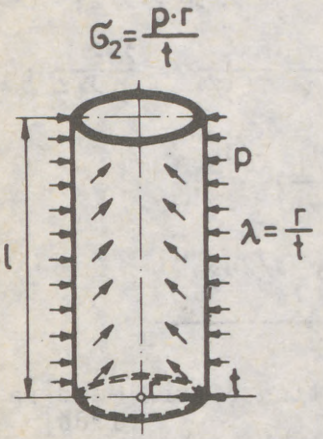

For $0{,}5 \le \frac{l}{r} \le 15$: $c = 0{,}55 \frac{r}{l}$; $m = 3/2$;

$$f_e = \frac{\pi \sqrt{6}\, r/l\, E}{9(1-\nu^2)^{3/4}\, \lambda^{3/2}}\, 0{,}6 = 0{,}55 \frac{r}{l} \frac{E}{\lambda^{3/2}} ;$$

$$\Lambda = \frac{\lambda}{0{,}67(\frac{r}{l})^{2/3}} \left(\frac{f_d}{E}\right)^{2/3} ;$$

$$\varphi \equiv \varphi_2 = (1 + \Lambda^{3/2u})^{-u}$$ Index $u = 0{,}5$

For $\frac{l}{r} > 20$: $c = 0{,}17$; $m = 2$;

$$f_e = \frac{E}{4(1-\nu^2)\, \lambda^2}\, 0{,}6 = \frac{0{,}17\, E}{\lambda^2} ;$$

$$\Lambda = \frac{\lambda}{0{,}41} \left(\frac{f_d}{E}\right)^{1/2} ;$$

$$\varphi \equiv \varphi_2 = (1 + \Lambda^{2/u})^{-u}$$ Index $u = 0{,}5$

3.6. CYLINDRICAL SHELLS UNDER TORSION $\lambda = \frac{r}{t}$;

After [Grigoliuk 1969]

For $10 \sqrt{\frac{t}{r}} \le \frac{l}{r} \le 3 \sqrt{\frac{r}{t}}$: $c = 0{,}5 \sqrt{\frac{r}{l}}$; $m = 5/4$

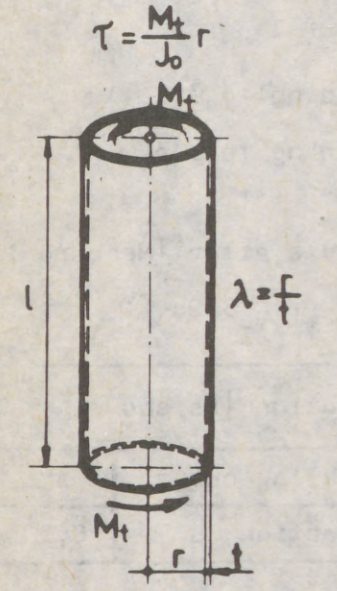

$$f_e = \frac{0{,}71(r/l)^{1/2}\, E}{(1-\nu^2)^{5/8}\, \lambda^{5/4}}\, 0{,}67 = 0{,}5 (\frac{r}{l})^{1/2} \frac{E}{\lambda^{5/4}} ;$$

$$\Lambda = \frac{\lambda}{0{,}57(\frac{r}{l})^{2/5}} \left(\frac{f_d}{\sqrt{3}\, E}\right)^{4/5} ;$$

$$\varphi \equiv \varphi_3 = (1 + \Lambda^{5/4u})^{-u}$$ Index $u = 0{,}5$

For $\frac{l}{r} > 3 \sqrt{\frac{r}{t}}$: $c = 0{,}17$; $m = 3/2$

$$f_e = \frac{E}{3\sqrt{2}(1-\nu^2)\, \lambda^{3/2}}\, 0{,}67 = \frac{0{,}17\, E}{\lambda^{3/2}} ;$$

$$\Lambda = \frac{\lambda}{0{,}31} \left(\frac{f_d}{\sqrt{3}\, E}\right)^{2/3} ;$$

$$\varphi \equiv \varphi_3 = (1 + \Lambda^{3/2u})^{-u}$$ Index $u = 0{,}5$

(9)

3.7. CYLINDRICAL SHELLS UNDER COMBINED STRESSES

After [DASt 013, 1980]

$$\left(\frac{\sigma_1}{f_d \cdot \varphi_1}\right)^{1,1} + \left(\frac{\sigma_2}{f_d \cdot \varphi_2}\right)^{1,1} + 3\left(\frac{\tau}{f_d \cdot \varphi_3}\right)^{2} \leq 1$$

φ_1 - according to 3.3.
φ_2 - according to 3.5.
φ_3 - according to 3.6.

3.8. SPHERICAL SHELLS UNDER EXTERNAL PRESSURE $\lambda = \frac{r}{t}$;

c = 0,6; m = 4/3

$$f_e = \frac{E}{[3(1-\nu^2)]^{1/2}\,\lambda}\,\frac{0,99}{\lambda^{1/3}} = \frac{0,6\,E}{\lambda^{4/3}} \quad ;$$

$$\Lambda = \frac{\lambda}{0,68}\left(\frac{f_d}{E}\right)^{3/4} \quad ;$$

$$\varphi = (1 + \Lambda^{4/3u})^{-u}$$

Class of imperfection after [Mendera b) 1986]

Buckling curve	a	b	c
Index u	0,333	0,667	1,000

CODES, SPECIFICATIONS AND STANDARDS

ISO 3898, 1987
Bases for design of structures - Notations - Generals symbols, International Standard, ISO 1987.

ISO/DIS 8930, 1986
General principles for reliability of structures - List of equivalent terms, International Standard (Draft), ISO 1986.

ČSN - 1978
Design of Steel Structures
Czechoslovakian State Standard, ČSN 73 1401, Prague 1978.

(10)

DASt 013, 1980

Beulsicherheitsnachweise für Schalen

Deutscher Ausschuss für Stahlbau, Richtlinie 013, Köln 1980.

PN - 1980

Steel Structures, Design Rules

Polish State Standard, PN-89/B-03200 (Draft 4), Warsaw 1989.

SNIP - 1981

Steel Structures, Design Rules

Soviet Union Standard, SNIP II-23-81, Moscow 1981.

REFERENCES

Allen, D. 1978
Merchant-Rankine Approach to Member Stability
Journal of Structural Division, ASCE Vol. 104, ST12.

Bornscheuer, B.-F. 1985
Stabilitätsnachweise für Platten und Schalen in gleicher Darstellung wie für Stäbe, Stahlbau 54, 1985, 12, 364-368.

Grigoliuk, E.J. and Kabanov, V.V. 1969
Stability of Circular Cylindrical Shells, Itogi Nauki, Moscow 1969.

Mendera, Z. a)1986
Interaction of Elastic and Plastic Instability in Cylindrical Shells with Imperfections, "SHELLS, MEMBRANES AND SPACE FRAMES", Editor Heiki, K., IASS Symposium, Osaka, 1986, Vol.1, pp.17-24.

Mendera, Z. b)1986
Interaction of Elastic and Plastic Instability in Thin-Walled Shells with Imperfections, "STEEL STRUCTURES", Editor Hajdin, N. and Sekulović, M., International Conference, Budva 1986, Part II pp. 581-590.

Mendera, Z. 1988
A Uniform Formula of Stability for Steel Structures, "STEEL STRUCTURES NOW AND IN THE FUTURE", 15th National Conference ČSVTS, Prague 1986, Part 2, pp. 13-16.

Mendera, Z. 1989
Load Carrying Capacity of Thin-Walled Tubular Structures, Proc. of Sci.-Techn. Conference KILIW PAN, Krynica 1989, Poland.

Murzewski, J. 1974
Random Analysis of Shells Carrying Capacity, Proc. of the Symposium on Shell Structures, Cracow 1974, Poland.

SESSION 2

COMPRESSION MEMBERS

(1)
BARSZCZ, Anna (1)
KARCZEWSKI, Jan A. (2)

ELASTIC-PLASTIC MODEL OF THE SPACE STRUCTURE'S MEMBER AXIALLY LOADED IN CYCLICALLY VARIABLE MANNER

INTERNATIONAL COLLOQUIUM
STABILITY OF STEEL STRUCTURES
BUDAPEST, HUNGARY, 1990
PRELIMINARY REPORT

Summary: The paper deal with the results of the experimental investigations of 23 specimens which were a members of a space structure. The length and the cross-sections area in the middle as well as in the ends of the investigated struts were diferentiated. The results of preliminary analysis were presented at previous Colloquium [3]. Here maximal values of an axial forces in compression and/or extension achieved in the following cycles of loading are examined with great care. The results of the theoretical considerations and experimental investigations were taken into account in modyfied mathematical model of the strut. In the model proposed the possibility of the plastic hinge forming in the middle of the strut as well as in the ends if they are connected with the nodes of restrained rotation is considered. To enable numerical analysis of the force-deformation function variability the computer program OPOS was worked out. The results of the computations are shown in the paper in the graphical shape.

---

(1) Lecturer Warsaw University of Technology
(2) Professor of Civil Engineering, Warsaw University of Technology

(2)

1. EXPERIMENTAL INVESTIGATIONS

The experimental arrangement description, goemetrical characteristic of the 13 from the 23 investigated specimens and obtained results are presented with full particulars in paper [3]. In the second stage of the investigations ten specimens were tested. There were two full-size struts of ring cross-sections ϕ 38x4 mm made with mild steel grade R35 - yield point stress and Young modulus evaluated with 95% probability σ_y= 245 MPa, E = 194975 MPa, and eigth full-size struts of ring cross-sections ϕ64x4 mm made with mild steel grade R45 - yield point stress and Young modulus σ_y= 341 MPa, E = 195434 MPa. The length all of them was 2000 mm.

The different ends restraint conditions were simulated by reduction of the ends cross-sections. The relation between moments of inertia of the cross-section in the middle of the specimen J_p and in the ends J_k was assumed 1, 5, 16 and 23.

During investigation above described specimens the deflections in the middle of the strut were taken additionally into account.

2. MAXIMUM VALUES OF THE AXIAL FORCES OBTAINED ON THE ANALYTICAL AND EXPERIMENTAL WAY

The maximum yielding force in extension for smallest cross-section of the strut were evaluated by formula

$$P_y = \sigma_y \cdot A$$

were

A - cross-sections area.

The critical force in the first cycle of loading was calculated as for strut with fixed ends. On the ground of experimental investigations results one assumed that residual strains which are occured after partially yielding of the cross-section in the first cycle of loading cause to reduction of the load carrying capacity. The critical force in second and following cycles of loading is evaluated like for strut with pin-jointed ends. In this case the Polish Cod of Practice's recomendations were adopted [5]

(3)

$$P_c = P_y/m_w$$

where

P_c - critical force,

m_w - factor of buckling.

$$m_w = \begin{cases} 1/[1 - 0,2\lambda' - 0,1(\lambda')^2 - 0,2(\lambda')^3 & \text{for } \lambda' \leqslant 1 \\ 2(\lambda')^2 & \text{for } \lambda' > 1 \end{cases},$$

$$\lambda' = \lambda/\lambda_p ,$$

λ - slenderness ratio,

$$\lambda_p = 2E_o/R ,$$

E_o - computational value of the Young modulus,

R - computational strength of the steel.

In comparative analysis of the computations and experiments results the characteristic values of σ_y, E were taken in the place of computational ones R, E_o.

The critical forces in first, second and third cycles of loading and maximum yielding forces for chosen struts obtained on the analitical and experimental way are compared in table 1. From second cycle of loading relation between critical forces in following cycles is described by coefficient η_3 shown in table 1.

3. MODIFIED COMPUTATIONAL MODEL OF THE STRUT

In order to attain more accura-te description of the strut's behaviour under cyclicaly variable loading the previously presented model [3] was modyfied. The modyfications refer in substance to first cycle of loading. The possibility of the punctual plastic hinge forming in the middle as well as in the ends of the strut is assumed. Behaviour of the strut as a member of a space structures can be described by function P(u) showing relationship between axial force P and displacement of the strut's ends in relation one to other u - see Fig. 1. In above mentioned function displacement u is composed with four integral parts

$$u = u^P + u^M + u^Y + u^R ,$$

where

(4)

Table 1

Cross-section		Length	Number of the strut	$\kappa = J_p/J_k$	COMPRESSION							EXTENSION		
					Critical force evaluated for end-restr. conditions	Experimental critical force						Theoretical yielding force	Experimental yielding force	
					fixed joined P_c^z	pin-jointed P_c^p	first cycle of loading P_c^1	second cycle of loading P_c^2	third cycle of loading P_c^3	$\eta_1 = P_c^1/P_c^z$	$\eta_2 = P_c^2/P_c^p$	$\eta_3 = P_c^3/P_c^z$	P_y	P_y^e	$\eta_4 = P_y^e/P_y$
	mm x mm	mm			kN	kN	kN	kN	kN				kN	kN	
ϕ 38 x 4	1	1500	1	1	-89,2	-53,5	- 68	- 38	- 42	0,76	0,71	1,10	104,7	114	1,09
			2				- 68	- 39	- 38	0,76	0,73	0,97		114	1,09
			3	5			- 70	- 35	- 34	0,78	0,65	0,97		123	1,17
			4	16			- 83	- 27	- 26	0,93	0,50	0,96	101,7	116	1,14
			5				- 82	- 29	- 29	0,92	0,54	1,00		-	-
			6	23			- 76	- 32	- 32	0,85	0,60	1,00	94,0	-	-
			7				- 77	- 29	- 29	0,86	0,54	1,00		-	-
		2000	8	1	-80,3	-30,1	- 59	- 30	- -	0,73	1,00	-	104,7	107	1,02
			9				- 69	- 31	- 30	0,86	1,03	0,97		112	1,07
			10	5			- 74	- 27	- 27	0,92	0,90	1,00		117	1,12
			11				- 72	- 30	- 31	0,90	1,00	1,03		113	1,08
			12	16			- 61	- 24	- 19	0,76	0,80	0,79	101,7	110	1,08
			13				- 67	- 28	- 27	0,83	0,93	0,96		128	1,26
			14	23			- 58	- 18	- -	0,72	0,60	-	94,0	108	1,15
			15				- 72	- 24	- 21	0,90	0,80	0,88		115	1,22
ϕ 60 x 4	1		16	1	-206,8	-132,2	-189	- 80	- 77	0,91	0,61	0,96	240,0	-	-
			17				-180	- 66	- -	0,87	0,50	-		-	-
			18	5			-163	- 91	- 84	0,79	0,69	0,92		-	-
			19				-170	- 89	- 82	0,82	0,67	0,92		-	-
			20	16			-157	- 50	- 47	0,76	0,38	0,94	182,3	-	-
			21				-140	- 72	- 68	0,68	0,54	0,94		-	-
			22	23			-187	- 56	- 52	0,90	0,42	0,93	148,6	-	-
			23				-191	- 54	- 52	0,92	0,41	0,96		-	-

(5).

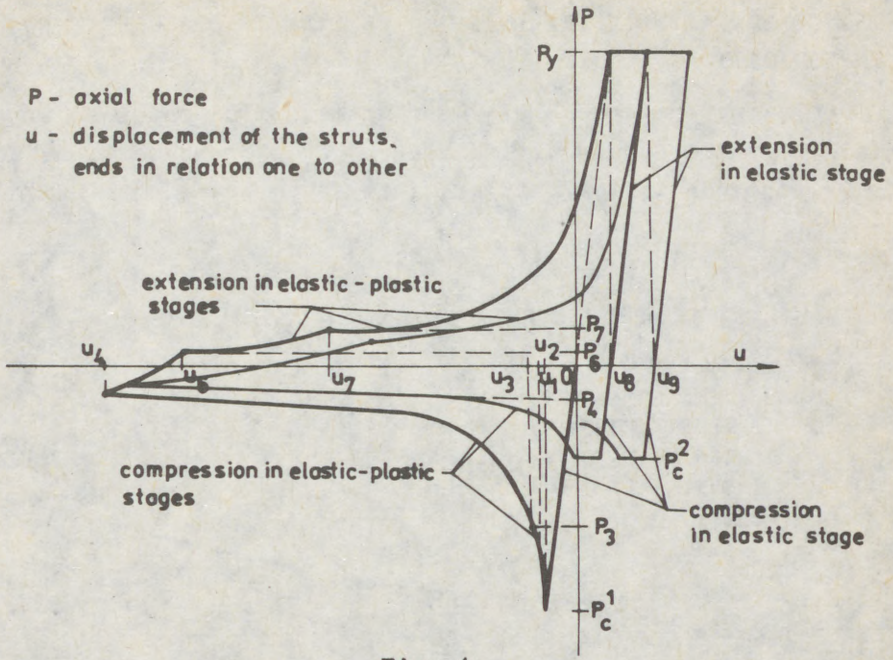

Fig. 1

$u^P = Pl/EA$ - displacement resulting with elastic deformations distributed along the length of the strut produced by axial force.

$u^M = \Phi(P,E,J,l,M_k,C)$ - displacement resulting with variability of the strut's geometry during elastic-plastic buckling. This function is continuous with different shape in compression and extension [2]. The stables of inte - grate C and moment in the end of strut M_k are evaluated indyvidually for every stages of the strut's behaviour after lost of stability.

$u^P = \int \dot{\Theta} \cdot M'(P)\, dt$ - displacement resulting with plastic axial deformation in plastic hinges during plastic rotation.

$\dot{\Theta}$ - velocity of the plastic rotation,

$M(P)$ - plastic conditions for cross-sections loading by axial force and bending moment.

u^R - displacement resulting with plastic deformation produced during extension where $P = P_y$.

(6)

4. THE CONFORMABILITY ANALYSIS OF THE EXPERIMENTAL AND THEORETICAL INVESTIGATIONS RESULTS

Comparing the graphs of the functions P(u) obtained experimentally for the struts with different ends cross-sections only -Fig. 2, one can notice that critical forces have nearing values.

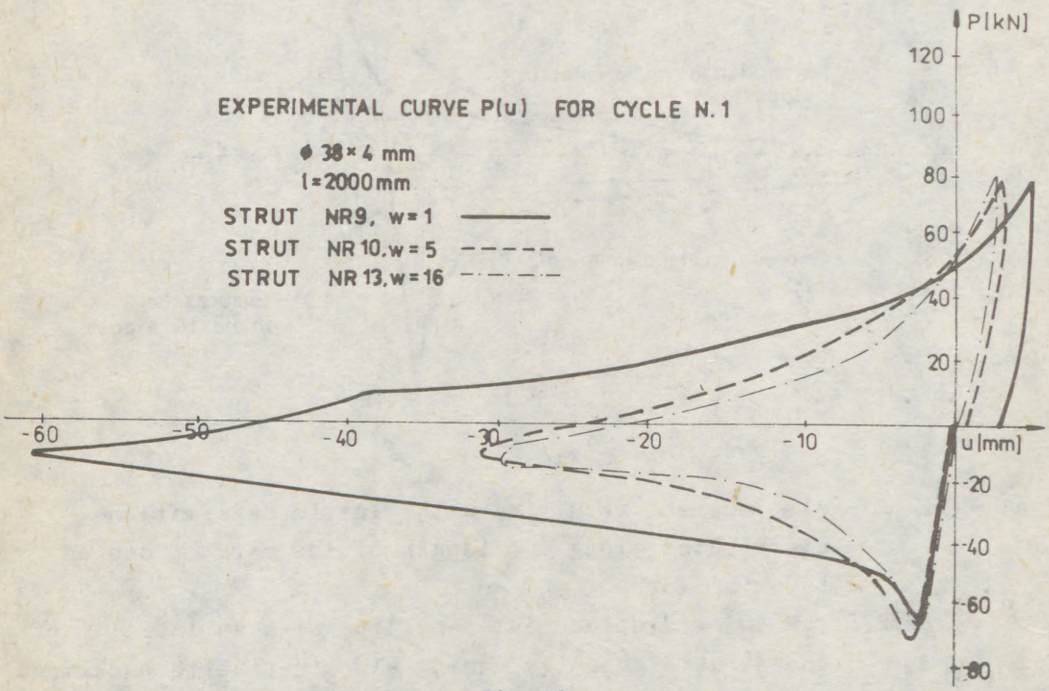

Fig. 2

The shapes of the function investigated are similar also. The same resulting with theoretical formulas - Fig. 3.

The curves P(u) obtained experimentally in second cycle of loading occured different for different ends cross-sections-Fig.4. Disagreements are enough small to omit they in the computational model of the strut.

For two described cycles of loading the value of the critical force were evaluated with taking into account average values of the ratio η computed on the ground of the experimental investigations results presented here - Tabl. 1.

The theoretical functions shown in figure were ploted auto-

(7)

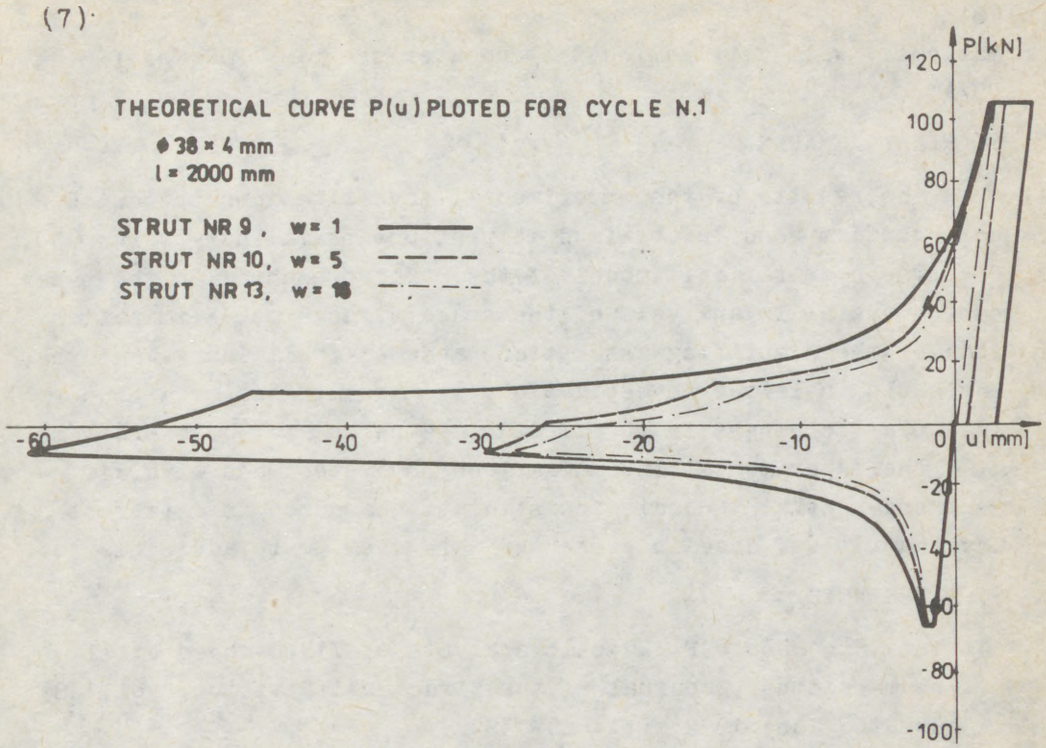
THEORETICAL CURVE P(u) PLOTED FOR CYCLE N.1
ϕ 38 × 4 mm
l = 2000 mm
STRUT NR 9 , w= 1
STRUT NR 10, w= 5
STRUT NR 13, w= 16
P[kN]
120
100
80
60
40
20
-20
-40
-60
-80
-100
-60
-50
-40
-30
-20
-10
0
u[mm]

Fig. 3

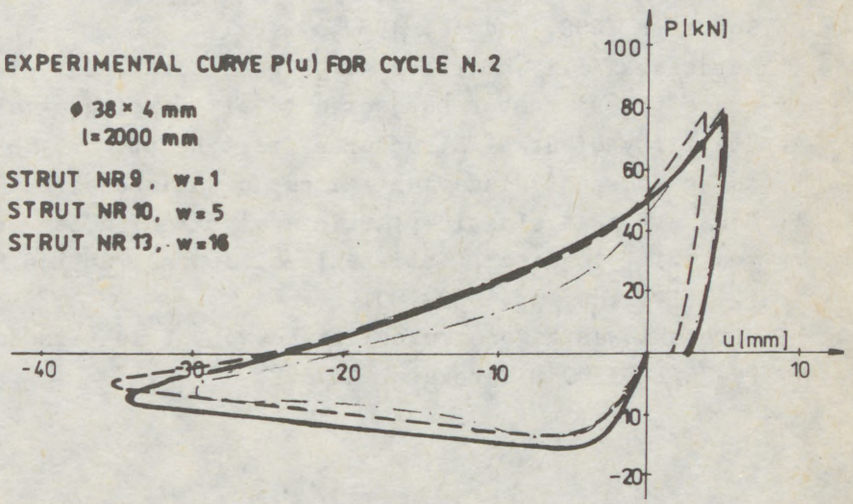
EXPERIMENTAL CURVE P(u) FOR CYCLE N. 2
ϕ 38 × 4 mm
l = 2000 mm
STRUT NR 9 , w = 1
STRUT NR 10, w = 5
STRUT NR 13, w = 16
P[kN]
100
80
60
40
20
-20
-40
-30
-20
-10
10
u[mm]

Fig. 4

(8)

matically with utilization the computer program OPOS for IBM PC/AT

5. FINAL REMARKS

The results of the experimental investigations presented here confirm results obtained in previous preliminary works [3].

The computational model of the strut presented in the paper can be useful in analysis of the space structures. Elimination some of the simplifing assumptions assumed preliminary would be advisable in leiter investigation. The assumptions about punctual plastic hinges in the first place belong to these problems.

The experimental investigations some specimens with different end-restraint conditions simulating assumed in different way that it was done in presented work seem to be advisable too.

6. REFERENCES

1. Toma S., Chen W.F.:„Cyclic analysis of fixed-ended steel beam-columns", Journal of the Structural Division, vol.108, nr ST6, June 1982, pp.1385-1399.
2. Karczewski J.A., Barszcz A.:„Behaviour of the space structures member subjected to cyclically variable loading", Congress IASS, Madrid, 1989.
3. Karczewski J.A., Barszcz A.:„Postcritical analysis of the space truss' member subjected to alternating axial loading", Stability of Steel Structures, part B, pp. 557-563, Publishing House of Hungarian Academy of Sciences, Budapest, 1988.
4. Nonaka T.:„An elastic-plastic analysis of a bar under repeated axial loading", International Journal Solids Structures, 1973, vol. 9, pp. 569-580.
5. „Projektowanie konstrukcji stalowych. Komentarz do normy PN-76/B-03200", Warszawa, 1976.

(1)

BJORHOVDE, Reidar[1]

THE STRENGTH OF HEAVY COLUMNS

INTERNATIONAL COLLOQUIUM
STABILITY OF STEEL STRUCTURES
BUDAPEST, HUNGARY, 1990
PRELIMINARY REPORT

Summary: The paper presents the results of a study on the maximum strength and behavior of wide-flange steel columns of large cross-sectional dimensions. Thus, hot-rolled and welded built-up shapes of flange thickness up to 150 mm and web thickness up to 75 mm were examined, using a variety of steel grades and manufacturing methods. It was found that there is a clear correlation between the relative maximum strength and the flange thickness for heavy hot-rolled wide-flange shapes. Specifically, the capacity drops by as much as 10 to 15 percent as the flange thickness goes from 25 to about 75 mm. As the thickness increases further, the relative maximum strength goes up, and it has regained its full value when the flange is 125 to 150 mm thick. The effect is a function of the slenderness ratio of the column; it is most pronounced in the intermediate range. Welded built-up shapes appear to be less heavily influenced by the flange thickness variation, especially for short and long members. However, the welded shape data base was limited, and further studies need to be conducted to verify the findings for these shapes. The results are currently being evaluated for design code recommendations.

INTRODUCTION

Although heavy steel shapes are commonly used in structures such as high-rise buildings and off-shore structures, relatively little

---

[1]Professor and Chairman, Department of Civil Engineering, University of Pittsburgh, Pittsburgh, Pennsylvania, U.S.A.

factual information is available on their strength and behavior. However, such columns are designed in the same way as those of small and medium size. The primary problem with this procedure is that the residual stresses and material properties of large thickness steel shapes and plates can be significantly different from those of smaller elements. It is therefore not clear whether the current design criteria can actually be applied for the design of such members.

The assumptions that sometimes have been used, namely, that columns are perfectly straight, made from isotropic and homogeneous materials, and free from any internal stresses, are convenient for limited theoretical analyses; they do not reflect actual member or material characteristics. Real elements display a variety of geometric and other imperfections, such as residual stress, variation of the yield stress, and initial crookedness, just to mention three of the primary parameters of the maximum strength. It is well established that these have a significant effect on the strength of such members (Galambos, 1988; Beer and Schulz, 1970; Bjorhovde, 1972; Bjorhovde, 1988).

The process of cooling of the steel, after hot-rolling, welding, or flame-cutting, is greatly influenced by the amount of material in the heat-sink. The size of the cross section and its elements therefore plays a major role in the formation of the residual stresses, as well as in the variability of the material strength. Studies have shown that the maximum compressive residual stress, for example, can be as high as 200 MPa in heavy shapes and plates, and the yield stress may vary by plus or minus 10 to 20 percent from the nominal, specified minimum value (Tall and Alpsten, 1969; Alpsten, 1968; Alpsten and Tall, 1970; Brozzetti et al., 1970; Bjorhovde et al., 1972). Further, the effects appear to be very different in rolled and welded shapes (Alpsten and Tall, 1970; Bjorhovde et al., 1972). The latter has important implications for the use of the largest of shapes that are commonly used in steel-framed structures.

The study that is detailed in this paper was undertaken to establish the characteristics of strength and stability of heavy rolled and welded built-up shapes, of the types that are used in steel construction today. Recognizing that physical testing would not be practicable, mostly because of the costs associated with such experiments, it was decided to base the evaluation on currently available data from tests and theoretical studies. The data base was expanded by making use of the knowledge that residual stresses, in particular, are not significantly influenced by the yield stress of the steel.

THE USE OF HEAVY COLUMNS

Heavy steel columns are used extensively in steel-frames for high-

(3)

rise buildings and industrial structures, and occasionally for larger bridge superstructures. The most common section is the rolled wide-flange (W-shape), but welded built-up H-sections and box shapes are also utilized, along with a large variety of other forms (Bjorhovde and Tall, 1970; Blodgett, 1978).

In the North American market, W-shapes are rolled in sizes with flange thickness up 125 mm, and welded section component plate thicknesses up to 200 mm are commonly found in a number of prominent structures (some examples are the World Trade Center, New York City; the Sears Tower and the John Hancock Building, Chicago; and the Toronto Dominion Tower and the Royal Bank Building in Toronto). In the Europe, traditional shape sizes have been limited in flange thickness to approximately 80 mm (Aschendorff et al., 1983), although this is currently changing, as the mills are examining the prospects for an increased share of the world construction market.

On the basis of the needs of the construction industry, therefore, it is evident that detailed data on the behavior and strength of heavy columns are much needed.

COLUMN STRENGTH MODEL

Several column strength models have been developed over the years, but the state of the art reflects the need to incorporate all of the major parameters of influence. Thus, it was decided to base the study on the maximum strength theory (Bjorhovde, 1972; Galambos, 1988). This approach considers the residual stresses and the initial out-of-straightness, and the model that was used also had the facility of accounting for the variation of the yield stress throughout the shape. Numerous studies have shown that the maximum strength model gives excellent correlation with full-size tests (Bjorhovde, 1972; Tebedge et al., 1972).

It is known that the maximum strength theory does not yield a closed-form solution for the capacity of the column. Rather, a computer solution is needed to give the capacity through an incremental, iterative procedure, while reflecting the variability of the various factors of influence. This approach was used in all of the studies that are the bases of the limit states design criteria for steel structures around the world today. The solutions for the heavy columns would therefore be transferable into the appropriate codes with the least amount of additional data evaluation.

A detailed presentation of the maximum strength model will not be presented in this paper. The principles are well known, and numerous applications have been given in the literature (Beer and Schulz, 1970; Bjorhovde, 1972; Galambos, 1988).

(4)

HEAVY COLUMN STRENGTH INVESTIGATION

The most important size data for the column shapes that were used in the investigation are summarized in Table 1. These shapes had all been the subject of detailed residual stress and material property tests (Bjorhovde, 1972; Brozzetti et al., 1970; Alpsten, 1968; Alpsten and Tall, 1970; Bjorhovde et al, 1972; Aschendorff et al., 1983). In addition, due to the insignificant effect of yield stress on the magnitude and distribution of the residual stresses, it was decided to expand the data base by using the same residual stress results for identical shapes in all of the common structural steel grades. Thus, steels with yield stresses of 175, 250, 350, and 700 MPa were used.

The strength data were developed for out-of-straightness values of L/500, L/1000, L/1500, and L/2000. The value of L/1000 was used in the development of the column strength criteria for the European (Beer and Schulz, 1970) and the Canadian (Bjorhovde, 1972; CSA, 1989) column curves; the value of L/1500, which is the approximate mean value, formed the basis for the American LRFD column design criteria (Bjorhovde, 1972; AISC, 1986).

TABLE 1: HEAVY COLUMN DATA

Shape Designation	Rolled or Welded	Flange Thk. (mm)
W 12x120 (US)	Rolled	28
HD 260x274 (Eur)	Rolled	50
W 14x426 (US)	Rolled	77
HD 400x685 (Eur)	Rolled	80
W 14x730 (US)	Rolled	125
H 12x210 (US)	Welded	51
H 14x15 (US)	Welded	60
H 20x354 (US)	Welded	51
H 24x428 (US)	Welded	51
H 24x1122 (US)	Welded	152

With 4 steel grades, as indicated above, a total of 40 complete column curves were developed. Although this is still a data base of limited magnitude, the results were consistent for the rolled shapes; they were not conclusive for the welded shapes. The reason for the latter finding is the relatively narrow range of sizes that were available for these types, and further study is therefore warranted for shapes of this type.

(5)

COLUMN STRENGTH RESULTS

Table 1 indicates the geometric shape parameter that was eventually found to be the most characteristic for the strength of the heavy columns. Thus, the influence on the results of various geometric parameters was evaluated, as follows: the flange and web thickness; the width-to-thickness ratio for the flange; the area of the flange; the ratio of the flange area to the web area; and the plate factor, given by $2(b + t)/bt$, which is a measure of the rate of cooling after rolling (Bjorhovde et al., 1972). In the preceding, b is the flange width and t is the flange thickness. It was determined that the flange thickness was the single most representative measure, and the final evaluations were therefore presented in this fashion.

As a sample of the results of the investigation, Figures 1 and 2 illustrate the relationship between the relative maximum column strength, given by the expression P_{max}/P_y, where P_y is the yield load, for buckling about the major and minor axes of the shape, and the flange thickness of hot-rolled shapes. The data also demonstrate the influence of the slenderness ratio of the column, using the common slenderness term. Finally, the curves represent the data for columns with an initial out-of-straightness of L/1500; this was used in recognition of the basis of the AISC LRFD Specification (AISC, 1986).

Similar results were developed for all of the major column strength parameters that were evaluated. In view of the limited space of the paper, only a sampling of the data is given. Briefly, given that residual stress and initial crookedness are the most important column strength factors, the data illustrate the variations that will occur for a given column as a function of the flange thickness only.

Some very important conclusions for hot-rolled shapes can be drawn on the basis of the results that are shown in Figs. 1 and 2. Thus, buckling about both major axes appears to be equally affected. Further, as would be expected, the strength of very short columns (curves for slenderness of 0.4) is very little influenced by the thickness variation. This observation also appears to apply to long columns (slenderness of 1.2).

The most important information is reflected by the middle curves of Figs. 1 and 2. These represent the variation of the strength of columns of intermediate slenderness, and thus the major share of all columns in structures. For minor axis buckling in particular, there is a drop in column strength of about 15 percent as the flange thickness increases from 25 to approximately 75 mm. Further, following this reduction of the column strength, the capacity then increases as the flange thickness continues to go up. The reason for this is that shapes with such large flange thickness

(6)

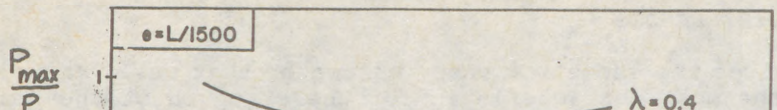

Fig. 1 Influence of Flange Thickness on Major Axis Maximum Strength for Hot-Rolled Wide Flange Shapes

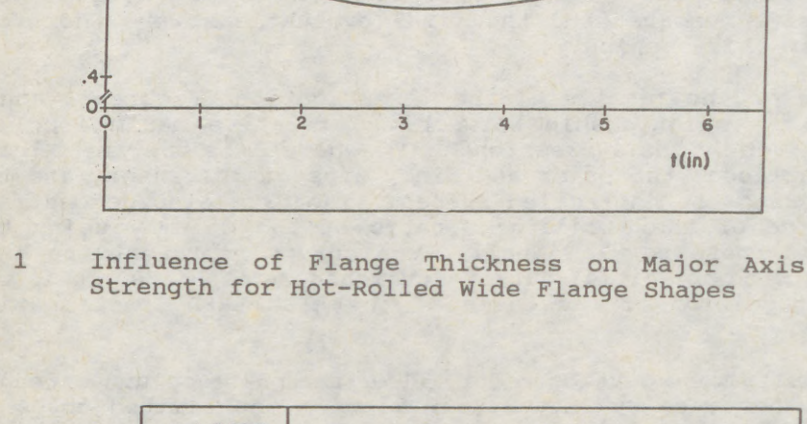

Fig. 2 Influence of Flange Thickness on Minor Axis Maximum Strength of Hot-Rolled Wide-Flange Shapes

(7)

also have a large cross-sectional area, and the strength decrease that is caused by the flange effect is offset by the amount of steel in the shape.

The results for the welded shapes are not presented in this paper. As already noted, these were not consistent as far as the various geometric parameters were concerned, and further study is needed. However, it is also reasonable to observe that differences in the method of manufacture between rolled and welded shapes, as well as the more favorable residual stress distributions in built-up sections are likely to be the cause of the differences. Thus, effects of flame cutting, for example, are significant.

SUMMARY AND CONCLUSIONS

The paper has presented a study of the maximum strength of heavy rolled and welded built-up steel columns. It is shown that the capacity of rolled shapes on the average decreases by about 15 percent as the flange thickness increases from 25 to 75 mm. Thereafter the strength is gradually regained, reaching its original value for thicknesses of about 150 mm.

The results are not conclusive for welded shapes at this time. This is attributed to the narrower range of shape sizes of the data base of the study. However, it is also noted that many of the fabrication operations for such members may tend to override the negative thickness influence.

REFERENCES

American Institute of Steel Construction (AISC) - 1986. "Specification for Load and Resistance Factor Design, Fabrication and Erection of Structural Steel for Buildings", AISC, Chicago, Illinois.

Alpsten, G. A. - 1968. "Thermal Residual Stresses in Hot-Rolled Steel Members". Fritz Engineering Laboratory Report No. 337.3, Lehigh University, Bethlehem, Pennsylvania.

Alpsten, G. A., and Tall, L. - 1970. "Residual Stresses in Heavy Welded Shapes". AWS Welding Journal, Vol. 49, No. 3, March, 1970.

Aschendorff, K. K., Bernard, A., Bucak, O., Mang, F., and Plumier, A. - 1983. "Knickuntersuchungen an Gewalzten Stutzen mit I-Querschnitt aus St 37 und St 52 mit Grosser Flanschdicke und aus St E 460 mit Standardabmessungen". Der Bauingenieur, Vol. 58 (pp. 261-268).

Beer, H., and Schulz, G. - 1970. "Bases Theoriques des Courbes Europeennes de Flambement". Construction Metallique, No. 3.

(8)

Bjorhovde, R., and Tall, L. - 1970. "Survey of Utilization and Manufacture of Heavy Columns". Fritz Engineering Laboratory Report No. 337.7, Lehigh University, Bethlehem, Pennsylvania.

Bjorhovde, R. - 1972. "Deterministic and Probabilistic Approaches to the Strength of Steel Columns". Ph.D. Dissertation, Lehigh University, Bethlehem, Pennsylvania.

Bjorhovde, R., Brozzetti, J., Alpsten, G. A., and Tall, L. - 1972. "Residual Stresses in Thick Welded Plates". AWS Welding Journal, Vol. 51, No. 8 (pp.392-406).

Bjorhovde, R. - 1988. "Columns: From Theory to Practice". AISC Engineering Journal, Vol. 25, No. 1 (pp. 21-34).

Blodgett, O. W. - 1978. "Usage of Heavy Columns in Structures". AWS Welding Journal, Vol. 57, No. 5.

Brozzetti, J., Alpsten, G. A., and Tall, L. - 1970. "Residual Stresses in a Heavy Rolled Shape W14x730". Fritz Engineering Laboratory Report No. 337.10, Lehigh University, Bethlehem, Pennsylvania.

Canadian Standards Association (CSA) - 1989. "Steel Structures for Buildings - Limit States Design". CSA, Rexdale, Ontario, Canada.

Galambos, T. V. - 1988. "Guide to Stability Design Criteria for Metal Structures". Wiley-Interscience, New York, New York.

Tall, L., and Alpsten, G. A. - 1969. "On the Scatter in Yield Strength and Residual Stresses in Steel Members". IABSE Symposium on Concepts of Safety of Structures and Methods of Design, London, England.

Tebedge, N., Chen, W. F., and Tall, L. - 1972. "On the Behavior of a Heavy Steel Column". Fritz Engineering Laboratory Report No. 337.33, Lehigh University, Bethlehem, Pennsylvania.

(1)
CARABA, Ioan (1)
DRUZENCO, Valentin (2)

THEORETICAL STUDIES UPON THE COMPRESSION STABILITY OF THE STANDARD BAR

INTERNATIONAL COLLOQUIUM
STABILITY OF STEEL STRUCTURES
BUDAPEST, HUNGARY, 1990
PRELIMINARY REPORT

Summary: Accepting the sine curve for the deformation of the standard bar of length "l" the "N" denominator of the relation $P = EI/N$ is studied with a numerical integration method when the bar deflection covers the interval $(0, 1/2)$, where P is the force which acts on the standard bar at the limit between the stable and unstable equilibrium, while E and I have known significances.

Thus I_{nec} and A_{nec} are determined in order that the bar would be on stable equilibrium under the force P.

The paper is finished with important conclusions for the design of bars, which are subjected to centric compression.

§ 1. Numerical integration method [1]. Let a function $F:A \longrightarrow R_+^*$, $A = [0,1] \subset R$, the ensembles $A_1 \subset A$, $A_2 \subset A$, $A_1 = \{\alpha_i\}$, $i = \overline{1,p}$, $A_2 = \{\beta_j\}$, $j = \overline{1,q}$ and the polynomial functions P_p, Q_q of the "p" degree, respectively of the "q" degree, where p and q are two natural numbers.

Proposition 1 . If the following conditions are accomplished:

C1) the function F is indefinite derivative

C2) $$\frac{1}{q} \sum_{j=1}^{j=q} F(\beta_j) > \frac{1}{p} \sum_{i=1}^{i=p} F(\alpha_i)$$

---

(1) Associate Professor, dr.eng. "Traian Vuia" Polytechnic Institute, Timişoara
(2) Eng., "Traian Vuia" Polytechnic Institute, Timişoara

(2)

C3) $$\frac{\frac{1}{q}\sum_{j=1}^{j=q} F(\beta_j) - \frac{1}{p}\sum_{i=1}^{i=p} F(\alpha_i)}{\frac{1}{q}\sum_{i=1}^{j=q} F(\beta_j)} = \varepsilon$$

C4) $$\int_0^1 P_p(x) = \frac{1}{p}\sum_{i=1}^{i=p} P_p(\alpha_i); \quad \int_0^1 Q_q(x) = \frac{1}{q}\sum_{j=1}^{j=q} Q_q(\beta_j)$$

C5) $A \subset D$, where D is the convergence domain of the Taylor's Series, then the following affirmations are correct:

a1) there are two numbers δ_1, δ_2 so that:

$$\int_0^1 F(x)dx - \frac{1}{p}\sum_{i=1}^{i=p} F(\alpha_i) < \delta_1; \quad \int_0^1 F(x)dx - \frac{1}{q}\sum_{j=1}^{j=p} F(\beta_j) < \delta_2$$

a2) $|e_\alpha| < 2\varepsilon$, $\quad |e_\beta| < \frac{\varepsilon}{1-\varepsilon}$, where

$$e_\alpha = \frac{\int_0^1 F(x)dx - \frac{1}{p}\sum_{i=1}^{i=p} F(\alpha_i)}{\int_0^1 F(x)dx};$$

$$e_\beta = \frac{\int_0^1 F(x)dx - \frac{1}{q}\sum_{j=1}^{j=q} F(\beta_j)}{\int_0^1 F(x)dx}$$

Remark upon C3). For $p = 3$ and $q = 4$ the ensembles:

$$A_1 = \{\alpha_i\}_{i=\overline{1,3}} = \{0{,}1464466 \cdot 1;\ 0{,}5 \cdot 1;\ 0{,}8535534 \cdot 1\}$$

$$A_2 = \{\beta_j\}_{j=\overline{1,4}} = \{0{,}1026739 \cdot 1;\ 0{,}4061987 \cdot 1;\ 0{,}5938013 \cdot 1;\ 0{,}8973261 \cdot 1\}$$

verify the third condition of the proposition.

The arrays of the nodes $\{\alpha_i\}$, $\{\beta_j\}$ are constant and they don't depend on the function F.

In this paper we consider:

(3)

$$\int_0^a F(x)dx = (a:4).(F(0,1026739a) + F(0,4061987a) + F(0,5938013a) + F(0,8973261a))$$

§ 2. Theoretical studies upon the standard bar. Let us consider the bar of figure 1.a and the initial conditions, i_k, $k = \overline{1,5}$, for investigations.

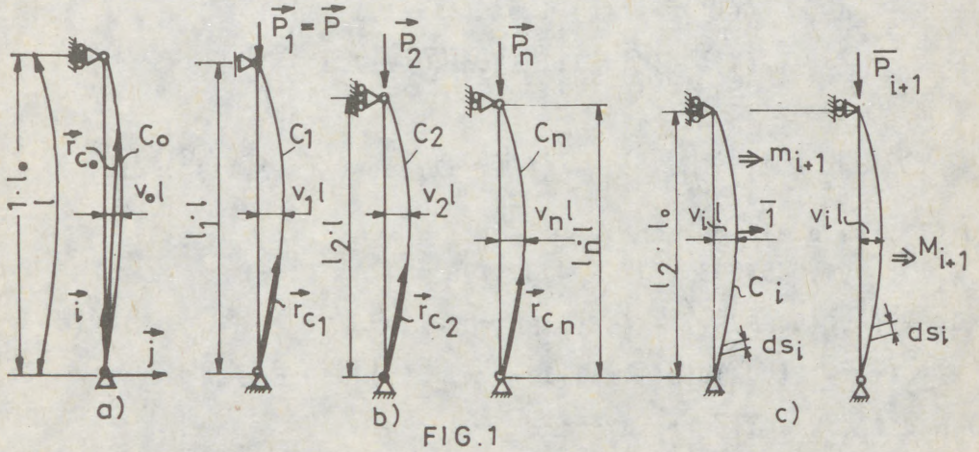

i1) The initial length of the bar is "l" and the longitudinal axis of the bar is represented by the curve (C_o) within vectorial form

$\vec{r}_{C_o} = x\vec{i} + v_o l \sin \frac{\pi x}{l_o} \vec{j}$, where "$v_o$" is the initial imperfection appraised to 1:1000.

i2) The bar is centrically compressed in stages under the forces $\vec{P}_1$ (in stage 1), $\vec{P}_2$ (in stage 2),..., $\vec{P}_n$ (in stage n); $\vec{P}_i = i.\vec{P}$; $P.\ l_i^2 : EI \cong 1$, for any "i".

In the stage "i" the longitudinal axis of the bar is represented by the curve (C_i) within vectorial form:

$$\vec{r}_{C_i} = x\vec{i} + v_i l \sin \frac{\pi x}{l_i} \vec{j} \quad \text{(figure 1.b)}$$

i3). We accept the calculation of the deflection $v_{i+1}{}^1$ with formula: $v_{i+1}{}^1 = \oint_{C_i} M_{i+1} m_{i+1} ds_i + v_i{}^1$, where M_{i+1}, m_{i+1} are the diagrams of the moments of flexure under the force $\vec{P}_{i+1}$, $\vec{1}$ (figure 1.c) and ds_i is the element of arc.

i4). Under deformations, it is accepted $\oint_{C_i} ds_i = 1$,

(4)

$i = \overline{o,n}$, with out consider the axial contraction.

i5). "n" is the integer solution of equation

$$l_n.l_o = l_o - nPl_o:EA = (1 - R:E).l_o ,$$

where R is the calculus resistance and $l_i.1$ is the chord of the sine curve. In the stage "n" the bar is at the limit between the stable and instable equilibrium. We consider $l_o \cong 1$.

The calculus of deflection $v_{i+1}l$.

$$ds_i = ((x')^2 + ((v_i l \sin(\pi x:l_i l))')^2)^{1/2} =$$

$$= (1 + ((\pi v_i l:l_i l)\cos(\pi x:l_i l))^2)^{1/2}$$

Of

$$\oint_{C_i} ds_i = 1, \quad \int_o^{l_i l} (1 + ((\pi v_i:l_i)\cos(\pi x:l_i l))^2)^{1/2} dx ,$$

and (1), we shall obtain:

$$l_i^2 l^2 = (4,0454283\ v_i^4 l^4 - 4,855198\ v_i^2 l^4 + l^4):l^2$$

$$l_i = (4,0454283\ v_i^4 - 4,855198\ v_i^2 + 1)^{1/2} \qquad (2)$$

$$M_{i+1}(x) = P(v_i l)\sin(\pi x:l_i l); \quad m_{i+1}(x) = 0,5\ x ,$$

(1) and i_k, $k = \overline{1,5}$ result in:

$$v_{i+1}l = 2 \int_o^{\frac{l_i l}{2}} (l:EI)P(v_i l)0,5x((1+(\pi v_i:l_i)\cos(\pi x:l_i l))^2)^{1/2} dx +$$

$$+ v_i l \qquad (3)$$

$$v_{i+1} = \frac{Pl_i^2}{EI} v_i(0,0010305(1 + 9,615102(v_i:l_i)^2)^{1/2} +$$

$$+ 0,0151216(1 + 6,3680592(v_i:l_i)^2)^{1/2} +$$

$$+ 0,0298109(1 + 3,5015422(v_i:l_i)^2)^{1/2} +$$

$$+ 0,0553551(1 + 0,2545013(v_i:l_i)^2)^{1/2}) + v_i$$

With the assistance of the computer we had obtained the graphic constituted of the couple $(i.P, v_i: \frac{P.l_i^2}{EI})$ (look at the first computation table).

Sentences. s1). For the bar in figure 2.a, the axial force n.P induces the longitudinal contraction $\Delta l_n =$ $= n.P.l:EA = (R:E).l$. After we remove the walls, the bar can pass to an unstable equilibrium (figure 2.b). We draw a reference line in computation table 1 for $l_n = 1-R:E$.

s2). The axial contraction Δl_i for the bar centrically compressed cannot exceed Δl_n. The bar is capable for

(5)

Computation table 1

i	P_i	v_i (for $Pl_i^2:EI \cong 1$)	l_i	
0	0	0,0009	0,999998	
1	P	0,001	0,999997	
2	2P	0,001101	0,999997	
3	3P	0,001212	0,999997	
4	4P	0,001334	0,999996	
5	5P	0,001465	0,999995	
6	6P	0,001617	0,999994	
7	7P	0,001780	0,999993	
8	8P	0,001960	0,999992	
9	9P	0,002158	0,999990	
10	10P	0,002376	0,999988	
11	11P	0,002616	0,999986	
12	12P	0,002881	0,999983	
13	13P	0,003173	0,999979	
14	14P	0,003494	0,999975	
15	15P	0,003848	0,999970	
16	16P	0,004237	0,999964	
17	17P	0,004666	0,999956	
18	18P	0,005138	0,999947	
19	19P	0,005658	0,999935	
20	20P	0,006231	0,999922	
21	21P	0,006862	0,999905	
22	22P	0,007557	0,999885	
23	23P	0,008322	0,999861	
24	24P	0,009165	0,999831	
25	25P	0,010093	0,999796	
26	26P	0,011115	0,999752	
27	27P	0,012241	0,999700	
28	28P	0,013481	0,999636	
29	29P	0,014847	0,999558	
30	30P	0,016351	0,999464	
31	31P	0,018008	0,999350	
32	32P	0,019833	0,999213	
33	33P	0,021843	0,999044	R=2100 $\frac{daN}{cm^2}$
34	34P	0,024057	0,998841	
35	35P	0,026495	0,998594	
36	36P	0,029181	0,998295	R=3600 $\frac{daN}{cm^2}$
37	37P	0,032140	0,997932	
38	38P	0,035400	0,997491	
39	39P	0,038991	0,996956	
40	40P	0,042948	0,996307	
41	41P	0,047308	0,995519	

(6)

stability on the condition that the moment of inertia should not permit the passing from $1 \cdot 1$ to $1_n \cdot 1 = (1 - \frac{R}{E})1$ under the action of the secondary bending moment.

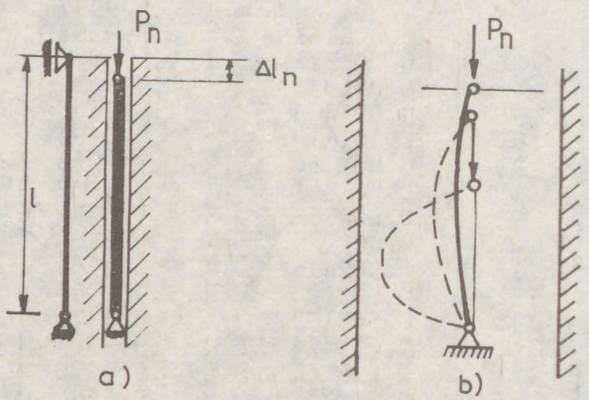

FIG. 2.

s3) $I_{necessary} \geqslant \frac{v_n}{v_1} I$, where $\frac{Pl_i^2}{EI} \cong 1$; $P = \frac{P_n}{n}$,

$$I_{necessary} \geqslant \frac{v_n}{v_1} \frac{Pl^2}{E} = \frac{v_n}{v_1} \cdot \frac{P_n}{n} \frac{l^2}{E} = \frac{v_n}{0,001n} \frac{P_n l^2}{E}$$

For $R = 2100$ daN/cm^2, $1_n = 0,999$, $n = 33$,

$$I_{necessary} = \frac{0,021843}{0,001.33} \frac{F.l^2}{E} = 0,6619 \frac{P_n l^2}{E},$$

where P_n is the force which acts on the standard bar.

s4). Of $\lambda^2 = \frac{l_f A}{I}$ and $\frac{P}{\varphi A} = R$ (4)

where λ, φ, R have the known significances and $\psi = \lambda^2 \varphi$ (see page 7), the second computation table), it result a calculus method for "$l_f = l$". We present their phases.

ph 1) $1_n = 1 - \frac{R}{E} \xrightarrow{\text{table 1}} n$, $v_n \Longrightarrow I_{necessary} = \frac{v_n}{0,001n} \frac{P_n l^2}{E}$ (5)

ph 2) (4), (5) and $l_f = l$ result in $\psi = \frac{0,001n}{v_n} \cdot \frac{E}{R}$

ph 3) Of computation table 2 we obtain:

(7)

$\Psi_{B24} = \lambda^2 \varphi$ Computation table 2

	0	1	2	3	4	5	6	7	8	9
0	0	1	4	9	15,984	24,975	35,928	48,902	63,808	90,727
10	99,6	120,39	143,13	167,81	194,43	222,75	253,18	285,24	319,46	355,22
20	393,2	432,62	473,83	516,83	561,6	608,12	655,72	705,67	756,56	809,88
30	864	919,67	976,89	1035,63	1095,88	1157,62	1220,83	1284,12	1350,14	1416,05
40	1483,2	1551,56	1621,11	1691,83	1763,69	1836,67	1908,63	1983,68	2057,47	2132,08
50	2207,5	2283,67	2360,59	2438,21	2516,50	2592,42	2671,87	2748,65	2825,76	2903,15
60	2984,4	3058,66	3136,70	3214,89	3293,18	3367,32	3445,59	3519,37	3597,47	3670,73
70	3743,6	3816,03	3888	3959,44	4030,33	4100,62	4170,27	4239,23	4307,47	4374,94
80	4553,33	4500,84	4565,59	4629,40	4692,24	4746,82	4807,4	4866,86	4925,18	4982,30
90	5038,2	5084,53	5137,64	5189,4	5239,74	5252,55	5336,06	5381,94	5435,86	5478,75
100	5520	5569,74	5607,75	5643,98	5689,21	5733	5764,06	5804,64	5843,66	5881,09
110	5904,8	5938,72	5983,48	6014,19	6043,14	6070,27	6109,02	6146,36	6168,33	6188,35
120	6220,8	6251,70	6266,16	6293,66	6319,53	6343,75	6366,27	6387,08	6422,52	6440,06
130	6455,80	6486,85	6499,15	6527,24	6535,98	6561	6584,57	6606,68	6627,31	6627,10
140	6644,40	6680,01	6694,44	6707,27	6718,46	6728	6757,17	6763,61	6790,24	6793,50
150	6817,50	6817,50	6838,78	6858,83	6853,92	6871,15	6887,08	6901,72	6915,02	6926,99
160	6937,60	6946,82	6954,66	6961,07	6966,06	6996,82	6999,22	7000,13	7027,77	7026,00
170	7051,60	7047,08	7070,57	7063,24	7084,58	7074,37	7093,50	7111,68	7097,21	7113,10
180	7128	7141,89	7154,78	7133,15	7143,61	7153,02	7161,37	7168,64	7174,83	7179,92
190	7183,9	7186,75	7225,34	7226,30	7226,11	7224,75	7222,20	7257,28	7252,74	7246,98

(8)

$$\lambda = \lambda(\psi) \; ; \quad A_{necessary} = \left(\frac{\lambda}{l}\right)^2 . I_{necessary}$$

Exemple. Determine the dimensions for a standard bar centrically compressed under the force F = 40000 daN. The length of the bar is l = 150 cm and R = 2100 daN/cm^2.

Resolution

ph 1). $l_n = l - \frac{R}{E} = 0,999$; n = 33; $v_n = 0,021843$

$$I_{necessary} = \frac{v_n}{0,001n} \frac{Fl^2}{E} = \frac{0,021843}{0,001.33} \cdot \frac{40000.150^2}{2100000} = 283,67 \text{ cm}^4$$

ph 2). $\psi = \frac{0,001n}{v_n} \frac{E}{R} = \frac{0,001.33}{0,021843} \cdot \frac{2100000}{2100} = 1510,78$

ph 3). $\lambda = 40,4$; $A_{necessary} = \left(\frac{\lambda}{l}\right)^2 . I = \left(\frac{40,4}{150}\right)^2 . 283,67 =$

$= 20,57 \text{ cm}^2$

Observation.

$$\frac{A_{necessary} - F:R}{A_{necessary}} 100 = \frac{20,57 - 19,04}{20,57} = 7,4 \%$$

3. Conclusions. This calculus method determines $I_{necessary}$ and $A_{necessary}$ for the standard bar without choose before the form of the section of the bar.

REFERENCES

1. Druzenco, V. - Modèle mathématique pour appliquer le principe du travail mécanique minimum dans le calcul des structures statiquement non-déterminées, Proceedings of National Conference on Applied Mathematics and Mecanics, 20-23 october, Cluj-Napoca, P.p.175-179.

GÁSPÁR, Zsolt[1]
DOMOKOS, Gábor[2]

GLOBAL DESCRIPTION OF THE EQUILIBRIUM PATHS OF A SIMPLE MECHANICAL MODEL

INTERNATIONAL COLLOQUIUM
STABILITY OF STEEL STRUCTURES
BUDAPEST, HUNGARY, 1990
PRELIMINARY REPORT

Summary

The equilibrium paths of a simple discrete model for the Euler problem have been determined. Beside the trivial equilibrium position several types of other equilibrium positions exist, i.e with horizontal symmetry-axis, with skew symmetry axis and with no symmetry axis at all. By changing the ratio of the spring constants among the critical points we discovered fold, standard and dual cusp, butterfly and elliptic umbilic catastrophe points. The behaviour of the imperfect structure will be demonstrated on the basis of the equilibrium paths of the perfect one.

1 Introduction

Let us determine the whole system of equilibrium paths for the structure illustrated in Fig.1/a. The structure consists of two bars with unstressed length L and axial stiffness a. The two bars are connected by a linear rotational spring with spring constant b, which is unstressed in the position illustrated in Fig. 1/a. The magnitude of the vertical conservative load is ΛaL.

The analysis will be carried out by investigating the total potential energy function of the structure and by utilizing the results of Catastrophe Theory. For convenience the energy function will be normalized.

[1]Research professor, Hungarian Academy of Science
[2]Assistant professor, Tech. Univ. of Budapest, Dept. for Strength of Materials

The structure has three degrees of freedom, but we did not find three parameters suitable to describe each position of the structure in a non-singular way, therefore other variables will be used for the description of the neighbourhood of the primary equilibrium path (Fig.1/b) and for other equilibrium paths (Fig. 1/c).

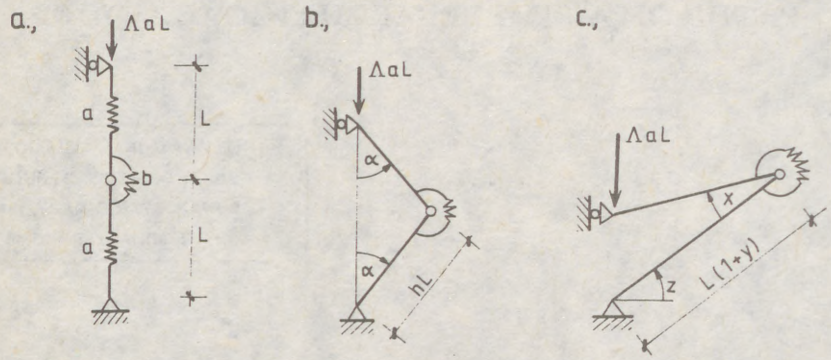

Fig.1: The structure and the coordinate systems

2 The primary equilibrium path

Based on simple considerations the existence of asymmetric equilibrium positions can be excluded in the neighbourhood of the original (Fig.1/a) position of the structure, therefore it is sufficient to use the coordinates α and h illustrated in Fig.1/b. The normalized potential energy function is the following:

$$V = \frac{\tilde{V}}{aL^2} = (h-1)^2 + \frac{c}{2}(2\alpha)^2 + 2\Lambda\cos\alpha, \tag{1}$$

where $c = \frac{b}{aL^2}$. The equation of the primary equilibrium path is

$$\alpha_0 = 0, \qquad h_0 = 1 - \Lambda \tag{2}$$

since by introducing the new variable

$$h = h_0 + u$$

the gradient of the function (1) is zero at the point (2). The stability of the equilibrium position can be investigated on the basis of the Hessian matrix of the function (1), composed of the second partial derivatives. In the case of stable equilibrium each eigenvalue of the matrix is positive. A subscript of V denotes partial differentiation with respect to the corresponding generalized coordinate, the 0 superscript denotes the equilibrium position. The Hessian matrix has now the following form:

$$\mathbf{H} = \begin{bmatrix} V^0_{uu} & V^0_{u\alpha} \\ V^0_{\alpha u} & V^0_{\alpha\alpha} \end{bmatrix} = \begin{bmatrix} 2 & 0 \\ 0 & 4c - 2\Lambda(1-\Lambda) \end{bmatrix}. \tag{3}$$

One eigenvalue is always positive, the other one is negative in the interval $(\Lambda_1^{cr}, \Lambda_2^{cr})$ and positive elsewhere. The endpoints of the interval are given by

$$\Lambda^{cr}_{1,2} = \frac{1}{2} \mp \sqrt{\frac{1}{4} - 2c}. \tag{4}$$

In the case of $c > \frac{1}{8}$ the values given in (4) are not real, i.e. the structure never looses its stability. To identify the type of the critical points the 4-jet of the Taylor expansion of (1) is derived:

$$j^4V = u^2 + (2c - \Lambda + \Lambda^2)\alpha^2 - \Lambda u\alpha^2 + (\Lambda - \Lambda^2)\frac{\alpha^4}{12}.$$

By substituting

$$u = v + \frac{\Lambda\alpha^2}{2}, \quad \Lambda = \Lambda^{cr}_{1,2} + \lambda$$

we arrive at

$$j^4V = v^2 + \left(\frac{2c}{3} - \frac{1}{8} \pm \frac{1}{8}\sqrt{1-8c}\right)\alpha^4 \mp (\lambda\sqrt{1-8c} + \lambda^2)\alpha^2.$$

Obviously v is the passive, α is the active variable. When substituting Λ_2^{cr} the coefficient of α^4 is negative, i.e. we have a dual cusp catastrophe (A_3^-, unstable symmetric bifurcation). When substituting Λ_1^{cr} the coefficient is positive for $c < \frac{3}{32}$, i.e. there is a standard cusp catastrophe (A_3^+, stable symmetric bifurcation), in the interval $\frac{3}{32} < c < \frac{1}{8}$ the coefficient is negative again. If $c = \frac{3}{32}$ then the analysis of j^6V yields the result, that we have a standard butterfly catastrophe (A_5^+). In the case of $c = \frac{1}{8}$ the coefficient of α^4 is positive, but in the coefficient of α^2 the term being linear in λ disappears. This does not change the type of the catastrophe, but as a consequence of the special role of λ the equilibrium path is given by the following equation in the neighbourhood of the critical point:

$$\alpha = \pm 4\lambda.$$

The distinct types of the investigated equilibrium paths are illustrated in Fig.2. (Stable equilibrium positions are represented by solid lines, unstable ones by broken lines.) Remark, that

the above problem is approached in POSTON & STEWART (1978) and in GOLUBITSKY & SCHAEFFER (1979), as well.

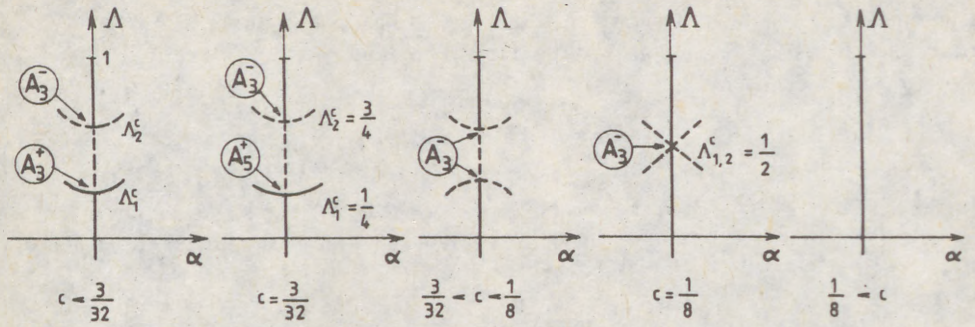

Fig.2: Distinct types of the primary equilibrium path

3 The secondary equilibrium paths

In this section the coordinates x, y and z will be used (illustrated in Fig.1/c). These coordinates have a singularity at the vertical position of the bars, but the neighbourhood of this position has been already discussed in the previous section. The normalized potential energy function has the following form:

$$V = \frac{1}{2}y^2 + \frac{1}{2}\left((1+y)\frac{\cos z}{\cos(z-x)} - 1\right)^2 + \frac{c}{2}(\Pi - x)^2 + \Lambda(1+y)\frac{\sin x}{\cos(z-x)}. \qquad (5)$$

The following equations describe the only secondary equilibrium path the limes of which is connected to the primary path:

$$\Lambda = \frac{1}{2\sin z}\left(1 \pm \sqrt{1 + 4c(2z - \Pi)\tan z}\right); \quad x = 2z; \quad y = -\Lambda \sin z, \qquad (6)$$

since at the points described by (6) the gradient of (5) vanishes. In the interval $-\frac{\Pi}{2} < z < 0$ one value for Λ is negative, the corresponding equilibrium position cannot be reached from the trivial one by continuous loading, therefore this case will not be discussed. If $z = 0$, then $\Lambda = c\Pi$. If $c \geq \frac{1}{8}$ then in the interval $0 < z < \frac{\Pi}{2}$ two real solutions exist for Λ, else , beyond a limit, the solutions are complex.

The determinant of the Hessian matrix composed of the second partial derivatives of (5) will be expressed by substituting the equilibrium equations (6):

$$|\,\mathbf{H}\,| = 2s(s + \Lambda - 2\Lambda s^2)(1 - \Lambda s)(2c - \Lambda(s + \Lambda - 2\Lambda s^2))(1 - s)^{-1},$$

where $s = \sin z$.

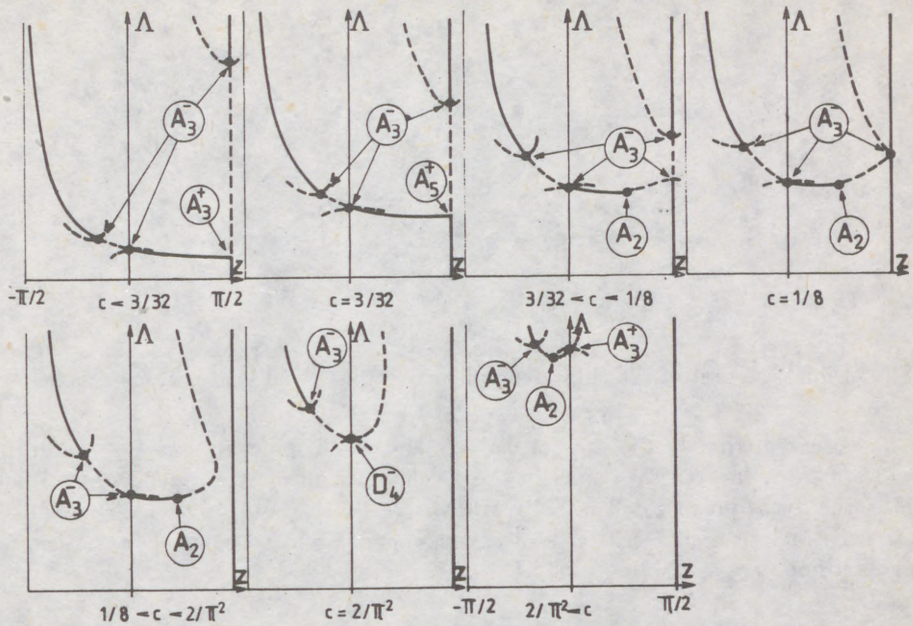

Fig.3: Distinct types of the primary and the secondary equilibrium paths

By using the symmetry of the structure it is sufficient to illustrate the equilibrium paths in the interval $-\frac{\Pi}{2} < z < \frac{\Pi}{2}$ (Fig.3). On the lower branch we have at $z = 0$ always a critical point, the state of equilibrium becomes stable again after a dual cusp catastrophe point. The first three diagrams illustrate the behaviour in the neighbourhood of a butterfly catastrophe point. (Observe the change of the number and type of the equilibrium states while changing the value of c.) When c became greater than $\frac{3}{32}$ then a fold catasrophe point appeared (A_2, limit point). This limit point approaches the dual cusp catastrophe point, and at $c = \frac{2}{\Pi^2}$ they are united in an elliptic umbilic catastrophe point (D_4^-). By increasing c they again fall apart, but the cusp catastrophe changes into a standard one. Between the two critical points a segment of the equilibrium path appears (represented by dotted line), where the Hessian matrix has two negative eigenvalues.

This pocess is well illustrated by the relation between the bifurcation set (see e.g. POSTON & STEWART (1978) or GÁSPÁR (1985)) and the load parameter Λ in the parameter space of one of the canonical forms of the elliptic umbilic catastrophe. (Minimum points are

denoted by ⊖ maximum points by ⊕ and saddle points by ○.)

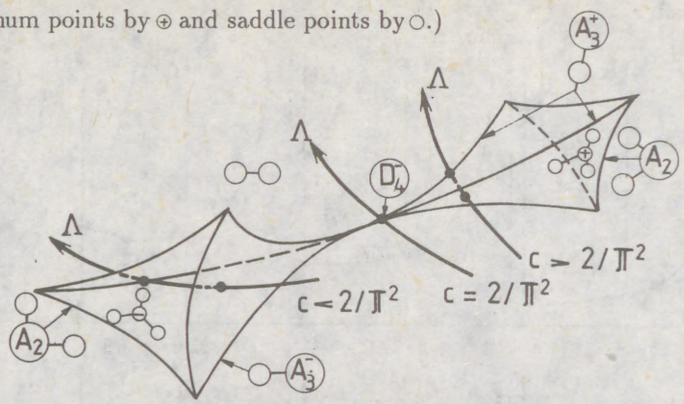

Fig.4:Bifurcation set of the elliptic umbilic catastrophe and load parameter axes

It can be observed, that in the case of $c = \frac{2}{\Pi^2}$ and small imperfections the equilibrium path will not have any critical points in the neighbourhood of the original critical point (inspite of the forms investigated by THOMPSON & HUNT(1984) and GÁSPÁR (1985), where to each imperfection a critical load corresponded) , and all equilibrium positions in the neighbourhood are unstable.

4 The tertiary equilibrium paths

The primary and secondary equilibrium paths describe all equilibrium positions with horizontal axis of symmetry. Point $z = 0$ is always critical. The tertiary equilibrium path passing through this point is described by

$$x = y = 0; \quad \Lambda = c\Pi \cos z, \tag{7}$$

since at these points the gradient of (5) vanishes. Equations (7) describe the positions, where the two bars cover each other, and there is no normal force in them. After a rotation of Π radians we arrive at position, which corresponds to the buckling of a structure upside down, but in the opposite direction and not to the buckling of the upright standing (original) structure in the opposite direction. These pieces of the equilibrium path repeat periodically, therfore only one period length will be illustrated in Fig.5 (with fixed value of c). This tertiary equilibrium path was first demonstrated by DOMOKOS (1989) for the continuous

beam.

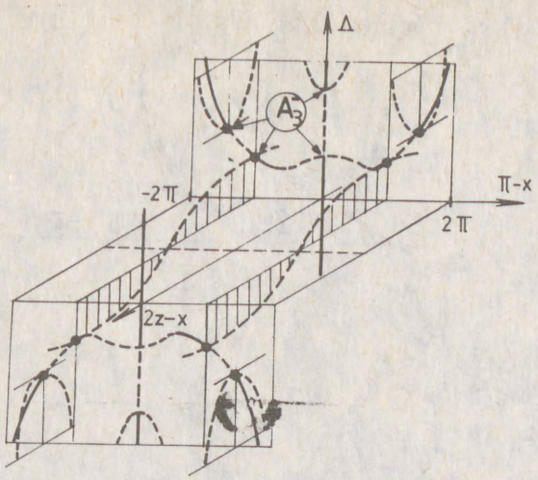

Fig.5:The complete system of equilibrium paths of the perfect structure

By substituting the equations of the equilibrium path (7) into the determinant of the Hessian matrix of (5) we arrive at

$$| \mathbf{H} | = -2c^2\Pi^2 \tan^2 z \leq 0,$$

i.e. only the point $z = 0$ is critical, all other equilibrium states are unstable.

In Fig.3 for each c-value we observed a dual cusp catastrophe point in the interval $-\frac{\Pi}{2} < z < 0$. The corresponding tertiary equilibrium path could be determined only numerically. The equilibrium states are unstable, there is no critical point except for the already mentioned one. Based on this it can be concluded, that no equilibrium path but those illustrated in Fig.5 are connected with the trivial one. There are, of course, other equilibrium positions, as well, but these positions can not be reached by „normal" loading procedure.

5 The imperfect structure

A real structure is never perfect. Due to the inavoidable imperfections the non-typical characteristics (bifurcation points) of the equilibrium paths disappear, and the connected system of equilibrium paths (e.g. the system in Fig.5) desintegrates into disjoint curves. In the neighbourhood of each non-singular point of the equilibrium path corresponding to the perfect strucure there exists an equilibrium position of the same (stable or unstable) type

for the imperfect structure. By using this information the equilibrium paths of the imperfect system (Fig.6) are easily derived from Fig.5.

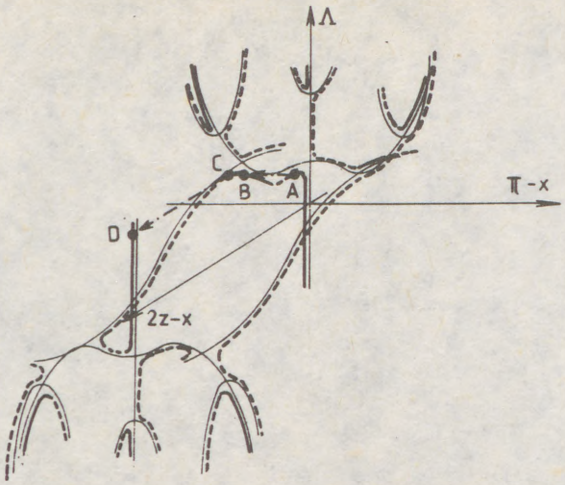

Fig.6:The complete system of equilibrium paths of the imperfect structure

The change of the critical load is proportional to the $\frac{2}{3}$rd power of the corresponding imperfections in the case of the cusp catastrophe points and to the 1st power, in the case of limit points. By increasing the load the state change of the structure is continuous up to the point A. At this point a snap-through occurs to point B. In the interval BC again continuous state-change can be observed, followed again by a snap-through from C to D, from the latter point the state-change remains continuous up to arbitrary load parameter. If we start to decrease the load at a structure upside down, then the snap-throughs will not occur at points D and B, i.e. as an effect of cyclic loading with large amplitude the equilibrium path describes a hystheresis loop.

References

DOMOKOS, G. (1989): *Large deflections of guyed masts* (in Hungarian) Thesis, Hung. Acad. of Sci.

GÁSPÁR, Zs. (1985): *Imperfection-sensitivity at near-coincidence of two critical points* J. Struct. Mech. **13** (1), 43-45.

GOLUBITSKY, M. & SCHAEFFER, D. (1979): *A theory for imperfect bifurcation via singularity theory* Comm. Pure and Appl. Math. **32**, 21-98.

POSTON, T. & STEWART, I.N. (1978): *Catastrophe theory and its applications* Pitman, London.

THOMPSON, J.M.T. & HUNT, G.W. (1984): *Elastic instability phenomena* Wiley, Chichester.

(1)
GIONCU, Victor (1)
BALUT, Nicolae (2)
MOLDOVAN, Adriana (3)
PACOSTE, Costin (3)
DUBINA, Dan (4)

THEORETICAL AND EXPERIMENTAL RESEARCH ON THE INTERACTION BETWEEN FLEXURAL AND FLEXURAL-TORSIONAL BUCKLING OF WELDED T SECTION COMPRESSION MEMBERS

INTERNATIONAL COLLOQUIUM
STABILITY OF STEEL STRUCTURES
BUDAPEST, HUNGARY, 1990
PRELIMINARY REPORT

Summary: In the introduction it is shown that the optimization of welded T section compression members leads to the coupling of flexural and flexural-torsional buckling. Chapter 2 presents theoretical research concerning the coupling of the above-mentioned two forms of instability, and the approximate interaction formulae which take into account the effects of plastic deformation. The theoretical data reveal an increase in the sensitivity to imperfections around the point where the coupling of the two forms of instability occurs, but the behaviour of welded T section compression members nevertheless falls within the range of "weak interaction". In order to provide confirmation of these findings, an experimental program was implemented, which is described in Chapter 3. A practical method for design is suggested in Chapter 4.

1. INTRODUCTION

Welded T sections are widely used in Romania for truss chords, because this is an economical solution. Due to the monosymmetry of the T section, instability of compression members can be

(1) Head of the ICCPDC Building Research Institute, Timisoara branch
(2) Senior Research Engineer, ICCPDC Building Research Institute, Timisoara branch
(3) Research Engineer, ICCPDC Building Research Institute, Timisoara branch
(4) Lecturer of Structural Mechanics, Polytechnic Institute of Timisoara

(2)

caused by flexural buckling or flexural-torsional buckling, assuming that the dimensions of the cross section are chosen in such a way as to prevent local buckling. In this case, since the members are manufactured from welded steel sheets, the dimensions of the cross section can be selected so as to obtain an economical section.

Mateescu, D., Dubina, and Mateescu, G. (1983) have recommended that this section should be optimised so that the ultimate loads, corresponding to the two forms of instability, be equal, and have developed a set of optimal cross sections, currently used in Romania in the design of trusses.

It is well known that when two forms of instability are coupled, member sensitivity to imperfections increases and the erosion of the bifurcation critical load is greater than that of either form of instability. The question therefore arises whether the common buckling curves can still be used for design. Gioncu (1989) has shown that the additional erosion caused by the coupling of two forms of instability can be weak or strong; in the first case, simple calculation methods can be used, whereas in the second case, specific methods must be devised.

This paper aims at presenting theoretical and experimental investigations carried out by the authors with a view to solving this problem in the case of welded T section members and providing a practical calculation method for design purposes.

2. THEORETICAL INVESTIGATIONS

The coupling of flexural buckling and flexural-torsional buckling was first studied by Grimaldi and Pignataro (1979). Systematic studies concerning elastic coupled instability were carried out by Gioncu and Ivan (1983) and Gioncu, Ivan, and Botici (1982).

Fig. 1 presents the three possible situations involving a T section member: the ideal unloaded member, the unloaded member with imperfections, and the deformed member with imperfections. The imperfections and deformations of the member are:

$$\{d_i\}^T = [u_i, v_i, \varphi_i] \; ; \; \{d\}^T = [u, v, \varphi] \qquad (1\ a, b)$$

Assuming that the imperfections are affined with the buckling shapes, and taking into account the fact that the deformations v and φ are coupled in flexural-torsional buckling, Gioncu and Ivan (1983) have shown that the coupling of the two forms of instability results in the appearance of an additional post-critical curve, which is unstable, and an increase in the sensitivity to imperfections (Fig. 2). The ultimate load N_u is calculated using the interaction formula

$$\left(1-\frac{N_u}{N_F}\right)\left(1-\frac{N_u}{N_{FT}}\right) = a_1 \frac{N_u}{N_F} u_i + a_2 \left[\frac{N_u}{N_F}\left(1-\frac{N_u}{N_F}\right)\Phi_i\right]^{2/3} \qquad (2)$$

where

- N_F : the flexural buckling critical load
- N_{FT} : the flexural-torsional buckling critical load
- a_1, a_2 : adimensional numerical coefficients which depend only on the geometrical characteristics of the

(3)

member undergoing buckling

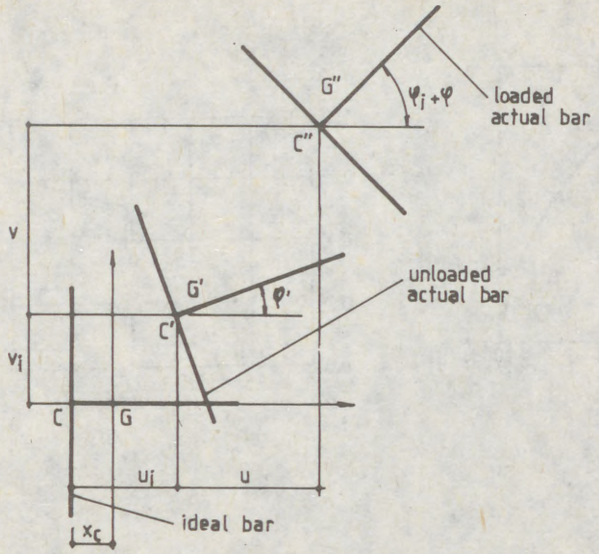

a)

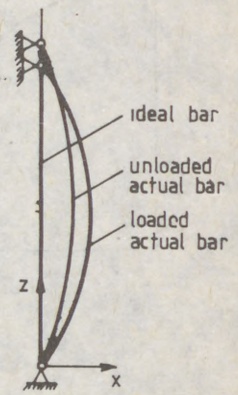

b)

FIG.1

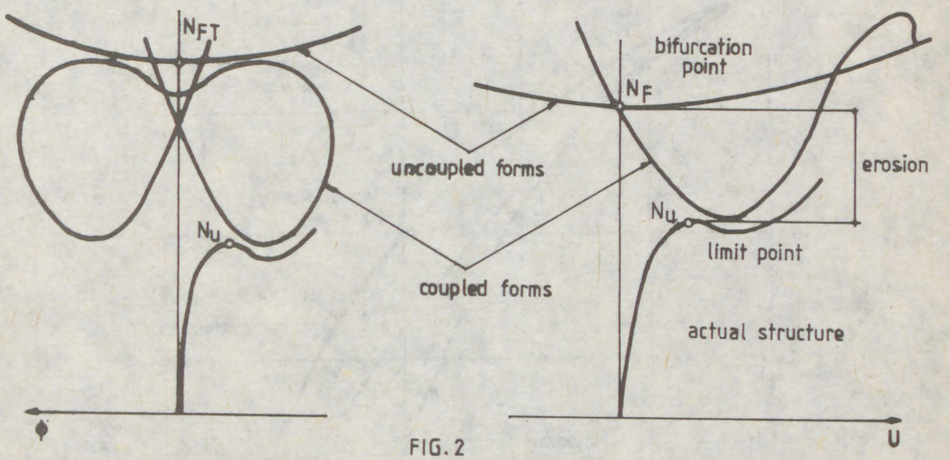

FIG.2

It is observed that when the member is ideal ($U_i = \Phi_i = 0$), the two forms of instability are uncoupled. For an ideal member, the interaction formula assumes the form in Fig. 3. The greatest erosion occurs when the two critical loads are equal. Fig. 4 presents the reduction in the buckling critical load for T sections in the case of the imperfections $U_i = \ell/500$, $v_i = \ell/600$, and $\varphi_i = 1/100$. It is seen that this reduction is not

(4)
very substantial, this type of interaction falling within the range of "weak interaction" as defined by Gioncu (1989).

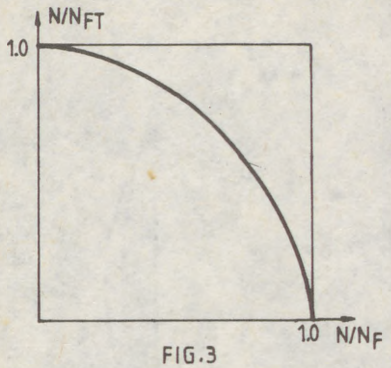

FIG.3

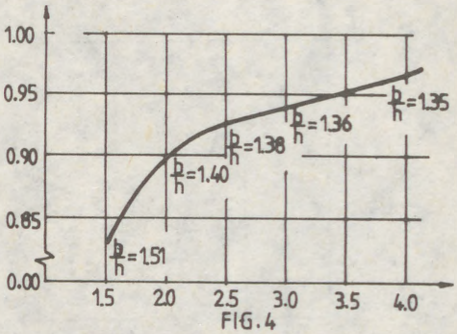

FIG.4

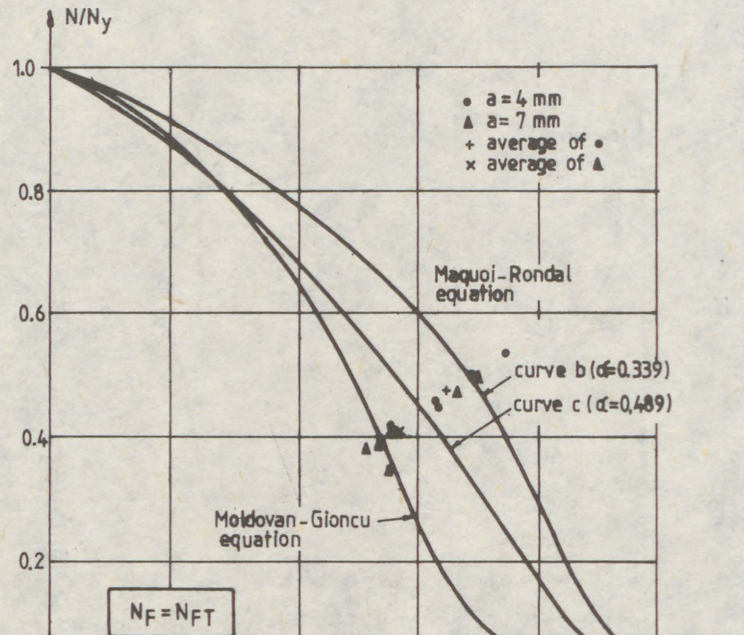

FIG.5

(5)
Moldovan and Gioncu (1986) have extended the scope of research concerning the interaction between these two forms of instability in order to allow for plastic deformations. Generalizing the formula for flexural buckling suggested by Maquoi and Rondal (1978), they have developed the following interaction formula

$$\left(1-\frac{Nu}{Ny}\right)\left(1-\frac{Nu}{N_F}\right)\left(1-\frac{Nu}{N_{FT}}\right)=\alpha\left(\sqrt{\frac{Ny}{N_{min}}}-0{,}2\right)\frac{Nu}{Ny} \qquad (3)$$

where α is the numerical coefficient specific to ECCS buckling curves (for curve b, $\alpha = 0.339$; for curve c, $\alpha = 0.489$).
Fig. 5 presents the curve yielded by Eq. (3) when $\alpha = 0.339$ and $N_y = A.fy$ for $N_F = N_{FT}$, plotted against that yielded by Maquoi and Rondal's formula. Sufficiently large reductions can be seen.
Because these theoretical investigations have indicated an increase in the sensitivity to imperfections when the two forms of instability are coupled, experimental investigations have been deemed necessary, which are presented in the next chapter.

3. EXPERIMENTAL INVESTIGATIONS

The experimental program implemented by the authors involved the testing of 48 members, 36 of which were subjected to buckling, while the other 12 were used for determining the mechanical characteristics and residual stresses.
The cross sections of the members were chosen so as to facilitate the experimental study of the various possible types of buckling.

TABEL 1

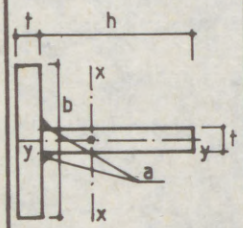

	L mm	h mm	b mm	t mm	$\frac{\lambda_y}{\varphi_y}$	$\frac{\lambda_{tr}}{\varphi}$	Nr. of specimens	a mm	Weld type
T1	2700	110	160	10	75	80	4	4	A
					0.544	0.566	3	7	B
T2	2700	80	160	10	107	73	2	4	A
					0.351	0.626	2	7	B
T3	2700	140	160	10	58	88	3	4	A
					0.679	0.502	3	7	B
T4	3600	140	210	10	80	84	3	4	A
					0.508	0.533	4	7	B
T5	3600	110	210	10	106	77	2	4	A
					0.355	0.591	3	7	B
T6	3600	160	210	10	69	90	5	4	A
					0.590	0.487	2	7	B

The members were made of OL52 grade steel sheets (f_y = 3,600 daN/cm^2) using common industrial processes.
This experimental program included the following stages:
1. stub column tests;

(6)

2. experimental determination of the residual stresses by means of the strip-cutting method, employing a Huggenberger mechanical extensometer;
3. determination of tensile yield strength and ultimate strength by tests performed on strips;
4. optical determination of the geometrical imperfections of the members chosen to undergo buckling tests;
5. buckling tests - carried out in the 200 ton hydraulic press.

For the buckling tests, support devices were developed which were meant to model as closely as possible the support conditions assumed in calculations, namely:

- the prevention of displacement in any direction perpendicular to the longitudinal axis of the member;
- the possibility of free flexural rotation in any direction;
- the prevention of torsional rotation.

In the case of T section members, there is no need to provide special support conditions as far as torsional warping is concerned.

In these circumstances, a system consisting of a relatively large hardened spherical surface bearing on a hard flat plate was devised for the application of the compression load. The support device generalizes that described by Klöppel and Unger (1971), in the sense that a system of bearings and guides in both directions x and y enables the end sections of the members to rotate freely around these axes (the principal axes of inertia). Fig. 6 shows a member being tested in the hydraulic press.

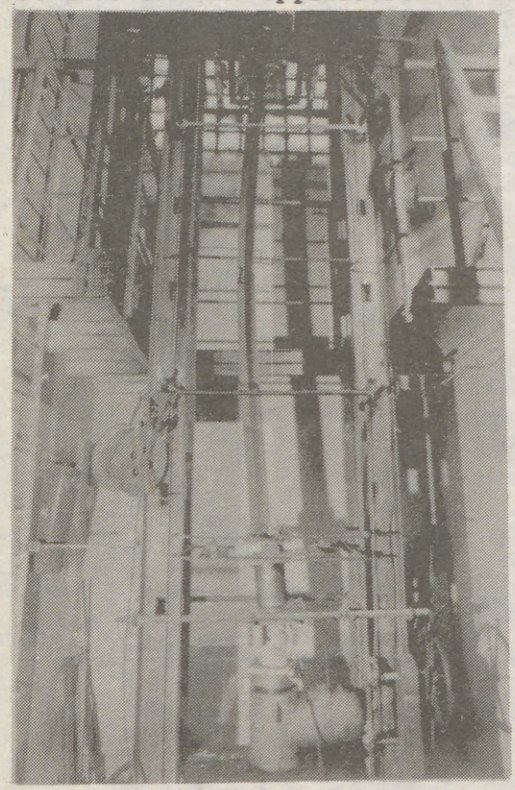

FIG. 6

For reasons of space, it is not possible to provide a detailed description of the results of the experimental program. This is why Figs. 7 and 8 present in a synthetical manner only the results concerning the buckling tests. Fig. 5 has put forth for comparison purposes the values determined experimentally for the members where theoretically $N_F = N_{FT}$.

(7)

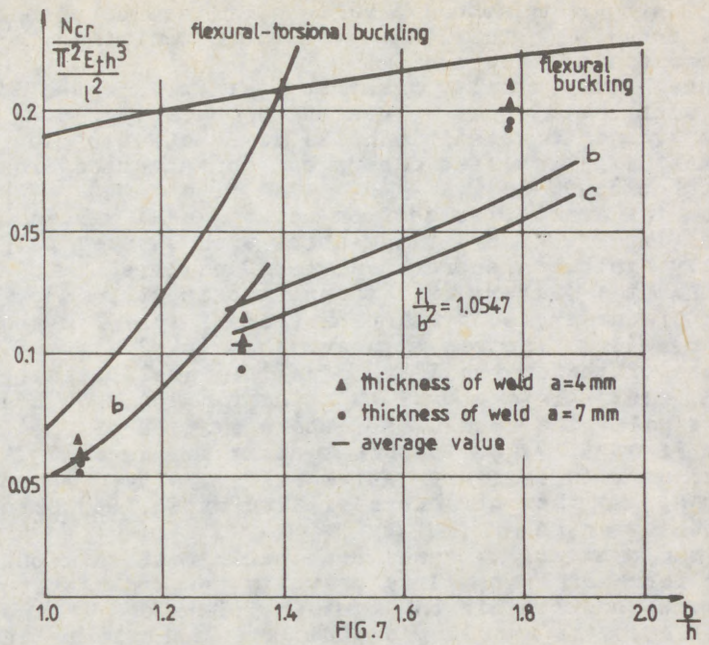
$\frac{N_{cr}}{\pi^2 E_t h^3 / l^2}$
flexural-torsional buckling
flexural buckling
0.2
0.15
0.1
0.05
b
c
$\frac{tl}{b^2} = 1.0547$
▲ thickness of weld a=4 mm
• thickness of weld a=7 mm
— average value
1.0
1.2
1.4
1.6
1.8
2.0
$\frac{b}{h}$

FIG.7

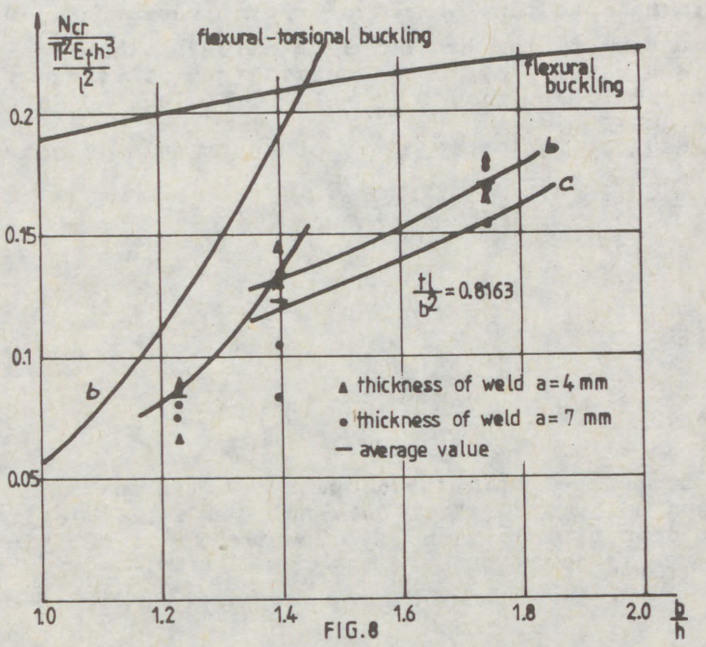
$\frac{N_{cr}}{\pi^2 E_t h^3 / l^2}$
flexural-torsional buckling
flexural buckling
0.2
0.15
0.1
0.05
b
c
$\frac{tl}{b^2} = 0.8163$
▲ thickness of weld a=4 mm
• thickness of weld a=7 mm
— average value
1.0
1.2
1.4
1.6
1.8
2.0
$\frac{b}{h}$

FIG.8

(8)

The following conclusions have been arrived at upon analyzing all the results (rather than just those mentioned herein) of the experimental program:

1. Although they display great scatter (within the limits common to such tests), the values of the buckling loads for the members T1 and T4 reveal both the interaction of the two forms of instability discussed herein and an increased erosion of the bifurcation load.

2. Given the same cross section and the same values of the geometrical imperfections, the members with thicker welds (type B) generally exhibit a poorer behaviour, collapsing under lower loads than the members with thinner welds (type A).

3. When discussing only the behaviour of type A members (the normal case), it becomes apparent that in almost all cases where one of the instability forms (flexural buckling for T2A and T5A, flexural-torsional buckling for T3A and T6A) plays a decisive role, the results are above curve b or immediately below it. Figs. 5, 7, and 8 show that in the case of T1 and T4 members, curve c is conservative as far as type A members are concerned, and that the curve yielded by Eq. (3) covers favourably both types, A and B.

4. In this context, it seems reasonable that when only one of the two forms of instability prevails (regardless of whether it is flexural buckling in the symmetry plane or flexural-torsional buckling), the buckling coefficient χ should be taken from curve b, and when the two forms of instability are coupled, this coefficient should be taken from curve c.

4. SUGGESTIONS FOR A FORMULA FOR PRACTICAL DESIGN PURPOSES

The authors suggest a generalisation of Maquoi and Rondal's (1978) formula so that when the critical loads N_{min} and N_{max} (corresponding to the two buckling modes of the ideal elastic member) are equal, the bearing capacity N_u fits curve c; in the other extreme case, when $N_{max} \to \infty$, N_u is calculated on the basis of curve b.

In this way the following interaction formula is obtained:

$$\left(1-\frac{N_u}{N_y}\right)\left(1-\frac{N_u}{N_{min}}\right)=\alpha_1\left(\sqrt{\frac{N_y}{N_{min}}}-0{,}2\right)\frac{N_u}{N_y} \qquad (4)$$

where

$$\alpha_1=\alpha_c-(\alpha_c-\alpha_b)\left(1-\frac{N_{min}}{N_{max}}\right)=0{,}339+0{,}15\left(\frac{\bar\lambda_{min}}{\bar\lambda_{max}}\right)^2 \qquad (5)$$

$$\bar\lambda_{max}=\sqrt{\frac{N_y}{N_{min}}}\quad;\quad \bar\lambda_{min}=\sqrt{\frac{N_y}{N_{max}}} \qquad (6\ a,\ b)$$

It will be assumed that the coupling of the two forms of instability can be ignored if it does not cause the buckling coefficient to drop by more than 3% below the value of χ corresponding to $\bar\lambda_{max}$ in curve b.

Given

(9)

$$\beta = \sqrt{\frac{\alpha_1 - 0{,}339}{0{,}15}} \qquad (7)$$

the condition that must be satisfied in order for the coefficient χ to be taken from curve b depending on $\bar{\lambda}_{max}$ is:

$$\bar{\lambda}_{min} \leq \beta \bar{\lambda}_{max} \quad , \qquad (8)$$

where $\bar{\lambda}_{max}$ and $\bar{\lambda}_{min}$ refer to the two buckling modes.
When $\bar{\lambda}_{max} < 0.4$, $\beta = 1$, and, therefore, since no coupling occurs, the coefficient χ can always be taken from curve b.
To facilitate practical calculations, it is recommended that the curve yielded by Eq. (7) be substituted with two straight lines and a second-degree parabola (Fig. 9).

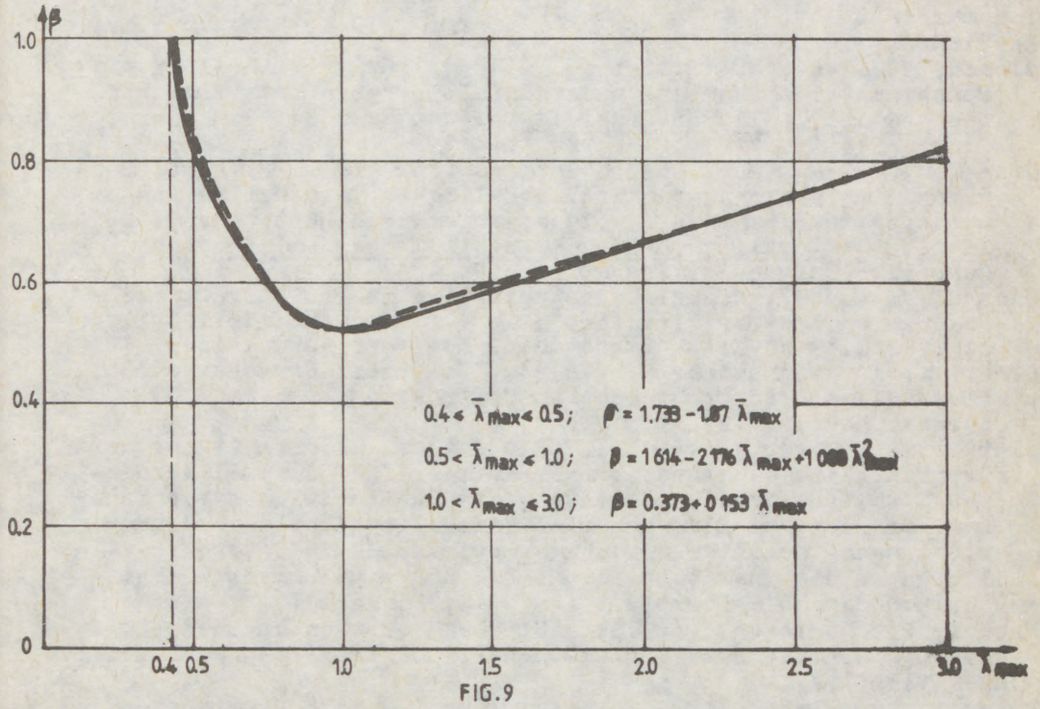

FIG.9

If $\bar{\lambda}_{min}$ does not satisfy the condition (8), the buckling coefficient χ can be determined using the approximate formula below:

$$\chi = \chi_b - \frac{\bar{\lambda}_{min}/\bar{\lambda}_{max} - \beta}{1 - \beta}(\chi_b - \chi_c) \qquad (9)$$

(10)

5. CONCLUDING REMARKS

1. The experimental results confirm the theoretical ones on the basis of which it has been concluded that the interaction of the two instability forms in T section members is of the "weak" type.
2. The buckling coeffcient for welded T section compression members with $\lambda_{max} \leq 0.4$, as well as the buckling coefficient for welded T section compression members where one of the possible forms of instability prevails - this is checked by means of the condition (8) - can be taken from curve b. If this condition is not satisfied, the buckling coefficients are located between curves b and c and can be calculated using Eq. (9).
3. This conclusion can be applied conservatively to other monosymmetrical members, such as hot-rolled channels, where residual stresses are at any rate lower than those in welded T section members.

REFERENCES

Gioncu, V., Ivan, M., Botici, I. (1982). "Spatial Buckling of Monosymmetrical Members under Axial Compression". Proc. of the 3rd Int. Coll. on Stability. First Session. Timisoara, October 16, p. 112.

Gioncu, V., Ivan, M. (1983). "Interaction between Flexural Buckling and Torsional-Flexural Buckling in Thin-Walled Compression Members", in J.M.Thompson and G.W.Hunt (eds.), Collapse: the Buckling of Structures in Theory and Practice. Cambridge University Press, p. 359.

Gioncu, V. (1989). "Coupled Instabilities in Bar Structures: Phenomenon, Theory, Practice". Rep. for the 4th Int. Coll. on Stability of Metal Structures. New York, April 18-19.

Grimaldi, A., Pignataro, M. (1979). "Postbuckling Behaviour of Thin-Walled Open Cross-Section Compression Members". J. Struct. Mech. 7 (2). p. 143.

Klöppel, K., Unger, B. (1971). "Ein Beitrag zur Ermittlung der Tragfähigkeit dünnwandinger offener Profile aus kaltgeformten Stahl bei Berücksichtingung des Zusammenwirkes von Knicken, Drillen und Elementbeulen einschliesslich der Berücksichtingung des überkritischen Bewlverhaltens". Veröffentlichungen des Instituts fur Statik und Stahlban der Technischen Hochschule Dormstadt, Heft 15, Dormstadt.

Maquoi, R., Rondal, J. (1978). "Mise en équation des nouvelles courbes europeennes de flambement". Construction Métallique, No. 1, p. 17.

Mateescu, D., Dubina, D., Mateescu, G. (1983). "Optimisation de la section en forme de T d'une barre biarticulée soumise en compression centrée". 3-ème Coll. Int. "Stabilité des structures métalliques", Paris, 16-17 Nov., Rap. preliminaire.

Moldovan, A., Gioncu, V. (1986). "Spatial Buckling of T-section Members" (in Romanian), in New and Efficient Solutions in the Design and Construction of Structures, Timisoara, nov. 14-15, section "Metal Structures and Welding in Construction", p. 91.

(1)

MAZZOLANI, Federico M. (1)

PILUSO, Vincenzo (2)

DIFFERENT USES OF THE PERRY ROBERTSON FORMULA FOR ASSESSING STABILITY OF ALUMINIUM COLUMNS

INTERNATIONAL COLLOQUIUM
STABILITY OF STEEL STRUCTURES
BUDAPEST, HUNGARY, 1990
PRELIMINARY REPORT

Summary: *This paper deals with a calibration procedure of the parameters defining the imperfection factor in a Perry-Robertson type formula for assessing stability of extruded aluminium columns.*

The obtained buckling curves are compared with the ones of some up-to-dated existing Recommendations.

INTRODUCTION

The subject of this paper is framed in the range of activity faced to the preparation of the Iso Recommendations for Aluminium Alloy Structures.

During the last meetings of the Committee ISO/TC 167/SC3 (Dubrovnik, October 1988 and Montreal September 1989), it was decided to develop a comparison between the method proposed in the first draft of ISO Recommendations for checking stability and the available expe-

(1) Professor of Structural Engineering, University of Naples, Italy
(2) Research fellow, University of Naples, Italy

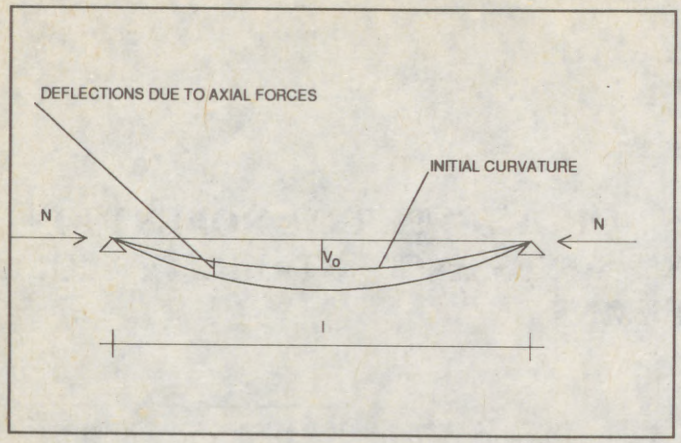

Fig.1

rimental results. This comparison was also extended to the up-to-dated existing Recommendations (i.e. ECCS Recommendations for Aluminium Alloy Structures, 1978; the italian UNI 8634, 1985 and the british BS 8118, now under public enquiry).

Different applications of the Perry-Robertson formula can be used to interpret the buckling curves whether they are derived from simulation (ECCS, UNI) or they are simple mathematical relation- ships (BS, ISO).

The new ISO proposal leads to a formulation whose parameters can be calibrated by means of the experimental evidence.

THE PERRY-ROBERTSON FORMULA

The deflections produced by an axial force acting on a bar are influenced by the initial curvature (fig.1).

If the initial shape of the axis of the bar is expressed by:

$$y_o = v_o \sin(\pi x/l) \qquad (1)$$

the bar remain elastic if the following condition is satisfied:

$$N/A + Nv_o/(1-N/N_{cr})W \leq f_y \qquad (2)$$

Equation (2) is the well-known Perry-Robertson formula, whose reputation is due to the possibility to interpret all geometrical and mechanical imperfections present in the industrial bars by introducing a fictitious initial curvature, expressed by v_o.

The collapse value N_c of the axial force is given by the condition:

$$N_c/A + N_c v_o/(1-N/N_{cr})W = f_y \qquad (3)$$

By introducing η as imperfection factor given by:

(3)

$$\eta = v_o A/W \tag{4}$$

equation (3) can be written as:

$$\sigma_c + \sigma_c\eta/(1 - \sigma_c/\sigma_{cr}) = f_y \tag{5}$$

and finally in the nondimensional form :

$$(1-\bar{N})\,(1-\bar{N}\,\bar{\lambda}^2) = \eta\,\bar{N} \tag{6}$$

being $\bar{N} = \sigma_c/f_y$ and $\bar{\lambda}$ the nondimensional slenderness: $\bar{\lambda} = (\lambda/\pi)(f_y/E)$.

The nondimensional Perry-Robertson formula (6) provides the nondimensional failure load:

$$\bar{N} = (1/2\bar{\lambda}^2)\{1+\eta+\bar{\lambda}^2 - [(1+\eta+\bar{\lambda}^2)^2 - 4\bar{\lambda}^2]^{1/2}\} \tag{7}$$

as a function of the imperfection factor η.

THE RECOMMENDATIONS FOR ALUMINIUM COLUMN BUCKLING

The check of the load carrying capacity of aluminium extruded members in pure compression is carried out in many codes by means of different methods. Many of them can be interpreted by eq. (7) [Mazzolani, 1985].

ECCS Recommendations [1978] use a formulation similar to eq. (7) but not rigorously of the Perry-Robertson type:

$$\bar{N} = (1/2\bar{\lambda}^2)\{1+\eta_1+\bar{\lambda}^2\eta_2 - [(1+\eta_1+\bar{\lambda}^2)^2 - 4\bar{\lambda}^2]^{1/2}\} \tag{8}$$

the ECCS buckling curves are obtained by introducing:

$$\eta_1 = \alpha(\bar{\lambda}^2 - \bar{\lambda}_o^2)^{1/2} \tag{9}$$

and:

$$\eta_2 = 1 - 2\beta(\gamma - \bar{\lambda})^{\mu}(\bar{\lambda}^2 - \bar{\lambda}_o^2)^{1/2} \tag{10}$$

where α,β,γ,μ and $\bar{\lambda}_o$ define two buckling curves (a) and (b) respectively for heat- treated and work-hardened alloys. The parameters $\bar{\lambda}_o$ represents the limit of the range of stocky columns where the buckling curve is cutted by $\bar{N}=1$. Their values are given in table 1.

The formulation adopted in the UNI 8634 Recommendations [1985] is rigorously of the Perry-Robertson type. In fact, it is obtained using for the imperfection factor η the following expression:

(4)

$$\eta = \alpha(\beta - \bar{\lambda})(\bar{\lambda}^2 - \bar{\lambda}_o^2)^{1/2} \qquad (11)$$

where α,β and $\bar{\lambda}_o$ define two buckling curves: curve (a) for heat-treated alloys and curve (b) for work- hardened alloys. The values of α,β and $\bar{\lambda}_o$ are provided in table 2.

The nondimensional curves C_1, C_2, C_3 given in the new BS 8118 are also derived from the Perry-Robertson formula, with $\bar{\lambda}_o$=0.2.

TABLE 1		
PARAMETER	CURVE a	CURVE b
$\bar{\lambda}_o$	0.2226	0.1876
α	0.1590	0.2420
β	0.083 if $\bar{\lambda} < 1.1$ 0.0 if $\bar{\lambda} \geq 1.1$	0.172 if $\bar{\lambda} < 1.4$ 0.0 if $\bar{\lambda} \geq 1.4$
γ	1.1	1.4
μ	0.966	1.478

TABLE 2		
PARAMETER	CURVE a	CURVE b
$\bar{\lambda}_o$	0.2226	0.1876
α	0.02	0.12
β	9.6	3.6

In the draft of the ISO Recommendations for Aluminium Alloy Structures the following relations for checking stability of extruded members in pure compression has been proposed:

$$\bar{N} = \beta - (\beta^2 - 1/\bar{\lambda}^2)^{1/2} \qquad (12)$$

being:

$$\beta = [1 + \alpha(\bar{\lambda} - \bar{\lambda}_o) + \bar{\lambda}^2]/2\bar{\lambda}^2 \qquad (13)$$

where the values of α and $\bar{\lambda}_o$, which define the buckling curves, are still matter of discussion.

Equation (12), with the notation (13), is a Perry-Robertson type formula. In fact it is easy to show that, by substituting eq. (13) in (12), we obtain eq. (7) provided that the imperfection factor is given by:

$$\eta = \alpha(\bar{\lambda} - \bar{\lambda}_o) \qquad (14)$$

The parameters α and $\bar{\lambda}_o$ can be evaluated using the available experimental results. Two numerical techniques for calculating α and $\bar{\lambda}_o$ are described in the following paragraph.

REGRESSION TECHNIQUES

Each series of experimental data is defined by the non dimensional slenderness $\bar{\lambda}_i$ and by the characteristic value (mean value minus k the standard deviation) of the nondimensional critical load $N_{i,exp}$.

The «best fit» technique for the characteristic values given by eq. (12) and (13) by means of the parameters α and $\bar{\lambda}_o$ requires the satisfaction of the following condition:

(5)

$$f(\alpha,\bar{\lambda}_o) = \Sigma_{i=1,n}\{\bar{N}_{i,exp} - [\beta_i - (\beta_i^2 - 1/\bar{\lambda}_i^2)^{1/2}]\}^2 = min \qquad (15)$$

with:

$$\beta_i = [1+\alpha(\bar{\lambda}_i - \bar{\lambda}_o)+\bar{\lambda}_i^2]/2\bar{\lambda}_i^2 \qquad (16)$$

being n the number of series of testing results.

The minimum conditions are:

$$\delta f/\delta\alpha = 0 \quad \text{and} \quad \delta f/\delta\bar{\lambda}_o = 0 \qquad (17)$$

and represent a system of equations in the unknowns α and $\bar{\lambda}_o$, which can be only solved in numerical way.

The formulation of the previous technique is not conservative because it doesn't take into account the fact that the scatters between experimental and theoretical values can be also negative, leading to cases in which the probability to compute values of N smaller than the experimental ones is greater than 5%. An alternative technique is therefore proposed.

We define:

n_v the number of cases in which the formulation is on the safe side:

$$\bar{N}_{i,exp} - [\beta_i - (\beta_i^2 - 1/\bar{\lambda}_i^2)^{1/2}] > 0 \qquad (18)$$

n_s the number of cases in which the formulation is unsafe:

$$\bar{N}_{i,exp} - [\beta_i - (\beta_i^2 - 1/\bar{\lambda}_i^2)^{1/2}] < 0 \qquad (19)$$

In order to assure that, for each value of $\bar{\lambda}$, the probability to obtain unsafe values is not greater than 5%, the parameters α and $\bar{\lambda}_o$ must satisfy the following condition:

$$n_s = 0 \qquad (20)$$

At the same time the formulation must fit as close as possible the characteristic values of testing results, what requires a second condition to be satisfied:

$$\Sigma_{i=1,nv}\{\bar{N}_{i,exp} - [\beta_i - (\beta_i^2 - 1/\bar{\lambda}_i^2)^{1/2}]\} = min \qquad (21)$$

Also in this case the values of α and $\bar{\lambda}_o$ can be derived in numerical way.

(6)

RESULTS AND COMPARISONS

The above techniques have been applied by using the testing results on aluminium alloy extruded columns, which are available in technical literature [Mazzolani, 1985].

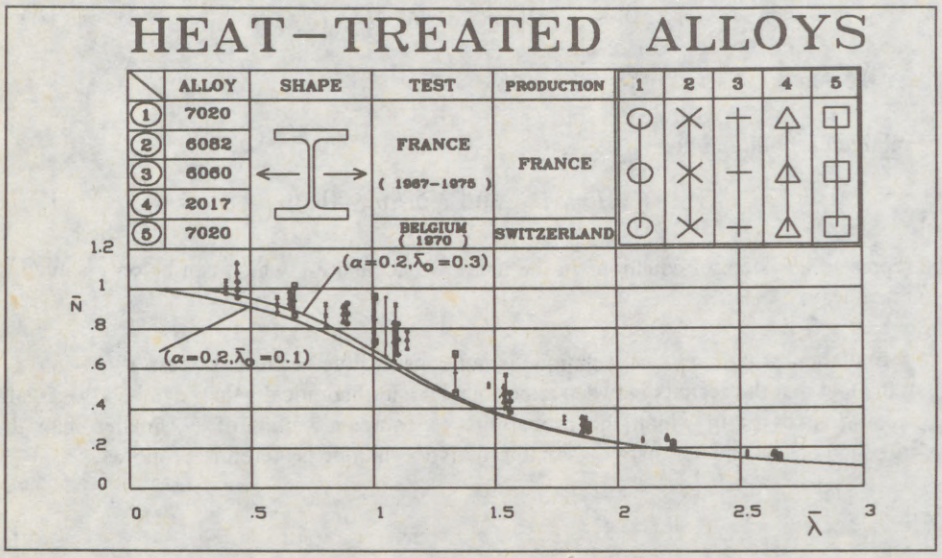

Fig. 2

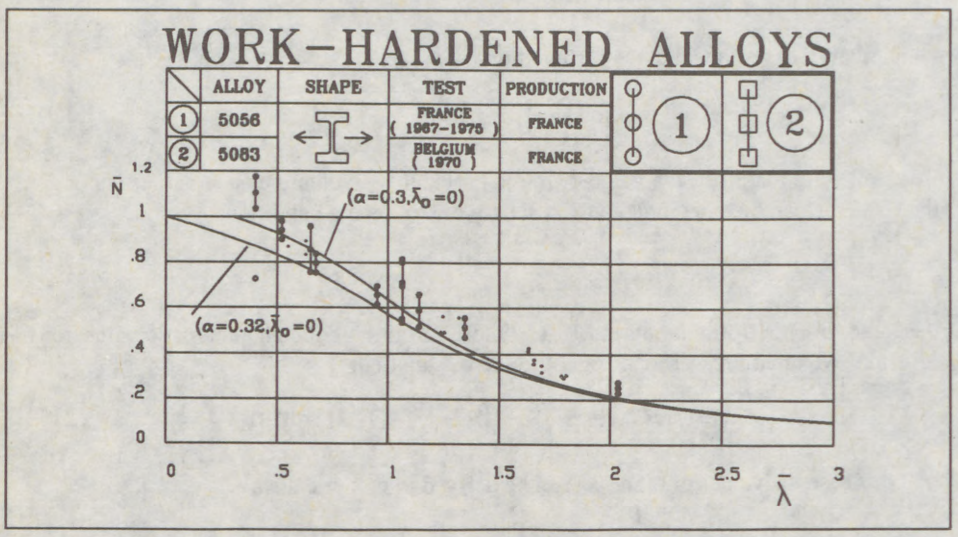

Fig. 3

(7)

The «best fit» technique provides values of parameters α and $\bar{\lambda}_o$, which are practically in accordance with those proposed by C. Marsh in the first draft of the ISO Recommendations. They are:

- $\alpha = 0.2$ and $\bar{\lambda}_o = 0.3$ for heat-treated alloys;

- $\alpha = 0.3$ and $\bar{\lambda}_o = 0.3$ for work hardened alloys.

The alternative technique, which can be defined as conditioned curvilinear regression, gives the following values:

- $\alpha = 0.20$ and $\bar{\lambda}_o = 0.1$ for heat-treated alloys;

- $\alpha = 0.32$ and $\bar{\lambda}_o = 0$ for work hardened alloys.

These values of α and $\bar{\lambda}_o$ are cohincident with those previously proposed in the discussion of the ISO draft [Mazzolani et al., 1989].

By introducing the above couples of values $(\alpha,\bar{\lambda}_o)$ in eqs. (12) and (13) we obtain the buckling curves plotted in figs. 2 and 3 for heat- treated and work-hardened alloys, respectively. The collected experimental data are also shown by means of their statistical scatters.

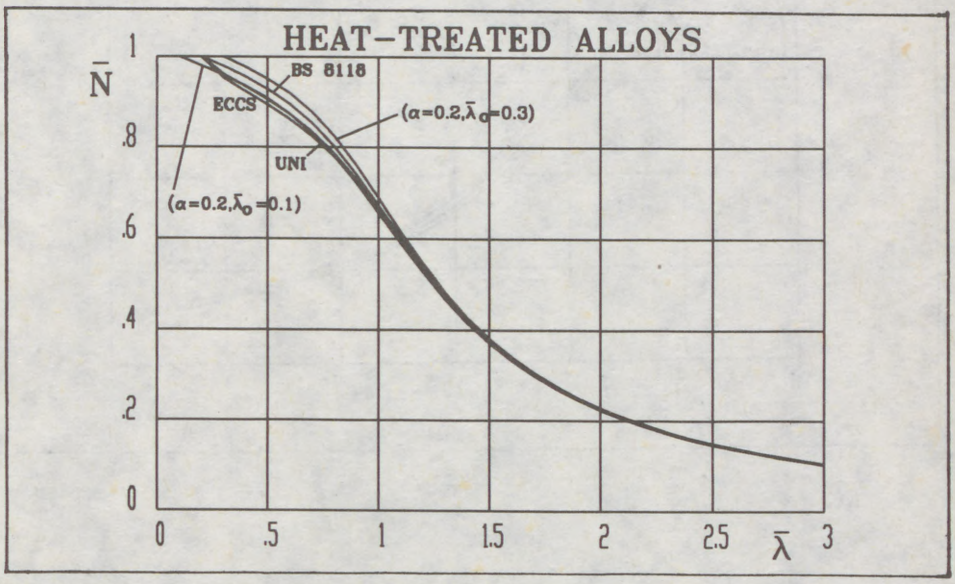

Fig.4

(8)

For both heat-treated and work-hardened alloys the proposed technique is the only one which assure a safe use of eqs. (12) and (13) in a strict agreement with the statistical interpretation of testing results. The same curves are also compared with the codified buckling curves for heat-treated (fig.4) and work- hardened alloys (fig.5).

The proposed curves are in good agreement with ECCS and UNI, both for heat-treated (α=0.20,$\bar{\lambda}_o$=0.1) and for work- hardened alloys (α=0.32,$\bar{\lambda}_o$=0), whereas the curves based on the «best fit» technique are unconservative.

REFERENCES

MAZZOLANI, F.M., 1985, «Aluminium Alloy Structures», Pitman Advanced Publishing Program, Boston-London-Melbourne.

MAZZOLANI, F.M., LANDOLFO, R., MANDARA, A., PILUSO, V., 1989, «Remarks to the Chapter 8 Ultimate Resistance of the Document N 122 E», Committee ISO 167/SC3.

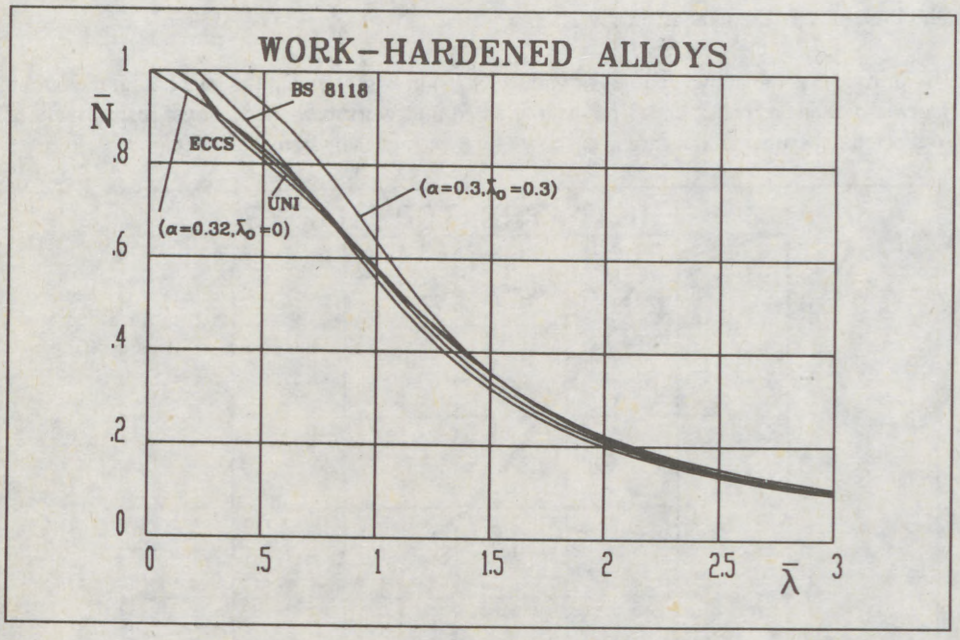

Fig. 5

(1)
NESALSOV, Oktavian (1)

COLUMN STABILITY INCREASING ON STEEL STRUCTURE RECONSTRUCTION

INTERNATIONAL COLLOQUIUM
STABILITY OF STEEL STRUCTURES
BUDAPEST, HUNGARY, 1990
PRELIMINARY REPORT

Summary: The present work is devoted to the problem of investigation of column carrying capacity reserves of steel structures at load increasing from bridge crane. The obtained results submit the ground to use existing columns without strengthening while steel structure reconstruction. New structures should be designed with the account of increased stability of the crane branch that permits to reduce steel expenditure . Crane branch stability research is carried out by matrix method. The evaluation of method accuracy is given by comparing with exact results. Calculated meanings of critical forces and corresponding designed length coefficients allow to make the design of new column structures. It is necessary to use direct matrix method according to given algorithm for more complicated cases.

(1) Professor, Steel Structure chair, Civil Engineering College, Dniepropetrovsk, USSR.

(2)

Old norms and standards of steel structure design in the USSR [1] which were used for column structure design contained recommendations for crane branch column stability design from plane as for hinge fastened bar in two points; on the foundation of the column and on the level of the crane beam supporting. In modern design [2] it is allowed to determine effective length on the basis of the effective scheme accounting real conditions of fastening column ends.

While reconstruction of metallurgic works the increasing of load-carrying capacity of bridge crane may take place. Therefore existing columns should accept the increased load. Crane beam branches of column appear to be more loaded. In connection with this the task of accounting of all factors influencing the carrying capacity of crane branch may appear. But we may have a hope that we shall find definite stock of carrying capacity on stability. This was proved by laboratory experimental data and tests of real columns under increased crane loads.

The task of bar system stability is solved more successfilly by direct method of matrix 3 which is especially realised by computors. It is connected with that all the initial data are put in as numerical matrix.

To consider and understand the essence of direct matrix method it is necessary to refer to differential eqations of equivilibrium for strait compressed bar.

$$EJ\frac{d^3y}{dx^3} = -Q(x) - N(x)\frac{dy}{dx};\quad EJ\frac{d^4y}{dx^4} = q(x) - N^{\circ}\frac{d^2y}{dx^2} \qquad (1)$$

(3)

Each of two equations are valid only under definite action character of longitudinal compressive forces which appears during bending bar deformations. The first equation corresponds to that case when longitudinal forces are having properties of weight forces during the bar deformation remain parallel to their initial direction (Fig.1a). The second equation corresponds to such character of longitudinal force action, which action line of these forces is located along tangent to resilient axis(tangent forces Fig.1b). The essence of direct matrix method consists of that the composition of outer load includes equivalent loads which reflect action of longitudinal compressed forces. Coming out of the differential equations (1) the equivalent loads will be those which contain longitudinal forces $N(x)$ and $N^{\circ}(x)$.

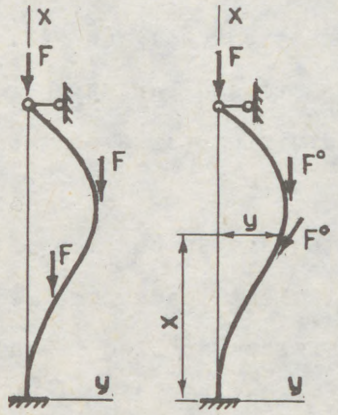

Fig.1

$$m^{e}_{(x)} = N_{(x)} \frac{dy}{dx} \; ; \quad q^{e}_{(x)} = N^{\circ}_{(x)} \frac{dy}{dx} \qquad (2)$$

The first expression for equivalent load in physisal sense corresponds to the intensity of the distributed bending moment and the second expression corresponds to the intensity of distributed transverse forces along bar length. To solve this task of stability it is necessary to show those loads

(4)

in discrete form. For longitudinal forces having properties of weight forces, discrete equivalent loads are finite number of concentrated moments applied in the middle of division parts of the compressed bar.

$$M_i^e = N_i \Delta y_i \qquad (3)$$

For this purpose we have one more expression.

$$M_i^e = N_i \varphi_i \Delta x_i \qquad (4)$$

The following notations are used in expressions (3) and (4). Δy_i - slope of division parts of the compressed bar, φ_i - corners of turn sections in the middle of division parts of the compressed bar.

If longitudinal compression elements have properties of tangencial forces N° then discrete equivalent loads are represented by the system of concentrated forces applied in the middle of division parts of compressed bars,

$$P_i^e = N_i^\circ \Delta \varphi_i \quad \text{or} \quad P_i^e = N_i^\circ y_i'' \qquad (5)$$

where $\Delta \varphi_i$ - mutual turn corners of bar section on the boundaries of each division part of the compressed bar, y_i'' - curvature of the division part middle.

Possibility of receiving of discrete equivalent loads which can be reffered to outer loads makes easier the solution of stability tasks essentially. Methods of building mechanics are more effectively used for bar statically undetermined systems. Using force method we can compose equation for displacement which come into the expression for equivalent loads and also for displacement in the direction of the

(5)

left ties which are equal to zero. Note slope vector of division parts as $\overrightarrow{\Delta y}$, vector of discrete equivalent loads as $\overrightarrow{M}$ and vector of unknown of force method as $\overrightarrow{X}$.

$$\overrightarrow{\Delta y} = \upsilon^{*}\overrightarrow{M} + \upsilon_1\overrightarrow{X} \quad \text{or} \quad \overrightarrow{\varphi} = \upsilon^{**}\overrightarrow{M} + \upsilon\overrightarrow{X} \qquad (6)$$

$$0 = \delta_1\overrightarrow{M} + \delta\overrightarrow{X} \qquad 0 = \delta_1\overrightarrow{M} + \delta\overrightarrow{X}$$

Longitudinal forces like N° give equations for displacement in matrix form like (6).

$$\overrightarrow{\Delta\varphi} = \xi^{*}\overrightarrow{P} + \xi_1\overrightarrow{X} \quad \text{or} \quad \overrightarrow{y''} = \xi^{**}\overrightarrow{P} + \xi_1\overrightarrow{X} \qquad (7)$$

$$0 = \delta_1\overrightarrow{M} + \delta\overrightarrow{X} \qquad 0 = \delta_1\overrightarrow{M} + \delta\overrightarrow{X}$$

In equations (6) and (7) multipliers at vectors represent matrix of single displacement which are calculated by multiplying single diagrams of strains of bending moments and as a result of multiplying diagrams of strains of single pair moments and single concentrated forces we can obtain matrix. The rest matrix are received analogically. (Fig.1b).

$\xi = \left(\frac{I}{6}\right)^3$

2.0 (2.75)	2.25	I.75	I.25	0.75	0.25	0.9I7
2.25	6.0 (6.75)	5.25	3.75	2.25	0.75	0.75
I.75	5.25	8.0 (8.75)	6.25	3.75	I.25	0.583
I.25	3.75	6.25	8.0 (8.75)	5.25	I.75	0.4I7
0.75	2.25	3.75	5.25	6.0 (6.75)	2.25	0.25
0.25	0.75	I.25	I.75	2.25	2.0 (2.75)	0.83

$\xi_1^{*} = \frac{I}{6}$

$\delta_1 = \frac{I}{6}$

5.27	II.8I	I3.85	I2.39	8.44	2.98

$\delta = \frac{I}{6}$

2

(6)

Matrix $\mathfrak{F}^{**}$ is received by $\mathfrak{F}^{*}$ changing of diagonal elements which are given in brackets. Stability task comes to the definition of own meanings of stability matrix which we receive from equations (6) and (7) using expressions for discrete eqivalent loads.

For forces stability we use stability matrix as

$$\beta(\upsilon - \upsilon_1\delta^{-1}\delta_1)$$

For forces stability matrix is

$$\beta(\mathfrak{F} - \mathfrak{F}\delta^{-1}\delta_1)$$

where β is a diagonal matrix of uncountable meanings of longitudinal compressing forces.

Accuracy of obtained data can be seen from table 1.

Table 1.

$N_{cr}=9.87\frac{EJ}{\ell^2}$ N 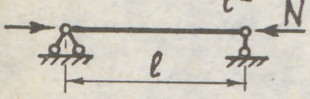				$N_{cr}=19.74\frac{EJ}{\ell^2}$ N 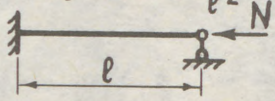				$N_{cr}=39.48\frac{EJ}{\ell^2}$ N 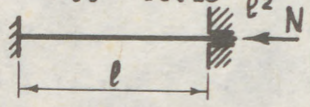			
υ^{*}	υ^{**}	$\mathfrak{F}^{*}$	$\mathfrak{F}^{**}$	υ^{*}	υ^{**}	$\mathfrak{F}^{*}$	$\mathfrak{F}^{**}$	υ^{*}	υ^{**}	$\mathfrak{F}^{*}$	$\mathfrak{F}^{**}$
9.98	9.66	9.98	9.65	20.6	19.3	20.6	19.3	40.9	36.1	41.14	36.3
9.82		9.81		19.95		19.95		38.5		38.72	
1.1%	2.1%	1.1%	2.3%	4.6%	2.5%	4.6%	2.5%	3.6%	8.7%	4.2%	8.0%
0.25%		0.37%		1.0%		1.0%		2.5%		1.9%	

More exact results are obtained as middle numbers between two meanings calculated by matrix $\mathfrak{F}^{**}$ and $\mathfrak{F}^{*}$, υ^{*} and υ^{**}. Table 2 and 3 gives design results on stability of hinge and rigid fixed columns with longitudinal tangential forces in the

Table 2

(7)

Scheme	No.	$\frac{l_1}{l}$	$\frac{F_1^\circ}{F_1^\circ+F_2^\circ}$	F_1° / F_2°	N_{cr}	μ
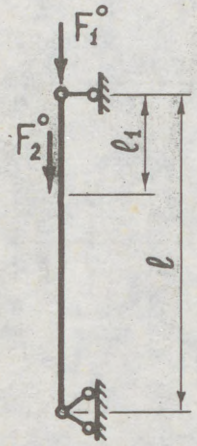	I	0	I.0	I / 0	9.87	I.0
	2	0.33	0	0 / I	II.6	0.92
	3		0.5	I / I	5.36	I.36
	4		0.67	I / 0.5	6.95	I.I8
	5	0.5	0	I / 0	I6.I	0.78
	6		0.5	I / I	6.35	I.25
	7		0.67	I / 0.5	7.76	I.I4
	8	0.67	0	0 / I	30.3	0.57
	9		0.5	I / I	8.04	I.I
	I0		0.67	I / 0.5	8.9	I.05

Table 3

Scheme	No.	$\frac{l_1}{l}$	$\frac{F_1^\circ}{F_1^\circ+F_2^\circ}$	F_1° / F_2°	N_{cr}	μ
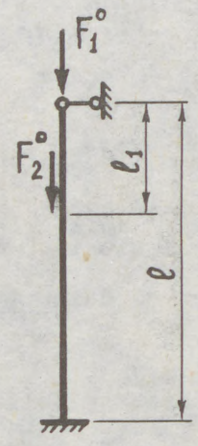	I	0	I.0	I / 0	I9.74	0.7
	2	0.33	0	0 / I	33.7	0.54
	3		0.5	I / I	I2.2	0.89
	4		0.67	I / 0.5	I5.22	0.80
	5	0.5	0	I / 0	56.0	0.42
	6		0.5	I / I	I7.I4	0.75
	7		0.67	I / 0.5	I8.6	0.69
	8	0.67	0	0 / I	I7.9	0.23
	9		0.5	I / I	2I.78	0.68
	I0		0.67	I / 0.5	20.66	0.65

(8)

span.

Data which are given in table 4 are calculated by direct matrix method and may be used in design practice.

Table 4

Scheme / F_1° / $F_1^\circ+F_2^\circ$		0	0.33	0.5	0.67	I.0
Scheme	F_1° / F_2°	0 / I	I / I	I / 0.5	I / 0.25	I / 0
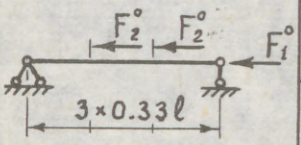	N_{cr}	8.93	4.78	6.45	7.8	9.87
	μ	I.05	I.43	I.2I	I.I2	I.0
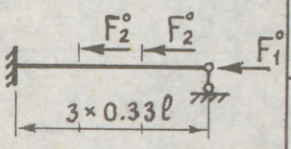	N_{cr}	I8.2	I2.89	I6.3	I7.6	I9.74
	μ	0.73	0.87	0.78	0.75	0.7

REFERENCE

1.СНиП II-B. 3 - 72

Steel Structures. Projection Norms. Moscow 1974,p.70

2.СНиП II - 23. 8I

Steel Structures. Projection Norms,M. 1982,p.93.

3.Nesalsov O.R. , 1970

Static forms of stability losses of bar construction under the action of tracing longitudinal forces and definition of their critical meanings.

Proceedings of Higher Educational Establishments,"Construction and Architecture" ,N 5,p.74 - 79.

(1)
Szabó, Gyula (1)
Szatmári, István (2)

COMPARISON OF NUMERICAL AND EXPERIMENTAL RESULTS OF BARS SUBJECTED TO LATERAL-TORSIONAL BUCKLING

INTERNATIONAL COLLOQUIUM
STABILITY OF STEEL STRUCTURES
BUDAPEST, HUNGARY, 1990
PRELIMINARY REPORT

Summary
The paper focuses on the experimental investigations of compression opened thin-walled members, made of high-strength structural steel. We compared the results we obtained with the analyses performed by numerical methods in oder to find out the reliability of high-strength materials.

I. Introduction

The modern manufacturing of structures can not be in lack of such structures that are made up from opened thin-walled members. Design for stength and deformation of thin-walled elements differs from the one of solid bars. Resistance of opened thin-walled members against torsion is very little. Their cross sections generally warp when under torsion. Should anything prevent warping of the cross section, warping normal stesses would arise in the cross section.

There is also a need of deeper theoretical thinking when tracing the isntability of sender compression members with opened cross sections. Thin-walled elements, when losing stability, deform as spacial plate-works. Plates building up the cross section might desplace both in the direction of their plane and also prependicular to it. Cross sections might twist with regard to each other and also might deform. Taking the simultaneous deformations into consideration, the element must be handled as spacial plate structure.

It is well-known that many disturbing effects appear in practice against the theroretical solutions with idealized condidtions describing the loss of stability of sender compression members.

- Disturbance is casued by the deviation of the physical properties in the material of the element alog or within the cross section,
- Problems are caused by the much different state and effect of residual stresses due to the manufacturing processes (e.g. rolling, forming, trimming, welding, etc. and

---

(1) First Assist. Prof. Department of Steel Structures TU Budapest
(2) Assoc. Prof. Department of Steel Structures TU Budapest

(2)
- also by the inaccuracy in the shape of the axle axis and the uncertainties in the location of application of forces, etc.

The following is the description of the experimental investigation of 12 thin-walled opened cross sectional members, completed by the results of a numerical analysis.

Elements were made of structural steel with increased yield stress (R_y=480 N/mm^2). The goal of the investigation was to check the reliability of computational methods by experiments with respect to structural steels with increased yield stress and also to see the reliability of the applied numerical method in this cese, too.

2. Experimental program

Thin-walled opened cross sections for the experiment were made by cold forming. Material was a 3 mm thick cold-rolled plate with a yield stress of R_y=480 N/mm^2. Table 1. contains the specific dimensions of the members.

We have investigated the initial imperfections and geometrical conditions of members. Figure 1. shows the results correspondig to members 6,9,10 and 11.

N°	G	O	V	L
1	40,24	42,29	3,0	1096
2	40,20	42,18	3,0	1101
3	60,38	60,23	3,0	1109
4	60,45	62,17	3,0	1104
5	40,35	41,43	3,0	1626
6	39,98	42,77	3,0	1600
7	60,53	60,42	3,0	1603
8	60,53	61,27	3,0	1622
9	40,28	42,65	3,0	2097
10	39,80	42,64	3,0	2096
11	60,25	61,18	3,0	2124
12	60,04	60,82	3,0	2125
[mm]				

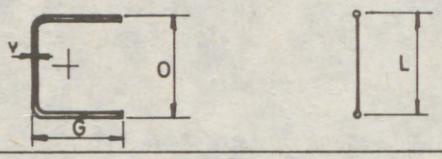

Table N° 1.

(3)
Figure 2. shows the sketch of the loading and the measuring system, while Figure 3. is an example for registrations.
For the sake of interest we determined the members' ultimate load-bearing capacity by reasonably applying the provisions of the Hungarian design Specification (MSZ 15024/1-85). Table 4. contains the sub-results of the calculations, as well as the values of the ratios $k = P_T/P_{KH}$.
k values for the elemets of the experiment are in all cases larger than 1.o., but their relation with slenderness is not expressed.

3. Numerical analyses
Those results of the experimental investigations, where the reason of losing the load-bearing capacity was obviouslythe elastic buckling (load instability or plastic deformation are excluded) were compared with the results of the STERUE computer program developed in the past few years for the analysis of spacial structures of bar elemets. (For more detailed informations on this program see the study of SZATMÁRI, I.: "A New Numerical Approach for the Calculation of 3-D Bar Systems ".)
Comparison was made with the members 6, 9, 10 and 11 of the experimental program. In Figures 1. through 4. we show the compression strain (e_z) of bars in the direction of the longitudinal axes according to the numerical and experimental analyses. Figure 5. shows the deflection of the mid-section of member 10 in the plane of symmetry of the bar (e_y), perpendicular to it (e_x) and its rotation about the axis ( ) parellel to the longitudinal axis of the member, also according to the numerical and experimental investigations.
Conclusions to be drawn by the figures:
- the STERUE program is capable to determine, with sufficiant accuracy, the load-bearing capacity of compression members of opened cross sections, loaded by arbitrary initial crookedness (imperfections), the ratio of numerical and experimental ultimate loads fell, in all four problems, between 0.95 and 1.05,
- in a compression member with irregular shape, the program can follow not only the value of the load carring capacity, but also the deflections of the member due to loading, with satisfactory accuracy therefore it can be fully considered as the numerical simulation of experimental investigations.

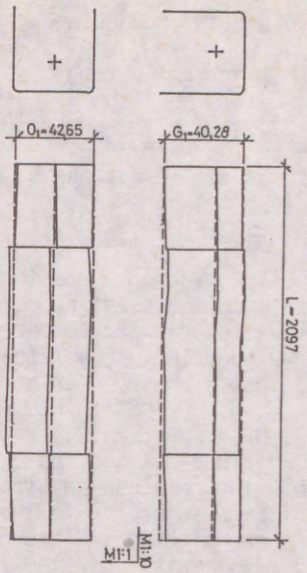

Spec. N°. 9.

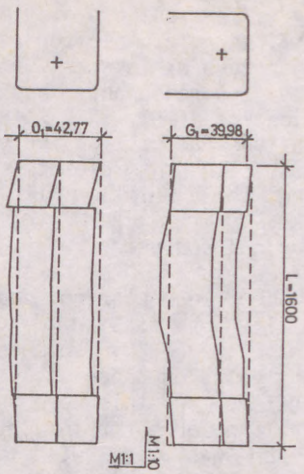

Spec. N°. 6.

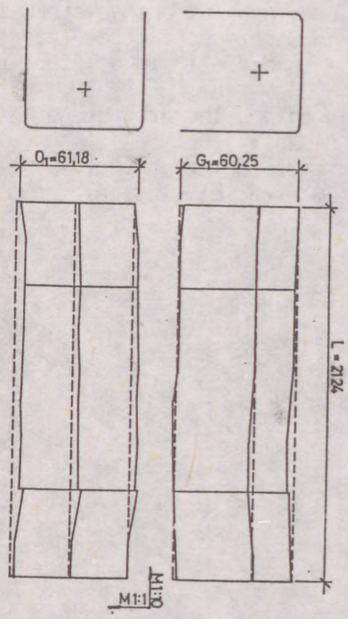

Spec. N°. 11.

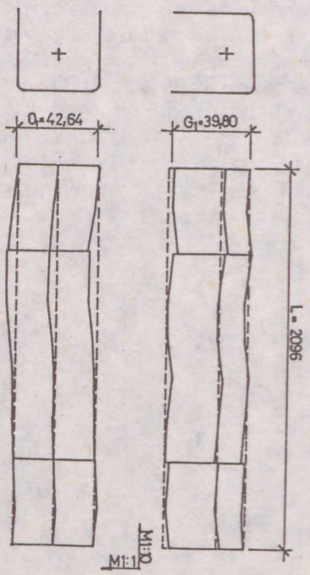

Spec. N°. 10.

Fig. 1.

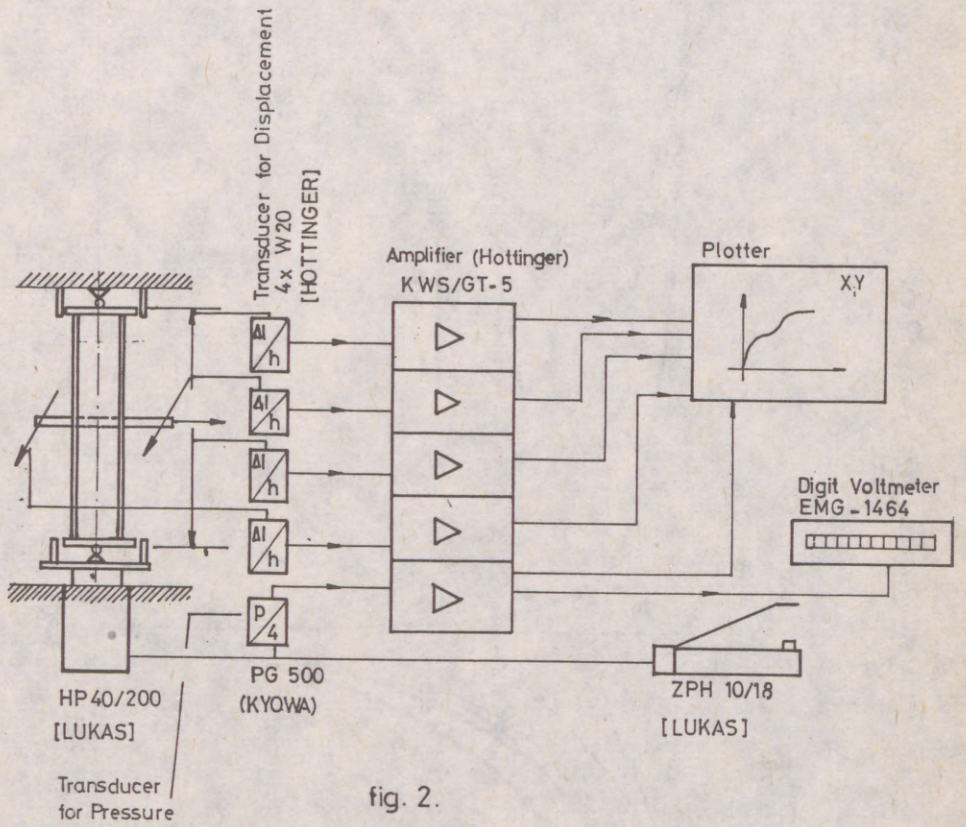
Transducer for Displacement
4 x W20
[HOTTINGER]
Amplifier (Hottinger)
KWS/GT-5
Plotter
X,Y
Digit Voltmeter
EMG-1464
Al/h
Al/h
Al/h
Al/h
p/4
PG 500
(KYOWA)
HP 40/200
[LUKAS]
Transducer
for Pressure
ZPH 10/18
[LUKAS]

fig. 2.

TEST SPECIMEN Nº 10.

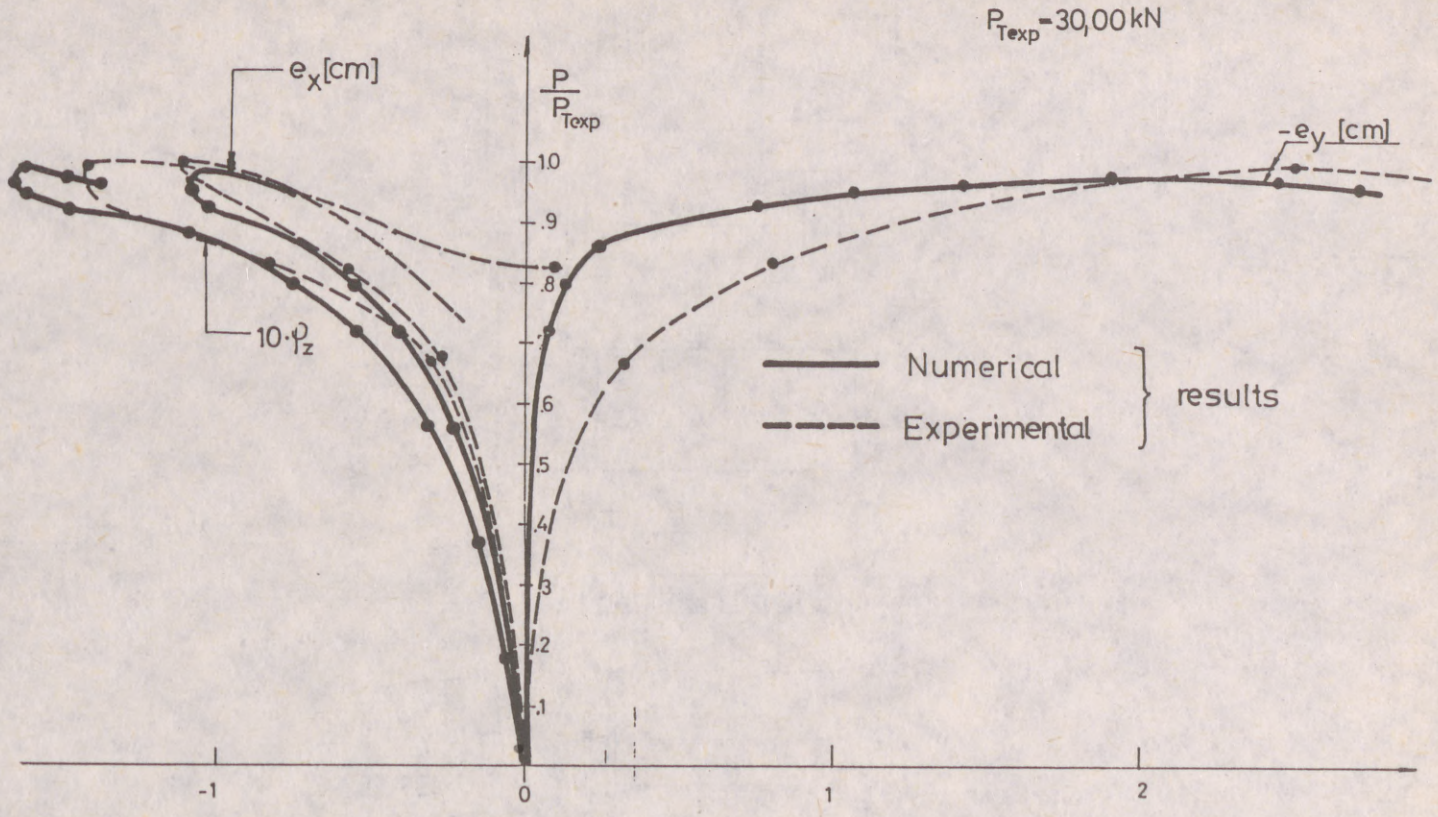

fig. 3.

TEST SPECIMEN Nº 6.

P_{Texp} = 35,00 kN

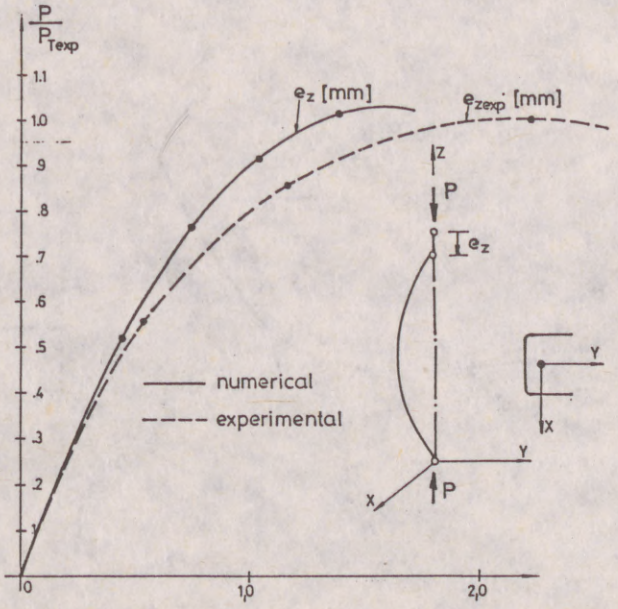

fig. 4.

TEST SPECIMEN Nº 9.

P_{Texp} = 28,00 kN

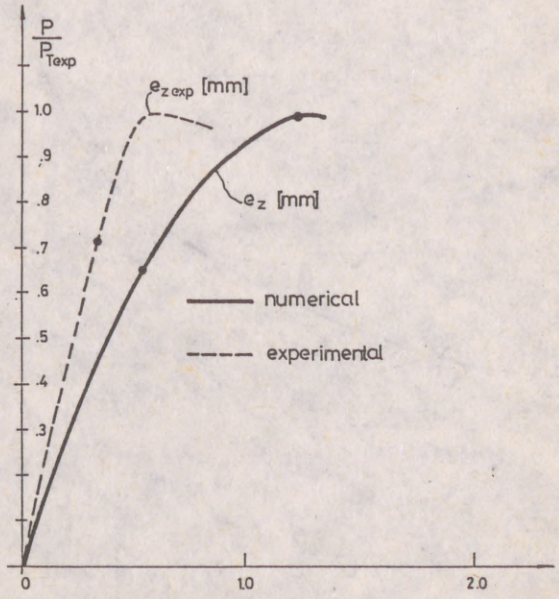

fig. 5.

TEST SPECIMEN Nº 10.

P_{Texp}=30,00kN

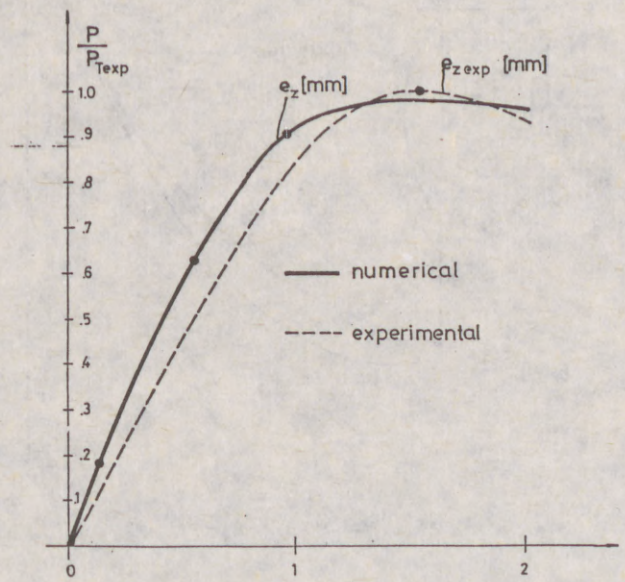

fig. 6.

TEST SPECIMEN Nº 11.

P_{Texp}=72,00 kN

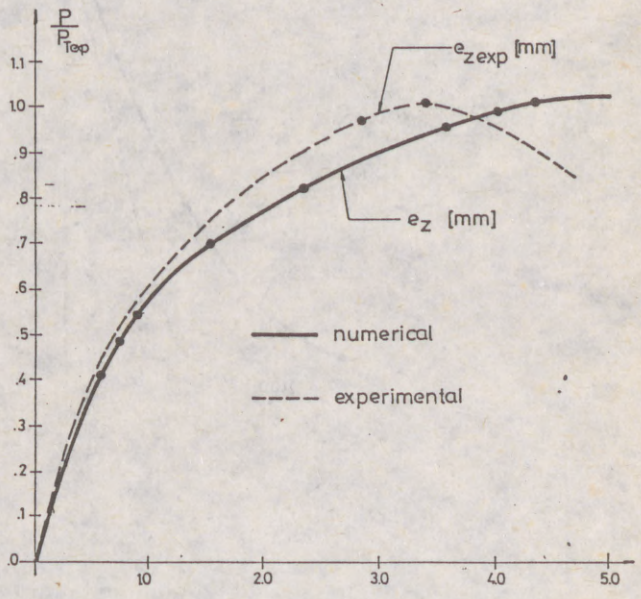

fig. 7.

(1)
SZYMCZAK, Czesław (1)

THE EFFECT OF MATERIAL NON-LINEARITY ON BUCKLING AND POST-BUCKLING BEHAVIOR OF AXIALLY COMPRESSED COLUMNS

INTERNATIONAL COLLOQUIUM
STABILITY OF STEEL STRUCTURES
BUDAPEST, HUNGARY, 1990
PRELIMINARY REPORT

Summary: The buckling and post-buckling behavior of axially compressed columns with bisymmetric open cross-section are investigated. A non-linear constitutive equation of the column material is assumed. The flexural and the torsional buckling are considered independently of each other because of bisymmetry of the column cross-section. The critical loads are calculated according to the tangent modulus theory. The considerations are based on the classical assuptions of the theory of bending and torsion of thin-walled beams with open non-deformable cross-section. The differential equations governing the initial post-buckling behavior are derived by utilizing the Euler conditions of stationary potential energy. The solution of the equations is obtained by means of a perturbation approach.
Some numerical examples, dealing with an aluminium I column are presented.

Introduction

The flexural and torsional buckling and post-buckling behavior problems have been extensively studied with aid of various methods [1,4,5]. The results of investigation dealing with an axially compressed column made of material with linear constitutive equation allow us to draw a conclusion that the bifuraction point of the flexural buckling is symmetrical and stable. Concerning the torsional buckling a detailed analysis [4] carried out for I columns shows that the bifurcation point is the same as in the case of the flexural one. The properties of the bifurcation point of the flexural buckling of a column made of a material with a cubic constitutive equation are considered by Haslach [2] . In this case the bifurcation point is also symmetrical, but it may be stable or unstable dependingon geometrical and mechanical parameters of the column. Unfortunately the solution obtained is not in line with the tangent modulus

(1) Technical University of Gdańsk

(2)
theory [5] .
The main purpose of the paper is to give a corrected analysis of the flexural bifurcation point of the axially compressed column with non-linear constitutive equation according to the tangent modulus theory. Moreover, the considerations of the torsional buckling and post-buckling behavior of a thin-walled column with an open, bisymmetric cross-section given in [4] are generalized for a non-linear constitutive equation.

Flexural buckling and post-buckling behavior of column

A critical stress of the flexural buckling σ_{cr} of the axially compressed column Fig. 1 , according to the tangent modulus theory [6] may be written as

$$\sigma_{cr} = \frac{\pi^2 E_t I_x}{l_w^2 A} , \tag{1}$$

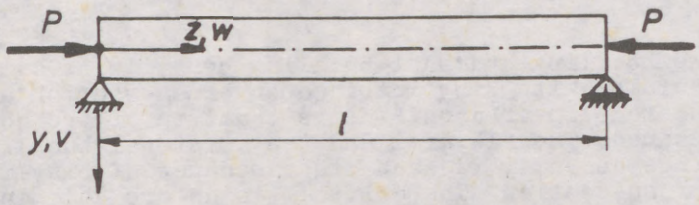

Fig. 1. Axially compressed column

where I_x is the moment of inertia of the column cross-section area about x-axis, A denotes the cross-section area, l_w stands for the effective length of the column and E_t is the tangent modulus of elasticity.
Differentiating a constitutive equation of the column material

$$\sigma = f(\varepsilon), \tag{2}$$

where σ is the normal stress, ε denotes the axial strain with respect to the strain ε , the tangent modulus can be obtained

$$E_t = \left.\frac{df}{d\varepsilon}\right|_{\varepsilon=\varepsilon_{cr}} , \tag{3}$$

where ε_{cr} is the critical strain.
After insertion of eqn.(3) into eqn.(1) and substitution $\sigma=\sigma_{cr}$ and $\varepsilon=\varepsilon_{cr}$ into eqn. (2), the equation for the critical strain may be derived

$$f(\varepsilon_{cr}) A l_w^2 - \pi^2 I_x \left.\frac{df}{d\varepsilon}\right|_{\varepsilon=\varepsilon_{cr}} . \tag{4}$$

The solution of eqn.(4) provides us with the critical strain ε_{cr} and after substituting it into eqn. (2) the critical stress is obtained.

(3)
The normal stresses σ_1 due to bending of the column after the flexural buckling may be written as the expansion of eqn. (2) into the Taylor's series around $\varepsilon = \varepsilon_{cr}$

$$\sigma_1 = E_t\varepsilon_1 + E_1\varepsilon_1^2 + E_2\varepsilon_1^3 \qquad (5)$$

where $\sigma_1 = \sigma - \sigma_{cr}$, $\varepsilon_1 = \varepsilon - \varepsilon_{cr}$, $E_1 = 0.5\, d^2f/d\varepsilon^2|_{\varepsilon=\varepsilon_{cr}}$ and $E_2 = \frac{1}{6} d^3f/d\varepsilon^3|_{\varepsilon=\varepsilon_{cr}}$.

The total potential energy V of the column of length l can be written as the sum of the strain energy V_i and the potential energy of the applied end loads V_e

$$V = V_i + V_e = \int_0^l \int_A \sigma_1 \delta\varepsilon_1 \, dA\, dz - P\int_0^l [1-(1-v'^2)^{0.5}]dz, \qquad (6)$$

where $\delta\varepsilon_1$ is the variation of the strain, P stands for the loads, v denotes the displacement of the column axis in the y-axis direction and $(\ldots)' = d(\ldots)/dz$.
After substituting eqn. (5) into eqn. (6) and utilizing the well known relation [5]

$$\varepsilon_1 = v''(1-v'^2)^{-0.5}y, \qquad (7)$$

the total potential energy (6) is

$$V = \frac{1}{2}\int_0^l [E_t I_x v''^2(1-v'^2)^{-1} + \frac{1}{2}E_2 I_{xx} v''^4(1-v'^2)^{-2}]dz - P\int_0^l [1-(1-v'^2)^{0.5}]dz, \qquad (8)$$

where $I_{xx} = \int_A y^4 \, dA$.

The differential equation governing the post-buckling behavior results from the Euler condition of the stationary potential energy

$$\begin{aligned} &E_t I_x [v^{IV}(1-v'^2)^{-1} + 4v'v''v'''(1-v'^2)^{-2} + v''^3(1+3v'^2)(1-v'^2)^{-3}] + \\ &E_2 I_{xx} [3v^{IV}v''^2(1-v'^2)^{-2} + 6v'''^2v''(1-v'^2)^{-2} + 24v'''v''^3v'(1-v'^2)^{-3} + \\ &3v''^5(1+5v'^2)(1-v'^2)^{-4}] + Pv''(1-v'^2)^{-1.5} = 0. \end{aligned} \qquad (9)$$

The initial post-buckling equilibrium path is determined by means of the perturbation approach. The deflection v(z) and the loads are expressed as follows

$$\begin{aligned} v(z) &= sv_1(z) + s^2v_2(z) + s^3v_3(z) + \ldots, \\ P &= P_{cr} + sP^{(1)} + s^2P^{(2)} + \ldots, \end{aligned} \qquad (10)$$

where s is the perturbation parameter, P_{cr} stands for the critical load and $v_i(z)$ for i=1,2,3,... are functions of variable z which should fulfil suitable boundary conditions. Substituting eqns. (10) into eqn. (9) and equating the coefficients of the power series in s to zero the following system of linear differential equations are obtained

$$E_t I_x v_1^{IV} + P_{cr} v_1'' = 0,$$

(4)

$$E_t I_x v_2^{IV} + P_{cr} v_2'' = -P^{(1)} v_1'',$$
$$E_t I_x v_3^{IV} + P_{cr} v_3'' = -E_t I_x (v_1^{IV} v_1'^2 + 4 v_1' v_1'' v_1''' + v_1''^3) - \quad (11)$$
$$E_2 I_{xx} (3 v_1^{IV} v_1''^2 + 6 v_1'''^2 v_1') - P^{(1)} v_2'' - P^{(2)} v_1'' - \frac{3}{2} P_{cr} v_1'' v_1'^2, \ldots.$$

In order to find the solution for the simply supported column /Fig. 1/, the following boundary conditions are assumed

$$v_i(0) = v_i(l) = 0, \; v_i''(0) = v_i(l) = 0 \quad \text{for} \quad i = 1,2,3,\ldots. \quad (12)$$

Moreover after insertion z=l/2 into eqn. (10) additional conditions are obtained

$$v_1(l/2) = 1, \; v_i(l/2) = 0 \quad \text{for} \quad i = 2,3,\ldots. \quad (13)$$

Using the conditions (12) and (13) in the first equation (11) and equating the perturbation parameter s to the mid-span deflection v_o we can obtain

$$s v_1 = v_0 \sin \frac{\pi z}{l}, \quad P_{cr} = \frac{\pi^2 E_t I_x}{l^2}. \quad (14)$$

After utilizing eqns. (14) the second equation gives

$$v_2 = 0, \; P^{(1)} = 0. \quad (15)$$

Insertion eqns. (14) and (15) into the third equation (11) yields after some algebra

$$v_3 = \frac{\pi^2}{64 l^2} \left(\frac{2\pi^2 E_2 I_{xx}}{E_t I_x l^2} - 1 \right) \left(\sin \frac{\pi z}{l} + \sin \frac{3\pi z}{l} \right), \quad (16)$$
$$P^{(2)} = \frac{\pi^4 E_t I_x}{8 l^4} \left(1 + 6 \frac{\pi^2 E_2 I_{xx}}{E_t I_x l^2} \right).$$

These results point out that the bifurcation point is symmetrical and it may be stable if $P^{(2)} > 0$ or unstable in the opposite case. It is easy to show that for the linear mateial ($E_2 = 0$) the bifurcation is symmetrical and stable.

Torsional buckling and post-buckling behavior of column

In the similar way the torsional buckling of an axially loaded thin-walled column with open, bisymmetric cross-section is investigated. The analysis is based on classical assumptions of the theory of thin-walled beams with non-deformable cross-section [4,7]. It is assumed that the ratio $a = E_t/G_t$ for non-linear constitutive equation is constant, where G_t is the tangent shear modulus of elasticity.
The total potential energy of the column due to torsion may be written as follows.

$$V = \int_0^l \int_A \sigma_1 \delta\varepsilon_1 \, dA \, dz + \frac{1}{2} \int_0^l G_t I_d \vartheta'^2 dz - P \int_0^l w' dz, \quad (17)$$

where I_d is the St. Venant's torsional constant, ϑ stands for the rotational displacement of cross-section and w denotes

(5)
the displacement of cross-section in the column axis direction. Utilizing eqn. (5) and the well known relationship [4]

$$\varepsilon_1 = w' + \frac{1}{2} r^2 \Theta'^2 - \omega \Theta'', \tag{18}$$

where $r^2 = x^2 + y^2$, ω is the sectorial area, in eqn. (17), we can express the total potential energy as a functional of displacements w, Θ and its derivatives.
The Euler conditions of stationary potential energy with respect to w and Θ, allow us to determine two differential equations which after elimination of the displacement w can be reduced to the fundamental differential equation depending on the displacement Θ

$$E_t I_\omega (1 - 2P\frac{E_1}{E_t^2 A})\Theta^{IV} + (P\frac{I_o}{A} - G_t I_d)\Theta'' + (6P\frac{E_1}{E_t}\frac{I_o^2}{A^2} - \frac{3}{2}E_t\bar{I}_{oo})\Theta'^2\Theta'' + [(E_1 - \tag{19}$$
$$3P\frac{E_2}{E_t A})\bar{I}_{o\omega} + 3P\frac{E_1^2 I_o I_\omega}{E_t^2 A^2}](\Theta''^3 + 4\Theta'\Theta''\Theta''' + \Theta'^2\Theta^{IV}) + 3E_2 I_{\omega\omega}(2\Theta''\Theta'''^2 + \Theta''^2\Theta^{IV}) = 0,$$

where I_o is the polar moment of inertia, $\bar{I}_{oo} = I_{oo} - I_o^2/A$, $I_{oo} = \int_A r^4\, dA$, $\bar{I}_{o\omega} = I_{o\omega} - I_o \cdot I_\omega / A$, $I_{o\omega} = \int_A \omega^2 r^2\, dA$, I_ω denotes the warping torsional constant and $I_{\omega\omega} = \int_A \omega^4 dA$.
Using the perturbation approach, the rotational displecement $\Theta(z)$ is expressed as

$$\Theta(z) = s\Theta_1(z) + s^2\Theta_2(z) + s^3\Theta_3(z) + \ldots, \tag{20}$$

where $\Theta_i(z)$ are functions of variable z which should fulfil suitable boundary conditions.
After insertion of eqn. (20) and second eqn. (10) into eqn. (19) and equating the coefficients of the power series of s to zero the system of linear differential equations is derived.
In similar way as above mentioned we can obtain the solution for the simply supported column

$$P_{cr} = \frac{A}{I_o}[G_t I_d + E_t I_\omega (\frac{\pi}{l})^2][1 + 2\frac{E_1}{E_t}\frac{I_\omega}{I_o}(\frac{\pi}{l})^2]^{-1}, \tag{21}$$

$$P^{(1)} = 0,\ s\Theta_1(z) = \Theta_o \sin\frac{\pi z}{l},\ \Theta_2 = 0,$$

$$P^{(2)} = \frac{3}{4}(\frac{\pi}{l})^2\{E_t\bar{I}_{oo} - 4P_{cr}\frac{E_1}{E_t}\frac{I_o^2}{A} + \frac{4}{3}(\frac{\pi}{l})^2[(E_1 - 3P_{cr}\frac{E_2}{E_t A})\bar{I}_{o\omega} + 3P_{cr}\frac{E_1^2}{E_t^2}\frac{I_o I_\omega}{A}]$$
$$+ \frac{3}{4}E_2 I_{\omega\omega}(\frac{\pi}{l})^4\}[\frac{I_o}{A} + 2\frac{E_1}{E_t}\frac{I_\omega}{A}(\frac{\pi}{l})^2]^{-1}.$$

It is easy to show that if the linear material is taken, ($E_1 = E_2 = 0$) then the results (21) correspond to those obtained in Ref. [4].

Numerical examples

The simply supported column made of aluminium is considered

(6)
(Fig. 2). The constitutive equation of the column material corresponds to the Ramberg-Osgood curve [3]

$$\varepsilon = \frac{\sigma}{E} + 0.002\left(\frac{\sigma}{\sigma_{0.2}}\right)^{n}, \tag{22}$$

where E is the modulus of elasticity, $\sigma_{0.2}$ stands for the conventional 0.2% offset yield stress and n characterizes the hardening of the alloy.
Figure 3 presents the graphs of the ratio P_{cr}/P_{cr}^{L} vs the column length and the post-buckling equilibrum paths (P/P_{cr}), where P_{cr} stands for the critical load of the flexural buckling and P_{cr}^{L} is the same load for the linear constitutive equation of the column material.
The same relationships for the torsional buckling are graphically presented in Fig. 4 where Θ_0 is the mid-span rotational displacement.

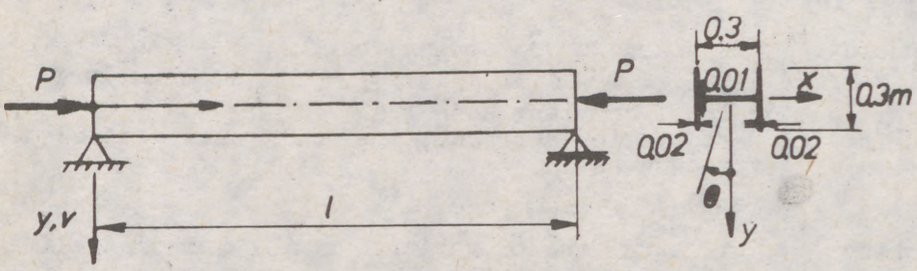

Fig. 2. Simply supported column

Conclusions

The results of investigations allow us to draw some conclusions regarding the bifurcation points of the torsional and flexural buckling of axially loaded columns made of material with nonlinear constitutive equations.
The critical loads of the flexural buckling for the non-linear material are smaller than the ones for the linear model, if $E_t < E$. Concerning the post-buckling behavior it should be noticed that the ratio $P^{(2)}/P_{cr}$ determining the initial curvature of the post-buckling equilibrium path depends on the geometrical dimensions of the column and the material parameters. Therefore the point of bifurcation may be stable $(P^{(2)}/P_{cr}>0)$ or unstable $(P^{(2)}/P_{cr}<0)$, whereas this point is stable for the linear constitutive equation. The bifurcation point is symmetrical independently of the column material property.
In the case of the torsional buckling of the column, the critical loads may be smaller or greater than the loads for the linear material. The bifurcation point is also symmetrical as in the case of the flexural buckling and it may be stable or

(7)
unstable. This property depends on the column geometry and the material constants but it is stable for the linear constitutive equation.

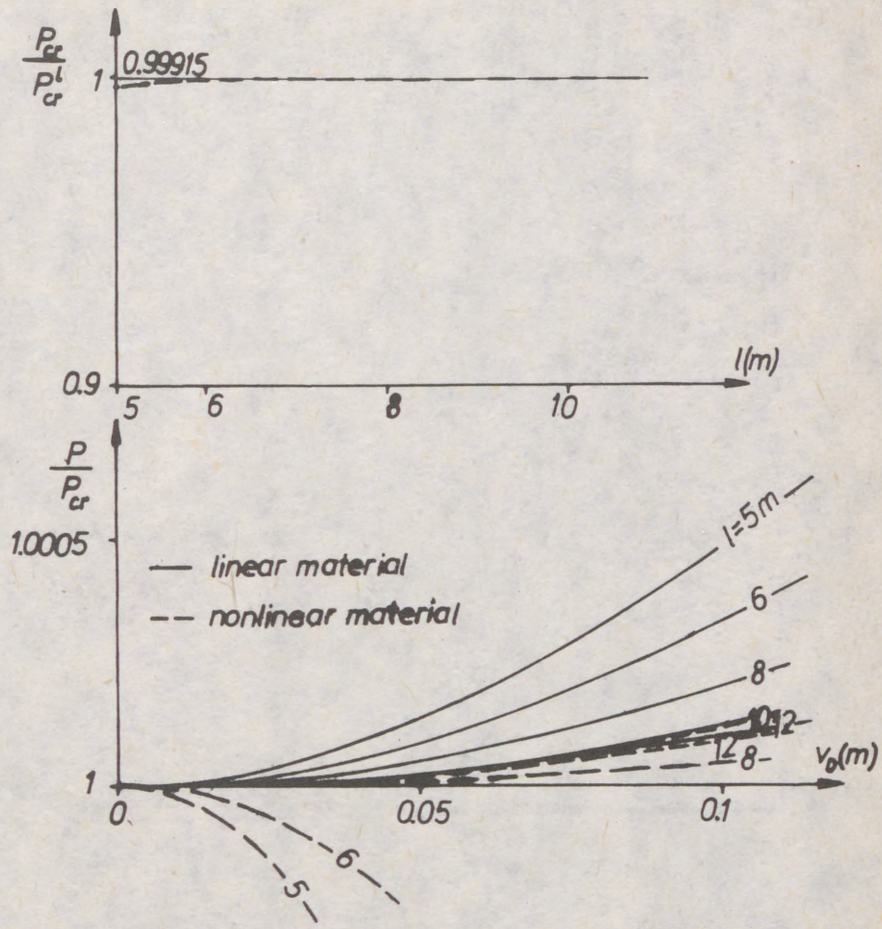

Fig. 3. Results for flexural buckling of column

References.

1. Brush D.O., Almroth B.O., (1975) Buckling of Bars, Plates and Shells. Mc Graw-Hill, New York.
2. Haslach H.W., (1985) Post-buckling Behavior of Columns with Non-linear Constitutive Equations. Int. J. Nonlinear Mechanice, 20, 53-67.
3. Mromliński R., (1964) Aluminium Structures. Arkady, Warsaw (in Polish).

(8)

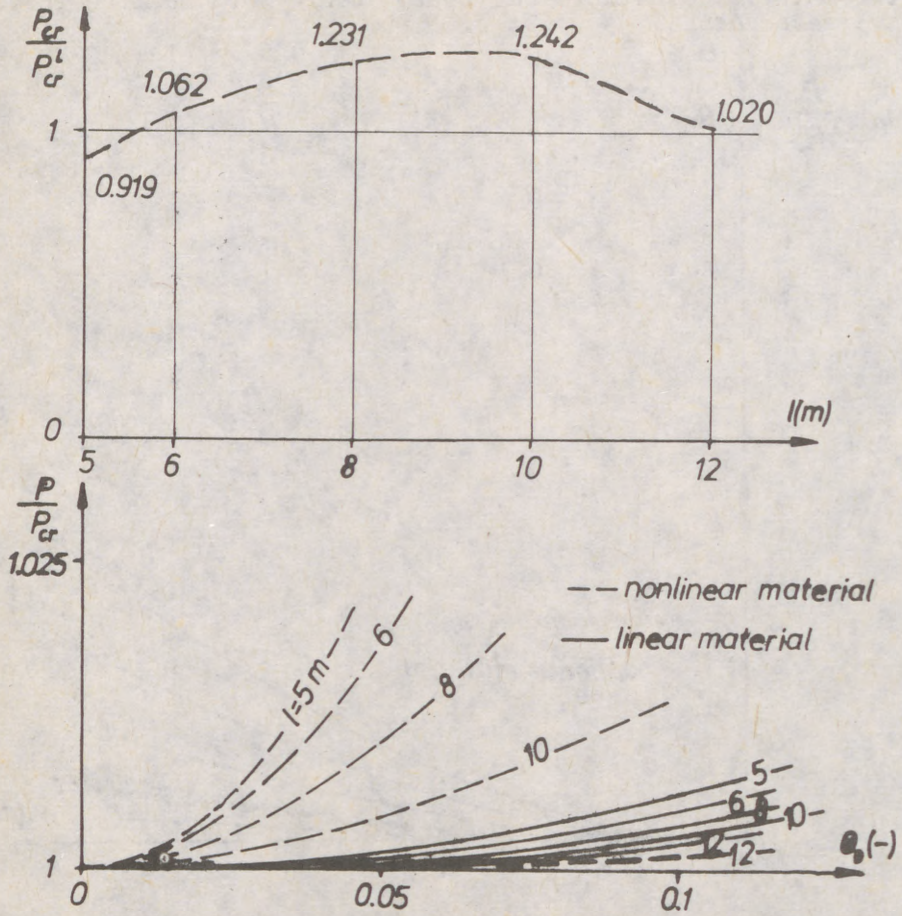

Fig. 4. Results for torsional buckling of column.

4. Szymczak C., (1980) Buckling and Initial Post-buckling Behavior of Thin-walled I Columns. Comput. Structures, 11, 481-487.
5. Thompson I.M.T., Hunt G.W., (1973) A General Theory of Elastic Stability. Wiley, London.
6. Timoshenko S.P., Gere I.M., (1961) Theory of Elastic Stability. Mc Graw-Hill, New York.
7. Vlasov V.Z. (1959) Thin-walled Elastic Beams. Fizmatgiz, Moscow(in Russian).

SESSION 3

BUILT-UP MEMBERS

(1)
RONDAL, Jacques (1)
NIAZI, Majid (2)

STABILITY OF BUILT-UP BEAMS AND COLUMNS WITH THIN-WALLED MEMBERS.

INTERNATIONAL COLLOQUIUM
STABILITY OF STEEL STRUCTURES
BUDAPEST, HUNGARY, 1990
PRELIMINARY REPORT

Summary :
The aim of the paper is to present experimental results on built-up elements composed of cold-formed C profiles with battened plates or C stitchs.

The test results are compared with theoretical predictions obtained by means of the classical design method taking into account the Q factor when the profiles are thin-walled, for battened plates, and by means of a new design method for elements using C stitchs.

The comparison of the results show that both methods lead to a safe and accurate design.

1. INTRODUCTION.

Battened columns composed of hot-rolled profiles are used since a long time for heavily loaded compressed elements. However, the use of battened elements using cold-formed C profiles is in increase for industrialized steel buildings.

The first objective of the paper is to present the results for an experimental research on the behaviour of battened steel struts composed of cold-formed C profiles with thin walls. The results of an experimental investigation on built-up struts where the members are connected by means of C stitchs are also given. This type of built-up profiles is normally not used as a column. In fact, this investigation is only the first step of a research devoted to the behaviour of lattice roof girders composed of C profiles (fig. 1).

---

(1) Associate Professor, University of Liège, Belgium.
(2) Research Engineer, University of Liège, Belgium.

(2)
In this type of girder, the chords are joined by the C web members and the most difficult design problem is the calculation of the ultimate load of the girder when subject to uplift wind loads which lead to a compression of the bottom chord.

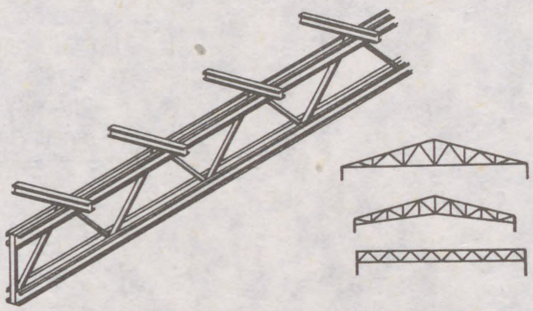

Figure 1 - Lattice roof girders with double C profiles.

2. EXPERIMENTAL INVESTIGATION AND NUMERICAL SIMULATION.

Eighteen tests have been performed on columns with battened plates and eighteen, also, on columns with C stitchs. Figure 2 shows the main dimensions of the elements. In each category, twelve specimens had four battened plates or stitchs and six specimens were tested with only three battened plates or stitchs.
The measured yield strength of the steel was of 455 N/mm^2 for the profiles with a thickness of 2.5 mm and of 428 N/mm^2, for the others, with a thickness of 3 mm.

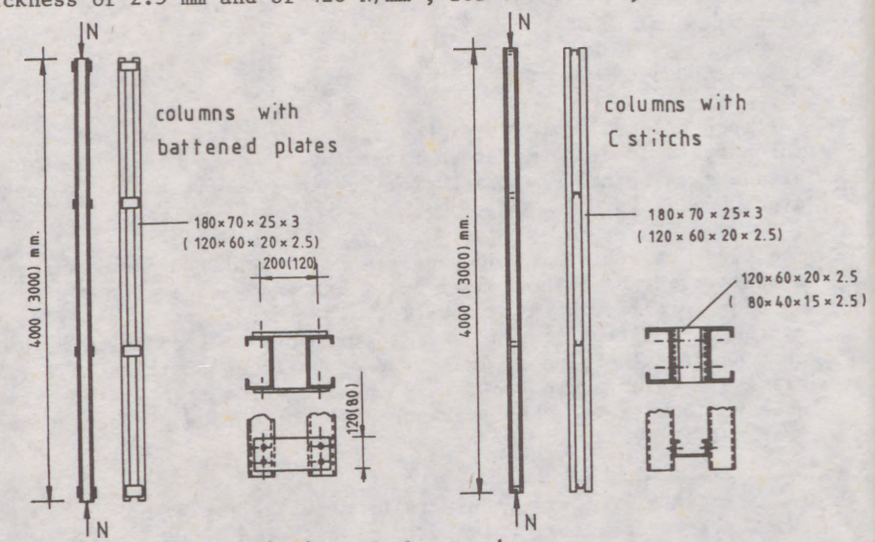

Figure 2 - Main characteristics of the specimens.

(3)
The dimensions of the profiles have been chosen in such a way that all the stability phenomena (local and global) can be met in the series of tests.

For some of the specimens, a numerical simulation has also been performed by means of the computer program FINELG:
This finite element program, developed at the University of Liège, takes account of the material and geometrical non-linearities. The local plate buckling of the profiles has been modelized by means of effective widths calculated in accordance with the Eurocode 3. (E.C.3, 1988).

Table 1 shows, for one profile with battened plates and one profile with stitchs that the results of the numerical simulations are in good agreement with the tests results. For the specimen with stitchs, the first and the second mode of buckling are very close to each other. For this reason, two geometrical imperfections have been used which are affine to the buckling modes. Figure 3 shows the load-displacement diagrams for a specimen with C stitchs and a geometrical imperfection corresponding to the second buckling mode.

Profiles	Type	l (mm)	N_{exp} (kN)	N_{num} (kN)
C 120	4 battened plates	4000	223 249 265	231
C 180	3 stitchs	3000	480 512 484	first mode: 497; second mode: 526

Table 1 - Comparison of experimental and numerical results.

(4)

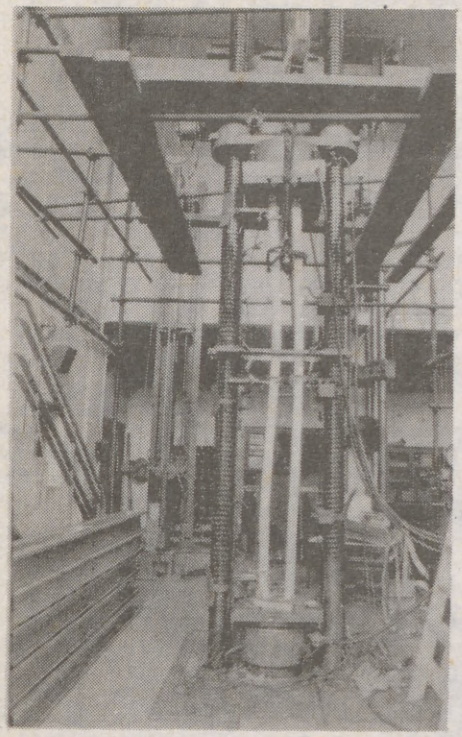

a.

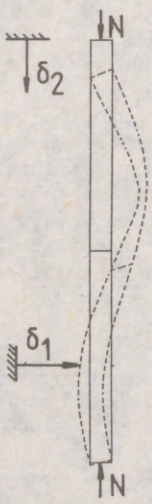

b.

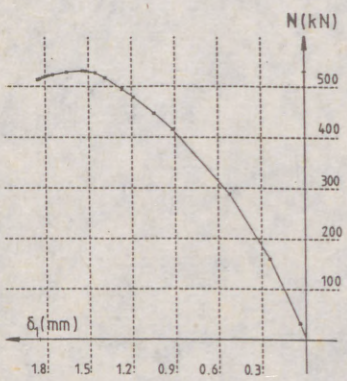

c.

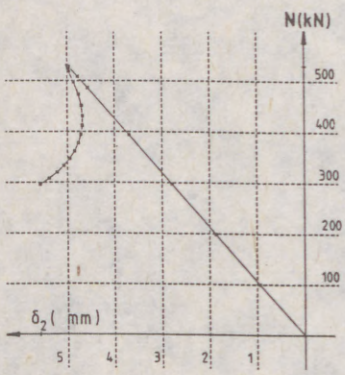

d.

Figure 3 - Column with C stitchs (profiles 180, l = 3000 mm, 3 C 120 stitchs) :
a) experimental test after failure ;
b) c) and d): numerical simulations: load-displacement curves.

(5)

3. DESIGN METHOD FOR COLUMNS WITH BATTENED PLATES.

The design method is based on the E.C.3 rules for built-up columns and the slenderness of the walls is taken into account by means of a Q reduction factor, which is calculated in accordance with the appendix on cold-formed sections of the E.C.3. (E.C.3., 1988).

Figure 4 shows the design curve in comparaison with the test results. For the series of tests, the mean value of the ratio N_{exp}/N_{th} is equal to 1.23 with a standard deviation of 0.08.

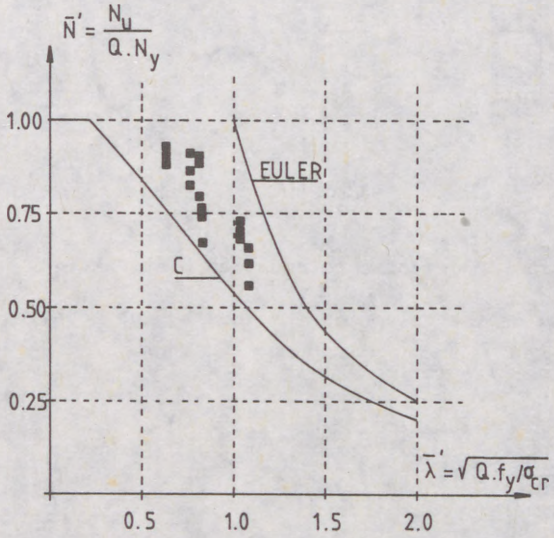

Figure 4 - Comparison of the experimental results and of the design curve for columns with battened plates.

4. DESIGN METHOD FOR COLUMNS WITH C STITCHS.

This type of junction between the profiles is more flexible than the battened plates. For this reason the model of the figure 5 has been adopted.

(6)

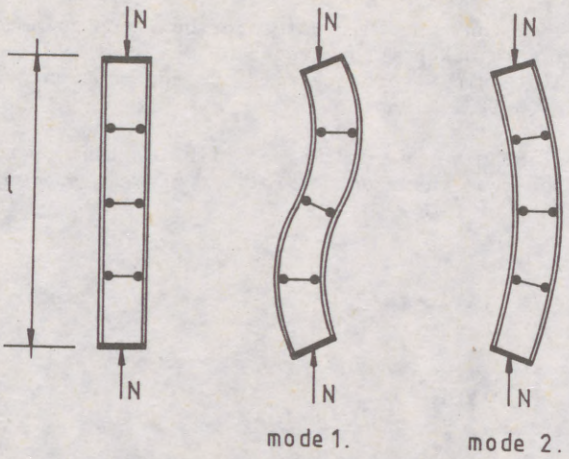

Figure 5 - Model of a column with C stitchs.

The critical load of the column is governed by the equation (JOHNSTON, 1971)

$$kl \sin kl + \left(\frac{I}{I_1} - 2\right)(1 - \cos kl) = 0 \qquad (1)$$

with

$$k^2 = \frac{N}{2EI_1} \qquad (2)$$

where I is the inertia of the whole column and I_1 is the inertia of a single profile.
This equation leads to an equivalent slenderness given by :

$$\lambda_{eq} = \frac{\pi l}{\sqrt{C_1}} \sqrt{\frac{A_1}{I_1}} \qquad (3)$$

where A_1 is the cross-section of one profile.

Figure 6 gives the coefficient C_1 as a function of the ratio I/I_1. The curve has been obtained, from equation (1), by means of an iterative solution technique.
This solution can be approximated, with a good precision, by the relation:

$$C_1 = 14.91 \ln \frac{I}{I_1} + 18 \qquad (4)$$

for $6 \leq I/I_1 \leq 42$ (5)

(7)

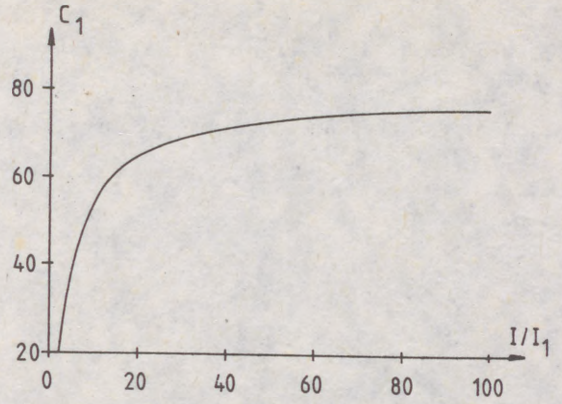

Figure 6 - Coefficient C_1 as a function of the ratio I/I_1

In the proposed design method, the equivalent slenderness calculated by means of equation (3) is then used in replacement of the equivalent slenderness used in E.C.3.

Figure 7 shows the design curve in comparison with the tests results. For the series of tests, the mean value of the ratio N_{exp}/N_{th} is equal to 1.25 with a standard deviation of 0.11.

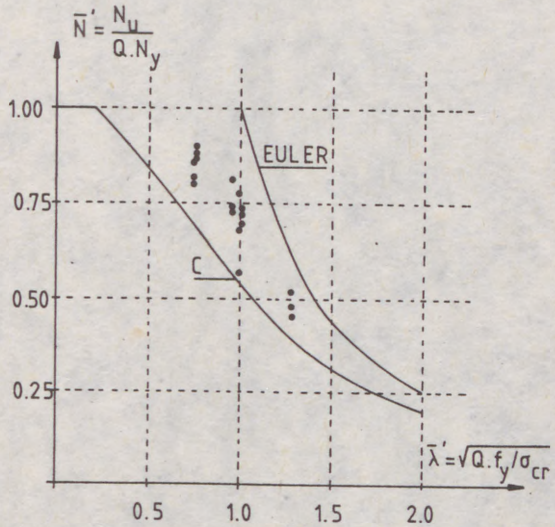

Figure 7 - Comparison of the experimental results and of the design curve for columns with C stitchs.

(8)
REFERENCES.

E.C.3., 1988 : Eurocode N° 3 - Design of Steel Structures, Commission of the European Communities, Final Draft.

JOHNSTON, B.G., 1971 : Spaced Steel Columns, Journal of the Structural Division, ASCE, Vol. 97, N° ST5, pp. 1465 - 1479.

(1)

dr. SZITTNER Antal

RESTAURATION OF DAMAGED COMPRESSION BARS ON SZABABSAG /LIBERTY/ BRIDGE, BUDAPEST

INTERNATIONAL COLLOQUIUM
STABILITY OF STEEL STRUCTURES
BUDAPEST, HUNGARY, 1990
PRELIMINARY REPORT

Summary: After the collapse of Reichsbrücke in Vienna, in 1976, a thorough inspection and reconstruction project was initiated by authorities, related to the Danube-bridges of Budapest -most of them had been blown up during the World War II. and rebuilt afterwards. Multiplication of traffic and accelerating corrosion due to salting (started in 1964) made the reconstruction necessary. The Department of Steel Structures of TU Budapest has been taking part in this project primarily as general adviser but carried out some delicate measurements too. This paper reports on the work performed by the Department in the reconstruction of the damaged compression columns of 'Szabadság' /Liberty/ bridge.

Liberty (formerly Ferenc József) bridge was originally constructed of Martin-Steel in 1894-96. Reconstruction of the bridge - reusing some of the old main elements - took place after the World War II. In 1979 the whole floor sytem and the balancing elements of the bridge were replaced. Replacement of walkways and the repair of main elements commenced only in 1985.

During the rehabilitation of the main structure the corrosion damage of the columns - especially that of noted by 6-6'- proved to be the most serious problem. This corrosion damage was found on those parts of the columns,

---

Senior scientific assistant, Dep't of Steel Structures,
Technical University Budapest

where they were led through the walkway slab and was due to clogging partially of the walkway supporting angles, partially of the gap between the asphaltic cover and the column. The salted sand did not leave the 28-42 mm. gap between the double webs - where there were heads of rivets as well -, and this, together with the scale flaking off due to corrosion, inhibited the outflow of dirty (salted) water. The severe corrosion along a length of about 150-200 mm - particularly at the original main columns - resulted in a 40-50 % reduction of the cross-section that had to be replaced properly.

Corrosion at the diagonals in tension, where there were no walkway slab supports, therefore the outflow of dirty water was inhibited less - fortunately didn't exceed 10 %. Similarly, less than 10 % corrosion damage was observed at every bridge components rebuilt after the War, where this gap was larger.

The rehabilitation had to be solved so, that

a) strengthening should ensure the full trimming of the compression member,
b) strengthening shouldn't inhibit gaps to be cleaned beween webs
c) shape of the bridge should not change for landscape purposes,
d) no elements inhibiting the outflow of salted water should be placed on columns at the support of walkway slab.

A larger problem arised during the reconstruction of the bridge, when - while opening the southern walkway on 17th of October, 1986 - the Buda South column 6-6' cracked, moved by 35 mm's sideway, shortened with about 15 mm. Fortunately, the broken ends were seated firmly on each other.

After having been closed the bridge from any traffic, the displaced ends were fixed first. Similar procedure was carried out at each columns still uncovered, but suscipious as possibly corroded. Afterwards the bar force in the damaged column was determined by measurement and the technology of rehabilitation was worked out.

The bar force in the damaged 6-6' bar and also in the neighbouring columns and diagonals was determined by the so-called trepanation method, by releasing the internal forces (stresses). Previous laboratory experiments showed favourable results using this method: the force at bar elements beeing in uniaxial state of stress can be determined with an accuracy of 15-20 %.

(3)

To release the internal stresses a pair of holes with a final diameter of 12 mm were drilled in several steps at both ends of previously bonded, 10 mm long strain gages. Stresses in different elements were calculated on the bases of strain measured after the drilling process. (Fig. 1.)

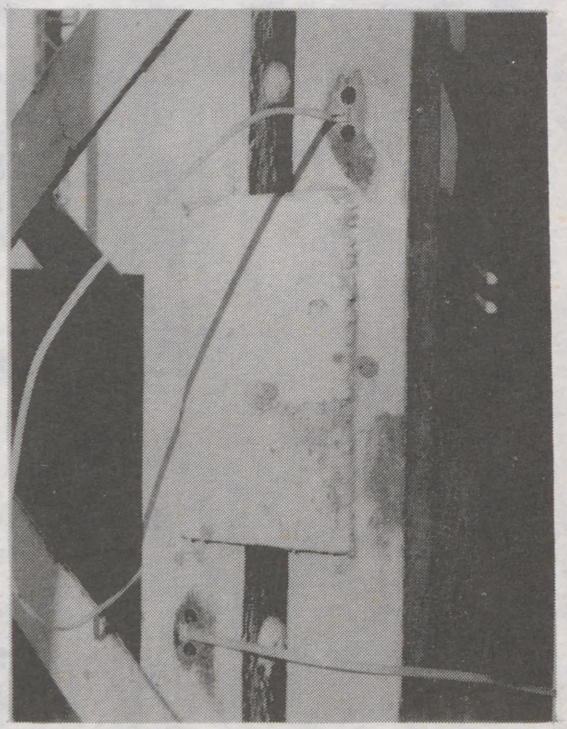

Fig.1.

As an interesting fact it should be mentioned, that these stresses in the webs of the columns proved to be compression but in the chord angles showed tension. The reason is, that during previous reinforcement longitudinal ribs and cover plates had been welded onto the chord angles causing tensile stresses.

From all of the results having been taken in many bars the ones measured in the damaged 6-6' column and in the 9-9'column were of great importance.

In bar 6-6'-871 kN resultant force was measured instead of the -1930 kN bar force, calculated theoretically from dead load. This theoretical value showed a very good correspondece with the force measured later, during rehabilitation. In the bar 9-9', - reconstructed after the War without pushing out the connecting chord points - the

(4)

measurement showed a practically unloaded state: -83 kN against the theoretical -1450 kN.

To reconstruct bar 6-6' a pair of trimming bar-ends was built in between the lower and upper joints of the bar. They were equipped by four hydaulic jacks with a capacity of 1000 kN each, enough to reach the designed -2500 kN bar force. (Fig. 2.)

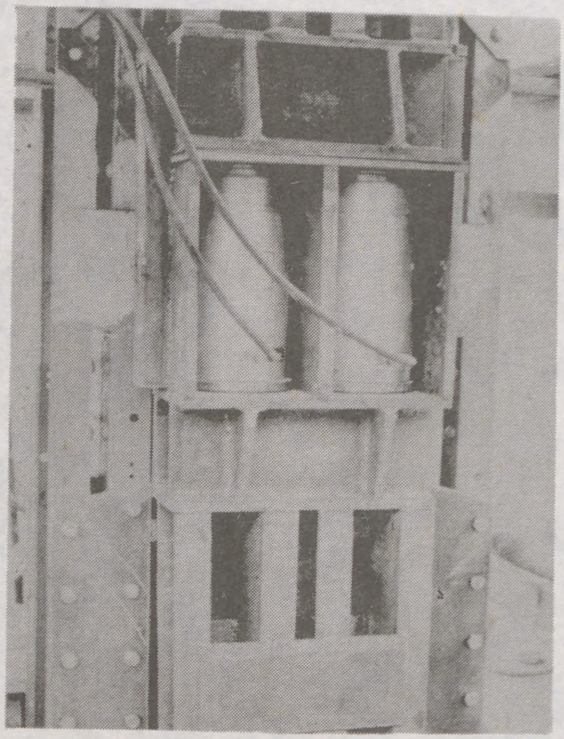

Fig. 2.

Strain gages were bonded to each elements of the upper end of bar 6-6' to keep the reconstruction process under control. The bar force calculated from the data of these strain gages was continously compared with the jack-force, calculated from the readings of a pressure gage, built into the hydraulic system. Measurement data were on-line collected, processed and displayed in the form of diagrams (Fig. 3) by the help of a microcomputer.

Reconstruction of bar 6-6'was carried out in the following steps:

a) After the trimming system and the hydraulic jacks had been built in, -20 kN force was applied and the

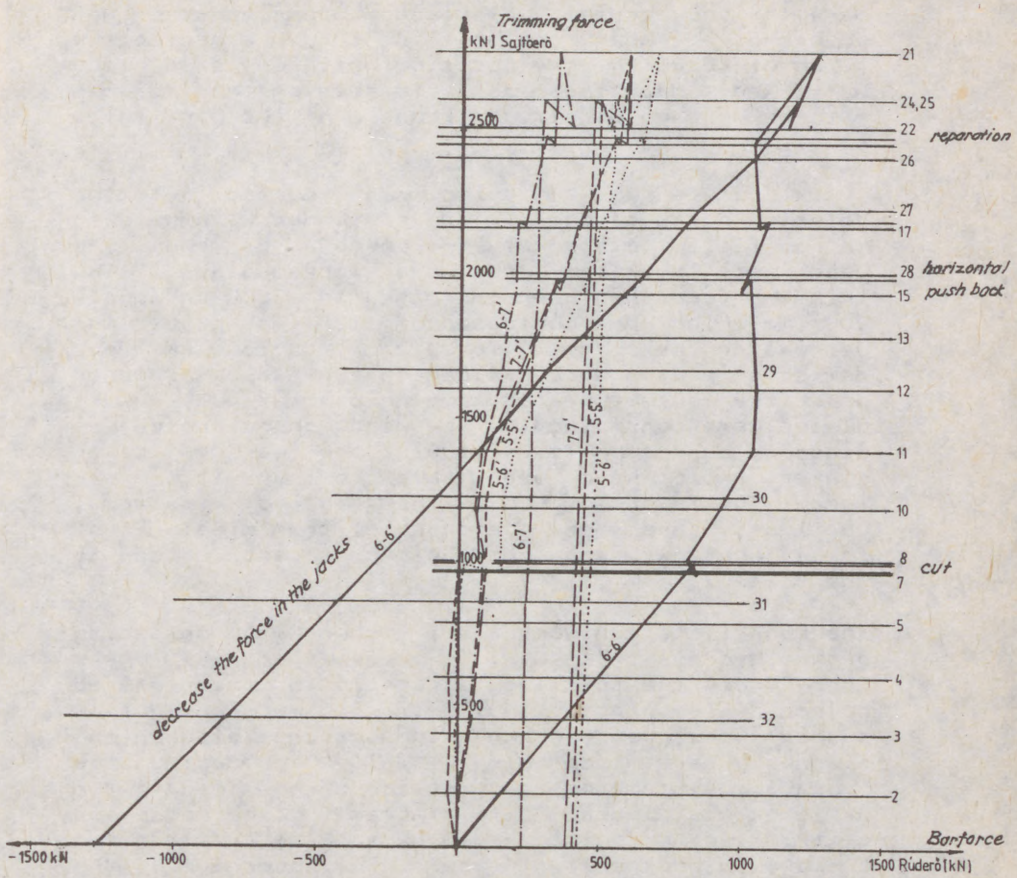

Fig. 3.

HS bolt connection, which temporarily fixed the broken bar ends, was released.

b) According to the -871 kN residual force determined earlier -1000 kN force was entered in 200 kN steps by the hydraulic jacks, trimming the bar this way. The force in bar 6-6' proved to be a little less, than forcasted (-800 kN), because a part of the force was taken by neighboring bars. After that the column ends at the location of damage were fully cut. During the successive cutting of the elements of the column's cross-section, - as it can be seen on the bar-force vs. press-force diagram - no considerable change has been observed either in the press- or in the bar-force.

c) The trimming force had been increased to -2000 kN.

(6)

Here the horizontally displaced upper bar-end was pushed back. When the trimming force acheived the value of -2500 kN, the position of the upper bar end was fixed. Meantime - as it is seen on the diagram - there were no significant change of the bar force 6-6'.

d) Next day's work started with cuttig out the defected parts of the bar and continued with welding in a filler plate at the corroded bar end. The upper and lower bar ends were worked plane. The trimming force had been increased to -2800 kN and a 200 mm high prefabricated filler was placed in. Decreasing the trimming force back to -2500 kN four new cover plates were welded to the flanges placed under the gusset plates, using butt-weld. Gusset plates were connected to the eight chord angles by close tolerance bolts. Altought the four new cover plates would have been able to transmit the bar force sufficiently, for the sake of material continuity and more favourable transmission of force, the lower and upper bar ends were welded to the filler.

e) The rehabilitation work was finished with unloading of the hydraulic jacks, i.e. transmitting the press force from the trimming structure to the repaired column. Temporarily built-in trimmer and gusset plates were removed and the bracings between the flanges were replaced. While unloading the hydraulic system the transmission of the load to the bar 6-6' was linear (c.f. diagram). The reduction of trimming-force from -2610 kN to 2 kN resulted in a -2548 kN compression force on the upper end of the bar and -2816 kN in the lower one.

After the reconstruction of bar 6-6'had been completed a loading test was carried out so as to examine the behaviour of the reinforced bar when the live load is close to its maximum design value. A similar loading for the column 9-9' was carried out at the same time. During the test strains of the bar elements were measured and from these stresses and bar forces were determined. Bar forces obtained in bars 6-6' and 9-9' were cca 20% less, then the calculated ones, probably due to approximations of the stringer's statical system. It was also observed that dispite of the crookedness of bar 9-9'the measured bending moment was not significant.

A second loading test (both static and dynamic) was carried out after the reconstruction had been finished, prior to the start of traffic, using 30 trucks, 20 tons each.

(7)

On the basis of experiences collected by the Departement during reconstruction work and loading tests we concluded that present public transport (trams and buses) can be maintaned till the centenary of the bridge, of assuming an enhanced controll. Afterwards only pedestrian and car traffic may be allowed. This decision means, that by the year of 2000 the construction of a new bridge (at Lágymányos) and a new subway line will be necessary.

(1)
TEMPLE, Murray C. (1)
MOK, Kenneth Hon-Wa (2)

STARRED ANGLES SUPPORTING SECONDARY TRUSSES

INTERNATIONAL COLLOQUIUM
STABILITY OF STEEL STRUCTURES
BUDAPEST, HUNGARY, 1990
PRELIMINARY REPORT

Summary: In some large industrial buildings it is common to span large areas by using primary trusses in one direction and secondary trusses in the other. The secondary trusses frame into the vertical web members in the primary truss. Because of their symmetrical cross-section and the ease with which the connections can be made, starred angles are frequently used as the vertical web members in primary trusses. These starred angles are usually designed as axially loaded members but the open nature of the cross-section and the fact that the secondary truss frames into one of the angles has raised some doubts about this loading assumption.

As a result of this concern, an experimental research program was undertaken to investigate the behaviour and strength of starred angles supporting secondary trusses. The results obtained indicate that these starred angle compression members are not concentrically loaded as the stress distribution across the angles varies greatly. It was found that if the slenderness ratio is modified, the load carrying capacity can be calculated in accordance with the requirements of the Canadian steel standard.

INTRODUCTION

The use of trusses is an economical way to support roofs which cover large areas. These trusses are often arranged in two mutually perpendicular directions but at different elevations. The secondary trusses support roof beams which run in the same direction as the primary trusses. Thus the secondary trusses must frame into the primary trusses at a lower elevation so that the top of the roof beams are at the same elevation as the top of the primary trusses. A convenient way of framing the

(1) Professor of Civil Engineering, University of Windsor, Windsor, Ontario, and
(2) Former Graduate Student, Department of Civil and Environmental Engineering, University of Windsor, Windsor, Ontario, N9B 3P4; currently Plan Examiner, City of Windsor, Windsor, Ontario.

(2)

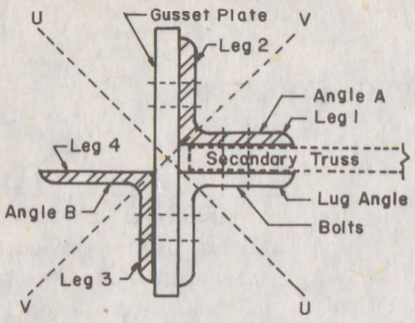

Fig. I - STARRED ANGLE

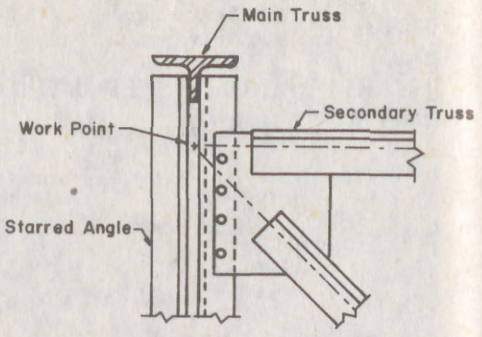

Fig. 2 - CONNECTION DETAIL

secondary truss into the primary truss is to use starred angles as the vertical web members in the primary truss.

The worst situation for this truss–to–truss connection occurs at the exterior of the building, with the primary truss parallel to the exterior of the building and a secondary truss framing into the primary truss from one side only. This unsymmetrical connection will be used in this research.

Because of the ease with which the connections can be made, starred angles (see Fig. 1) are often used as vertical web members in primary trusses to support the end reactions from the secondary trusses. A typical connection is illustrated in Fig. 2. It will be noted that the work point of the connection coincides with the longitudinal centroidal axis of the starred angle. Thus, in design, the starred angle is designed as if the member is axially loaded. The open nature of the cross section and the fact that the secondary truss frames into one angle only, has resulted in some concern about this axial loading assumption. This concern was the reason this research was undertaken.

REQUIREMENTS IN VARIOUS STANDARDS AND SPECIFICATIONS

An examination of the standards and specifications reveals nothing directly related to the design of starred angles supporting secondary trusses. ASCE Manual 52 "Guide for Design of Steel Transmission Towers" (American Society of Civil Engineers 1988) specifies that the effective length factor, K, depends upon the type of connection used. For example, with single angles with normal framing eccentricities at both ends of the unsupported panel and with an $L/r \leq 120$

$$[1] \quad \frac{KL}{r} = 60 + 0.50 \left(\frac{L}{r} \right)$$

where L = length of the compression member, and r = the least radius of gyration. For members unrestrained against rotation at both ends of the unsupported panel, and $120 \leq L/r \leq 200$

(3)

[2] $\frac{KL}{r} = \frac{L}{r}$

EXPERIMENTAL PROGRAM

Test Program

The experimental program involved the testing of eleven starred angle compression members. Five specimens were tested as concentrically loaded compression members and the other seven were tested with the main load being applied through a truss. In order to reduce the number of variables the same size angles 1 3/4 x 1 3/4 x 3/16 in. (45 x 45 x 5 mm), were used in all tests. Two different lengths of specimens were used and these were 2100 and 1270 mm. These lengths were measured from the knife edge at the top to the corresponding knife edge at the bottom of the specimen. The two lengths resulted in slenderness ratios, L/r_v, of 124 and 75, respectively, where r_v = the minimum radius of gyration of the cross section. Thus the specimens can be classed as "slender" or of "intermediate length."

For simplicity the specimens will be referred to as a Type C, B or W in order to differentiate between loading conditions and connection details. The different types of columns may be described as follows:

(a) Type C Specimens. The letter "C" indicates that the specimen is a starred angle that is loaded concentrically. These test results were run to provide "base data" that can be used as a basis for comparison with the load carrying capacities of starred angles loaded through secondary trusses. Five type C specimens were tested, three 2100 mm in length and two 1270 mm long.

(b) Type B Specimens. The letter "B" is used to denote a specimen in which a bolted connection is used to connect a truss to a starred angle. The starred angle was loaded to failure by applying a load to the truss. This is the most common type of arrangement and is illustrated in Fig. 2. Four type B specimens, two 2100 mm long and two 1270 mm in length, representing the vertical web-members of a primary truss, were loaded to failure by applying a load to the secondary truss.

(c) Type W Specimens. The letter "W" indicates that the gusset plate is welded to the angles. In all other respects the specimens were the same as the Type B specimens.

Specimen Designation

Each specimen, for simplicity, was designated by a test series number. For example, B2100.1 indicates that the specimen was a Type B specimen, 2100 mm in length, and the first specimen of its type tested.

Test Set-Up

All specimens were tested with double knife edges top and bottom.

(4)

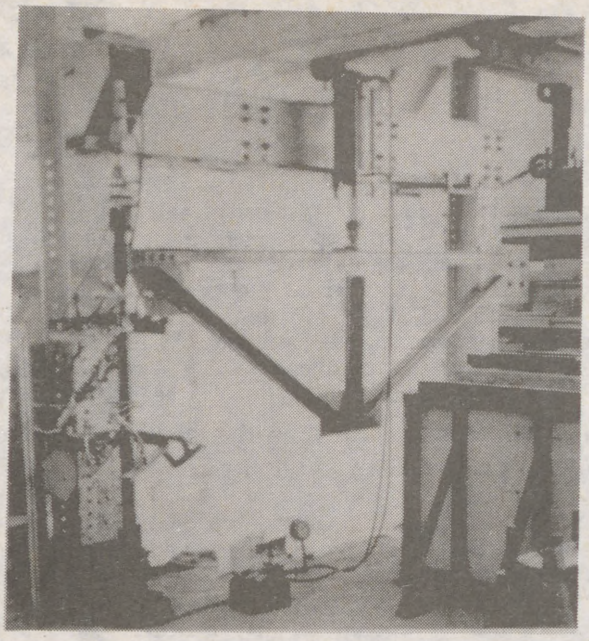

FIG. 3 – TEST SET–UP

The Type C specimens were tested under an axial load in a loading frame in the Structural Engineering Laboratory.

The complete test set–up for Type B and Type W specimens is shown in Fig. 3. A simple steel truss was fabricated and bolted at one end to the specimen and at the other end to an existing column of the structural testing frame in the Structural Laboratory.

Strain Gages

Strain gages were attached to the legs of the angles in the Type B and Type W specimens in order to determine the stress distribution across each leg of each angle of the specimen. As many as twenty–four 90 degrees rosette strain gages were installed across the legs of the angles.

Test Procedure

During the testing of the Type C specimens, the load was applied slowly in increments of 8.9 kN. At about 80 percent of the predicted failure load, the load increment was reduced to 2.2 kN. The load increment was applied until failure occurred, which was taken as the load at which a large increase in lateral deflection resulted from a very small increase in load.

(5)

At the start of each test for a Type B or Type W specimen, a load of 4.45 kN was first applied by using the jack at the top of the specimen. This load was kept constant throughout the test. This axial load was used to represent the load in the vertical web member of the truss that resulted from the loads applied directly to the primary truss but not including the end reactions from the secondary trusses. The total load applied to the specimen was measured by the load cell at the bottom of the specimen. The load was applied to the truss so that 4.45 kN increments resulted in the specimen. This load increment was used until the specimen failed.

RESULTS

General

The mechanical properties of the steel were determined from tensile tests. The average value of the yield stress and modulus of elasticity were determined to be 390 and 205 400 MPa, respectively. These values were used in all computations.

Failure Loads

Theoretical Results. The compressive resistance for the Type C specimens, as listed in column 3 of Table 1, were calculated using the equations in the Canadian Steel Standard. A resistance factor of 1.0 was used.

Experimental Failure Loads. The experimental failure loads are tabulated in Table 1.

Table 1. Experimental Failure Loads

Specimen Number	Experimental Failure Load P_{ex} (kN)	Compressive Resistance C_r (kN)	$P_{ex}C_r$ (%)
C2100.1	89.0	88.0	101
C2100.2	93.9	88.0	107
C2100.3	93.4	88.0	106
C1270.1	197.3	177.5	111
C1270.2	216.9	177.5	122
B2100.1	91.9	88.0	104
B2100.2	91.9	88.0	104
B1270.1	133.8	124.3#	108
B1270.2	123.8	124.3#	100
W2100.1	97.9	88.0	111
W2100.2	99.9	88.0	113

#Values are based on the modified slenderness ratios suggested by ASCE Manual 52.

(6)

The experimental failure loads for the Type C specimens agree quite well with those predicted using the requirements of the Canadian Steel Standard. Hence, it can be concluded that these values can be used as "base data" for comparison with the failure loads obtained for the Type B and W specimens.

The slender Type B and Type W specimens, the starred angles loaded primarily through the secondary truss, had failure loads which are very close to those obtained for the same length Type C specimens, i.e. C2100. The reason for this will become evident when the stress distribution in the legs of the angles is examined. The W2100 specimens had failure loads which are six to eight percent higher than the failure loads obtained for the B2100 specimens.

For the B1270 specimens, the failure loads are 133.8 and 123.8 kN. These failure loads are some 30 to 40 percent lower than the failure loads obtained for the C1270 specimens. The drop in load carrying capacity can be explained when the stress distribution in the legs are examined. Thus, it can be concluded that starred angles of intermediate length supporting secondary trusses cannot be designed as axially loaded columns.

In order to achieve a better relationship between the experimental and theoretical results, a combined approach is suggested. In this approach, the starred angle members supporting secondary trusses are designed as axially loaded members according to the requirements of the Canadian Steel Standard. The effective length factors, however, are modified in accordance with the requirements of ASCE Manual 52. In Table 1, a comparison is made between the compressive resistances calculated using this approach and the experimental results. It is observed that by modifying the slenderness ratio, the Canadian Steel Standard gives better results than simply calculating the compressive resistance of the starred angle as an axially loaded member.

Stress Distribution

Fig. 4 shows the stress distribution across the angles for Specimen B2100.1. In these figures, the angles have been straightened out to lie flat on the sheet of paper. Angles A and B, and Legs 1 to 4 are shown in Fig. 1. Both angles display a similar trend. The stress relationship is linear at small loads. This probably reflects the influence of the 4.45 kN axial load applied at the top of the specimen. As the load on the truss is increased, and hence the load on the specimen, the stress across the cross section becomes nonlinear. When the failure load is reached, the tips of Legs 2 and 4 are subjected to tensile stresses while the other edges of the angles are subjected to high compressive stresses, up to about 300 MPa, but still below the yield stress of 390 MPa. It should be pointed out that the stress distribution curves for the W2100 specimens are very similar to those shown in Fig. 4.

It will be noted that Angle A carries more of the applied load than Angle B. At about 50 percent of the failure load, Angle A carries about 60 percent of the load, but this gradually reduces to 55 percent at the failure load. It will also be noted that Legs 1 and 3 carry most of the applied load.

In the intermediate length columns B1270, the stress, as shown in Fig. 5 (a) and (b), at failure in Leg 1 is equal to the yield stress of 390 MPa. In Leg 2, although

(7)

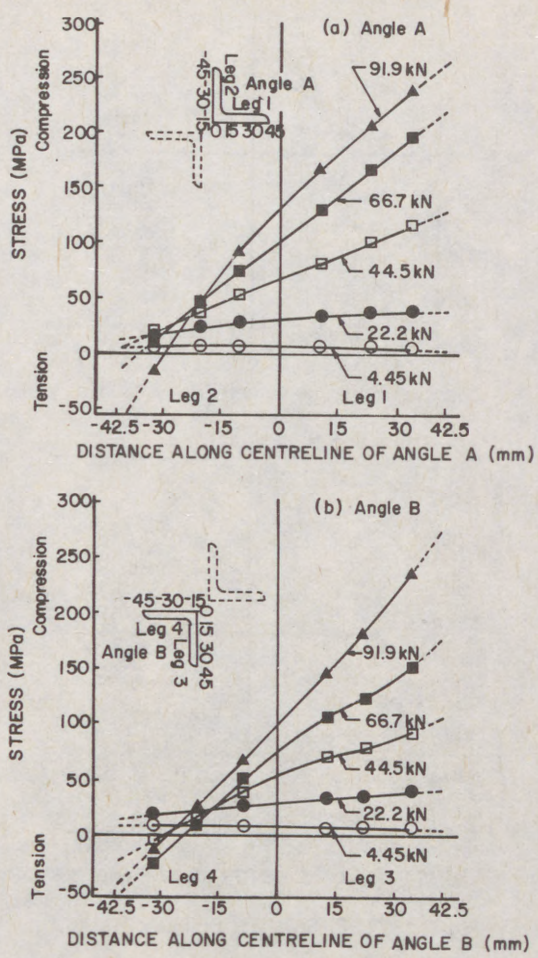

Fig. 4- STRESS DISTRIBUTION B2100.1

measurements of strain were not made right at the tip, it appears that the stress reached the yield stress in tension. It will be noted that in Leg 3, the stress at high loads actually started to decrease. This is due to local buckling of the leg.

CONCLUSIONS

The following conclusions for starred angles supporting secondary trusses are based on the preceding work:

1. Standards and specifications do not cover the design of such members.

(8)

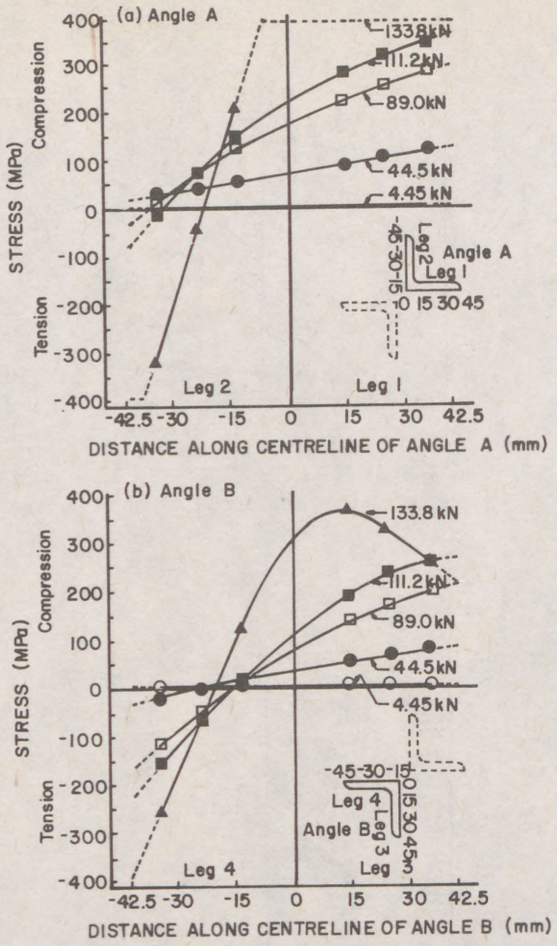

Fig. 5 - STRESS DISTRIBUTION B1270.1

2. The experimental results for intermediate length members indicate that such members cannot be designed as axially loaded members.

3. A simplified design method for such angles is proposed. In this approach the effective length factors are modified in accordance with the requirements of ASCE Manual 52. The compressive resistance is then calculated according to the requirements of the Canadian Steel Standard.

4. Angle A carries more load than Angle B (see Fig. 1) and Legs 1 and 3 carry much more load than Legs 2 and 4.

REFERENCES

American Society of Civil Engineers. 1988. Guide for design of steel transmission towers. ASCE Manuals and Reports on Engineering Practice. No. 52, New York, N.Y.

SESSION 4

BEAMS

(1)

AGOCS,Zoltan [1]

ANALYSIS OF THIN-WALLED MULTI CELLS BEAMS WITH DEFORMABLE CROSS SECTION.

INTERNATIONAL COLLOQUIUM
STABILITY OF STEEL STRUCTURES
BUDAPEST, HUNGARY, 1990
PRELIMINARY REPORT

Summary:
A method for analysis of multi cells thin-walled beams with deformable cross section according the Sedlacek's theory is carried out.The opportunity of simplification of the solution by "beams on elastic foundation" analogy is studied.

1.INTRODUCTION.

Many different methods for the analysis of thin-walled beams have benn presented in recent time.A good view of them is given in [5].The exact solution using numerical methods(finite elements,finite strips,folded plates) needs powerful computer programs and doesn't offer the opportunity for studying the structural response to different kinds of actions.

Simplified models are applicable in everyday engineering practice.They are expected to give correct insight into the analysis of the various aspects of the structural behavior. Sedlacek's theory [6] gives an opportunity for following the influence of the different kinds of loading to the structural response(axial loading, bending, torsion, distortion, shear lag, etc.).A relatively simple analytical model for each of them can be obtained.The influence of various symplifying assumptions in the accuracy of the analysis of single cell beams is studied in [3],[5],[8].

This article deals with a suitable method for analysis of three cells box girders using Sedlacek's theory.

---

[1] Ph.D.student
Department of Steel and Timber Structures
Slovak Technical University, Bratislava, Czechoslovakia

(2)

2.THEORETICAL FOUNDATIONS OF THE METHOD.

The basic assumptions of the theory are presented in [6], [8]. According them a beam, with deformable cross section of three cells (fig.1), has three additional degree of freedom (cross sectional displacement) due to distorsion (fig.2).The associated deplanations (shape functions) obtained after the orthogonalization with the deplanations of rigid body ($1,x,y,\omega - v_1,\ldots,v_4$) are showed on fig.2, too.

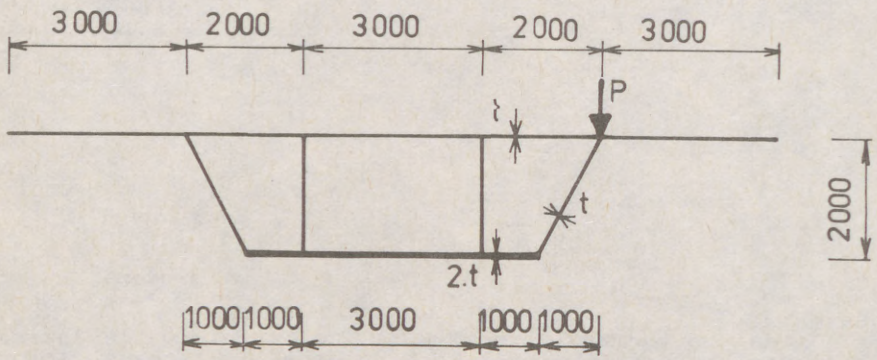

Fig.1

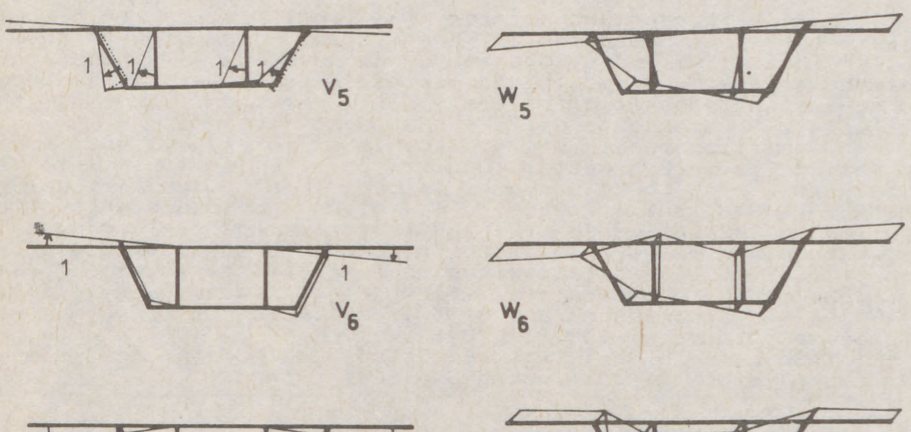

Fig.2

(3)

The system of differential equations describing the problem in terms of displacements can be obtained from the conditions of equilibrium of the virtual works in form :

$$E.J_{ij}.v_i^{IV} - G.K_{ij}.v_i^{II} + R_{ij}.v_i = P_i \qquad i=1,2,..,7 \qquad (2.1)$$

where :

$J_{ij} = \int_A w_i . w_i . dA$ is the axial.bending and warping stiffness respectively

- A is the area

$K_{ij} = \int_A \frac{\psi_i}{t} . \frac{\psi_j}{t} . dA$ is the shear stiffness

- ψ_i is the shear flow in closed parts

$R_{ij} = \int_A \frac{m_i . m_j}{E.J_R} . dA$ is the transverse bending stiffness

- m_i is the transverse bending moment
- I_R is the transverse moment of inertia

Four equations from this system are independent (v_1, v_2, v_3, v_7)- have only diagonal members. Three other are coupled together due to extra-diagonal members in matrices J^* and R^*. A linear combination of the general coordinates has to be done to obtain a separate differential equation for each degree of freedom. The full forms of stiffness matrices are :

$$J = \begin{bmatrix} J_{11} & 0 & 0 & 0 & & & 0 & \\ 0 & J_{22} & 0 & 0 & & & & J^* \\ 0 & 0 & J_{33} & 0 & & & & \\ 0 & 0 & 0 & J_{44} & J_{45} & J_{56} & 0 & \\ & & & J_{54} & J_{55} & J_{56} & 0 & \\ & 0 & & J_{64} & J_{65} & J_{66} & 0 & \\ & & & 0 & 0 & 0 & J_{77} & \end{bmatrix} \qquad K = \begin{bmatrix} 0 & & & & 0 & K^* \\ & K_{44} & & & & \\ & & & 0 & 0 & 0 \\ 0 & & & 0 & K_{66} & 0 \\ & & & 0 & 0 & J_{77} \end{bmatrix}$$

$$R = \begin{bmatrix} 0 & & & 0 & R^* \\ & & & R_{55} & R_{56} & 0 \\ & 0 & & R_{65} & R_{66} & 0 \\ & & & 0 & 0 & J_{77} \end{bmatrix} \qquad (2.2)$$

Where :

J_{11} is the area

J_{22}, J_{33} are the moments of inertia for bendig (J_x, J_y)

J_{44} is the moment of inertia for torsion (J_ω)

J_{55}-J_{77} are the moments of inertia for distorsion

The full orthogonalization of all three matrices is not possible, mathematically. The selection of suitable pair of matrices for orthogonalization is studied in [1],[7],[9]. The works [7],[9] deal with the method using the pair of matrices J and R. Results obtained in [7] shows, that the neglecting of the coupling effects in matrix K is not acceptable for the solution

(4)

3. THE ORTHOGONALIZATION METHOD FOR MATRICES J AND K.

The process of orthogonalization of matrices J and K consists of two steps :

1. Zero setting the extra-diagonal members in sub matrix J^* see (2.2)
2. Zero setting the members on opposite diagonal by solving the characteristic system :

$$| I_{ij} - \lambda_i . K_{ij} | . e_{ij} = 0 \qquad (3.1)$$

After the orthogonalization process the sub matrices J^*, K^*, R^* become forms :

$$J^* = \begin{bmatrix} J_{\bar{4}\bar{4}} & 0 & 0 \\ 0 & J_{\bar{5}\bar{5}} & 0 \\ 0 & 0 & J_{\bar{6}\bar{6}} \end{bmatrix} \qquad K^* = \begin{bmatrix} K_{\bar{4}\bar{4}} & 0 & 0 \\ 0 & 0 & 0 \\ 0 & 0 & K_{\bar{6}\bar{6}} \end{bmatrix} \qquad R^* = \begin{bmatrix} R_{\bar{4}\bar{4}} R_{\bar{4}\bar{5}} R_{\bar{4}\bar{6}} \\ R_{\bar{5}\bar{4}} R_{\bar{5}\bar{5}} R_{\bar{5}\bar{6}} \\ R_{\bar{6}\bar{4}} R_{\bar{6}\bar{5}} R_{\bar{6}\bar{6}} \end{bmatrix} \qquad (3.2)$$

The shapes functions of the cross section are transformed due to orthogonalization process (fig.3) and a fictive value of "transverse bending stiffness" for the torsion evaluates in matrix R^*. The system of differential equations is coupled only throw the extra-diagonal members in matrix R^*.

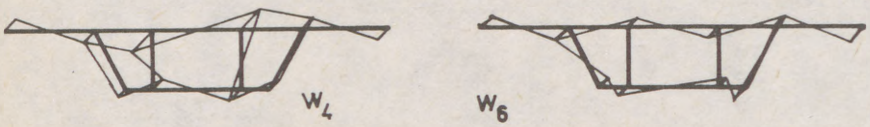

Fig.3

Each of the equations is analogous to the equation of straight prismatic bar on elastic foundation subjected to bending and axial loading (fig.4). The "axial loading" exists only in the case of antisymetrical shape function and the "elastic foundation" exists only if the transverse bending stiffness has nonzero value.

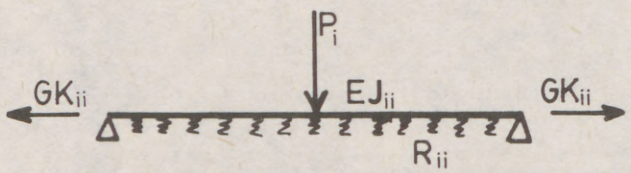

Fig.4

Ordinary beams static can be used for the solution if the coupling effect of the system is neglected. The influence of such assumption is parametrically studied in part 4.

(5)

4.NUMERICAL EXAMPLE.

The above method for using Sedlacek's theory is applycated for three cells simply supported box girder according the static scheme on fig.5.

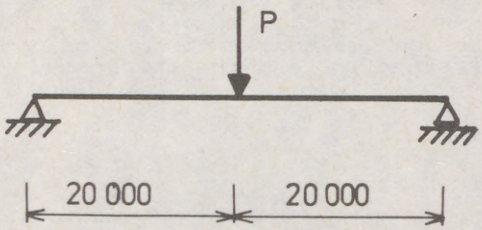

Fig.5

For solving the full system of differential equations an iteration was used. The influence of the simplified solution for changeable thickness of panels is showed in diagrams on the fig.6 in terms of the values of distortional bimomets for the cuopled degrees of freedom. The curves for the solution without and with the effect of shear deformations according the Heilig's theory [3],[8] are presented.

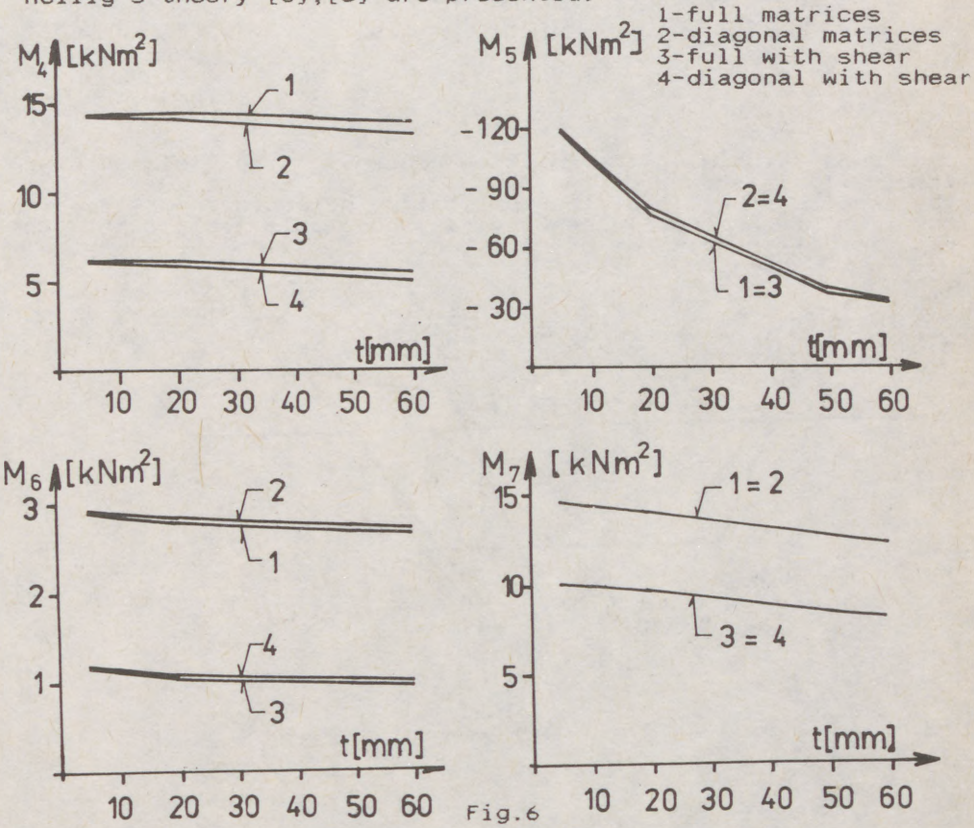

Fig.6

(6)

The longitudinal stress is calculated from :

$$\sigma = \sum \frac{M_i}{J_{ii}} \cdot w_i \qquad (4.1)$$

The influence of the plate thickness for the values of global stresses is exspressed by the coefficient γ (fig.7). The additional stresses due to the distortion of the cross section get smaller with the increassing thickness.

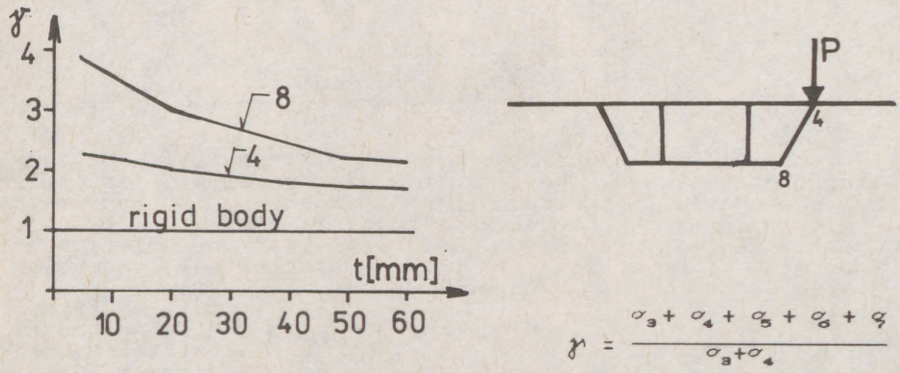

Fig.7

The comparision with the solution according the folded plate theory [2] is showed on fig.8.
The results shows, that the application of above theory for the solution of three cells beams gives acceptable insight into the behavior of these kinds of structures.

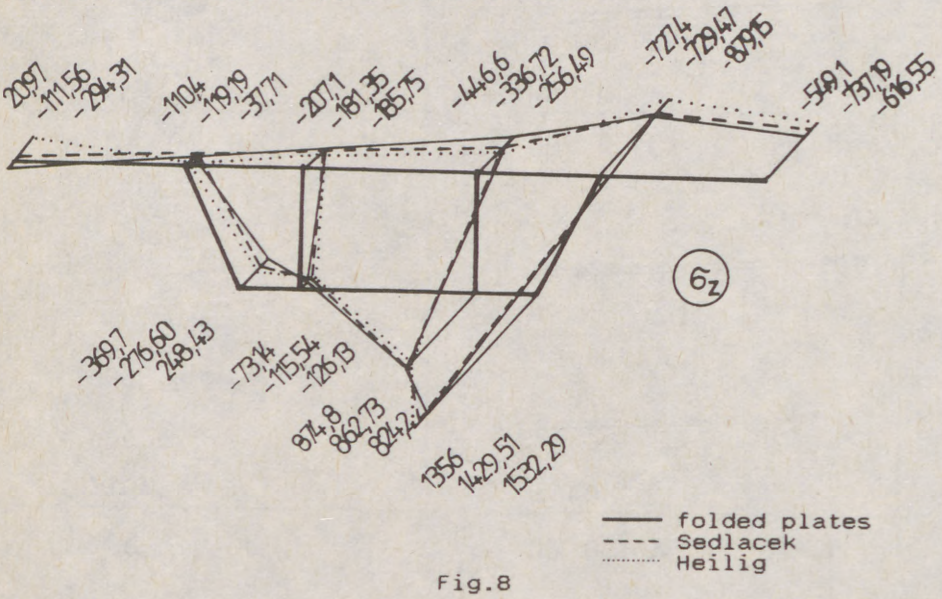

Fig.8

(7)

REFERENCES.

[1] Agocs,Z. (1987):Pridavna napatost tenkostennych komorkovych nosnikov od zmeny tvaru prierezu.(Additional stresses in thin-walled box beams due to distortion.)
Diploma thesis.SVST Bratislava

[2] Belica,A.(1988) :Unosnost tenkostennych uzavretych prierezov (Load bearing capacity of thin-walled box girders)
PhD thesis.SVST Bratislava

[3] Hajdin,N.,Mandic,R.(1988):A contribution to the analysis of box beams with deformable cross section.
Journal of Constructional Steel Research,Vol.9,No.2

[4] Heilig,R.(1961,1963):Beitrag zur Theorie der Kastenträger beliebiger Querschnittsform.
Der Stahlbau 11/61,2/63

[5] Maisel,B.I.(1982):Analysis of concrete box beams using small computer capacity.
Cement and Concrete Association,Development Report 5

[6] Sedlacek,G.(1968):Sytematische Darstellung des Biege und Verdrehvorgamges für prismatische Stäbe mit Dünnwandige Querschnitt unter Berucksichtignung der Profilverformung
Fortschritt-Berrichte VDI-Zeitschrift,Tiehe 4,Nr 8

[7] Sokol,M (1986):Parametricka studia na vystihntie ochabnutia smykom pri uzavretych prierezoch mostneho typu.(Parametric study for description of shear lag in bridge box girders)
Diploma thesis.SVST Bratislava

[8] Tesar,A.(1977):Kovove konstrukcie a mosty.Moderne ocelove mosty.I,II (Metallic constructions and bridges.Modern steel bridges)
ES SVST,Bratislava

[9] Tesar,A.& col.(1986):Priecne stuzenie tenkostennvch sustav. (Transverse stiffness of thin-walled systems)
Zaverecna sprava temy c. III-3-4/10.4a,I.cast
Closing report of the theme.

Dr. H. de Jong (1)

AN APPROACH TO MORE COMPLICATED LATERAL BUCKLING PROBLEMS

INTERNATIONAL COLLOQUIUM
STABILITY OF STEEL STRUCTURES
BUDAPEST, HUNGARY, 1990
PRELIMINARY REPORT

SUMMARY In this paper the lateral buckling of a girder with varying cross section, varying loading and one or two planes of symmetry is discussed. It is shown that the adapted Merchant-Rankine formula can be replaced by an ECCS-buckling curve.

1. Introduction

The codes regarding lateral buckling deal with the simplest, though very important, cases. Disregarding the finite element method and considering rigid cross sections only, some cases - to be met frequently in daily practice - cannot be dealt with:
- Cross sections with only one plane of symmetry are not discussed.
- If the cross section varies, it is not clear which full plastic moment has to be inserted in the adapted Merchant-Rankine formula:

$$\frac{1}{M^{1,5}_{r;lb}} = \frac{1}{M^{1,5}_{pl}} + \frac{1}{M^{1,5}_{E;lb}} \qquad (1)$$

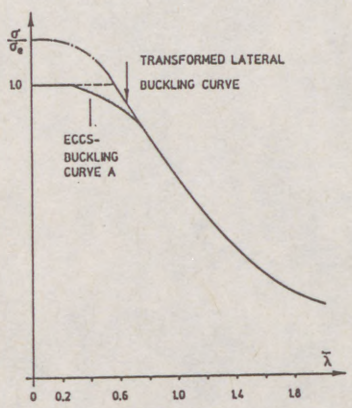

Fig. 1

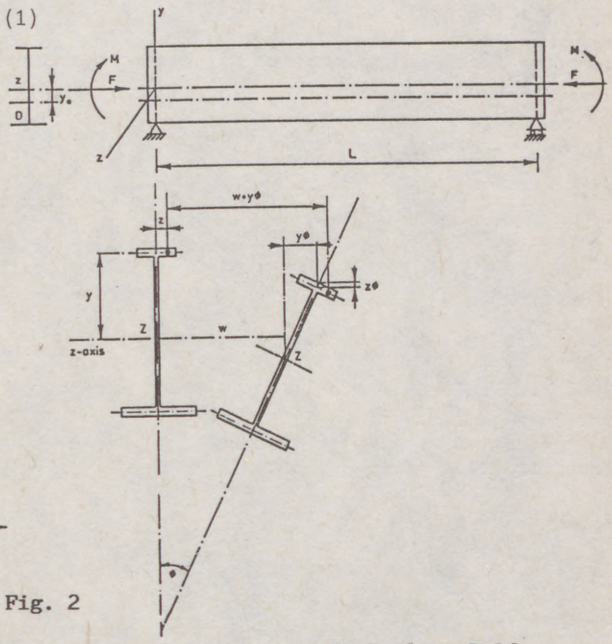

Fig. 2

(1) Senior lecturer Steel structures, University of Technology Delft

2. The Merchant-Rankine curve / ECCS-curve

Lateral buckling is composed of two components: buckling and torsional buckling (Eq. (27)). For each buckling mode the (dutch) code allows the use of the ECCS-buckling curves. For lateral buckling however the Merchant-Rankine concept, Eq. (1), is used. This seems to be inconsistent. The two extreme situations, buckling and torsional buckling, are calculated using the ECCS-buckling curves, while a combination of the two requires a different curve.
A simple transformation of Eq. (1) shows the similarity between the curve obtained from Eq. (1) and the ECCS-buckling curve-a (fig. 1).

Conclusion:
Eq. (1) may be replaced by the ECCS-buckling curve-a.

3. The energy equation.

The energy equation describing the lateral buckling problem can be derived after some tiresome mathematical operations. Only an outline is presented here.
The displacement of the centre of gravity in z-direction, is w (fig. 2-b).
The rotation of the cross section is ϕ.
In an arbitrary point of the cross section, (y,z), the displacement in x-direction, u, is:

$$u = (w' + y\,\phi')\,z \tag{2}$$

Starting from the fundamental situation, the strain energy in the girder, due to bending, is given by:

$$U_1 = \int_V \frac{E}{2}\,u'^2\,dV = \frac{E}{2}\int_0^L dx\,\left[\int_A (w'' + y\,\phi'')^2\,z^2\,dA\right] \tag{3}$$

With:

$$\int_A y^2\,z^2\,dA = \Gamma \tag{4}$$

$$\int_A y\,z^2\,dA = \psi \tag{5}$$

we obtain the equation for strain energy:

$$U_1 = \int_0^L \frac{E}{2}\left[\,I_y\,w''^2 + \Gamma\,\phi''^2 + 2\,\psi\,w''\,\phi''\,\right]dx \tag{6}$$

This equation is simplified by a transformation (fig. 2-b and 3):

$$w + y\,\phi := w + (y - y_o)\,\phi \tag{7}$$

and for the centre of gravity Z,(0,0):

$$w := w - y_o\,\phi \tag{8}$$

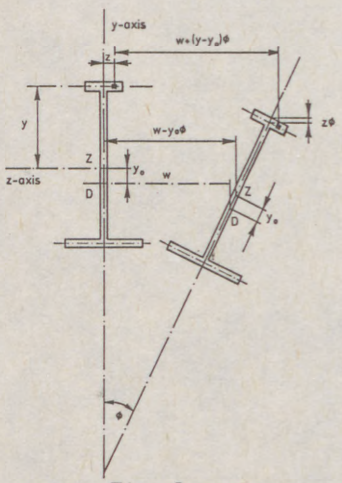

Fig. 3

Substituting Eq. (8) into Eq. (6) we obtain:

$$\int_0^L \frac{E}{2} [I_y (\ddot{w}^2 - 2 y_o \ddot{w} \ddot{\phi} + y_o^2 \ddot{\phi}^2) + \Gamma \ddot{\phi}^2 + 2 \psi (\ddot{w} - y_o \ddot{\phi}) \ddot{\phi}] \, dx \qquad (9)$$

Suppose y_o to be chosen so that: $y_o = \frac{\psi}{I_y}$ (10)

From Eq. (7) it follows that the displacement of point D,$(y_o,0)$, is no longer determined by rotation, which means that D must be the centre of shear. Substituting Eq.(10) into Eq. (9), eliminating ψ, leads to:

$$U_1 = \int_0^L [\frac{EI_y}{2} \ddot{w}^2 + \frac{E(\Gamma - y_o^2 I_y)}{2} \ddot{\phi}^2] \, dx \qquad (11)$$

Strain energy due to torsion is given by:

$$U_2 = \int_0^L \frac{GI_t}{2} \dot{\phi}^2 \, dx \qquad (12)$$

The increase in potential energy is given by:

$$U_3 = \frac{1}{2} \int_V \{ [\underline{u}^2_{,x} + \underline{v}^2_{,x} + \underline{w}^2_{,x}] \sigma_x + [\underline{u}^2_{,y} + \underline{v}^2_{,y} + \underline{w}^2_{,y}] \sigma_y +$$

$$[\underline{u}_{,x}\underline{u}_{,y} + \underline{v}_{,x}\underline{v}_{,y} + \underline{w}_{,x}\underline{w}_{,y}] \tau_{xy} + [\underline{u}_{,x}\underline{u}_{,z} + \underline{v}_{,x}\underline{v}_{,z} + \underline{w}_{,x}\underline{w}_{,z}] \tau_{xz} \} \, dV \qquad (13)$$

Considering that:

- $\underline{u}_{,x}$ and $\underline{u}_{,y}$ are relatively small and may be neglected,

- $\sigma_y \ll \sigma_x$, so terms with σ_y may be neglected.

$$- \sigma_x = \frac{M_z}{I_z} y + \frac{F}{A} \qquad (14)$$

$$- \underline{v} = v - z \phi \quad ; \quad \underline{v}_{,x} = \dot{v} - z \dot{\phi} \quad ; \quad \underline{v}_{,y} = 0 \; ; \; \underline{v}_{,z} = - \phi \qquad (15)$$

$$- \underline{w} = w + \phi (y - y_o) \; ; \; \underline{w}_{,x} = \dot{w} + \dot{\phi} (y - y_o) \; ; \; \underline{w}_{,y} = \phi \; ; \; \underline{w}_{,z} = 0 \qquad (16)$$

substituting : Eq. (14) to (16) into Eq. (13),
eliminating : v, as buckling with respect to the strong axis is of no importance
introducing : the boundary conditions: for
x = 0 and x = L: $\phi = 0$, $\ddot{\phi} = 0$, $w = 0$, $\ddot{w} = 0$ (17)
using : the identities

$$\int_A \frac{y(y^2 + z^2)}{2I_z} \, dA = C_y \qquad (18)$$

$$\int_A \frac{y^2 + z^2}{A} \, dA = i_p^2 \qquad (19)$$

we finally obtain the expression for the total potential energy U :

$$U = U_1 + U_2 - U_3 \qquad (20)$$

$$U = \int_0^L \left[\frac{EI_y}{2} w''^2 + \frac{E(\Gamma - y_o^2 I_y)}{2} \phi''^2 + \frac{1}{2} GI_t \phi'^2 - M_z \phi' (w' - y_o \phi') - M_z C_y \phi'^2 \right.$$

$$\left. - \frac{F}{2} \{ (w' - y_o \phi')^2 + i_p^2 \phi'^2 \} \right] dx \qquad (21)$$

The principle of minimum total potential energy requires U to be a minimum. If necessary Eq. (21) can be extended by :
- additional conditions by means of the Lagrange multiplier method,
- additional energy terms to allow for lateral elastic springs.

4. Application of the energy equation

Consider a simply supported girder with one plane of symmetry, unchanged cross section, fork-like supports, loaded in bending and compression (fig. 2-a). The boundary conditions Eq. (17) are fulfilled by the formulae:

$$w = a \sin \frac{\pi x}{L} \qquad (22)$$

$$\phi = b \sin \frac{\pi x}{L} \qquad (23)$$

Substitution of Eq. (22) and (23) into Eq. (21) and integration leads to:

$$U = \frac{EI_y}{2} a^2 \left(\frac{\pi}{L}\right)^4 \frac{L}{2} + \frac{E(\Gamma - y_o^2 I_y)}{2} b^2 \left(\frac{\pi}{L}\right)^4 \frac{L}{2} + \frac{1}{2} GI_t b^2 \left(\frac{\pi}{L}\right)^2 \frac{L}{2}$$

$$- M_z (ab - y_o b^2) \left(\frac{\pi}{L}\right)^2 \frac{L}{2} - M_z C_y b^2 \left(\frac{\pi}{L}\right)^2 \frac{L}{2}$$

$$- \frac{F}{2} \{ (a - y_o b)^2 + i_p^2 b^2 \} \left(\frac{\pi}{L}\right)^2 \frac{L}{2} \qquad (24)$$

From the conditions:

$$\frac{\delta U}{\delta a} = 0 \qquad \frac{\delta U}{\delta b} = 0 \qquad (25)$$

it follows that there is a solution, only if:

$$(M_z - y_o F)^2 = \left(\frac{\pi^2 EI_y}{L^2} - F\right) \left[\frac{\pi^2 E(\Gamma - y_o^2 I_y)}{L^2} + GI_t + 2 M_z (y_o - C_y) - \right.$$

$$\left. F (i_p^2 + y_o^2)\right] \qquad (26)$$

As there is only one plane of symmetry we obtain two values for M_z, different in sign and different in absolute value.
For a cross section with two planes of symmetry Eq. (26) reduces to:

$$M_z^2 = M_{E;1b}^2 = \left(\frac{\pi^2 EI_y}{L^2} - F\right) \left(\frac{\pi^2 E\Gamma}{L^2} + GI_t - F i_p^2\right) \qquad (27)$$

Obviously lateral buckling is composed of two components: buckling due to bending and due to torsion. Due to double symmetry we find two values for M_z, equal in absolute value, but different in sign.
To understand the practical implications a simply supported beam with two planes of symmetry, constant bending moment and axial force is investigated.

Suppose F = 0. From Eq. (27) we find, according to the usual procedure:
- the elastic bending moment causing lateral buckling: $M_{E;lb}$
- the elastic lateral buckling stress: $\sigma_{E;lb}$
- the relative slenderness ratio: $\bar{\lambda}$
- the reduction factor χ, using the appropriate ECCS-buckling curve.

However if F ≠ 0, this method gives unreliable results. As lateral buckling is composed of a bending and a torsion component we start with reducing these two components:

$$\left[\frac{\pi^2 EI_y}{L^2} - F \right] \quad \text{is replaced by} \quad \left[\frac{\pi^2 EI_y}{L^2} - \beta_1 F \right] \tag{28}$$

$$\left[\frac{\pi^2 E\Gamma}{L^2} + GI_t - i_p^2 F \right] \quad \text{is replaced by} \quad \left[\frac{\pi^2 E\Gamma}{L^2} + GI_t - \beta_2 i_p^2 F \right] \tag{29}$$

in which: $\beta_1 = \frac{F_{E;b}}{\chi_1 F_{pl}}$ and (30a)

$\beta_2 = \frac{F_{E;t}}{\chi_2 F_{pl}}$ (see fig. 4) (30b)

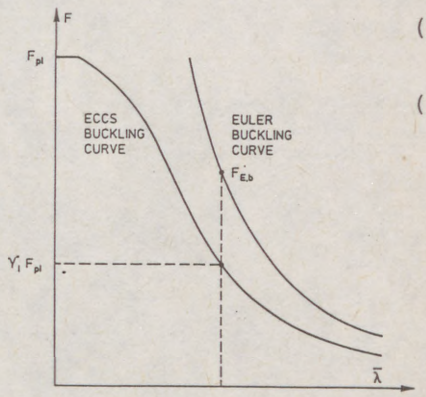

Fig. 4

Substitution into Eq. (27) gives:

$$M^2_{E;lb} = \left(\frac{\pi^2 EI_y}{L^2} - \beta_1 F \right) \left(\frac{\pi^2 E\Gamma}{L^2} + GI_t - \beta_2 i_p^2 F \right) \tag{31}$$

Having introduced these two corrections we can again follow the procedure listed above.
The buckling term and the lateral buckling term are adapted so as to find correct buckling and torsional buckling loads. Consequently the calculated moment might be supposed to equal the correct bending moment for lateral buckling. This leads to an inconsistent calculation method if F = 0. We are then left with the wellknown formula for lateral buckling, to which still the reduction factor χ should be applied.
Matching the sort of cross section to the appropriate buckling curves, we determine β_1 and β_2; for instance for a rolled section, using the ECCS-curve b.

5. Extension of the scope

- There is no problem in extending the method discussed, to cross sections with only one axis of symmetry.
  If $M_z - y_o F = 0$, F acts in the required position for all lateral buckling problems: the centre of shear.

M_z can now be eliminated from the torsional buckling term of Eq. (26) and one value of F is found, generating torsional buckling. The above procedure to determine β_1 and β_2, can be applied again.
For beams with varying cross section, we determine the equivalent I_y, I_t I_z, Γ, y_o, i_p and C_y by equating similar terms in the energy in the real situation and the energy in an equivalent girder with constant cross section.

- An arbitrary loading leading to lateral buckling is replaced by equivalent end moments at both ends of the girder. A varying axial force leading to buckling, is replaced by an equivalent force acting at both ends of the girder, through the centre of shear. Supposing the relationship between the real loading and equivalent loading to be linear, the problem can be solved.
By combination of these options we obtain a solution for arbitrary loading and varying cross section with one or two planes of symmetry.

6. Outline of the solution of the problem, shown in fig. 5.

1. Determine allowable P_{1b} supposing F to be constant.

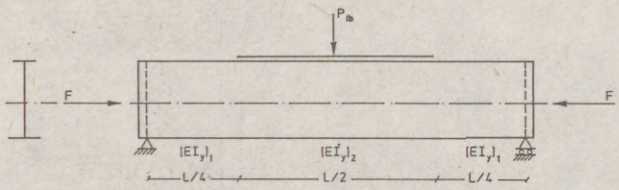

Fig. 5

2. Calculate the cross section constants in sections 1 and 2:
I_y, I_z, I_t, Γ, y_o, i_p, C_y.

3. Calculate the equivalent EI_y from:

$$2 \int_0^{L/4} [EI_y w''^2]_1 \, dx + 2 \int_{L/4}^{L/2} [EI_y w''^2]_2 = \int_0^{L} EI_y w''^2 \, dx$$

with $w = a \sin \frac{\pi x}{L}$

4. In this case the equivalent upper flange thickness can be determined from I_y and the values for I_z, I_t, Γ, y_o, i_p and C_y, matching with the cross section with the equivalent upper flange.

5. From Eq. (21) to (23) we calculate P_{1b} elastically,

   - including β_1 and β_2, determined according to Eq. (30) and par. 5.
   - $M_z = \frac{1}{2} \times P_{1b}$
   - using the correct cross section constants (step 3 and 4),

6. From Eq. (26) we calculate the equivalent end moments M_z elastically, with:
   - M_z is constant and
   - using the equivalent cross section constants (step 4)

7. From Eq. (14) we determine maximum compression: σ

$$\bar{\lambda} = \sqrt{\frac{\sigma_e}{\sigma}}$$

8. From the ECCS buckling curve we determine γ

$$\bar{P}_{lb} = \gamma \frac{\sigma_e}{\sigma} P_{lb}$$

7. Conclusions

- The Merchant-Rankine equation can be abandoned and replaced by an ECCS-buckling curve.
- The presented method:
  - avoids the Merchant-Rankine concept and generalizes the use of the ECCS-buckling curves.
  - can be easily adapted if ever a torsional buckling curve is presented.
  - allows the calculation of a girder with varying cross section, one plane of symmetry and arbitrary loading.
  - allows lateral springs to inserted.

8. Notations

A	:	Cross section of the beam
C_y	:	Constant defined in Eq. (19)
D	:	Centre of shear
E	:	Young's modulus
F	:	Axial force in compression
$F_{E;b}$	:	Euler buckling load; collapse due to bending
$F_{E;t}$	:	Euler buckling load; collapse due to torsion
F_{pl}	:	Full plastic axial force
G	:	Shear modulus
I_y	:	Second moment of inertia with respect to the y-axis
I_z	:	Second moment of inertia with respect to the z-axis
I_t	:	Torsion constant
L	:	Span of the beam
M_y	:	Bending moment with respect to the y-axis
M_z	:	Bending moment with respect to the z-axis

M_{pl} : Full plastic moment with respect to the z-axis
$M_{E;lb}$: Elastic lateral buckling moment
$M_{r;lb}$: Factored lateral buckling moment
U : Total potential energy
U_1 : Strain energy due to bending
U_2 : Strain energy due to torsion
U_3 : Potential energy
V : Volume of the beam
Z : Centre of gravity
i_p : Polar radius of gyration
u : Displacement in x-direction
v : Displacement in y-direction
w : Displacement in z-direction
y_o : Distance between Z and D
Γ : Warping constant
Ψ : Constant defined in Eq. (5)
β : Ratio,defined in Eq. (30), and explained in fig. 4
σ_x : Stress parallel to the x-axis
σ_y : Stress parallel to the y-axis
σ_e : Yield stress
$\sigma_{E;lb}$: Elastic lateral buckling stress
$\bar{\lambda}$: Relative slenderness ratio
γ : Reduction factor, according to the ECCS-buckling curve
ϕ : Rotation of the rigid cross section
τ_{xy} : Shear stress in the cross section, parallel to the y-axis
τ_{xz} : Shear stress in the cross section, parallel to the z-axis

Note

- w' means differentiation of w, or any other variable, with respect to x
- index ,x or ,y or ,z means differentiation with respect to x, y or z respectively.

References

Jong, Dr. H. de, 1981, De Arbeidsmethode toegepast op kipproblemen, Stevin report 6-81-16. University of Technology, Delft, The Netherlands.

(1)
Dr.DULÁCSKA, Endre (1)

LATERAL BUCKLING OF SLANDER BEAMS MADE OF ELASTIC-PLASTIC STEEL MATERIAL

INTERNATIONAL COLLOQUIUM
STABILITY OF STEEL STRUCTURES
BUDAPEST, HUNGARY, 1990
PRELIMINARY REPORT

SUMMARY: Stability problems of slender steel beams are handled by the equilibrium method using a sinle sinusoidal deformation as an approximation. Initial curvature of the beam, nonlinear deformational properties and restraint by the transversal ultimate moment are taken into consideration. A table has been compiled for several load cases, simplifying analiysis of simple beams encountered in practice.

1. INTRODUCTION

The problem of buckling of slander flexural beams made of a linear elastic material may be considered to be solved [Prandtl (1901), Timoshenko (1961)]. So are the buckling problems of beams suspended on vertical [Csonka (1954)] and on skew cables [Korda (1963)], and even the problem of the gradual deformation of suspended beams of an imperfect elastic material. Several achievements in the scope of plastic buckling of steel beams are presented in [Trairhar (1977)]. Analysis methods for the buckling of beams with an initial imperfection on forked-end supports, and for the effect of nonlinear deformability of r.c. beams and of the transverse ultimate moment to reduce the critical load are, however, missing.

These effects will be analysed in the following. For the sake of simplicity, only beams with ends suspended on cables, of with forked-end supports at the extremities will be examined, approximating by lateral deformation a single sinusoidal buckling were due eclusively to the buckling effect of dead load acting in the beam gravity line.

---

(1) Structural chief engineer of
Institute of Architectural Development and Technology
HUNGARY, 1075. Budapest VII. Asbóth u. 9-11.

(2)

2. THE SIMPLIFIED ANALYSIS METHOD

The applied analysis method will be illustrated on a straight, compressed bar. Let the bar be initially rectilinear, with an initial imperfection $w_o=0$ (Fig. 1a). In this case the bending moment M for a slight displacement w:

$M = Nw$.

The sinusoidal deformation has an amplitude $w=Ml^2/\pi^2EI$. Substituting the M value above, $N = \pi^2EI/l^2$, the Euler's critical force, in the following denoted by N_E.

Next, let the amplitude of sinusoidal imperfection be w_o (Fig. 1b), the incremental deformation w_h, and the total deformation $w = w_o+w_h$. Now,

$$w_h = M\, l^2/\pi^2\, EI, \text{ and } M = Nw = N(w_o+w_h), \tag{1}$$

leading to the well-known relationship:

$$w = w_o/\left(1-N/N_E\right). \tag{2}$$

The lateral buckling analysis may be similar to that. Let us consider first a straight beam suspended both ends, such that $w_o = 0$ (Fig. 2a). For a slight lateral twist of the beam, it is bent by horizontal load $p_h=\alpha g$. Centroid of the deflected beam is absolutely in the plane of suspension.

Under this condition, $\alpha = 2w/\pi e$, where e is the height of the point of suspension above the beam gravity line. Hence $w=\pi e\alpha/2$. Or, expressing w in terms of deformation, $w = \left(p_h l^2/8\right)\left(l^2/9.6EI_y\right) = \alpha g l^4/76.8EI_y$. Equating both w values leads to the well known relationship:

$$g \approx 120\ EJ_y e/l^4. \tag{3}$$

It being a critical load similar to the Eulerian critical force of the straight bar, it will be termed Euler-type critical load, denoted by g_E.

Let us consider now the suspended beam with initial imperfection w_o. In this case $w = w_o+w_h$ and $\alpha=2(w_o+w_h)/\pi e$.

Furthermore, $w = \pi e\alpha/2 = \alpha g\, l^4)76.8EI_y + w_o$.

Substituting g_E, and simplifying, $1 = g/g_E + w/w_o$.

Expressing w:

$$w = w_o/\left(1-g/g_e\right). \tag{4}$$

(This formula is similar to (2), thus, the suspended curved beam behaves similarly to the compressed curved bar.) Introducing notation $\xi = w/w_o$,

$$g/g_E = \eta = 1-1/\xi. \tag{5}$$

For a beam suspended on skew rather than on vertical cables, horizontal component of the cable force causes a compressive force in the bar (Fig.2b). The compressive force $N=gl/2\,tg\varphi$, where the cables include an angle φ with the horizontal. The horizontal bending moment

$$M_h = p_h l^2/8+Nw = \frac{2w}{e}\, g\, \frac{l^2}{8} + \frac{gl}{2\ tg\,\varphi}\, w.$$

(3) The deformation:

$$w=w_o+w_h=w_o+\frac{l^2}{\pi^2 EI_y}\left(\frac{2w}{\pi e}\,g\,\frac{l^2}{8}+\frac{glw}{2tg\varphi}\right)=w_o+w\left(\frac{g}{g_E}+\frac{N}{N_E}\right). \qquad (6)$$

Hence $w = w_o/\left(1+g/g_E+N/N_E\right)$,

where g_E is the Euler-type critical load (3), and

N_E the Euler-type critical force.

In conformity with (6),

$$w \to \infty \qquad \text{for } g/g_E + N/N_E = 1 \qquad (7)$$

the Dunkerley formula.
Using notations $B = 6e/l\,tg\varphi$, $\eta = g/g_E$ and $\xi = w/w_o$,

$$\eta = \left(1 - 1/\xi\right)/(1+B) . \qquad (8)$$

Let us consider now the case of a simple beam on forked-end support (Fig. 3). In this case, mid-beam deflection α has to be written as twist of length 1/2.

The torsional moment of the beam end:

$$M_T = \int_0^{1/2} \frac{g}{8}\left(l^2-x^2\right) w_o \frac{\pi^2}{l^2} \cos\frac{\pi x}{l}\,dx = 0.38\ gwl. \qquad (9)$$

Twist angle of middle cross section:

$$\alpha = \int_0^{1/2} \frac{M_T}{GI_T}\,dx = 0.38\ gwl^2/\pi GI_T, \qquad (10)$$

and the horizontal mid-beam deformation:

$$w = \frac{ph\,l^2}{\pi^2} \cdot \frac{l^2}{\pi^2 EI_y} = \frac{\alpha g\, l^4}{\pi^4 EI_y} . \qquad (11)$$

For $I_\omega \neq 0$, substitute torsional moment of inertia in twist:

$$\overline{I}_T = I_T\left(1 + 10\ I_\omega/I_T l^2\right). \qquad (12)$$

Expressing w from (10) and equating to (11):

$$g^2 = \frac{\pi^5}{0.38} \cdot \frac{EI_y\, GI_T}{l^6} .$$

Hence

$$g_E = 28.4\,\frac{\sqrt{EI_y\, GI_T}}{l^3} , \qquad (13)$$

practically identical to the value pbulished in [Timoshenko (1961)].

(4)

For a curved bar, $w_o \neq 0$, then:

$$w=w_o+w_h=w_o+\frac{\alpha g\, l^4}{\pi^4 EI_y}=\frac{0.38 g l^2 w_o}{\pi GI_T}+\frac{0.38\alpha g^2 l^6}{\pi^5 GI_T\, EI_y} \quad . \tag{14}$$

Taking values of (10) and (13) into consideration,

$$w=\frac{w_o}{1-(g/g_E)^2} \quad . \tag{15}$$

Hence $$\eta=\sqrt{1-1/\xi} \, . \tag{16}$$

It is obvious from (15) that deformation under load of the curved beam on forked-end support grows slower than that of the suspended beam. It has the physical explanation that the torsional moment of the suspended beam is limited by the equilibrium condition of suspension while the same for forked end support is not. The lesser deformation is due to the higher torsional moment.

3. NONLINEAR DEFORMATION

The applied steel material is elastic-plastically characteristic, and these are causing nonlinear deformability, to be reckoned with in terms of the curvature:

$$\frac{1}{R}=\frac{M}{EJ}\left[\frac{1}{1-(M/M_u)^m}\right] . \tag{17}$$

The same results from the substitute moment of inertia:

$$\overline{I}=I_o\left[1-(M/M_u)^m\right] \, , \tag{18}$$

where I_o is the initial "elastic" moment of inertia, and M_u the ultimate moment.

Taking m = 6 for the cross section of a beam of ideal elastoplastic material is a rather close approximation of the exact curvature (Fig. 4).

Our analysis showed curvature of lateraly bent elastic-plastic, elasto-plastic steel I beam, to be fairly approximated for a value m=6.

For ideal elasto-plastic cross sections under eccentric load, the ultimate condition is better expressed in terms of ultimate force N_u of the cross section for a given eccentricity t. In this case, M/M_u has to be replaced by N/N_u in (17) and (18) where

$$N_u \approx N_{u,o} / \left(1+nt/h\right) . \tag{19}$$

The $N_{u,o}$ being ultimate force of the cross section under axial load. Factor n was found to be fairly approximated as:

$$n \approx 2\left(2-\frac{1}{1+1.5\, t/h}\right) . \tag{20}$$

4. DETERMINATION OF THE CRITICAL FORCE OR LOAD

Let us consider first a straight bar of an ideal elasto-plastic material, with an initial imperfection of amplitude w_o. Takint (18), (19) and (20) into consideration, and introducing notations $\xi = w/w_o$, $\nu = w_o/h$ and $\beta = N_{u,o}/N_E$, (5) may be written as:

$$\eta = \left(1-1/\xi\right)\cdot\left\{1-\left[\frac{\eta}{\beta}\left(1+n\xi\nu\right)\right]^m\right\}. \qquad (21)$$

Assuming a value $\xi > 1$ in (21), the equation may be satisfied by assigning values to η by the trial and error method, to obtian an N value for a given w. Assuming a succession of ξ values yields a set of N values. This set yields curves N/w/ and $\eta(\xi)$ convex from upside, with the critical load for a given eccentricity w_o as maximum.

For slander beams, equations η similar to (21) may be written. These equations η, and the resulting critical load paramteres η_{cr} have been plotted in Fig. 5. In cases a) and b), parameter $A = N_E w_o/M_{u,o}$ has been applied. For the sake of uniform treatment, in case c) parameter β has been replaced by parameter A in the value $M_{u,o} = N_{u,o}\cdot\left(\frac{h}{4}\right)$ of the ideal elasto-plastic cross section.

As an axample, variation of the critical load parameter η_{cr} of a beam suspended on skew cables vs. parameter A and cableskewness-dependent parameter B has been plotted in Figs. 6a,b, while variation of load parameter η is in Fig. 6c.

Diagrams point out that neglect of the initial imperfection and of the material nonlinearity may cause serious errors to the detriment of safety.

5. ACCOUNTING FOR INITIAL IMPERFECTIONS

Stability of suspended beams is impaired by the inaccurate position of lugs, by beam twisting, and by its curvature in the horizontal or vertical plane. Of them, horizontal curvature is the most essential, the other inaccuracies may be converted to horizontal curvatures by some convenient method. This is why our former studies concerned the effect of horizontal curvature alone.

A beam may suffer horizontal curvature from the following causes:

a) Manufacturing inaccuracies caused by the rolling and velding an curvature, of an empirical value

$$w_{o,a} \approx 1/500, \qquad (22)$$

i.e., for $l = 24$ m, $w_{o,a} \approx 2400/500 = 4.8$ cm.

b) Curvature due to unilateral warming by sunshine, amounting to

$$w_{o,b} = \frac{\alpha_t\ \Delta t\ l^2}{8\ b}, \qquad (23)$$

where α_t is the coefficient of thermal expansion, b the beam width, and t the thermal gradiant across width b.

For b= 30 cm, $_t$= 0,00001 and t= 20°C, and l= 24 m, $w_{o,b}$ = 4.8 cm.

c) Horizontal wind load on the beam, causing a displacement

$$w_{o,c} = \frac{5}{384} \cdot \frac{Pwind\ l^4}{EI_y} \cdot \qquad (24)$$

For l= 24 m, I_y= 15750 cm^4, E= 20600 kN/cm^2, Pwind= 0.45 kN/m^2:

$w_{o,c}$ = 5.98 cm.

d) Horizontal bending caused by slanting roadway. The resulting displacement:

$$w_{o,d} = \frac{5}{384} \cdot \frac{G\ l^4}{EI_y} \qquad (25)$$

where G - uniform dead load of the beam, - slope of the roadway. For G= 3,0 kN/m, and = 0.03, $w_{o,d}$= 1,20 cm for the same beam as above.

e) Beam curvature due to the centrifugal force exerted by the transport vehicle in a bend. The resulting horizontal displacement at mid-beam:

$$w_{o,e} = \frac{5}{384} \bar{m} \frac{v^2}{R} \frac{l^4}{EI_y} \cdot \qquad (26)$$

where v is the vehicle speed, R the curvature radius of the bend, and $\bar{m} = G/g$ where g is the gravity acceleration.
Be R= 150 m, v= 30 km/h=8.4 m/sec, $\bar{m}$= 3.0/9.8=0.305 kNm^2/sec^2, $w_{o,e}$=3.85cm.

The w_o values sum up to 20.63 cm. Coincidence of w_o values from different causes is, however, rather unlikely. The probable value may be estimated as

$$w_{o,max} = \sqrt{w_{o,i}^2} \qquad (27)$$

or, in our example:

$$w_{o,max} = \sqrt{4.8^2+4.8^2+5.98^2+1.20^2+3.85^2} = 9.9 \text{ cm.}$$

For the considered beam of width b= 30 cm, relative curvature = 9.9/30 = 0.33.

REFERENCES

Böröcz, I.(1956): Kiviteli pontatlanságok hatása a végein felfüggesztett négyszögkeresztmetszetü rud stabilitására. (Effect of Constructional Inaccuracies on the Stability of a Rectengular Bar Suspended at Extremities). Mélyépitéstudományi Szemle 6 pp. 105-115.

Csonka, P.(1954): Standsicherheit des an zwei Punkten aufgehängten Rechteckbalken. Bauplanung - Bautechnik 8 pp. 290-293.

Korda, J.(1963): Ferde kötelekkel emelt gerenda stabilitása. (Stability of a Beam Suspended on Skew Cables). Magyar Epitőipar 12 pp. 285-285.

Pettersson, O.(1960): Vippiningsproblem vid hissing och montering av slanka balkar. Nordisk Betong 4 pp. 231.

Prandtl, L(1901): Kipp-Erscheinungen. Dissertation, München. Buchdruckerei R.Stich, Nürnberg.

Tarnai, T.(1978): Lateral Buckling of Elastic Beams with Initial Stresses and Initial Deformations. Acta Techn.Hung. 87 pp. 187-192.

Timoshenko, S.P.(1961): Theory of Elastic Stability. Mc.Graw-Hill Book Comp. New York-Toronto-London.

Traihair, N.S.(1977): Lateral Buckling of Beams and Beam-Columns: (in Chen, W.F. - Atsuta, T.: Theory of Beam Columns. Vol.2) Mc.Graw-Hill Book Comp. New York-Toronto-London.

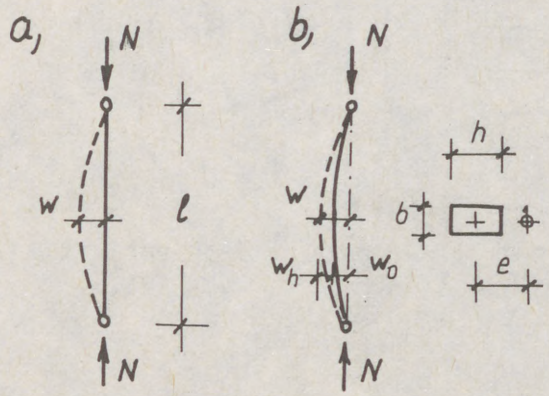

Fig. 1 Bar in compression

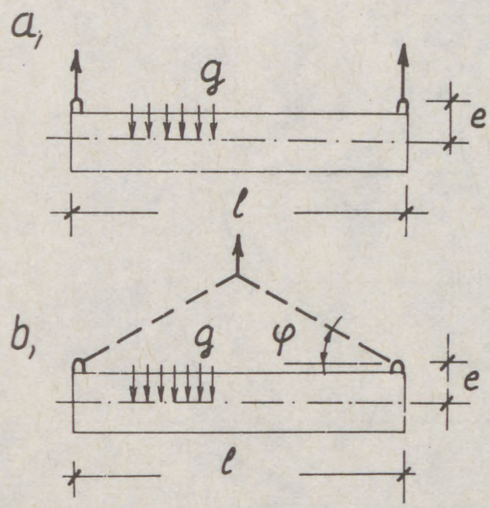

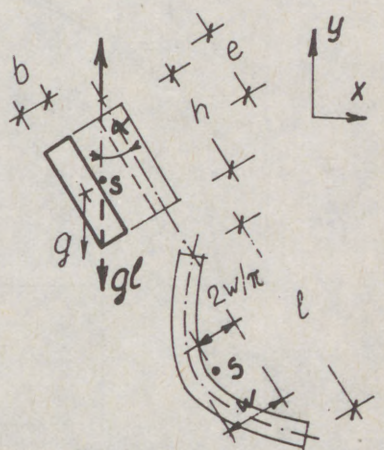

Fig. 2 Suspended beam

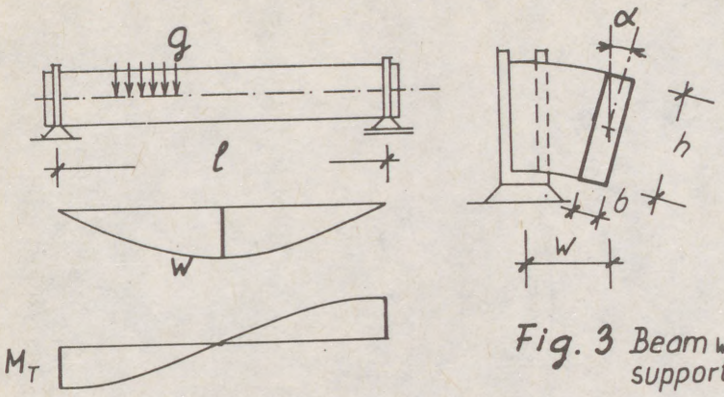

Fig. 3 Beam with „fork-like" supports

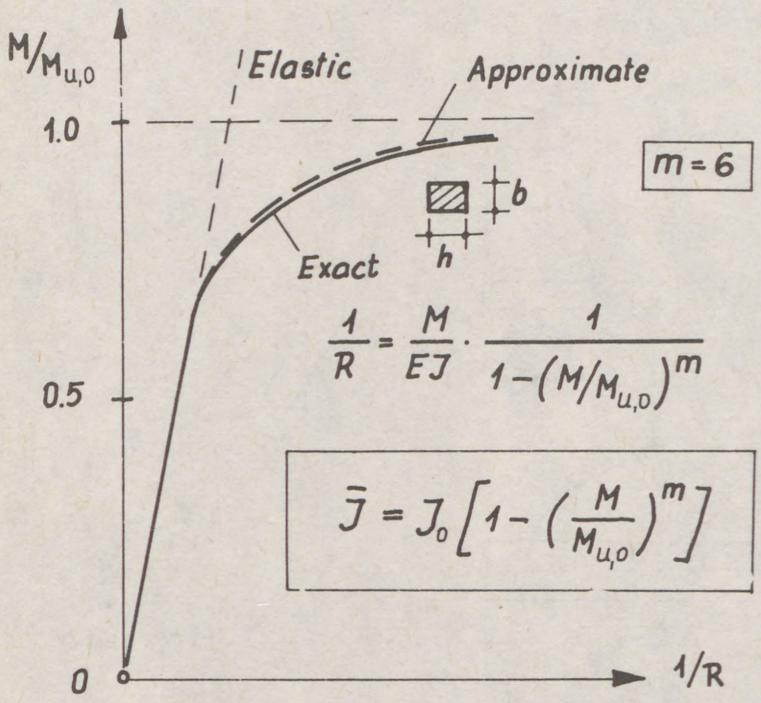

Approximation of the „nonlinear" curvature Fig. 4

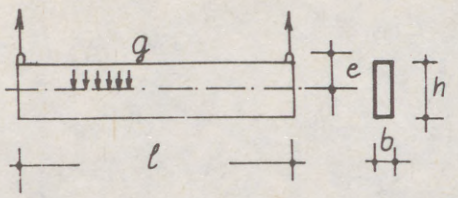

$$\eta = \left(1 - \frac{1}{\xi}\right)\left[1 - (\eta\xi A)^m\right],$$

$$g_E = \frac{120\,E\,J_y}{l^4}\,e.$$

$g_{cr} = \eta_{cr}\, g_E$

a,

A	0	0.2	0.4	1.0	2.0	5.0	10
η_{cr}=	1.0	0.72	0.59	0.39	0.26	0.13	0.07

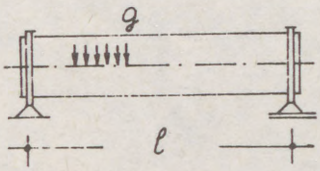

$$\eta = \sqrt{1 - \frac{1}{\xi}}\left[1 - (\eta^2\xi A)^m\right],$$

$$g_E = 18.6\,\frac{E}{l^3}\sqrt{J_y J_T}.$$

b, $g_{cr} = \eta_{cr}\, g_E$

A	0	0.2	0.4	1.0	2.0	5.0	10
η_{cr}=	1.0	0.84	0.75	0.61	0.49	0.35	0.26

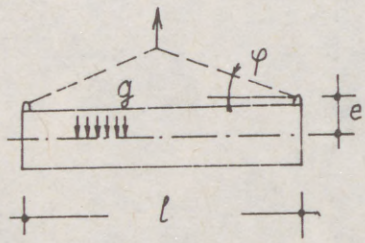

$$\eta = \left(1 - \frac{1}{\xi}\right)\frac{1 - \left\{\frac{AB\eta}{4\vartheta}\left[1 + n\left(1 + \frac{1}{B}\right)\vartheta\xi\right]\right\}^m}{1 + B},$$

$$g_E = \frac{120\,E\,J_y}{l^4}\,e,$$

$$n = 2\left[2 - \frac{1}{1 + 1.5\,\xi\vartheta\,(1 + 1/B)}\right]$$

$g_{cr} = \eta_{cr}\, g_E$

C,

$\eta = g/g_E$; $\xi = w/w_o$; $\vartheta = w_o/b$;

$m = 6$; $B = 6e/l\,\mathrm{tg}\,\varphi$;

$N_E = \pi^2 E J_y / l^2$; $A = N_E w_o / M_{u,o}$.

A	0	0.2	0.4	1.0	2.0	5.0	10
η_{cr}=	0.67	0.48	0.39	0.26	0.17	0.08	0.05
B = 0.5 ϑ = 0.25							

The critical loads of slander steel beams **Fig. 5**

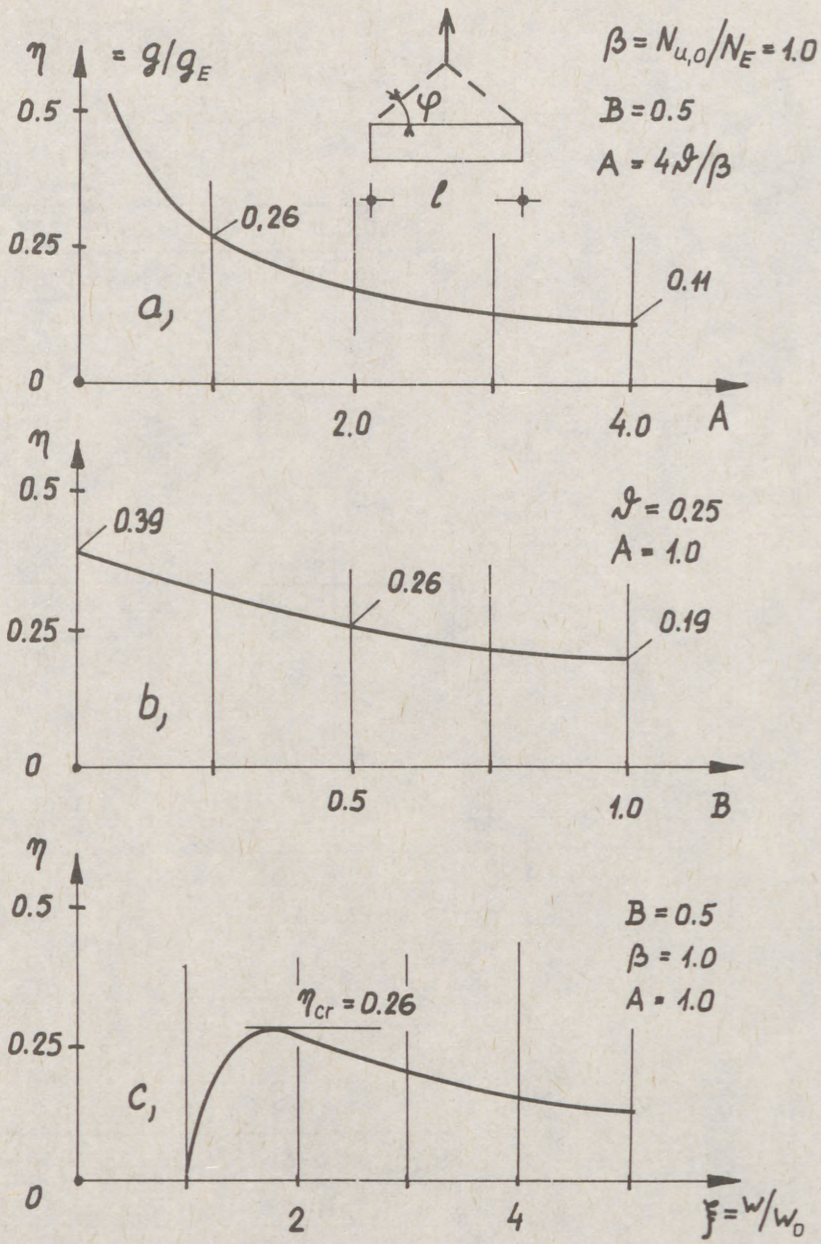

Example of a suspended beam

Fig. 6

(1)
LOOS, Wolfgang (1)
GOEBEN, Hans-Ehrenfried (2)
LEHMANN, Edwin (3)

SYSTEMATICS FOR A RESEARCH SYSTEM (EXPERT`S) IN THE FIELD OF "STABILITY OF BEAMS"

INTERNATIONAL COLLOQUIUM
STABILITY OF STEEL STRUCTURES
BUDAPEST, HUNGARY, 1990
PRELIMINARY REPORT

Summary: Precondition of an analysis of knowledge available in journals, research reports, dissertations etc. is its systematization as a field of knowledge. Such a systematics has been developed for the analysis in the field of stability of steel columns. An account of it will be given as well as an explanation by an example.

1. Introduction

In GOEBEN, LOOS /1/ an attempt is made to analyse the field of knowledge "Stability of steel beams". The knowledge of this problem important for design an existing throughout the world will be made available. Thus unsolved problems in research become evident on which in GOEBEN, LOOS /2/ a preliminary report was given, with an important partial aspect of this work, i.e. the systematization of this field being dealt with.
This is not only done because this systematics is of general scientific concern, but to stimulate similar analyses in other fields at the same time.

2. Systematics of the field of knowledge

The knowledge to be systematized exists in the form of information sources. These are in order of frequency: articles from journals, conference papers, research reports, dissertations, special technical books, monographs, manuals, codes, guidelines, commemorative volumes.
Way of description, aims etc. of authors are as different as those types of publication. The present tasks consists in systematizing the scientific content of those publications.

---

(1) Dr. sc. techn., VEB Entwicklungs- und Musterbau Berlin, DDR
(2) Dr. sc. techn., Technische Hochschule Leipzig, DDR
(3) Dr.-Ing., VEB Entwicklungs- und Musterbau Berlin, DDR

(2)
A systematics is to be established which makes it possible to systematize easily any item occuring in practice. According to this systematics, after breaking it down into individual results, the content of each source can be used in practice.
To put it metaphorically: The field of knowledge is to be subdivided into drawers, into which the knowledge to be analysed is distributed and from where it can be retrieved by the user on request.
Before systematizing knowledge, i.e. breaking it down into its constituent parts, the framework is to be clearly defined. The present limited field is flexural torsion as a problem of bifurcation, stress or ultimate load of the second order of single steel bars or bar systems subjected to bending and/or lateral loading at any load level, cross section, shape of cross section, and shape of the bar axis.
Thus the following related fields have been distinguished from the field to be systematized:
- buckling, torsional buckling, flexural torsional buckling (also constant moment, if any axial force exists)
- dynamic stability
- lateral buckling of compressed flanges of through bridges
- stability under simple torsional load
- stability of ribs of plate structures
- stability of lattice beams
- stability of beams made of other materials than steel (timber, aluminium, concrete etc.), if the investigation concerned does not deal with material-independent problems
- fields whose results serve as aids for the present limited field (general bar theory, torsion theory, elasticity and plasticity, mathematics, testing etc.)

The remaining field of knowledge make up practical partial problems, which are determined by 15 independent parameters:
These are:

a. Configuration of the bar axis (Fig. 1)

Position 1

Code	Description	Explanation
A	general	
B	bar system; spatial	
C	bar system; plane , xz-plane	
D	bar system; plane, yz-plane	
E	single bar; spatial	
:		
P	single bar; plane; yz-plane; discontinuous; knee-shaped once	
Q	single bar; straight	
:		
Z	single bar; straight; preformed; about z-axis	

Fig. 1 Systematics Pos. 1 - configuration of bar axis

(3)
Here, as with all other parameters, the general case comes first, the most specialised is the last.
Problem solutions of general cases apply to all kinds of configurations, irrespective of the fact whether the bar axis is spatial or in a plane, straight, knee-shaped or curved, whether it is a bar system or a single bar. This case can bi coordinated with all special cases. Problem solutions for other cases would not be required, if there were a solution for those most general cases that would meet all requirements.
Principally this seems to be the case. Theoretical fundamentals have been adequately investigated. Computing has attained a level that makes it possible to cope with any work load required. Only the expenditure of work is tremendous because the present problem is demanding mathematically and mechanically. In the design process stability is a partial problem only, the expenditure of work being inappropriate. Simple cases require simple solutions to be found in manuals an specifications as simple formulas, tables an graphs. Therefore, in addition to general cases, all special cases are given, as to parameters of "Configuration of bar axis". For the same reason the same approach is used with the remaining parameters.

b. Number of supports in the main load plane
c. Location of supports in the main load plane

For reasons of practicality three parameters concerning complex parameters "Supports for the main load plane" are summed up. With these parameters an unexpected problem was encountered which became increasingly evident with the following parameter of "Supports in the subordninate load plane", i.e. denoting support conditions. It is common to denote support conditions by symbols rather than verbally. Such an approach is practical and, what is more important, familiar to the designer.
The problem was that symbols commonly used are rather complex and denote one support condition only. But such symbols were not known and used for all support conditions that were encountered when the present field was analysed. Many new symbols would have been necessary in order to meet all requirements. Instead a new approach was used. New symbols similar to those already known have been divised that characterize each constituent of a support condition individually. Summing them up results in the entire support condition. This practical, can be overlooked easily, an extended any time (Fig. 2).

(4)

Position 2

Code	Description	Explanation
A	general	
B	point supports; any number of supports	
:		
F	point supports; 2 supports; at bar ends	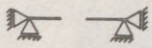
:		
P	point supports; 2 supports; at bar ends	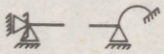
:		
W	point supports; 1 support; at bar end	
:		
Z	point supports; deviation of positions	

Symbols for support conditions:

spring support about x-axis 

rigid support about x-axis 

rigid support in direction of y-axis 

rigid support in direction of z-axis 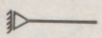

Fig. 2 Systematics Pos. 2 - supports in the main load plane

The following three parameters (Fig. 3) can also be summed up forming a complex parameter "Supports for the subordinate load plane".
The yz-plane is the main load plane and the xz-plane the subordinate load plane, with y being the minimum mean axis and x the maximum mean axis and z the bar axis.

e. Number of supports in the subordinate load plane
f. Location of supports in the subordinate load plane on the bar axis
g. Type of supports in the subordinate load plane

The following two parameters refer to the beam cross section.

h. Type of bar cross section
i. Shape of the bar cross section about the bar axis

Fig. 4 and Fig. 5 show each, as Fig. 2 and Fig. 3 do, part of the parameter concerned.

(5)
Position 3

Code	Description	Explanation
AA	general	
:		
AG	point supports and linear support	 and 
:		
AP	point supports and linear support	 and 
:		
CE	point supports; two different types of support	 and 
:		
DA	point supports	
:		
EA	linear support	
:		
FA	no support	

Symbols for support conditions:

spring support in direction of x-axis	
rigid support in direction of x-axis	
spring support about y-axis	
rigid support about y-axis	
spring support in direction of z-axis	
rigid support in direction of z-axis	
spring support about z-axis	
rigid support about z-axis	
spring support against cross section distortion	
rigid support against cross section distortion	

Fig. 3 Systematics Pos. 3 - Supports for subordinate load plane

(6)

Position 4

Code	Description	Explanation
AA	general	
:		
BC	asymmetrical;	
:		
CC	monosymmetrical about x-axis	
:		
EC	point symmetrical about z-axis	
:		
FF	double symmetrical	
:		
GA	various types of cross sections	

Fig. 4 Systematics Pos. 4 - Types of bar cross section

Position 5

Code	Description	Explanation
A	general	
:		
G	variable cross section dimensions; depth, width, wall thickness of plates variable	
:		
N	variable cross section dimensions; depth variable; discontinuos	
O	variable cross section dimensions; depth variable; discontinuous	
:		
S	variable cross section dimensions; depth variable; disontinuous	
:		
Z	cross section values and cross section dimensions respectively of each type of cross section occuring invarible	

Fig. 5 Systematics Pos. 5 - Shape of bar cross section about bar axis

(7)
Position 6

Code	Description
AA	general
BA	invariable direction; general
:	
FA	invariable direction; linear loads; point loads; general
:	
NE	invariable direction; point loads; one moment; at the end
:	
OK	invariable direction; moments; one moment; at the end
:	
OB	variable direction; general
:	
RA	no loads

Fig. 6 Systematics Pos. 6 - Loads in the main load plane

The parameters j to l (Fig. 6) and m to o (Fig. 7) can also be summed up, forming one complex parameter.

j. Number of loads in the main load plane
k. Location of the loads in main load plane on the bar axis
l. Type of loads in the main load plane
m. Number of loads in the subordinate load plane
n. Location of loads in the subordinate load plane on the bar axis
o. Types of loads in the subordinate load plane

Thus each case is described eventually by seven rather complex parameters. The discription ist done alphabetically. A code word emerges consisting of seven digits, whose constituents are made up by one or two digits depending on the complexity of a parameter.

Position 7

Code	Description
A	general
B	uniform and different from main load plane; general
:	
I	different from main load plane; general
J	different from main load plane; linear loads
K	different from main load plane; point loads
R	uniform from main load plane
S	no loads

Fig. 7 Systematics Pos. 7 - Loads in the subordinate load plane

(8)

3. Example

This will be demonstrated by an example. In an article published in a journal Kitipornchai, Trahair /3/ report on research results on elastic stability of tapered I-beams. An analysis has shown than this work contains useful solutions an results concerning six different individual problems. One of them is shown in Fig. 8.

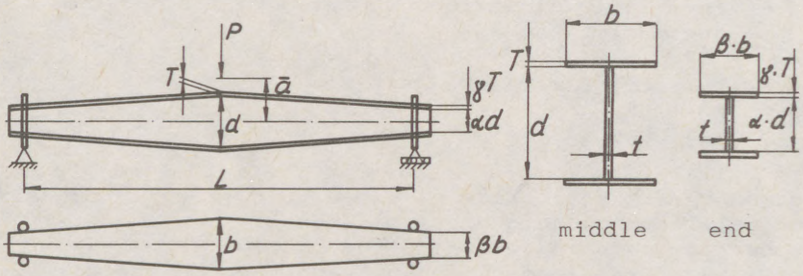

Codeword: Q G DA FF O NE S

Fig. 8 - Example for the systematic description of an individual problem

The code word characterising it is obtained as follows:

(1) Configuration of bar axis: It is a single bar, which is straight. The systematics gives: Q
(2) Supports in the main load plane: The bar has statically determinate supports at the ends. The systematics shows: G
(3) Supports for the subordinate load plane: Both supports are identical, are rigid against torsion, displacement free under bending and distorsion. The systematics shows: DA.
(4) Type of bar cross section: Double symmetrical I-cross section: FF
(5) Shape of the bar cross section about the bar axis: This symmetrically tapered shape is denoted with O by the systematics.
(6) Loads in the main load plane: A point load in the middle with invariable direction: NE.
(7) Loads in the subordinate load plane: In the subordinate load plane, perpendicular to the bar axis, there are no loads: S.

By the way, the analysis of the present field concerning this code word resulted in 10 different entries. In 10 scientific papers results on this problem have been presented which are now available the user as a result of the present analysis and systematics.

(9)

References:

/1/ Goeben, H.-E.; Loos, W., 1986, Stabilität von Trägern aus Stahl - Analyse eines Wissensgebietes, Technische Hochschule Leipzig, Dissertation B.

/2/ Goeben, H.-E.; Loos, W., 1986, Stability of Beams Made of Steel - an Analysis of a Field of Knowledge, Proceedings and Final Report of the Colloquium on Stability of Steel Structures, p. 339.

/3/ Kitipornchai, S.; Trahair, N.S., Elastic Stability of Tapered I-Beams, Proc. ASCE, J. Struct. Div. 98 (1972) ST 3. p. 713

POSTOYAN, YURIY (1)
CHAPLIGINA, SVETLANA (2)

TORSIONAL STABILITY OF NEW CONSTRUCTIONS OF SPAN'S BEAMS.

INTERNATIONAL COLLOQUIUM
STABILITY OF STEEL STRUCTURES
BUDAPEST, HUNGARY, 1990
PRELIMINARY REPORT

Summary: In experimental-theoretical way the problems of torsion and stability of plane-bend of cross-section thin-walled metalic beams with pipe belts were investigated. It is discovered that the real moment of inertia of tested sections at free torsion is lower in comparison with theoretical premise. Corrected coefficient is within 0.18 - 0.83. In this work the corrected coefficients are given and the analyses of stability of open section beams with pipe belts supported with bars are done.

---

(1) Professor of Civil Engineering, Dniepropetrovsk Civil Engineering Institute.
(2) Professor of Mechanics, Dniepropetrovsk Civil Engineering Institute.

The development of engineering thought led to creation of new constructions of open cross-section beams with large spans and belts of pipes. It's known that efficiency of using of open cross-sections is often limited with stability of plane bend and increase of stability may be got at the expense of torsional rigidity. As open cross-sections, as a rule, consist of sheets, they don't possess large torsional rigidity. The use of beams with box-like cross-section that have considerable torsional rigidity is not economic profitable for large spans because of its large weight and labour-intensiveness making.

New constructions of thin-walled metalic open cross-sections beams with belts of pipes are successfully used for travelling gantry cranes frameworks for woods with carring capacity 16 and 12.5 tons and operation zones in 63 and 81 m (1). Such beams have significant moment of inertia in torsion tests that allows in some cases to cancel the usage of box-like beams.

In order to eliminate deformation and to increase the plane bend stability the travelling gantry cranes frameworks with carring capacity 12.5 tons are reinforced in a span and on cantilevers with bars (fig.).

The analysis of construction decisions of open cross-section beams with large spans and belts of tubes shows that their large practical usage is limited because of the shortage of studing their work at torsion and plane bend stability.

As it shown (2) moment of inertia of tested beams with belts of pipes is largely depended upon the rigidity of lateral diaphragms. With the help of tests in our institute the torsion of such beams at free and limited torsions is investigated. With the methods of mathematic statistics the experimental data reduction has been done and analytic expression for moment of inertia in torsion test has been received.

It is known, the moment of inertia of beams consisted of open and closed areas of sections at free torsion has been taken as equal to algebraic sum of moments of inertia of its separate elements (3):

$$J_t^{\Sigma} = J_t^{(3)} + J_t^{(0)} , \qquad (1)$$

where the first item is corresponded to closed and the second to open contours of sections. As it is said in (3) it is true only in the case of installation of "great ammount of sufficiently rigid lateral diaphragms". Due to our tests on 212 large-scale models with spans from 0.25 to 4.00 m it is investigated the moment of inertia at free torsion of beams with belts of pipes have decreased numeral value in comparison with those calculated by the formula (1).

It is suggested to evaluate this effect with the help of coefficient γ^3 which takes into account the level of "switching on" closed elements to the operation of the whole section to free torsion. In this case the coefficient γ^3 is determined as relation of pilot value moment of inertia at free torsion J_t^3 to the moment of inertia J_t^Σ theoretically calculated. Tests data determine the coefficient γ^3 has the interval of values within 0.07-0.83. To determine the influence of lateral diaphragms rigidity on the grade of "switching" of pipes belts at free torsion dimensionless parameter k is calculated in accordance with the following formula:

$$k = a J_s l / J_t^\Sigma h_\omega, \qquad (2)$$

where J_s is a reduction moment of inertia of cross-section diaphragm determined from the condition of equivalent deflection of fixed in cantilever bar with consideration of vertical wall operation on l = 1.0 m from horizontal force action T = 1, applied in centre of gravity of pressed belt, a - dimensionless coefficient (a = 100), h_ω - distance between beam belts centres of gravity.

Tests showed the increasing of parametre k increases "switching" coefficient γ^3. The relation between unknown value k and γ^3 is determined to be described with such equation:

$$\gamma^3 = 0.0178 + 0.0754\, k \qquad (3)$$

It is possible to assume the theoretical "switching" coefficient for open-section beams with pipes belts γ is equal to γ^3, so the moment of inertia for tested beams

at free torsion can be valued with the formula:

$$\bar{J}_t = \gamma J_t^{\Sigma} , \qquad (4)$$

where $\bar{J}_t$ - is the reduction moment of inertia of open-section beams with pipes belts at free torsion.

Test results proved the sector moment value of inertia of beams with pipes belts can be determined as for compound open profile thin-walled bars and their value does not depend upon the type of fixing of cross diaphragms to belts.

Knowing the geometric characteristics of tested open-section beams with pipes belts we now evaluate their stability of plane bend with fixing them by bars (see fig.).

For the investigation of stability of plane bend of tested beams with bars direct matrix method has been used (5).

The direct matrix method is based on the idea of load brokenness equal to parameteric forces action. Equal loads are obtained from prof. Vlasov's differencial equilibrium equations for thin-walled bars.

To get equal loads the components relative to the presence of parametric loads in Vlasov's equations are transfered to the right part and considered to be external. The same is done with component which takes into account free torsion.

Integrating these equations we get the following equal loads (4):

$$\Delta M_i = M_i \theta \; ; \quad H_i = -M_i \Delta U_i' \; ;$$

$$H_j = P_j d_j \theta \; ; \quad B_i = (M_i K_i - C_i) \Delta \theta_i \; . \qquad (5)$$

Using equal loads (5) we compose the relations which connect linear and anglular displacements with forced action

$$\begin{aligned} \Delta \vec{U}' &= \varsigma \Delta \vec{M} \; ; \\ \vec{\theta} &= g \vec{H} + g_0 \vec{H}_0 + g_1 \vec{B} \; ; \\ \vec{\theta}_0 &= g_{10} \vec{H} + g_{00} \vec{H}_0 + g_{01} \vec{B} \; ; \\ \Delta \vec{\theta} &= \vartheta_1 \vec{H} + \vartheta_0 \vec{H}_0 + \vartheta \vec{B} \; . \end{aligned} \qquad (6)$$

The solution of obtained equations (6) is own numbers of determinant

$$|\mathcal{D} - \lambda E| = 0 .$$

Minimum crucial force value corresponds to maximum own number λ_{max} ;

$$F_{cr} = 1/\lambda_{max}$$

The physical sense of these dependences is given in the work (5). Three possible schemes of fixing bars on span structures are taken for searching these problems. Due to scheme "a" (see fig.) bars with area of cross section A_T support the carrying beam along the line of cross section bend centres. Due to scheme "b" the bars are installed on the upper belt of carrying beam. Due to the travelling gantry crane КК П-8 type scheme the bars are installed on the upper belt of span beam (see scheme "c" on fig.).

Cross section tested beam is given in fig., scheme "c". For calculated schemes "a" and "b" the deformation of bars and span structures was taken into consideration, as for scheme "c" the pliability of bars, span beams, crane supports and struts was taken into consideration as well.

For all calculated schemes it is considered that the cross load is applied to the centre of the beam span (see fig.).

Test results of investigation of plane bend stability for calculated schemes are given in figure as a dependence $F_{cr} \rightarrow A_T$ where F_{cr} - the parameter of crucial load, A_T - area of bar cross-section.

The analysis of obtained results showed:

1. Presence of bars on the span beams increases the stability of plane bend of beams up to 2 times.

2. The most effective method of fixing the bars in beam span is on the upper belt level (see fig., scheme "b").

3. The stability of plane bend is increasing when the bars section area is growing.

4. The pliability of supports is considerably lowing the parameter of critical force (see schemes "b", "c") which must be considered in calculations.

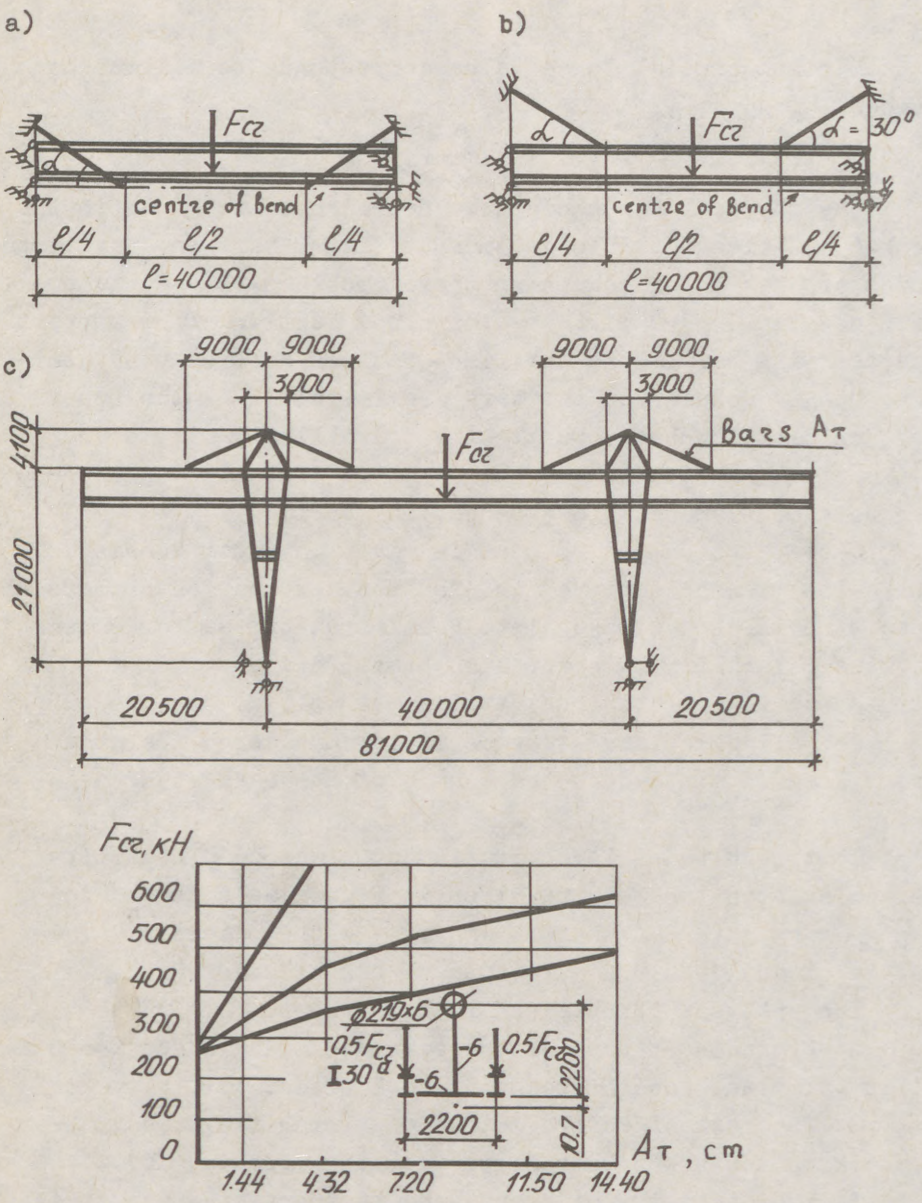

Fig.

a) Bars are installed in the centre of bend
b) Bars are installed on the upper belt
c) Bars are on the travelling gantry crane ККЛ-8 type.

REFERENCES

I.Абрамович И.И. I979, Новые козловые краны для перегрузочных работ. - "Вестник машиностроения", № II.

2.Постоян Ю.А. I987, Кручение пролетных балок с поясами из труб. - "Известия ВУЗОВ. Машиностроение", № 3.

3.Любаров Б.И. I972, Кручение тонкостенных стержней открыто-закрытого профиля. - Материалы УI научной конференции молодых ученых-строителей "Исследования по строительным конструкциям", Ленинград.

4.Незальзов О.Р. I972, Прямой матричный метод определения критических сил при потере устойчивости плоской формы изгиба. Сопротивление материалов и теория сооружений. - БудIвельник, Киев, ХУI.

5.Постоян Ю.А. I982, Исследование устойчивости плоской формы изгиба тонкостенных металлических балок открытого сечения с поясами из труб. - Диссертация на соискание ученой степени кандидата технических наук, Днепропетровск.

(1)
RABOLDT, Karl (1)

BENDING AND TORSION OF TRAVERSES WITH CHANNEL SECTIONS

INTERNATIONAL COLLOQUIUM
STABILITY OF STEEL STRUCTURES
BUDAPEST, HUNGARY, 1990
PRELIMINARY REPORT

Summary: For traverses with channel sections and suspension rods the analysis has to take into account the deformations of the beam and of the suspension rods, the rotations of the suspension rods and the special condition of the introduction of the load. The equations of the mathematical model are presented, which are nonlinear. An incremental-iterative procedure is used for solution. The results of the application are demonstrated by examples.

1. Introduction

Traverses with channel sections and round suspension rods (Fig. 1) are often used in industrial building to carry technological equipment. So it is usefull, to investigate the mechanical behaviour of the system. The analysis has to take into consideration:

1. the deformations of the channel-beam (bending and torsion II. order)
2. the bending deformation of the suspension rods
3. the rotation of the suspension rods, which are fastend with a hinge at the bearing construction,
4. the special condition of the introduction of the load

(1) Professor of Civil Engineering, Hochschule für Bauwesen Cottbus

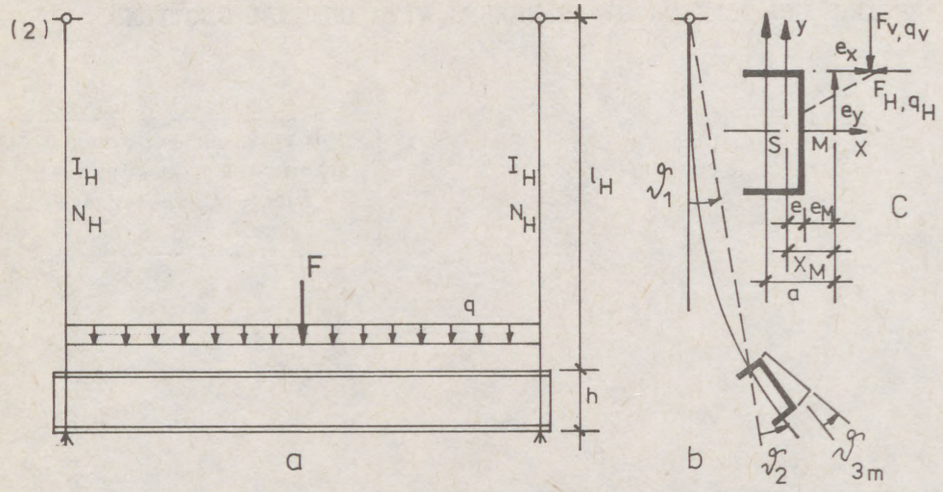

Fig.1 a System, b characteristic angles, c cross sektion

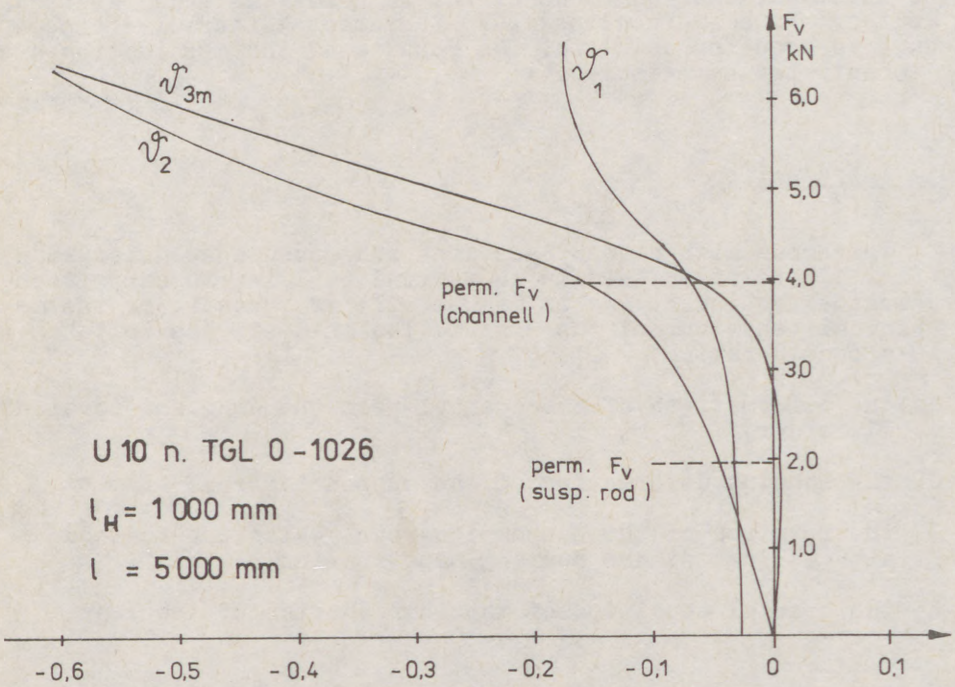

Fig.2 Example 1: Characteristic angles in dependence of a vertical single load at the back of the profile

(3)

The first three effects are considered in the mathematical model presented in 2. The solution of this problem is used in 3. to implement the 4. condition.

The load may be an inclined uniformly distributed load q or an inclined single load F (Fig. 1).

The deformation state of the system (Fig. 1b) is characterized by the rotation of the suspension rod ϑ_1, the relative rotation of the beam at the suspension points ϑ_2 and the relative deformations of the shear centre of the cross section at the middle of the span u_m, v_m, ϑ_{3m}.

For the calculation of the action effects a elastic theory is used, which takes into account little deformations for the evaluation of the elastic resistance and arbitrary angles ϑ_1, ϑ_2, ϑ_{3m} for the distribution of the action components.

The proof of the cross-section capacity considers an elastic-partially plastic behaviour.

Imperfections may be taken into account using an angle ϑ_o, considering the slip at the bore-holes of the beam and added to $(\vartheta_1 + \vartheta_2)$, or an additional horizontal load component.

2. Mathematical model and solution method

In this part the case is investigated, when the in 1. specified loads act at an abitrary point (Fig. 1c). For the evaluation of the unknown deformations ϑ_1, ϑ_2, u_m, v_m, ϑ_{3m}

- the equilibrium conditions of the whole system
- the deformation relations of the suspension rods and
- the solutions of the bending-and-torsion-problem of the channel-beam with supports, which prevents lateral deflection and twist but which allows both lateral bending and warping to occur freely, (Roik, Carl, Lindner 1972, TGL 13503)

are available.

The equations of the mathematical model are derivated in (Raboldt 1990). Here the final equations are presented.

The moment equilibrium condition of the whole system gives:

$$R_V e_{V1} + (F_V + 0{,}637\, Q_V)\, e_{V2} + R_H e_{H1} + (F_H + 0{,}637\, Q_H)\, e_{H2} = \\ = -R_V l_H \sin\vartheta_1 - R_H l_H \cos\vartheta_1 \qquad (1)$$

(4)

with: $Q_v = q_v\, l$; $Q_H = q_H\, l$; $R_v = F_v + Q_v$; $R_H = F_H + Q_H$ (2 a,b,c,d)

$$e_{v1} = a_H \cdot \sin\vartheta + a_v \cdot \cos\vartheta \quad (3\ a)$$

$$e_{v2} = -u_m \cos\vartheta + v_m \sin\vartheta + \vartheta_{3m}\,(a_H \cos\vartheta - a_v \sin\vartheta) \quad (3\ b)$$

$$e_{H1} = a_H \cos\vartheta - a_v \sin\vartheta \quad (3\ c)$$

$$e_{H2} = u_m \sin\vartheta + v_m \cos\vartheta - \vartheta_{3m}\,(a_H \sin\vartheta + a_v \cos\vartheta) \quad (3\ d)$$

$$a_H = 0{,}5\ h - e_y;\ a_v = a + e_x;\ \vartheta = \vartheta_1 + \vartheta_2 + \vartheta_o\ \mathrm{sign}(\vartheta_1 + \vartheta_2) \quad (4\ a,b,c)$$

The deformation relations of the suspension rods give:

$$\vartheta_2 = 0{,}167\,(R_v \sin\vartheta_1 + R_H \cos\vartheta_1)\, l_H^2\,(3/\gamma_1 + h/l_H)/(E\, I_H) \quad (5)$$

with: $\gamma_1 = \varepsilon^2 \sinh\varepsilon\,/(\varepsilon \cosh e - \sinh\varepsilon)$; $\varepsilon = l_H \sqrt{/N_H//EI_H}$ (5 a,b)

The solutions of the bending-and-torsion-problem of the channel-beam (Roik, Carl, Lindner 1972, TGL 13503) give:

$$\vartheta_{3m} = Z/N;\ \vartheta_G = \vartheta + \vartheta_{3m} \quad \text{with:} \quad (6)\ (7)$$

$$Z = 1{,}273(-q_y e_x + q_x e_y) + 0{,}0139\, q_x q_y\, l^4/(E\, I_y) + 2\,(-F_y e_x + F_x e_y) + 0{,}0368\, F_x F_y l^3/(E\, I_y) \quad (6\ a)$$

$$N = D_M - 0{,}01218\, l^2\,(q_y^2\, l^2/E\, I_y + q_x^2 l^2/E\, I_x) - (q_y \bar{\bar{e}}_y + q_x \bar{\bar{e}}_x) - 0{,}0335\, l\,(F_y^2 l^2/E\, I_y + F_x^2 l^2/E\, I_x) - (F_y \bar{\bar{e}}_y + F_x \bar{\bar{e}}_x) \quad (6\ b)$$

$$D_M = \pi^2(\pi^2\, E\, C_M/l^2 + G\, I_D);\ \bar{\bar{e}}_y = \bar{e}_y;\ \bar{\bar{e}}_x = \bar{e}_x - f_R(r_y - 2x_M) \quad (6c,d,e)$$

$$f_R = 0{,}57 \text{ for } F = 0;\ q \neq 0;\ f_R = 0{,}37 \text{ for } F \neq 0;\ q = 0 \quad (7)$$

$$E\, I_y\, u_m = \frac{5}{384}\, l^4\,(q_x \cos\vartheta_{3m} + 0{,}97\, q_y \sin\vartheta_{3m}) + \frac{1}{48}\, l^3\,(F_x \cos\vartheta_{3m} + 0{,}90\, F_y \sin\vartheta_{3m}) \quad (8)$$

$$E\, I_x\, v_m = \frac{5}{384}\, l^4\,(q_y \cos\vartheta_{3m} - 0{,}97\, q_x \sin\vartheta_{3m}) + \frac{1}{48}\, l^3\,(F_y \cos\vartheta_{3m} - 0{,}90\, F_x \sin\vartheta_{3m}) \quad (9)$$

(5)
with:

$$F_y = F_v \cos\vartheta - F_H \sin\vartheta;\quad F_x = F_v \sin\vartheta + F_H \cos\vartheta \qquad (10\ a,b)$$

$$q_y = q_v \cos\vartheta - q_H \sin\vartheta;\quad q_x = q_v \sin\vartheta + q_H \cos\vartheta \qquad (10\ c,d)$$

The basic equations (1), (5), (6), (8), (9) are nonlinear. An incremental-iterative solution procedure is used in a computer program. The following measures are taken to avoid divergence:

- incremental proceeding:

• internal determination of the start value
◦ regulation of the hight of the incremental steps dependent on the Euclidean norm of the three characteristik angles
• stop at a small value of step hight and possibility of further regulation by dialogue

- iterative proceeding:

• use of an Aitken acceleration
• end of iteration, if $\|\Delta\vartheta(i)\| / \|\vartheta(i)\| < \varepsilon (=0{,}002)$ (11)
with:

$$\|\Delta\vartheta(i)\| = (\vartheta_1(i)-\vartheta_1(i-1))^2+(\vartheta_2(i)-\vartheta_2(i-1))^2+(\vartheta_3(i)-\vartheta_3(i-1))^2 \qquad (11\ a)$$

$$\|\vartheta(i)\| = \vartheta_1(i)^2 + \vartheta_2(i)^2 + \vartheta_3(i)^2 \qquad (11\ b)$$

◦ divergence or poor convergence, if $i > 50$ (12 a)
or $\|\Delta\vartheta(i)\| / \|\Delta\vartheta(i-1)\| \geq 1$ (12 b)
with: i ... ordinal number of the iteration step

Figure 2 shows as results of an example the dependences of the characteristic angles from a vertikal single load at the back of the profile. The system with a span of l = 5000 mm is slender. The typical effects of deformations are to be seen, but they appear clearly above the permissible loads F_v, characterizing the elastic-partially plastic carrying capacity of the suspension rod respectively the channel-beam.

3. Influence of load introduction

For the realistic analysis of the traverses the influence of the special load introduction has to be taken into consideration. As a rule the traverses bear bar-like elements with an effective bending stiffness like pipes or ventilation channels. If the traverse twists, the bar-like elements are supported by the highest point of the cross section.

(6)
In figure 3a the dependence of the angle ϑ_G on the load position along the upper flange is shown for an example. If the vertikal load acts at the back of profile ($e_L = 0$) the total angle $_G$ becomes negative and the highest point of the cross section is the free end of the flange, where a bar-like loading element would be supported. The position of the load at the free end of the flange results in a positive angle ϑ_G and the supporting for a bar-like element at the back of the profile. So a bar-like loading element counteracts a rotation ϑ_G and acts as a rotation restraint.

This behaviour may be described by a modified mathematical model with new boundary conditions. But there is another possibility, using the solution method, described in 2.. A rotation restraint means that the rotation ϑ_G becomes zero. Such a supporting effect transmits the load F or q, acting on the upper surface of the profile and additionally a fixing moment. The combination of the vertical component of the load F_v or q_v and the fixing moment may be substituted only by F_v or q_v acting at a horizontal displaced position. In order to evaluate this position, the vertical load is moved on the upper surface of the profile perpendicular to the axis of the beam until the rotation ϑ_G becomes zero. If a determinate load level is given, the relation between the rotation ϑ_G and the characteristic value of the load position e_L is linear (fig. 3 a) and the substituting position of the vertical load is easy to evaluate. An imperfection $_o$ causes a parallel displacement in sections (fig. 3 a).

Figure 3 b shows the influence of the load position on the stresses in the profile (σ_2, σ_4) and in the suspension rod (σ_H). In the environs of the axis throuqh the suspension rods the stresses in the suspension rod are low. They increase linear with the eccentricity of the load position from the suspension rod. This fact influences the permissible load, how fig. 4 shows.

4.References

/1/ Raboldt,K.,1990: Berechnung der Verformungen und Spannungen von pendelnd aufgehängten Trägern mit U-Querschnitt, Wissenschaftliche Zeitschrift HfB Cottbus 12 (1990) 1

/2/ TGL 13503 - Stahlbau,Stabilität von Stahltragwerken, 01: Vorschriften,02: Erläuterungen und Berechnungsmöglichkeiten,April 1982

/3/ Roik,K., Carl, J.,Lindner, J.:1972: Biegetorsionsprobleme gerader Stäbe,Berlin,München,Düsseldorf

(7)

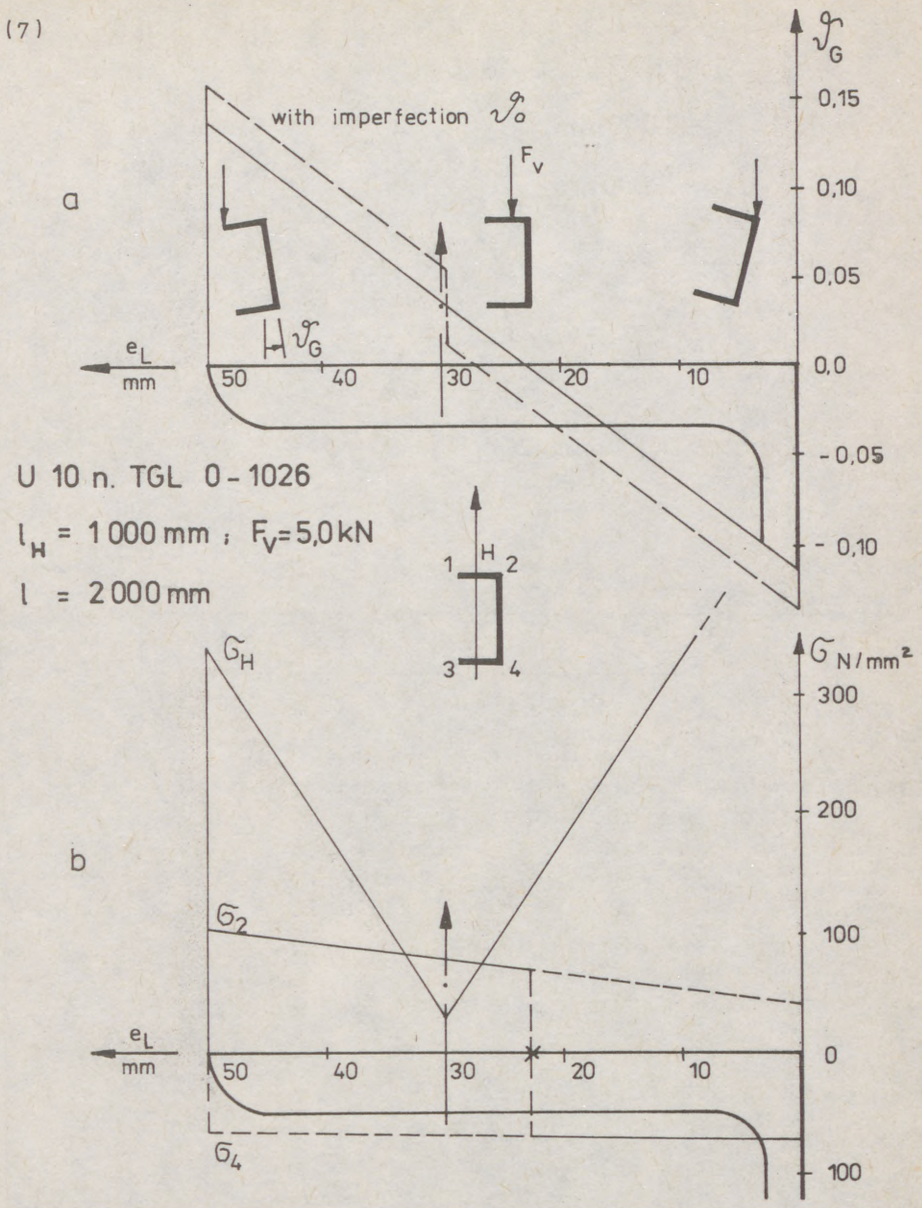

Fig.3 Example 2: Dependence from the load position - a angle ϑ_G ; b stresses in the profile σ_2, σ_4 and in the suspension rod σ_H

(8)

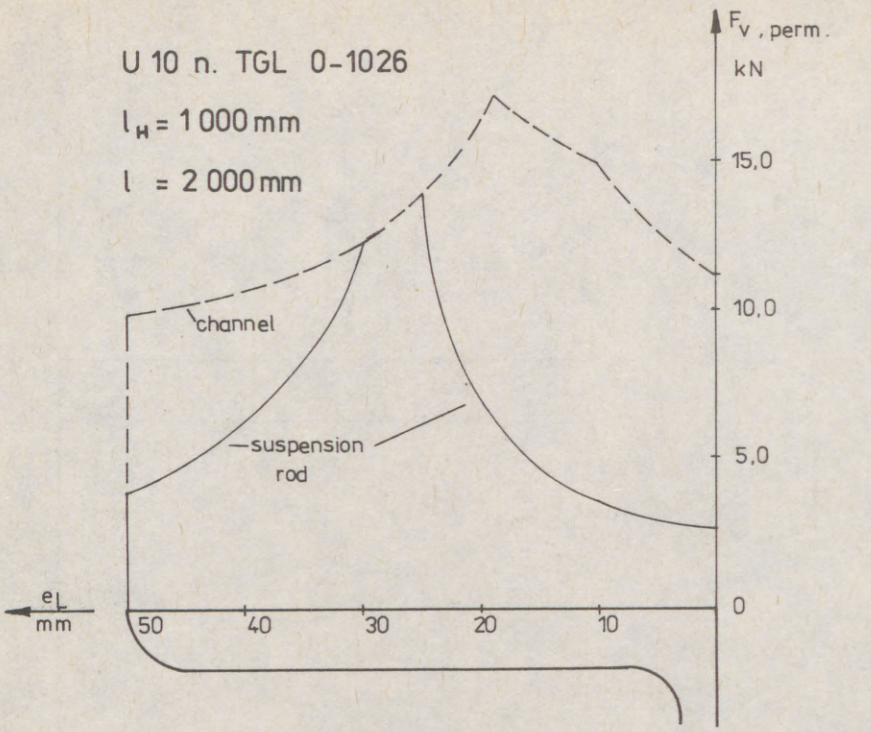

Fig. 4 Example 2 : Depence of the permissible load F_V, perm from the load position e_L

(1)
RAHAL, Mohsen (1)
GOEBEN, Hans-E. (2)

SOLUTION OF THE ELASTIC AND UNELASTIC FLEXURAL TORSION PROBLEM ACCORDING TO THE SECOND-ORDER THEORY BY MEANS OF THE FINITE-ELEMENT-METHOD

INTERNATIONAL COLLOQUIUM
STABILITY OF STEEL STRUCTURES
BUDAPEST, HUNGARY, 1990
PRELIMINARY REPORT

Summary: This article gives a survey on how the finite-element method (FEM) is used to solve flexural torsion problems and describes algorithm and programmes to solve flexural torsionally stressed straight bars with any load and support in case of the existence of geometric and structural imperfections (internal stresses) in the elastic and unelastic ranges of stress. The programmes are available for large computer systems and, for the first time, for a 16-bit PC.

1. Introduction

The need for an economical utilization of steel in building construction and the development of modern strength technologies of steel construction resulted in using preferably supporting members with open thin-walled cross sections today. Therefore more emphasis has to be placed on the questions of spatial instability phenomena. The elastic flexural torsion problems which have been subject of research work over a long time were replaced by researches to utilize the plastic material reserves.

The solution of the general flexural torsion problem is complicated and it is advisable to use large computer systems or 16-bit personal computers /1/. For this the finite-element method (FEM) has proved to be specially suitable. By 1981 appro-

(1) Aspirant, Dipl.-Ing., Technische Hochschule Leipzig, GDR
(2) Dr. sc. techn., Technische Hochschule Leipzig, GDR

(2)
ximately 90 publications were available for axially and transversely loaded bars /2/. Early applications of the method can be traced back to BARSOUM/GALLAGHER (Diss. Cornell Univ., 1970), POWELL/KLINGNER (Proc. ASCE, 1970, ST) and NETHERCOT (Diss. Univ. Wales, 1970). Other authors perfected the solution for elastic bifurcation problems of beams with specific loads and boundary conditions, e. g. NETHERCOT/ROCKEY (Internat. J. Mech. Sci., 1970), HANCOCK/TRAHAIR (Civil Eng. Trans., 1978), ATTARD (Diss. Univ. New South Wales, 1984), with variable stiffness behaviour, e. g. NETHERCOT (Mém. AIPC, 1973), TEBEDGE (Diss. Lehigh Univ., 1972), SCHROETER (Diss. TU München, 1979), and for elastic stress problems, e. g. EHELEBE /3/ (Diss. TH Leipzig, 1986) as well as unelastic stress problems with imperfections, e. g. RAJASEKARAN (Diss. Univ. Alberta, 1971), KINDMANN (Diss. Ruhr-Univ. Bochum, 1981) and RAHAL /1/ (Diss. TH Leipzig, 1989). In the following a solution according to FEM for the general flexural torsion problem is given /3/ /1/.

2. Basis

The starting point for deriving an FEM solution for thin-walled, true to shape and flexural torsionally stressed bars is the potential energy of the work performed by internal and external forces. The potential energy (1) (2) is formulated for the analysis of an optionally loaded and supported bar with geometric and structural imperfections in the unelastic range of stress. The deformations u, v, ϑ, and w are related to any reference point s (see fig. 1) because of the asymmetric, elastic residual cross sections developed by plasticization:

$$\pi = \pi^{(i)} + \pi^{(a)} \tag{1}$$

$$\begin{aligned}\pi = \frac{1}{2}\int_0^l \{ & EA w_S'^2 - 2EA_x w_S' u_S'' - 2EA_y w_S' v_S'' - 2EA_\omega w_S' \vartheta'' + EA_{xx} u_S''^2 \\ & + 2EA_{xy} u_S'' v_S'' + 2EA_{x\omega} u_S'' \vartheta'' + EA_{yy} v_S''^2 + 2EA_{y\omega} v_S'' \vartheta'' \\ & + EA_{\omega\omega} \vartheta''^2 + 2M_y \bar{v}_S'' \vartheta + 2M_x \bar{u}_S'' \vartheta + N[\bar{v}_S'^2 + \bar{u}_S'^2] + M_r \vartheta'^2 \\ & + GI_D \vartheta'^2 + c_x[u_S - e_{cx}]^2 + c_y[v_S + e_{cy}\vartheta]^2 + c_\vartheta \vartheta^2 \} dz \\ & - \int_0^l \{ f_x u_S + f_y v_S + f_z w_S + m_z \vartheta + [f_y e_{fy} - f_x e_{fx}]\vartheta \\ & - \frac{1}{2}[f_y e_{fy} + f_x e_{fx}]\vartheta^2 \} dz \\ & - \sum_i \{ F_{xi} u_S + F_{yi} v_S + F_{zi} w_S + [F_{yi} e_{Fyi} - F_{xi} e_{Fxi}]\vartheta \\ & - \frac{1}{2}[F_{xi} e_{Fxi} + F_{yi} e_{Fyi}]\vartheta^2 \} - \sum_i [M_{xi} v_i' + M_{yi} u_i' + M_{zi}\vartheta + M_{\omega i}\vartheta'] \end{aligned} \tag{2}$$

(3)

with $\bar{u}_S = u_{S0} + u_S$; $\bar{v}_S = v_{S0} + v_S$; $\bar{\vartheta} = \vartheta_0 + \vartheta$

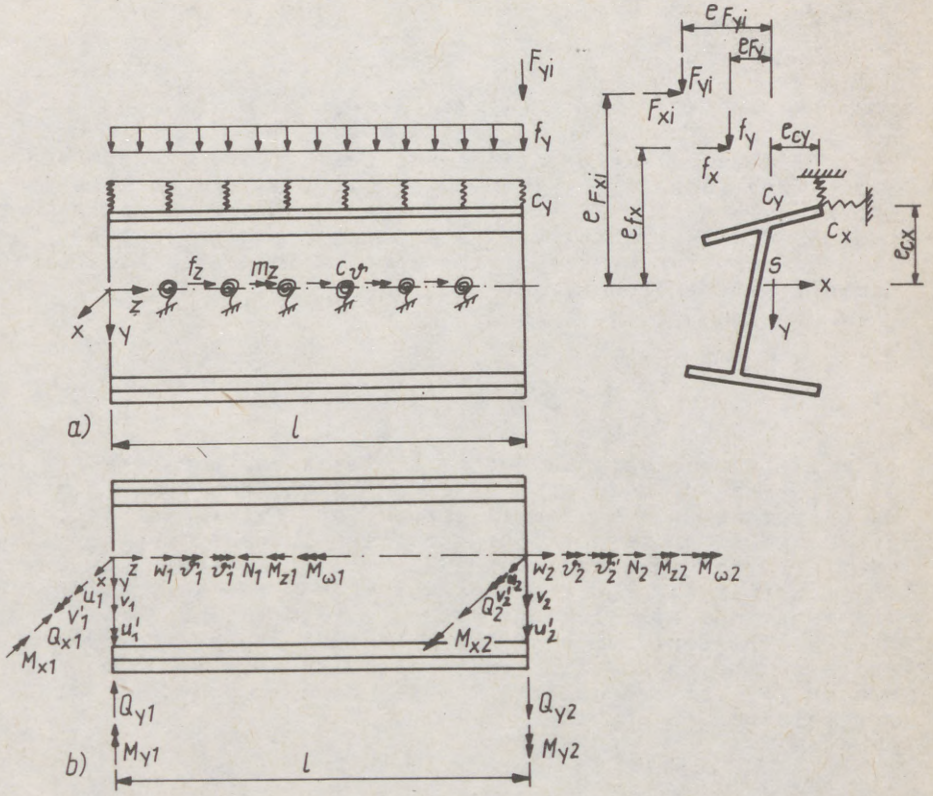

Fig. 1 Definitions along bar element subjected to any loads and supports
a) Loads and supports
b) Deformations and cross section forces

A loaded system is in the equilibrium when the first variation of the potential energy disappears:

$$\pi = \text{Min.} \longrightarrow \delta\pi = 0 \tag{3}$$

$$\delta\pi = \frac{\partial\pi}{\partial V_i}\, dV_i = 0 \tag{4}$$

The spatial state of deformation of a beam divided into elements is given by 7 deformation values at every element edge and by 14 deformation values at the element as a whole which 14 components of cross section forces are attributed to. The criterion for the equilibrium at the bar

(4)
(3) is then:

$$d\pi = \sum_{i=1}^{14(15)} \frac{\partial \pi}{\partial V_i} dV_i = 0 \qquad (5)$$

$$\{V_i\}^T = \{ \underset{1}{w_1}, \underset{2}{u_1}, \underset{3}{u_1'}, \underset{4}{v_1}, \underset{5}{v_1'}, \underset{6}{\vartheta_1}, \underset{7}{\vartheta_1'}, \underset{8}{w_2}, \underset{9}{u_2}, \underset{10}{u_2'}, \underset{11}{v_2}, \underset{12}{v_2'}, \underset{13}{\vartheta_2}, \underset{14}{\vartheta_2'}, \underset{(15)}{(w_3)} \} \qquad (6)$$

For the flexural deformations and twist there are applied cubic functions of solution by use of the Hermite interpolation polynomials of the 4th degree and for the bar's longitudinal displacement there is applied a square or cubic function of solution by use of the Hermite interpolation polynomials of the 3rd degree.

$$\begin{aligned} u &= a_1 u_1 + a_2 u_2 + a_3 u_1' + a_4 u_2' \\ v &= a_1 v_1 + a_2 v_2 + a_3 v_1' + a_4 v_2' \\ \vartheta &= a_1 \vartheta_1 + a_2 \vartheta_2 + a_3 \vartheta_1' + a_4 \vartheta_2' \\ w &= a_5 w_1 + a_6 w_2 + a_7 w_3 \end{aligned} \qquad (7)$$

It will be necessary to choose at least one square function of solution for w in case of an unelastic analysis if any fixed reference axis system is chosen for the asymmetric unelastic residual cross sections occurring in case of plasticization /1/. For an elastic analysis with principal axis system there are linear functions of solution for w sufficient /3/. The functions of solution (7) are put in the potential energy (2). The derivation of the potential energy to the components of the deformation vector results in a local equation system (7) for every element which is composed of matrices and vectors.

$$[K_i]\{V_i\} + [G_i]\{V_i\} + [G_i]\{VO_i\} = \{F_i\} \qquad (8)$$

$[K_i]$ *element stiffness matrix*

$[G_i]$ *element geometric matrix*

$\{V_i\}$ *element displacement vector*

$\{VO_i\}$ *element initial displacement vector*

$\{F_i\}$ *element load vector*

The local equation systems (8) of the elements are compiled in a global system equation (9) by incidence tables /4/ under consideration of geometric compatibility conditions at the element boundaries. The matrices $[K_i]$ $[G_i]$ and vectors $\{V_i\}$ $\{VO_i\}$ $\{F_i\}$ are superposed in global matrices $[K]$ $[G]$ and global vectors $\{V\}$ $\{VO\}$ $\{F\}$.

$$[K]\{V\} + [G]\{V\} + [G]\{VO\} = \{F\} \qquad (9)$$

(5)
The system equation can be homogeneous or inhomogeneous. The inhomogeneous system equation of a stress problem will result in deformations which can be used to find out cross section forces and stresses according to equations (10) (11).

$$N = \int_A \sigma_z \, dA \qquad M_x = \int_A \sigma_z \, y \, dA \qquad M_y = \int_A \sigma_z \, x \, dA \tag{10}$$

$$M_\omega = \int_A \sigma_z \, \omega \, dA \qquad M_r = \int_A \sigma_z \, r^2 \, dA \qquad r^2 = x^2 + y^2$$

$$\sigma_z = [w_S' - x(u_S'' + \vartheta' v_S'') - y(v_S'' - \vartheta' u_S'') - \omega \vartheta'' + \frac{1}{2}(w_S'^2 + y'^2 + r^2 \vartheta'^2)] \tag{11}$$

3. Determination of critical loads

The system equation (10) provides the critical loads of bifurcation, stress, or ultimate load problems depending upon the valuation of the equation systems and the determination of the stress-strain relation.

a) Bifurcation loads
Bifurcation loads are calculated from the homogeneous system equation (9) according to the following condition:

$$Det([K] + [G]) = 0 \tag{12}$$

It is the minimum eigenvalue of the problem only which is of interest for the construction. It is found out according to the incremental method with correction of loading (see ultimate loads).

b) Yielding loads
The system equation (9) of the elastic, geometrically nonlinear flexural torsion problem is inhomogeneous in case of a stress problem. The critical load is found out iteratively according to the Newton-Raphson process, the 1st iterative step according to equation (13) being the solution according to the first-order theory providing an associated residual load vector (14) (see fig. 2a).

$$[K]\{V1\} + [G]\{V0\} = \{F\} \rightarrow \{V1\} \quad 1^{st} \text{ order theory} \tag{13}$$

$$\{RF1\} = \{F\} - [K]\{V1\} - [G]\{V1\} - [G]\{V0\} \tag{14}$$

The 2nd iterative step together with the cross section forces of the 1st step will provide the solution according to the linearized second-order theory.

$$[K]\{V2\} + [G]\{V2\} + [G]\{V0\} = \{RF1\} \quad 2^{nd} \text{ order theory} \tag{15}$$

If the iteration is continued with improved deformations and cross section forces the solution will be found after

(6)
approximately 5 steps according to the non-linear second-order theory.

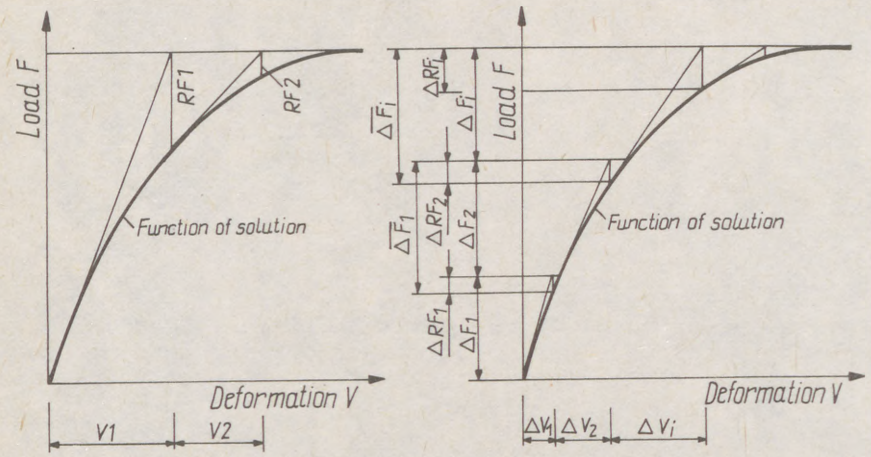

Fig. 2 Iteration procedures for determination of critical load
a) Yielding load problems (Newton - Raphson - method)
b) Ultimate load problems (Incremental method with correction of loading)

c) Ultimate loads
The ultimate loads of geometrically and physically non-linear problems can be calculated by means of the total-step iteration and incremental iteration methods. The incremental method with correction of loading according to fig. 2b has proved to be specially efficient using a bilinear stress-strain diagram.

$$[K]\{\Delta V\}+[G]\{\Delta V\}+[G]\{V0\}=\{\Delta F\} \qquad (16)$$

By checking the equilibrium in every load increment, the residual loads of the system weakened by partial plasticization are recorded as follows:

$$\{\Delta RF\}=[\Delta G]\{V\} \qquad (17)$$

[ΔG] being the change of the geometric matrix in the load increment under consideration compared with the previous load step.
The elastic residual cross sections developed by plasticization are recorded in the iteration process by a cross-sectional iteration through the cross section forces N, M_x, M_y, and M_ω. Here it is possible to take into consideration the initial stresses.

(7)

d) Computer programmes

The algorithms were transformed into the following computer programmes:

- programme BIETO for the elastic flexural torsion problem in the large computer system EC 1040 in FORTRAN /3/
- programme IMBIT for the unelastic flexural torsion problem for a 16-bit PC with 460 Kbyte RAM capacity in FORTRAN 77 /1/

The implementation of the programme into a personal computer required an extremely economical utilization of the memory space whereby an element number of 40 was achieved.
The critical loads can also be limited by the condition that the torsion must not be higher than $\vartheta \leq 0{,}2$.

4. Examples of calculations

a) Yielding and ultimate loads of a rigidly stressed beams with distributed loads

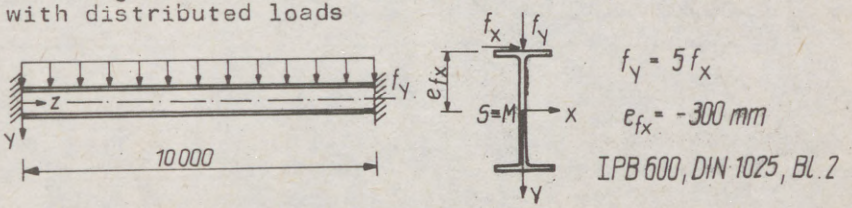

Critical load	Load	Dim.	LINDNER /6/	KINDMANN/7/	EHELEBE/3/	RAHAL /1/
Yielding load	$f_{y,el}$	N/mm	47,2	—	48,45	48,32
Ultimate load	$f_{y,u}$	N/mm	95,9	108,2	—	108,44/111,6 *
Error to /1/	Δ	%	-12,37	-1,13	—	0

* by nonlinear second-order theory

The comparison between the results shows that there are plastic ultimate reserves of up to 100 % available for statically indeterminate systems due to transposition of the cross-section force. Calculations for statically determinate systems have shown that those reserves are between 20 and 50 % only. The loads according to the non-linear second-order theory are within practically interesting ranges of beam lengths by approximately 0,5 to 2 % above the values found out according to the linear second-order theory. The differences are still smaller in case of an elastic analysis and, thus, without any importance for practical use.

b) Comparison between ultimate loads by means of flexural torsion according to TGL 13503/02 /5/

In line with the stability regulation of the GDR, TGL 13503/02, it is possible to make a stress proof according to the second-order theory for flexural torsionally stressed bars. Here approximately plastic material reserves can be used if partially plastic section moduli W_T are applied. The proof by means of a global safety factor has to be made as follows:

(8)

$$\sigma = \frac{M_x - M_y \vartheta}{A_{xx}} \; y\, k_x + \frac{M_y + M_x \vartheta}{A_{yy}} \; x\, k_y - 0{,}9\, E\, \omega_M \vartheta \leq \sigma_F \qquad (18)$$

$$k_x = \frac{W_{x,el}}{W_{Tx}} \qquad k_y = \frac{W_{y,el}}{W_{Ty}} \qquad W_T = \frac{W_{el} + W_{pl}}{l} \leq 1{,}2\, W_{el} \qquad \sigma_F = \text{yield stress}$$

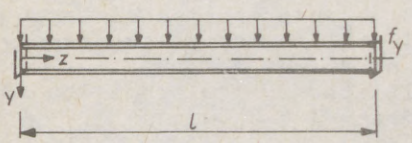

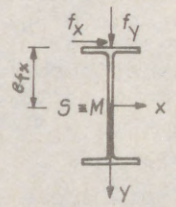

$f_y = 5 f_x$

$e_{fx} = -300\,mm$

IPB 600, DIN 1025, Bl. 2

Ultimate load	Dim.	f_y					
Length l	mm	2500	5000	7500	10000	12500	15000
FEM /1/	N/mm	953,7	222,72	91,28	47,19	27,60	17,42
TGL 13503 /5/	N/mm	553,6	193,6	65,05	36,45	22,85	15,3
Difference	%	41	35	28	22,7	17,2	12,1

The example shows the considerable ultimate reserves of the calculation according to /5/ which can be reduced by adapting of W_T.

References

/1/ Rahal, M., 1989, Beitrag zur Traglastermittlung von räumlich belasteten Durchlaufträgern mit Hilfe der Finiten-Element-Methode, Technische Hochschule Leipzig, Diss. A

/2/ Goeben, H.-E., Loos, W., 1986, Stabilität von Trägern aus Stahl - Analyse eines Wissensgebietes, Technische Hochschule Leipzig, Diss. B

/3/ Ehelebe, K., 1986, Beitrag zur Lösung des allgemeinen Biege-Torsionsproblems als Spannungsproblem der Theorie II. Ordnung nach der Finiten-Element-Methode, Technische Hochschule Leipzig, Diss. A

/4/ Szilard, R., 1982, Finite Berechnungsmethoden der Strukturmechanik, Bd. 1 - Stabwerke, Berlin (W) - München

/5/ TGL 13503/01 and /02, April 1982, Stabilität von Stahltragwerken, Berlin

/6/ Lindner, J., 1970, Näherungsweise Ermittlung der Traglasten von auf Biegung und Torsion beanspruchten I-Trägern, Technische Univ. Berlin (W), Diss.

/7/ Kindmann, R., 1981, Traglastermittlung ebener Stabwerke mit räumlicher Beanspruchung, Inst. Konstr. Ing.-Bau, Ruhr-Univ. Bochum, Techn.-wiss. Mitt. Nr. 81-2, Diss.

(1)
SZATMÁRI, István (1)
TOMKA, Pál (2)

ANALYTICAL AND NUMERICAL STUDY ON THE LATERAL INSTABILITY OF A PLATED BRIDGE

INTERNATIONAL COLLOQUIUM
STABILITY OF STEEL STRUCTURES
BUDAPEST, HUNGARY, 1990
PRELIMINARY REPORT

Summary: Theoretical and experimental investigation of simple supported cantilevered beam with open, monosymmetrical cross-section is given. Approximate energy solution for the critical load, results of second-order computer analysis, model tests and actual design problem are presented. Numerical approaches were developed or applied with special attention to critical situation that may arise at free erection of continuous beams.

1. Introduction

At the free erection of bridges especially in case of continuous beams special problems arise. Relatively long cantilever as a continuation of the erected simple supported beam in itself requires close attention. Furthermore, some technologies use cranes where the application point of the load due to the unit to be built in is relatively high above shear center as it is illustrated in fig. 1.

The above mentioned circumstances may cause critical situation, especially in case of open cross-sections restrained only at internals by cross-beams and cross-ties.

Because of the relatively few available theoretical result the paper offers three approches for the analysis of the problem:

- energy method to obtain the critical load,
- a second-order elastic computer analysis with program STERUE (Szatmári 1990.),
- test results of small scale model specimens.

---

(1) Assoc. Prof. Department of Steel Structures TU Budapest
(2) Senior research assistant, Research Group for Applied Mechanics of the Hungarian Academy of Sciences, Department of Steel Structures, Technical University Budapest

(2)

2. CRITICAL LOAD BY ENERGY METHOD

The notations are shown in fig. 1. Actual dimensions refer to the test specimen discussed later.

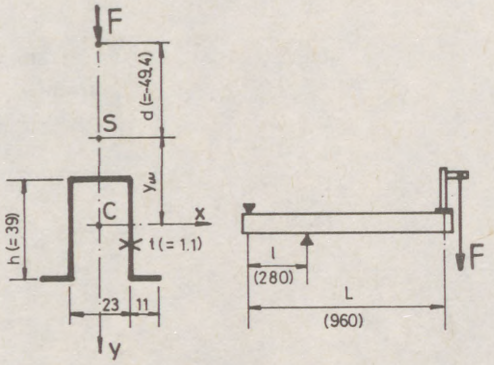

figure 1

The angle of rotation γ and the lateral deflection u are assumed in the form of polynom of forth degree:

$$\gamma = a_0 + a_1 z + a_2 z^2 + a_3 z^3 + A z^4 \qquad (1)$$

$$u = b_0 + b_1 z + b_2 z^2 + b_3 z^3 + B z^4 \qquad (2)$$

The constants a_0 through a_3 and b_0 through b_3 can be obtained by substituting the four boundary conditions for γ and u respectively:

$$\begin{aligned} u = u'' = \gamma = \gamma'' &= 0 \quad \text{at } z = 0 \\ u = \gamma &= 0 \quad \text{at } z = \ell \\ u'' = \gamma'' &= 0 \quad \text{at } z = L \ . \end{aligned}$$

The above listed boundary conditions do not take into consideration the shear force in the plane of lateral deflection u and the torque at z=L. Furthermore, one free parameter per displacements γ and u allows only an upper bound solution.
Leaving the estimation of the degree of approximations induced for subsequent discussion of numerical and experimental results, after substitutions the assumed functions may be written in the following form:

$$\gamma = A L^4 f \qquad (3)$$

$$u = B L^4 f \ , \text{ with} \qquad (4)$$

$$f = b\zeta - 2\zeta^3 + \zeta^4$$

$$b = 2\lambda^2 - \lambda^3$$

$$\lambda = \ell / L$$

$$\zeta = z / L$$

(3)
The total potential energy of the system is expressed by the well-known equations:

$$P_1 = \frac{1}{2}\left[EJ_y\int_0^L (\gamma'')^2 dz + 2\int_0^L M\gamma' u' dz\right]$$

$$P_2 = \frac{1}{2}\left[EC_w\int_0^L (u'')^2 dz + EJ\int_0^L (\gamma')^2 dz + \int_0^L M\gamma' u' dz + 2\beta_y\int_0^L (\gamma')^2 dz + Fd\frac{\gamma_L^2}{2}\right]$$

where:

$$M = F(1 - 1/\lambda)z \qquad 0 \le z \le \ell$$

$$M = F(z - L) \qquad \ell < z \le L$$

$$\beta_y = \frac{\int y(x^2 + y^2)}{J_x} - y_\omega$$

$\gamma_L = b - 1$ (angle of rotation at z = L)

Substituting the functions (3) and (4) for γ and u, putting the first variations of the total potential energies P_1 and P_2 equal to zero the determinant of the system of linear equations obtained must vanish. Finally, the critical value of F may be obtained by the following non-dimensional formula:

$$\frac{F_{CR} L^2}{\sqrt{GJEJ_y}} = C_1\left[\sqrt{1 + \alpha(\beta^2 C_2 + C_3)} + \beta\sqrt{C_2\alpha}\right] \qquad (5)$$

where

$$C_1 = \sqrt{\frac{I_1 I_2}{I_3^2}}; \qquad C_2 = \frac{I_1}{\pi^2\varepsilon_w^2 I_1 I_3^2}; \qquad C_3 = \frac{I_1}{\pi^2 I_2}$$

$$\beta = 2\varepsilon_y I_3 + \varepsilon_d\gamma_L^2$$

$$\varepsilon_w = \frac{2}{h}\sqrt{C_w / J_y}$$

$\varepsilon_y = \beta_y / h$ (positive if application point is below shear center)

$\varepsilon_d = d / h$

$$I_1 = \int_0^1 (f'')^2 d\zeta; \qquad I_2 = \int_0^1 (f')^2 d\zeta$$

$$I_3 = (1 - 1/\lambda)\int_0^\lambda (f')^2\zeta d\zeta + \int_\lambda^1 (f')^2(\zeta - 1) d\zeta$$

(4)
To check the results equation (5) was applied to a simple cantilever beam completely fixed at the support by putting $\lambda = 0$.
The results for doubly symmetric I section ($\varepsilon_w \sim 1$, $\varepsilon_y = 0$) with

$\varepsilon_d = 0$ (loading at shear center)
$\varepsilon_d = -0{,}5$ (loading on top flange)

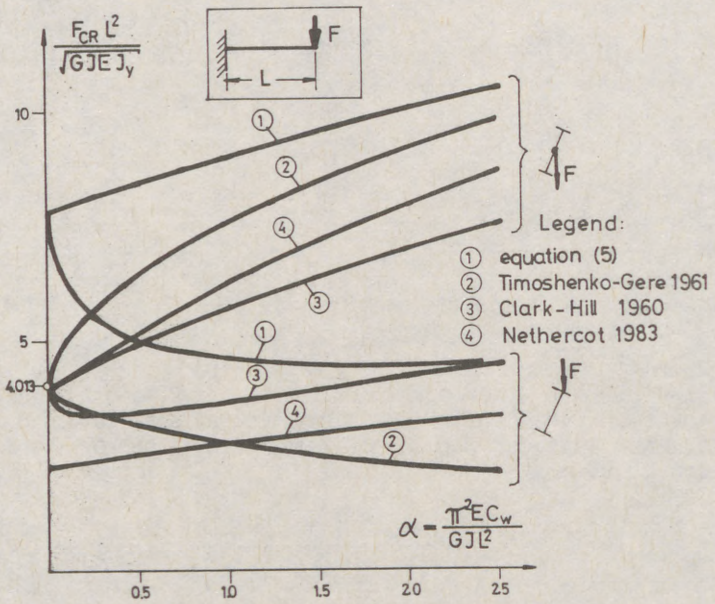

figure 2

are shown in fig. 2. For comparison some of the available solutions are also plotted. Due to the nature of the method applied the curves computed from equation (5) lie above the other, partly exact but partly also appoximate curves. The agreement is closer in case of top flange loading at relative high value of α .

3. Experimental investigations

Arrangement and dimensions of the specimens are given in fig. 3. Test specimen No 1 was made with open cross-section while No 2 was restrained at intervals by flats. Equivalent thickness of the restraint on lower flange was found as 0.012 mm.

The load was applied on the attachement fastened to the end of the cantilever. The application point was adjustable in steps. Lateral deflections were measured at the top of the attachment and the bottom of the beam allowing to evaluate the angle of rotation γ and the lateral deflection of the shear center u respectively. Tests were carried out using a small initial twist γ_0 .

(5)

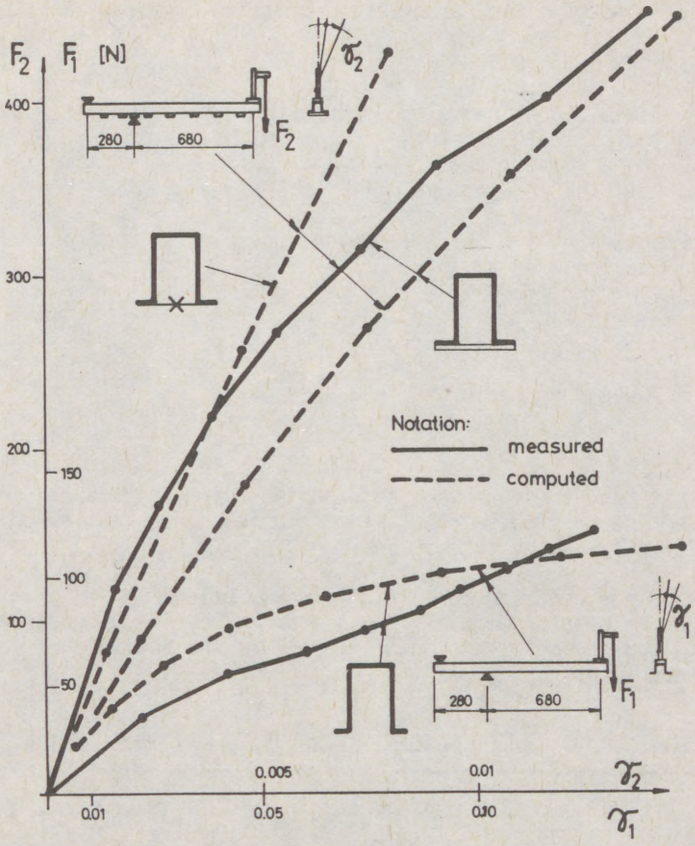

figure 3

The plot of experimental data is given with solid line on fig. 3. in the form of angle of rotation ϑ versus load F. The ultimate loads were

$$F_{u1} = 122 \text{ N} \quad \text{and} \quad F_{u2} = 451 \text{ N}.$$

Experimental data were confronted by two numerical approaches.
The results of program STERUE are also given on fig. 3. The ϑ versus F curve of test speciemen No 2 was computed in two different ways:

- with varying cross-section due to the exact geometry and
- assuming a constant closed profile using the previously mentioned $t_{equ.} = 0.012$ mm.

It can be seen that in case of the open profile the agreement of measured and computed ultimate load is quite satisfactory. On the other hand, in case of the restrained cross-section the application of semi-opened, true numerical model results in a good match while the use of the equivalent closed profile can be accepted only as a first-order approximation.

(6)
Critical forces for the two cases were calculated by formula (5) giving

F_{CR1} = 141N and F_{CR2} = 2500N.

In praxis it was found that a good approximation of the ultimate load can be get using the following formula:

$$F_u/F_y = 0.5(\beta - \sqrt{\beta^2 - 4n\, F_{CR}/F_y}) \qquad (6)$$

where
F_y - the force causing full plastic moment (with a yield stress of 270 N/mm^2 in our case F_y = 715 N)

$\beta = n\,(1 + F_{CR}/F_y)$ and

n = 1.2
Applying the above formula to the test specimens:

$$F_{u,appr,1} = 136\ N \text{ and } F_{u,appr,2} = 673N.$$

In the first case the agreement between the approximation and test result seems to be surprisingly good. The second approximation exceeds the measured ultimate load by some 50 per cent.

4. Analysis of the erection phase of a highway bridge
Having proven the efficiency of program STERUE by the comparison with the results of model test the next example is the analysis of the lateral buckling of a highway bridge at the erection phase.

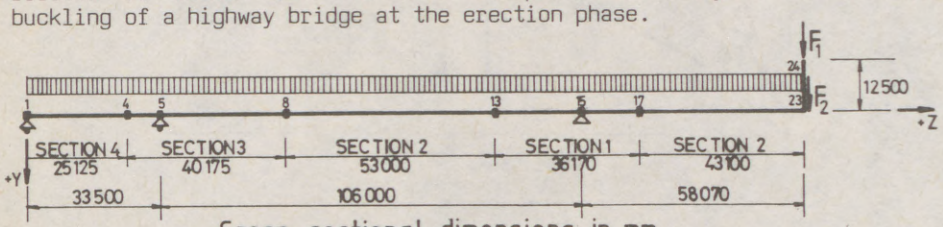

Cross-sectional dimensions in mm

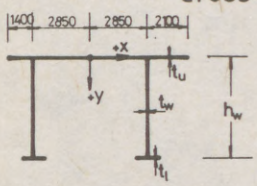

	1	2	3	4
t_u	16	12	12	12
h_w	5000	4000	2900	2500
t_w	16	12	12	12
b_l	1200	720	720	540
t_l	50	40	40	30

figure 4

For the input of the computer program a slightly modified layout shown in fig. 4 was used. This was the most critical stage of the free erection from point of view of lateral buckling: continuous beam over three supports with a 58 m long cantilever. The crane at the end of this cantilever raises the application point of the loading by 12.5 m above the traffic deck. Actual cross-sections were appriximated by four typical ones (notation 1 to 4).

(7)
Actual loadings are the nominal values of dead- and erection loads, the weight of the crane and the last unit to be built in, the latter magnified by a dynamic factor of $\mu = 1.5$ (see figure).
Displacements and stresses were computed as functions of a loading parameter p. This way the actual numerical values of loadings at different loading levels can be obtained from the following formulae:

$$f_{eff} = p\, f$$
$$F_{1,eff} = p\, F_1$$
$$F_{2,eff} = p\, F_2,$$

that is full intensity of loading would be reached at p = 1.0.

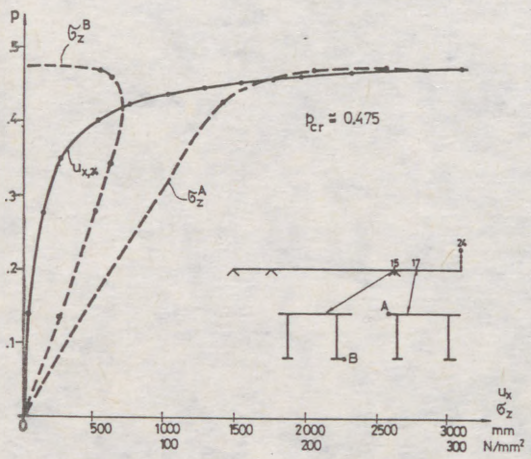

figure 5

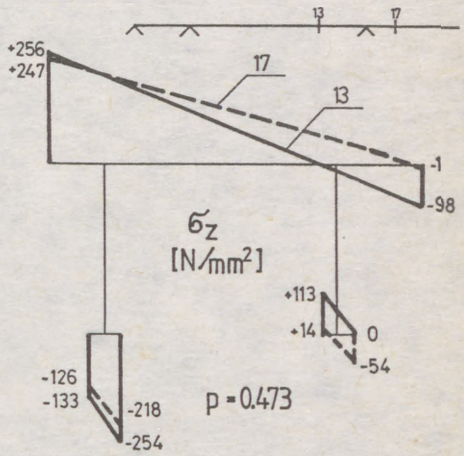

figure 6

Horizontal displacement normal to the longitudinal axis of nodal point 24 (u_x) and normal stresses at cross-sectional points of special interest versus p are shown on fig. 5. The distribution of normal stresses over the cross-sections 17 and 13 can be seen on fig. 6 et loading level of p = 0.473. The results illustrated by the two figures indicate a lateral buckling at critical value of $p_{CR} \sim 0.475$. The conclusion is that the erection of the given structure can not be carried out in the form illustrated by the scheme in fig. 4.

5. Conclusion

In case of delicate problems associated with lateral buckling where exact solutions are not available relatively simple analytical and numerical approaches give satisfactory results for the design praxis.
It should also be noted that at the free erection of bridges with open cross-section the use of temporary bracing against lateral buckling is generally unavoidable.

(8)

REFERENCES

Clark, I. W., and Hill, H.NM., 1960: LATERAL BUCKLING OF BEAMS, Journal of the Structural Division, ASCE, Vol. 86., No. ST7, pp. 175-196.

Nethercot, D.A.,: 1983: Beams and Beam-Columns-Stability and Strength, Elsevier Applied Science Publishers, London and New York, Chapter 1.

Szatmári, I., 1990: A New Numerical Approach for the Calculation of 3D Bar Systems. International Colloquium on Stability of Steel Structures, Budapest (under edition).

Timoshenko, S.P., and Gere, I. M., 1961.: Theory of Elastic Stability McGraw-Hill Book Company, Ins., New York-Toronto-London, Chapter 6.

(1)
TOMKA, Pál (1)

Lateral buckling of haunched members

INTERNATIONAL COLLOQUIUM
STABILITY OF STEEL STRUCTURES
BUDAPEST, HUNGARY, 1990
PRELIMINARY REPORT

Summary : The paper is a contribution to the complex problem arising at the design of members with varying section subject to non-uniform moment. Restraint of upper flange at intervals is assumed. Details of a parametric study illustrate the effect of different structural parameters. A practical design proposal based on the results of the parametric study is also given. The proposal is supported by other solutions and experimental evidence.

1. Introduction

Haunching is frequently used at the ends of rafters to reduce the value of normal stresses arising from the relatively high but rapidly descending bending moment.

In almost all cases rafters are restrained at intervals by purlins ensuring full restraint against lateral displacements at their attachments. Conservative approaches developed for the design of overall lateral buckling of rafters and columns take into consideration the above mentioned restraint only, neglecting the torsional restraint supplied by purlin to rafter connection, elastic restraint against warping and lateral twist at the ends.

Test programs carried out by the Department for Steel Structures of TUB yielded precious informations about the nature and extent of the contribution of cladding, purlins, side rails and other structural elements of secondary importance to the load bearing capacity of frames. The general conclusion was that this composite action, with careful consideration, may be explored at the design , and conclusively, at the check of overall lateral buckling as well.

---

(1) Senior research assistant, Research Group for Applied Mechanics of the Hungarian Academy of Sciences, Department for Steel Structures, Technical University Budapest

(2)

The aim of the paper is doublefold: to give a qualitative view to illustrate the effect of some of the factors influencing the structural performance of the member in question, and, based on the critical loading obtained by elastic stability, to suggest practical design method for the praxis.

2. Elastic lateral buckling

To survey the effect of different structural factors influencing the critical value of the uniformly distributed load w a parametric study was made using the Timoshenko-Ritz method. Roots of the non-standard eigenvalue problem were obtained by iteration.

Some of the numerical results are listed below. The notation is given in fig. 1. The common parameters and circumstances are:

- haunching is made by halfing the profile of rafter,
- enforced axis of rotation and application level of loading is assumed at a distance of 0.25h above upper flange,
- boundary conditions: free warping and lateral twist,
- both end moment parameters m are taken as unity,
- the effect of axial force is neglected.

Plots are given in non-dimensional form. In the ratio of moments:

$M_{CR} = mw_{cr}L^2/12$: critical end moment,

M_{OCR} : critical value of uniform bending moment with constant cross-section, without haunching.

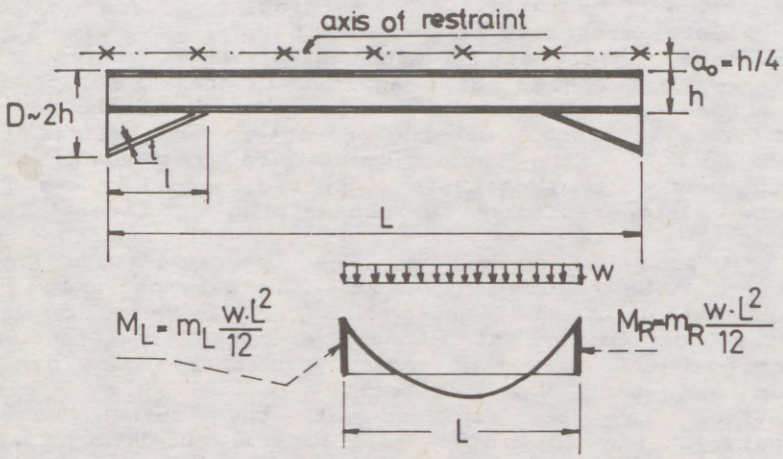

Figure 1

(3)

The effect of variation in the length of haunching can be seen in fig. 2. It is of interest that for stocky beams the critical moment decreases at longer haunches. It is to be mentioned that a similar anomaly was experienced by Bradford 1988. as well. By aspection the curves it is clear that the increase in the length of haunch itself has not a decisive effect on the stability . Therefore the choice of the length depends rather on the proper reduction of compressive normal stresses arosen from major axis bending moment.

The influence of uniformly distributed torsional restraint k is shown in fig. 3. There is a remarkable increase in critical moment even in case of relatively low k values. On the other hand, at the choice of the numerical value of k a careful consideration has to be done involving all circumstances mentioned by Horne and Morris 1977.

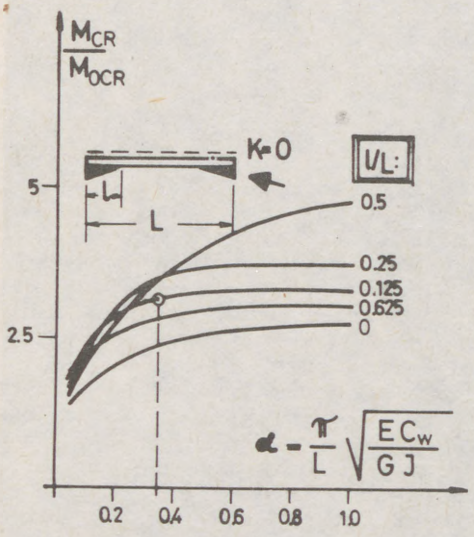

figure 2

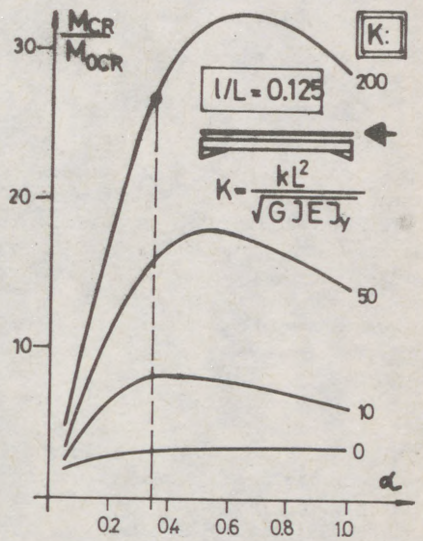

figure 3

Solution for negative value of w is given in fig. 4. This is a problem of semi-closed and open buildings with light weighted cladding on the roof subject to wind suction. Despite of the fact that in this case a relatively long part of the outstanding flange in span is in compression, values of critical moment show a marked increase. This is due to the advantegeous position of the application level of loading.

Finally, the stabilising effect of restraint against lateral displacement of lower flange at midspan is illustrated in fig. 5. In the lack of other restraints this solution - represented for example by a longitudinal tie or rafter bracing - is used to increase the resistance of rafters.

(4)

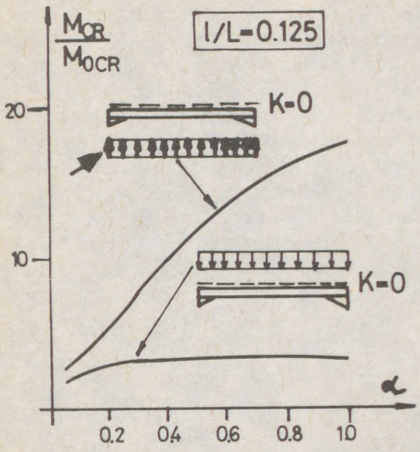

figure 4

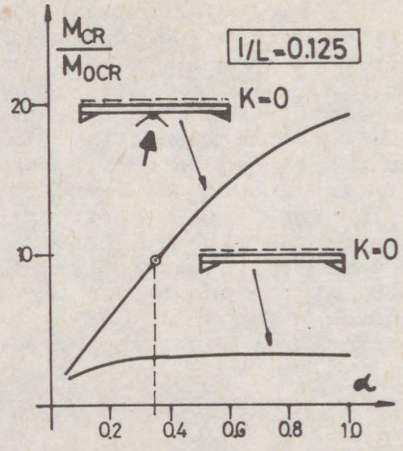

figure 5

3. Practical application

The advantage of the use of the bifurcation theory lies in the fact that by means of relatively simple algorithm practically all structural factors can be taken into consideration. A parametric study with properly chosen parameters may cover all practical situations, or, alternatively, even a home computer may give instant answers for particular problems.

On the other hand, all effects of initial imperfections can not be analysed this way. For this reason, results of elastic stability require transition for practical use.

This transition is illustrated by a practical example, taken with slight modification from the experimental program mentioned in Iványi-Kálló-Tomka 1986.

Geometrical dimensions of the rafter in question are shown in fig. 6. Results of subsequent procedures are given in term of load factor defined by the ratio of design moment M_d over the full-, or in some cases the modified plastic moment $M(\bar{M}_y)$ of the deep cross-section.

3.1 Problem 1 : Restraint against torsion at midspan but no uniformly distributed restraint (k =0)

3.11 Proposed design due to Hungarian Standard MSZ 15024/1-85 (HS)

The critical moment derived from the value marked on fig. 5 is:

M_{CR} = 273 kNm

(5)

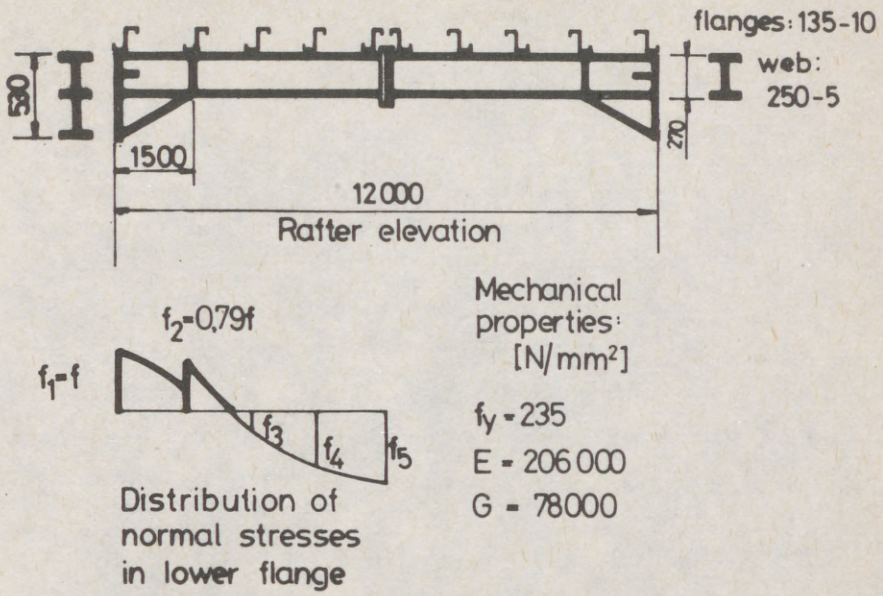

figure 6

As it can be seen from the distribution of normal stresses in the outstanding lower flange the critical cross-section is at left end with critical stress of

$$f_{CR} = 295 \text{ N/mm}^2 .$$

The equivalent slenderness ratio can be obtained from the general formula slightly modified by HS :

$$\lambda = \sqrt{\frac{1.1\ E}{f_{CR}}}$$

The design stress :

$$f_d = \varphi_{LT}\varphi_y \ / \text{ Factor of Safety}$$

where :

$$\varphi_{LT} = \left[\frac{1}{1 + \left(\frac{\lambda_{LT}}{\lambda_E}\right)^5}\right]^{0.4}$$

and with

λ_E = 93 (for low carbon steel)

φ_{LT} = 0.806

The design moment:

$M_d = \bar{W}\varphi_{LT}f_y$ / F.S. ($\bar{W}$ = 1.1 x elastic sectional modulus)

(6)

The modified plastic moment:

$\bar{M}_y = \bar{W} f_y / F.S.$

Consequently :

$M_d / \bar{M}_y = \varphi_{LT} = 0.806$.

3.12 Design moment obtained by transition formulae

3.121 Formula derived on the basis of experimental evidences

$$M_{ultimate} / M_y = \frac{1}{2} \left\{ \beta - \sqrt{\beta^2 - 4n\varphi} \right\}$$

where:

$\varphi = M_{CR} / M_y$

$\beta = n (1 + \varphi)$

$n = 1.2$,

and the full plastic moment :

$M_y = 244$ kNm .

In our case, with $M_{ultimate} = M_d$:

$M_d / M_y = 0.748$.

3.123 Formula suggested by Klöppel and Unger 1969

$$\frac{f_{LT}}{f_y} = \frac{c}{\sqrt[n]{1 + \left(\frac{c f_y}{f_{CR}} \right)^n}}$$

with

$c = S_{el} / S_{pl}$

S_{el}, S_{pl} : elastic and plastic cross-sectional moduli, respectively,

f_{LT} : design stress for lateral buckling for the use in formula : $M_d = f_{LT} S_{el}$,

$n = 3.35$.

In our case $c = 1.12$ thus

$\frac{f_{LT}}{f_y} = 0.959$, and this way :

$$\frac{M_d}{M_y} = \frac{f_{LT} S_{el}}{f_y S_{pl}} = 0.856 .$$

(7)

3.13 Design procedure introduced by Horne and Morris 1977.

The basis of this procedure is the torsional differential equation applied to a member of constant, double symmetrical cross-section, with an assumed initial deflection of the outstanding lower flange subject to uniform bending moment.

The solution is an equation for the normal stress from bending moment about the minor axis. The design criterion is that the sum of normal stresses from major and minor axis bending moment shold not exceed the yield stress. The basic formula was extended to non-uniform members subject to varying major axis bending moment. Hereby an effective length factor was defined computed from the distribution of normal stresses in the outstanding flange. In case of haunching the benefit of the increase in torsional costant due to the middle flange was also explored.

Experimental verification was done by Morris and Packer 1977.

Because of the differences in Universal sections and the fabricated profile in question cross-sectional properties of the reference section (the deep section at the left, see fig. 6) were substituted into the original formula (equ. (8) loc. cit.) giving a design criterion with only slight deviation from the original one:

$$f_{S,max} + \frac{2.1 f_y \bar{\lambda}}{20.6 + \left[3760(t/D)^2 - 0.069 f_y \right] \bar{\lambda}^2} \leq f_y \quad \text{with}$$

$$\bar{\lambda} = \sqrt{k}\, L / 100\, r_y$$

Introducing load factor γ the effective length factor is :

$$k = \frac{1}{12 f_y} \left(\gamma f_y + 3 \times 0.79 \gamma f_y + 0 + 0 + 0 + 0 \right) = 0.281 \gamma$$

Substituting the above expression for k and, assuming that the function of angle of rotation is non-symmetrical, for the maximum stress in span the one at the end of the haunching into the design criterion the solution for the load factor is :

$$\gamma = 0.720$$

Regarding γf_y as the design value of stress, according to 3.11 :

$$M_d / \bar{M}_y = \gamma = 0.720 .$$

The range of the different load factors obtained extends from 0.720 to 0.856 .Keeping in mind that the procedure giving the lowest value, due to the approximations involved and experimental evidences, is on the safe side the proposal seems to be satisfactory at least in this particular case. Therefore the next problems are analysed by this proposal.

(8)

3.2 Problem 3 : no intermediate restraint against torsion and k = 0

The cririticall moment according to fig. 2 is :

M_{CR} = 89.1 kNm .

The load factor computed by the method shown in 3.11 :

$M_d / \bar{M}_y$ = 0.362 ,

consequently the rafter under these circumstances is quite unpractical.

3.3 Problem 3 : same as Problen 2, but the uniformly distributed restraint k ≠ 0

Practically, this was the configuration investigated by the experimental program previously mentioned. The corrugated steel cladding was supported by Z purlins of 200 mm heigth with 1500 mm spacing and 6000 mm span. Purlin to rafter cleat connection was made by a four bolt moment resisting one. This allowed to consider the elastic restraint against torsion. In the lack of stiffeners the spring constant computed from the flexural rigidity of purlin has to be reduced. Examples for this reduction is given in Dooley 1967. and Lindner 1986. Additionally, the constant was further reduced so that actual bending moment at purlin to rafter connection due to a predetermined value of angle of rotation should not exceed 50 per cent of the lesser of the load bearing capacity of purlin and connection. Numerically, a uniformly distributed restraint represented by K=200 was adopted.

The corresponding critical moment using fig. 3 is :

M_{CR} = 761 kNm .

the load factor in this case :

$M_d / \bar{M}_y$ = 0.979 ,

almost full load bearing capacity. This was supported by the actual test because no sign of overall lateral instability could have been detected even at ultimate load of frames under test. On the other hand free lateral buckling - not discussed by this paper - developed near midspan between the purlins at the vicinity of ultimate load.

Summarising the last example, the proposed method is in good agreement with the experimental experience.

4. Conclusions

A parametric study based on elastic critical load is in itself a powerful help to analyse the effects of different structural parameters influencing the stability of members with non-uniform sections, restrained at intervals subject to practical loading conditions. Moreover, results obtained by the bifurcation theory, with a relatively simple transition, may be used for practical design too, as proven by detailed comparisons with other methods and experimental evidences.

(9)

References

Bradford, M. A., 1988 : Stability of Tapered I-Beams, Journal of Constructional Steel Research, 0143-974X, pp. 195-216.

Dooley, J. F., 1967 : ON THE TORSIONAL BUCKLING OF COLUMNS OF I-SECTIONS RESTRAINED AT FINITE INTERVALS, International Journal of Mechanical Sciences, Vol. 9., pp. 1-9.

Horne, M. R. and Morris, L. J., 1977 : The Design against Lateral Instability of Haunched Members Restrained at Intervals along the Tension Flange, International Colloquium on Stability of Sructures under Static and Dynamic Loads - Washington D. C., pp. 618-629.

Iványi, M., Kálló, M., Tomka, P., 1986 : EXPERIMENTAL INVESTIGATION OF FULL-SCALE INDUSTRIAL BUILDING SECTION, Second Regional Colloquium on Stability of Steel Structures - Hungary, Final Report, pp. 163-170.

Klöppel, K. and Unger, B. 1969 : Kippen von Durchlaufträgern bei seitlich und gegen Verdrehen gelagertem Obergurt, Der Stahlbau, 38, pp. 203-207.

Lindner, J., 1986 : COMMENTS TO THEME III: LATERAL BUCKLING, Second Regional Colloquium on Stability of Steel Structures - Hungary, Final Report, pp. 119-122.

Morris, L. J. and Packer, J. A., 1977 : STABILITY OF HAUNCHED RAFTERS, 2nd Colloquium on Stability of Steel Structures -Liege, Preliminary Report, pp. 539-544.

Y.C. Wang /1/ and
D.A. Nethercot /2/

"BRACING REQUIREMENTS FOR LATERALLY UNRESTRAINED BEAMS"

INTERNATIONAL COLLOQUIUM
STABILITY OF STEEL STRUCTURES
BUDAPEST, HUNGARY, 1990
PRELIMINARY REPORT

Summary

Results from a finite element program specially developed to study the behaviour of braced beams are presented. These show that providing a beam is braced with restraints of stiffness sufficient to induce "complete support", a force of 1% of the axial load in a flange at failure may generally be assumed as the bracing strength requirement.

Introduction

For a laterally unrestrained beam, lateral torsional buckling is often the controlling failure mode. The stability of a beam may, however, be improved through the provision of lateral bracings, which, in many practical arrangements will be present to some degree in the form of components such as floors, purlins, secondary beams etc. Although research into the bracing of beams and columns has a long history, rarely have the two key aspects of this problem, - the bracing stiffness necessary to increase the loading carrying capacity of the main member to the required level and the bracing strength necessary to withstand the loads transmitted to the bracing by the main member - been addressed satisfactorily.

Flint [1] showed that the ratio of the buckling load for a braced beam of zero warping stiffness to that for an equivalent unbraced one was $\sqrt{1+\lambda}$, where λ is defined as:

/1/ Postdoctoral Fellow, Department of Civil and Structural Engineering, University of Sheffield, U.K.
/2/Professor of Civil Engineering, University of Nottingham, U.K.

$$\lambda = \frac{\textit{bracing stiffness} \times [\textit{beam length}]^3}{48 \times [\text{beam rigidity about its minor axis}]} \qquad (1)$$

but did not address bracing strength requirements. In an ingenious simplified approach that assumed a fictious hinge at the bracing point, Winter [2] determined the minimum bracing stiffness necessary for "complete bracing" on a column i.e the bracing stiffness which causes the bracing to have the same effect on the main member as a rigid support. He also found in a series of simple tests that increasing the bracing stiffness in excess of this minimum value resulted in the reduction of bracing strength requirement. Zuk [3] obtained the bracing strength requirement for 8 cases of braced beams and columns by solving the differential equation of equilibrium or using the energy method. For elastic members without imperfections, Trahair and Nethercot [4] summarised the minimum stiffness necessary for complete bracing for a number of cases. Large-scale experimental studies conducted by Wakayabashi and Nakamura [5] have confirmed the theoretical view that comparatively light bracing can improve the stability of beams enormously; tests by Wong-Chung and Kitipornchai [6] have confirmed the ineffectiveness of bracing located on the tension flange of a beam and showed that shear centre bracing would be as effective as torsional bracing.

Realistic study of the bracing requirements for real structures requires that the effects of plasticity and imperfections be taken into consideration. With this in mind, the authors have extended a rigorous finite element program for three dimensional ultimate strength analysis of beam-columns to include bracing effects. This paper presents the results from a study using the modified program, in which the interrelationship between bracing stiffness, bracing strength and load carrying capacity for a number of representative cases of braced beams, are presented.

Theoretical Analysis and Program Verification

Theoretical Analysis

A finite element approach has been used to produce the results reported herein. This represents three dimensional beam-column behaviour with a line element, which has seven degrees of freedom at each node representing the actions of thrust, bending about both major and minor axes, torsion and warping of a thin-walled open cross-section. Using the virtual work principle, a second order analysis has been performed by Rajasekaran [7] to derive the tangent stiffness matrix for this type of element. This stiffness matrix formed the basis for extensions by El-Khenfas [8] to consider ultimate strength problems of simply supported beam-columns. In this analysis, instability effects are accounted for by a geometrical stiffness matrix; plasticity is considered by dividing the cross-section into a number of small regions; imperfections (including initial deflections) are included by establishing the member stiffness matrix for the deformed position

and transforming it to the reference coordinate system using a geometrical transformation matrix. This program has now been extended by the authors to study the effects of end restraint and intermediate bracings. Bracings are assumed at nodal points and their effects are included by adding their contribution to the energy of the overall system, which result in an additional stiffness matrix for each braced node. These matrices are simply added to the overall stiffness matrix for the member as explained in ref. [9].

Program Verification

One series of validations for the program has used the set of tests on I-beams braced by either purlins or sub-beams of Wakayabashi and Nakamura [5]. Purlins were modelled as torsional braces with an elastic perfectly plastic moment-rotation curve and an elastic stiffness of $8.88 kNm/rad$ and a limiting moment of 0.444 kNm. The sub-beam was assumed to be an elastic rotational spring with a stiffness of $6.24 \times 10^{-3} kNm/rad$ located at the beam's shear centre. Table 1 gives the ultimate strength comparison between the authors' results and the test results in terms of the ratio of applied maximum moment M_u to the plastic moment capacity of the beam M_p. That the analytical result is generally lower than that from the test, especially for beams involving a large amount of yielding, is principally due to the neglect of strain hardening in the analysis. Figure 1 compares selected calculated and experimental load-deflection curves. A second validation using

Type of major axis moment	Type of bracing	Length (m)	Slenderness	M_u/M_p Ref.5	M_u/M_p Present Analysis	percentage difference
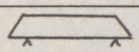	Unbraced	5.0	459	0.35	0.33	-6.0
		2.5	229	0.59	0.573	-4.4
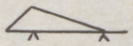	Unbraced	6.5	596	0.45	0.42	-7.0
		5.0	459	0.58	0.53	-8.4
		3.5	321	0.80	0.80	0.0
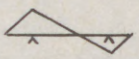	Unbraced	6.5	596	0.60	0.54	-10.0
		3.5	321	0.86	0.82	-5.2
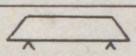	Purlins	5.0	459	0.63	0.63	0.0
		2.5	229	0.84	0.83	-1.3
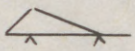	Purlins	5.0	459	0.92	0.88	-4.4
		3.5	321	1.08	0.90	-17.0
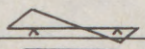	Purlins	6.5	596	0.99	0.89	-10.0
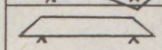	Sub-beam	5.0	459	0.52	0.49	-6.0
		2.5	229	0.90	0.83	-7.5
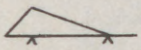	Sub-beam	6.5	596	0.60	0.56	-6.3
		3.5	321	0.90	0.88	-2.3

Table 1 Comparison of author' results with tests of Ref. 5 - ultimate loads.

the tests of Wong-Chung and Kitipornchai [6] gave discrepancies of less than 2% for most cases and less than 5% for every case considered. Numerous checks for unbraced members, covering a variety of load types, cross-sections, slendernesses etc. [8] [9] have also been made.

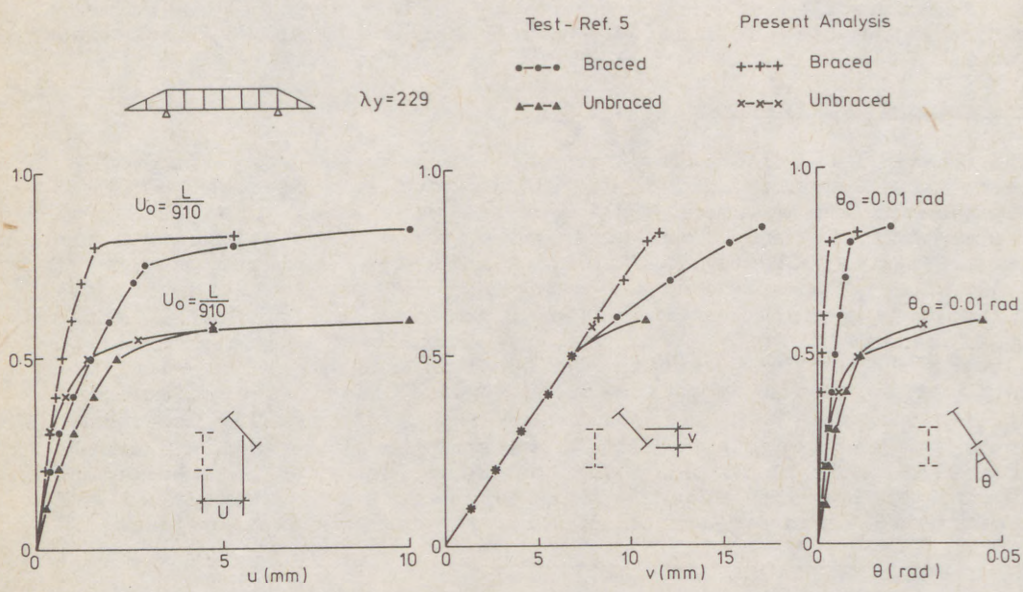

Fig. 1 Comparison of authors' results with tests of ref. 5 uniform moment on central segment.

Results of Parametric Study

The program has been employed to study the interrelationship

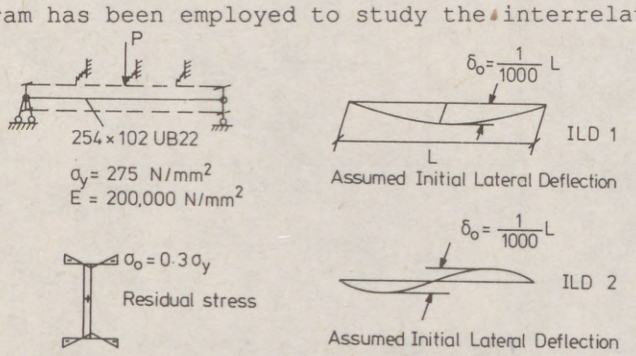

Fig. 2 Basic data for Parametric Study.

between bracing stiffness, bracing reaction force and the ultimate strength of the main member for a number of representative cases of beams with single or multiple bracing systems. In all cases the beam was assumed simply supported at both ends and load was applied to the upper flange at midspan. Figure 2 illustrates the basic arrangement used in the parametric study.

Single Bracing System

Type 1 ILD was assumed for this case. Figures 3(a) and 3(b) give the load versus shear centre deflection and load-bracing force relationship for a brace located at the upper flange with a stiffness of $1.0 \times \frac{48EI_y}{L^3}$. (Trahair and Nethercot [4] gave a value of $\frac{\pi^2}{3} \times \frac{48EI_y}{L^3}$ as the value required for "complete support" for this

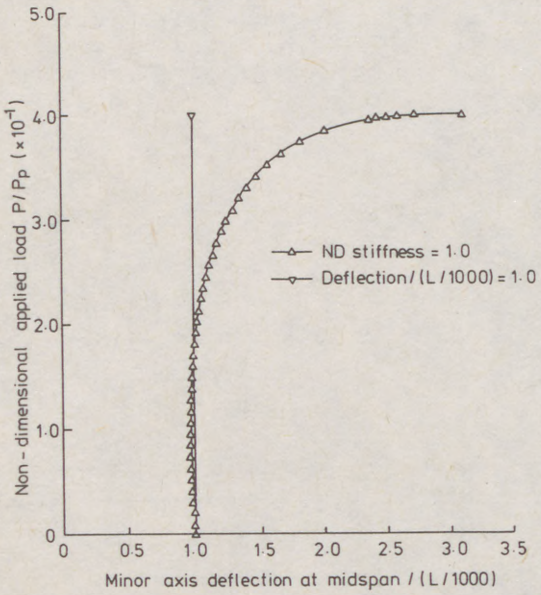

Fig. 3a Load-deflection relationship for upper flange bracing, upper flange loading $\frac{}{S_b} = 1.0$

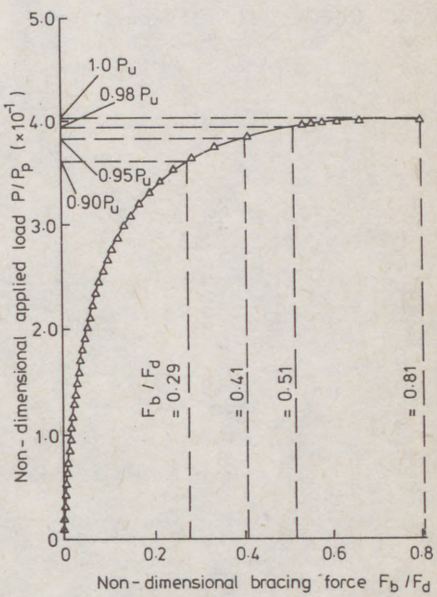

Fig. 3b Load versus bracing force relationship for upper flange loading, upper flange bracing. $\frac{}{S_b} = 1.0$

type of bracing arrangement). Although given for a particular combination of problem parameters, the behaviour is generally representative of the results as a whole.

It is apparent that both curves are highly non-linear from the start. A tendency for the sign of the deflection to reverse is present in Figure 3(a). This is expected since the brace at the upper flange initially holds the movement of the flange but the shear centre tends to deform towards the straight beam position relative to the upper flange because of torsion. At higher loads, however, the rapid increase in lateral deflection overcomes this tendency. For stiffer braces, the effect is more pronounced, leading to a slight deformation in the opposite direction and thus a slight reduction in the ultimate strength [9]. Fig 3(b) indicates that bracing force increases rapidly as beam failure is approached. Figure 4 presents the main member ultimate load - bracing stiffness and bracing force - bracing stiffness relationships for both upper flange bracing and shear centre bracing. The bracing stiffness S_b is nondimensionalised as $S_b/(48EI_y/L^3)$, while the ultimate load P_u and the ultimate bracing force F_u are expressed as P_u/P_p and F_u/F_d respectively. P_p is the load when the beam cross-section at midspan reaches its plastic moment carrying capacity M_p i.e. $P_p = 4.0 \times M_p/L$ and F_d is one percent of the axial load in a flange at this state i.e. $F_d = 0.01\sigma_y t_f d_f$.

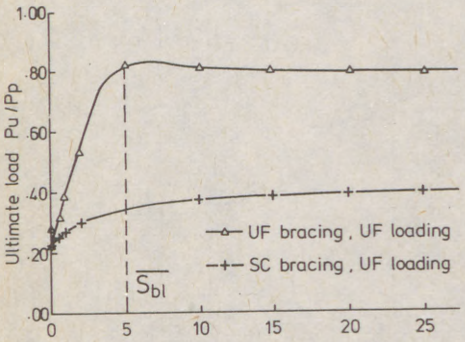

Fig. 4a Ultimate load - bracing stiffness curves for translational bracings.

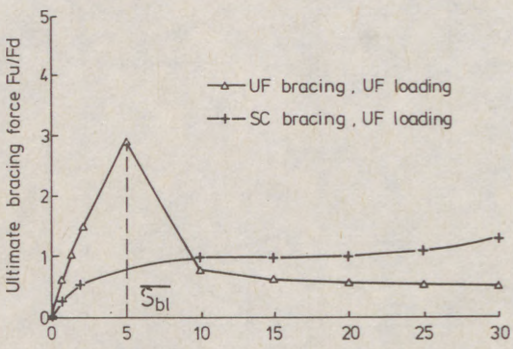

Fig.4b Bracing force - bracing stiffness curves for translational bracings.

Clearly placing the bracing at the upper flange means that "complete support" is achieved with bracing of quite modest stiffness, while the improvement for the main member due to the shear centre bracing is small principally because of its inability to restrain torsional deformation. Fig. 4b shows how the bracing force decreases with the use of braces stiffer than those needed to just provide "complete support". Providing the bracing

stiffness exceeds about twice the value for "complete support", bracing forces are relatively insensitive to changes in stiffness and Fig 4b suggests that taking F_u/F_d as 1 percent would be safe and reasonable.

This agrees quite well with the value specified in the British Standard [10] for lateral and torsional restraint, although the standard does not link the force requirement to any particular bracing stiffness level. Torsional bracing has also been considered [9] and similar conclusions emerge. Furthermore, changes in initial deflection seem to result in a straightforward proportional change in the bracing force [9].

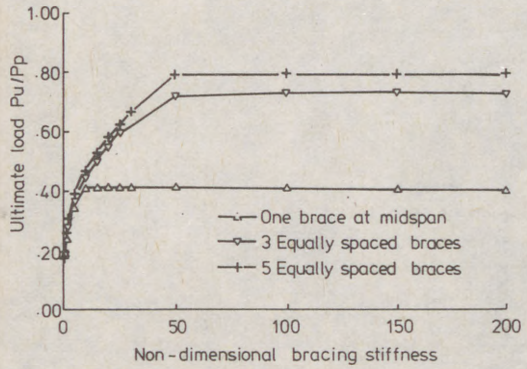

Fig.5a Ultimate load - bracing stiffness curves for beam slenderness = 600 (L=12m). UF bracing, UF loading. ILD type 1.

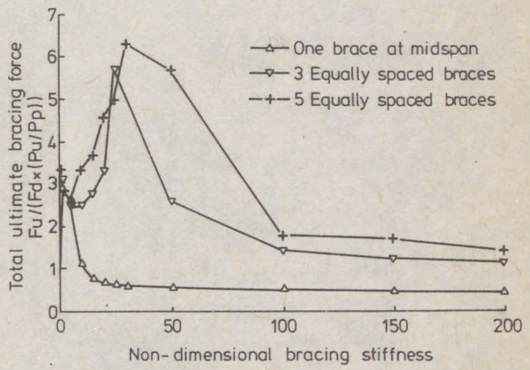

Fig.5b Bracing force - bracing stiffness curves for bea slenderness = 60 (L=12m). UF bracing, UF loading. ILD type 1.

Multiple Bracing

A beam slenderness of 600 was assumed in this study so as to provide a large margin for bracing enhancing main member strength. Equally spaced arrangements of 1,3 and 5 braces were considered. Figure 5 shows similar behaviour in all cases, although the bracing stiffness for complete bracing and the bracing strength requirements are higher when more braces are present. In figure 5, a non-dimensional stiffness value of 40 is obtained for the 3 & 5 restraint arrangements compared with a value of 5 for a single bracing system. Nevertheless, figure 5(b) indicates that a value of less than 2 percent of the axial load in a flange at failure is still sufficient as the total bracing strength requirement provided, of course, that sufficiently stiff bracing is used.Whilst the bracing strength requirement for the whole of the multiple system is quite steady, the requirement of an individual brace varies significantly according to its location and the assumed initial deflection type. Figure 6 shows an example of

bracing force distribution along the beam for the 3 brace case. It clearly demonstrates that the highest values always occur in the brace at the highest initial deformation and that a maximum value of 1% of the flange axial force at failure is required in design as the bracing strength for each brace regardless of its location.

Conclusions

A brief parametric study has been performed using a rigorous finite element program to address the problem of bracing

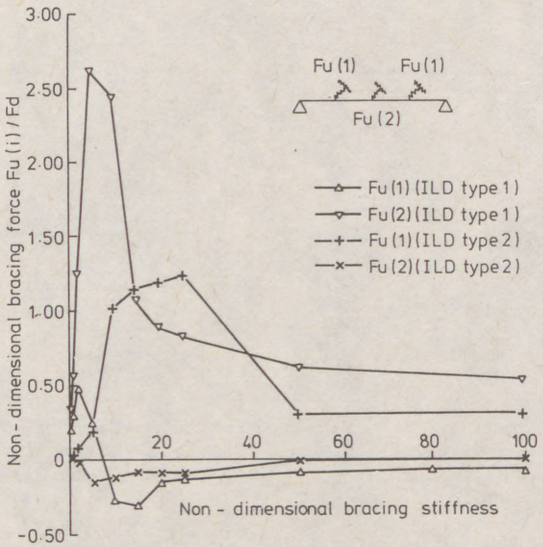

Fig. 6 Bracing forge versus bracing stiffness relationship for different bracing components for different initial lateral deflection (ILD) types. Upper flange loading, upper flange bracing.

requirements for unrestrained beams. It is concluded that for a single bracing system, one percent of the axial force in a flange at failure may be taken as the bracing strength requirement in design. For multiple bracing systems, this value may be unsafe in certain cases, especially for beams with high slenderness. However, a value of 2% may be considered more appropriate as a total figure, with a maximum value of 1% for each brace.

Acknowledgement

This work forms part of the first author's Doctoral research project financed by the British Council. The program used is based on that originally developed by Dr El-Khenfas.

References

(1) Flint A.R. The Influence of Restraints on the Stability of Beams. *The Structural Engineer.* September 1951, pp. 235-246.
(2) Winter G. Lateral Bracing of Columns and Beams. ASCE *Journal of Structural Division,* 1958, **84**, ST2, Mar., pp. 1-22.
(3) Zuk W. Lateral Bracing Forces on Beams and Columns. *ASCE Journal of Engineering Mechanics Division.* Vol. **82**, No. EM3, July 1956, pp. 1032(1-11).
(4) Trahair N.S. and Nethercot D.A., (Rhodes J. and Walker A.A.(eds)). Bracing Requirements in Thin-Walled Structures. *Developments in Thin-Walled Structures-2.* Elsevier, London, 1984, pp. 93-130.
(5) Wakayabashi M. and Nakamura T. Buckling of Laterally Braced Beams. *Engineering Structures.,* 1983, **5**, No. 2, Apr., pp. 108-118.
(6) Wong-Chang A.D. and Kitipornchai S.T. Partially Braced Inelastical Beam Buckling Experiments, *J. Construct. Steel Res., 1987,* **7**, *No. 3 pp. 189-211.*
(7) Chen W.F. and Atsuta T. Theory of Beam-Columns. Chapter 12, Vol. 2, McGraw-Hill International Book Company, 1980.
(8) El-Khenfas M.A. *Analysis of Biaxial Bending and Torsion of Open Section Beam-Columns.* University of Sheffield, 1987, PhD Thesis.
(9) Wang Y.C. *Ultimate Strength Analysis of Three-Dimensional Structures with Flexible Restraints.* University of Sheffield, 1988, PhD Thesis.
(10) British Standards Institution. *Structural Use of Steelwork in Building.* BSI, London, 1985, BS 5950: Part 1.

SESSION 5

BEAM-COLUMNS

(1)
BĂLUȚ, Nicolae (1)

A SUGGESTION FOR THE SEPARATE CONSIDERATION OF GEOMETRICAL AND MECHANICAL IMPERFECTIONS

INTERNATIONAL COLLOQUIUM
STABILITY OF STEEL STRUCTURES
BUDAPEST, HUNGARY, 1990
PRELIMINARY REPORT

Summary: While geometrical imperfections are equivalent to additional transverse loads, mechanical imperfections cause a decrease in stiffness. Since these two categories of imperfections are different by their nature, and their effects on the behaviour of structures are different (which can be easily observed by comparing for instance the cases of braced and of unbraced frames), it is preferable to consider them separately whenever the deformation caused by primary loads includes the fundamental buckling shape. A simplified method (based on the equivalent stiffness concept) is suggested for the second-order analysis of frames.

1. Introduction

Second-order analysis methods are more appropriate for checking the stability of frames, as compared to the traditional approach based on the effective length concept. The inadequacies of the latter concept have been clearly demonstrated by Vogel (1986).

More accurate results can be obtained by using the second-order plastic zone theory; however, approaches based on the plastic hinge theory or the elastic theory are generally preferred for practical design purposes. Their use requires some simplifying assumptions about the influence of imperfections. The most habitual procedure is to assume an equivalent geometrical imperfection, allowing for both categories of imperfections: geometrical (mainly initial deformations) and mechanical (mainly residual stresses). The equivalent geometrical imperfection concept was brought in by Ayrton and Perry (1886) for flexural buckling of compression members. Maquoi and Rondal (1978, 1979) suggested an equation based on a single imperfection parameter, which is able to offer

(1) Senior Research Engineer, Building Research Institute ICCPDC, Timișoara, Romania

(2)
the most accurate analytical expressions for the ECCS column curves. A few years later, Boraeve, Maquoi and Rondal (1983) formulated the equivalent imperfection in such a way that it reflects the decrease in the detrimental effect of residual stresses with increasing yield strength and allows for any amplitudes of geometrical and mechanical imperfections. More recently, Costa Ferreira and Rondal (1987) proved the applicability of the Ayrton-Perry formulation for the mathematical modelling of instability phenomena, such as: flexural, torsional or flexural-torsional buckling of compression members; lateral buckling of beams; local buckling of plates.

However, the author's opinion, expressed in a previous paper (1988), is that the use of this concept should be restricted to cases when the deformation caused by primary loads does not include the fundamental buckling shape, i.e. when the deformation characterizing the instability phenomenon under examination is merely due to imperfections. If this is not the case, it seems preferable to consider separately the effects of the two kinds of imperfections.

To illustrate this view-point, the simple example of a beam-column made of an ideal elasto-plastic material will be considered here (Fig.1a). The first yield condition can be expressed as:

$$\sigma = \frac{N}{A} + \frac{M + Nf_o}{(1 - N/N_E)W} \leq \sigma_y \qquad (1)$$

where N is the axial load, M are the equal end moments, f_o is the initial bow, A is the cross section area, W is the elastic section modulus, σ_y is the yield strength and N_E is the Euler load:

$$N_E = \pi^2 EI/l^2 = \pi^2 S/l^2 \qquad (2)$$

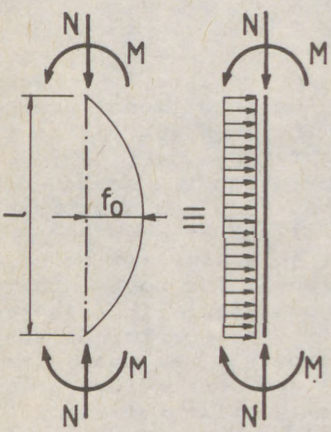

Fig. 1

In this case, the nonlinearity is merely geometrical. According to some recent design specifications (e.g. Eurocode Nr.3 and DIN 18800), the geometrical imperfection can be replaced by a uniform transverse load (Fig.1b).

By actual members, mechanical imperfections occur besides geometrical ones. If the maximum compressive residual stress in an extreme fibre is

$$\sigma_r = \alpha_r \sigma_y \qquad (3)$$

then the first yield condition becomes:

$$\frac{N}{A} + \frac{M + Nf_o}{(1 - N/N_E)W} \leq (1 - \alpha_r)\sigma_y \qquad (1')$$

If the load is increased beyond this limit, the bending stiffness of the mem-

(3)
ber is gradually diminished, because partial plasticizing occurs in certain zones. The curvature is known to be a nonlinear function of the axial load N, the second-order bending moment M^{II}, the yield strength σ_y and the residual stress pattern, see e.g. the paper by Beer and Schulz (1969). Since the bending moment varies along the member, the bending stiffness is also variable; the exact solution of this problem can only be obtained by a finite element analysis. Chen (1971) suggested analytical nonlinear moment-curvature-thrust relationships for different cross section shapes and residual stress patterns. For current design, however, one can be tempted to define an equivalent constant bending stiffness S_e. The limit state criterion for plastic (Class 1) or compact (Class 2) sections can be approximated as follows:

$$\frac{N}{A} + \frac{M + Nf_o}{(1 - N/N_{Ee})W_{pl}} \leq \sigma_y \qquad (1'')$$

Here

$$N_{Ee} = \pi^2 S_e / l^2 \qquad (2')$$

where S_e is the equivalent bending stiffness. For semi-compact (Class 3) sections, which are often used especially by welded columns, it is suggested to replace W_{pl} by KW:

$$K = (W + W_{pl})/2 \qquad (4)$$

where W_{pl} is the plastic section modulus. It can be shown that the longitudinal strain in the most compressed fibre corresponding to this partial plasticizing is still at the beginning of the yield plateau and therefore can be accepted for Class 3 sections. Eq.(1") becomes:

$$\frac{N}{A} + \frac{M + Nf_o}{(1 - N/N_{Ee})KW} \leq \sigma_y \qquad (1''')$$

According to the equivalent geometrical imperfection concept, the material is assumed to behave elastically, but the actual geometrical imperfection is replaced by a greater imperfection f_{oe}:

$$\frac{N}{A} + \frac{M + Nf_{oe}}{(1 - N/N_E)KW} \leq \sigma_y \qquad (1^{IV})$$

By comparing Eqs.(1''') and(1^{IV}), it can be observed that the first is more correct, because it allows for the detrimental effect of mechanical imperfections in increasing both the primary bending moment M and the moment Nf_o from geometrical imperfections. The two kinds of imperfections are different by their nature: while geometrical imperfections are equivalent to additional transverse loads, mechanical imperfections bring about a decrease in the member stiffness. These effects are by no means identical.

(4)

It should be recalled here that, in a comment concerning the well-known secant formula, Vinnakota (1973) emphasized the arbitrary character of an equivalent eccentricity e_o (the effect of which is similar to an equivalent initial bow f_o): 'Finally, the formula though simple, is irrational in that, this single variable e_o, has to do the job of so many variables...'

In the case of frames (braced or unbraced), geometrical imperfections are always detrimental to columns. As for mechanical imperfections, their influence in decreasing the stiffness of columns causes by unbraced (sway) frames an amplification of the bending moments produced by horizontal loads. On the contrary, by braced frames, moments are mainly due to vertical loads and therefore column end moments are decreased by the second-order effect. This decrease is intensified by the influence of mechanical imperfections. It follows that a conservative procedure would be to check the stability of each column of a braced frame by considering an isolated beam-column with the end moments resulting from a second-order analysis. But one would thus overestimate the restraint degree of the beams and consequently underestimate the beam moments in the span, especially in the case of single-bay frames, see the paper by Kindmann (1984).

2. The Equivalent Stiffnesses

Returning to the case of Fig.1, it must be pointed out that the equivalent bending stiffness S_e cannot result directly from the assumption that N_{Ee} is the buckling load of an imperfect compression member (according to a column curve), since such curves include the effects of both geometrical and mechanical imperfections and do not include the effect of primary bending moments. Instead, an interaction equation for flexural buckling of beam-columns will be considered, namely in the form specified by Eurocode Nr.3:

$$\frac{N}{\chi N_{pl}} + \frac{1}{1 - [N/(\chi N_{pl})](\chi\bar{\lambda})^2} \frac{\beta M}{M_u} \leq 1 \qquad (5)$$

where

$$N_{pl} = A\sigma_y \; ; \; M_u = 1.1\, W_{pl}\sigma_y \; ; \; \bar{\lambda} = \sqrt{N_{pl}/N_E} \; ; \; \beta M \cong 1.1\, M_e \qquad (6\text{–}9)$$

In Eq.(9), M_e is the equivalent uniform bending moment. Replacing W_{pl} by KW (for the above mentioned reasons), one obtains:

$$\frac{N}{\chi A} + \frac{1}{1 - [N/(\chi A\sigma_y)](\chi\bar{\lambda})^2} \frac{M_e}{KW} \leq \sigma_y \qquad (10)$$

Denoting

$$\sigma_N = N/A \; ; \; e = M_e/N \; ; \; \rho_K = KW/A \; ; \; \eta = N_{Ee}/N_E = S_e/S \leq 1 \qquad (11\text{–}14)$$

then assuming that N and M_e are a set of limit values, and comparing Eqs.(1^{IV}) and (10), the limit value of η is obtained:

(5)

$$\eta_l = \frac{\bar{\lambda}^2}{1 - \dfrac{f_o + e}{(1/\chi - 1)\beta_k + \dfrac{e}{1 - (\sigma_{Nl}/\sigma_y)\chi\bar{\lambda}^2}}} \cdot \frac{\sigma_{Nl}}{\sigma_y} \leq 1 \qquad (15)$$

where σ_{Nl} results from Eq.(11), replacing N by N_l (the limit value of N complying with Eq.(10) for a given e). If $N \leq N_o$ (the limit value of N complying with Eq.(1') for a given e), the member behaves elastically and $\eta = 1$. Assuming a linear variation of the stiffnesses as N varies between N_o and N_l, one obtains:

$$\eta = F(A, W, K, \bar{\lambda}, \sigma_y, \alpha_r, f_o, M_e, N) = \begin{cases} 1 \ (\text{for } N \leq N_o) & (16) \\ \eta_l + \dfrac{N_l - N}{N_l - N_o}(1 - \eta_l) \ (\text{for } N > N_o) & (17) \end{cases}$$

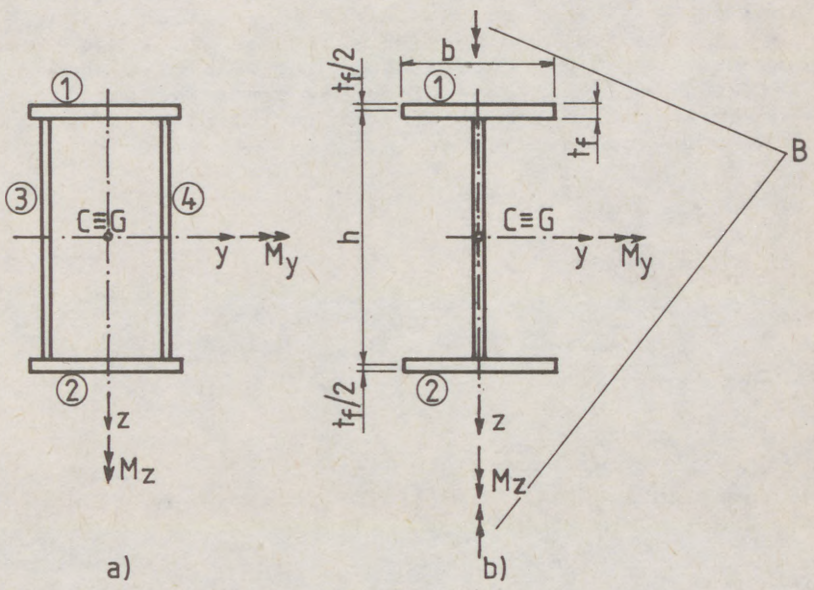

Fig. 2

Once the member forces have been computed, the strength of each column must be checked for compression and in-plane bending. An additional check is required against flexural-torsional buckling

(6)

(based on an interaction equation). This check becomes unnecessary if a second-order space-frame analysis is carried out (which is advisable in all cases when primary biaxial bending occurs). If mechanical imperfections are considered separately, then the bending stiffnesses about both principal axes of inertia are affected. One cannot use the same procedure as in the case of plane bending, because only one equation is available, while the number of unknowns is two (if only biaxial bending is considered) or more (if bimoments from torsional warping are also taken into account). In the case of box-sections (Fig.2a), the bending moment M_y is mainly carried by the flanges 1 and 2, and the moment M_z by the webs 3 and 4. Therefore, it will be assumed that the bending stiffness about a principal axis of inertia is not influenced by the moment about the other axis:

$$\eta_y = F(A, W_y, K_y, \bar{\lambda}_y, \sigma_y, \alpha_{ry}, f_{oz}, M_{ey}, N) \qquad (18)$$

$$\eta_z = F(A, W_z, K_z, \bar{\lambda}_z, \sigma_y, \alpha_{rz}, f_{oy}, M_{ez}, N) \qquad (18')$$

where α_{ry} refers to the maximum compressive residual stress in the flanges, and α_{rz} refers to the webs.

For I-section members, the problem becomes even more intricate, because torsional warping (which is usually disregarded by box-section members) must be considered in addition to bending. It can be assumed that the bending stiffness about the strong axis remains unaffected by bending about the weak axis and η_y is given by Eq.(18). Only the case of doubly symmetric sections will be considered herein. The axial forces in the flanges (assumed to be positive when compressive) are due to N and M_{ey}:

$$N_{f1,2} = \left[\frac{N}{A} \pm \frac{N(f_{oz} + e_z)}{(1 - N/N_{Eey})W_y}\right] A_f =$$

$$= \left\{1 \pm \frac{f_{oz} + e_z}{\left[1 - \left(\sigma_N/\eta_y\sigma_y\right)\bar{\lambda}_y^2\right]\rho_y}\right\} A_f \sigma_N \qquad (19)$$

where

$$e = - M_{ez}/N \; ; \quad \rho_y = W_y/A \qquad (20\text{-}21)$$

The bending moments (about the z-axis) in the flanges are due to M_{ez} and the bimoment B:

$$M_{f1z} = M_{ez}/2 + B/h \; ; \quad M_{f2z} = M_{ez}/2 - B/h \qquad (22\text{-}22')$$

The geometrical imperfections of the flanges in the y-axis direction are:

$$f_{o1y} = f_{oy} + \varphi_{ox} h/2 \; ; \quad f_{o2y} = f_{oy} - \varphi_{ox} h/2 \qquad (23\text{-}23')$$

where f_{oy} is the initial bow at the shear centre level in the y-axis direction and φ_{ox} is the initial twist at mid-length (posi-

(7)

tive when directed clockwise). It will be assumed that these geometrical imperfections are affined with the fundamental elastic flexural-torsional buckling shape of a beam-column under compression and bending (with zero lateral displacement and torsional twist, and respectively free flexural rotation and torsional warping at each of the member ends):

$$f_{oy} = \frac{\gamma e_z}{\gamma e_z + h/2} f_{o1y} \; ; \; f_{ozy} = \frac{\gamma e_z - h/2}{\gamma e_z + h/2} f_{o1y} \qquad (24\text{-}25)$$

$$\gamma = N_{zt}/(N_z - N_{zt}) \qquad (26)$$

where N_z and N_{zt} are respectively the elastic critical loads for flexural buckling about the z-axis under axial compression and for flexural-torsional buckling under compression and bending. The value of f_{o1y} (the maximum initial transverse deflection of the most compressed flange) is chosen in accordance with the design specifications, and its sense must be the most unfavourable (so that it increases the maximum stress resulting from a first-order analysis without imperfections).

The equivalent stiffnesses in bending about the z-axis and respectively in warping, are:

$$S_{ez} = \eta_z S_z = \eta_z EI_z \; ; \; S_{ew} = \eta_w S_w = \eta_w EI_w \qquad (27\text{-}28)$$

$$\eta_z = (\eta_{1z} + \eta_{2z})/2 \; ; \; \eta_w = 2\eta_{1w}\eta_{2w}/(\eta_{1w} + \eta_{2w}) \qquad (29\text{-}30)$$

$$\eta_{1z} = F(A_f, W_{fz}, K_{fz}, \bar{\lambda}_z, \sigma_y, \alpha_{ry}, f_{o1y}, M_{f1z}, N_{f1}) \qquad (31)$$

$$\eta_{2z} = F(A_f, W_{fz}, K_{fz}, \bar{\lambda}_z, \sigma_y, \alpha_{ry}, f_{ozy}, M_{f2z}, N_{fz}) \qquad (31')$$

where I_w is the cross section warping constant,

$$W_{fz} = t_f b^2/6 \qquad (32)$$

and $K_{fz} = 1.25$. The factors η_{1w} and η_{2w} are obtained by merely replacing $\bar{\lambda}_z$ by $\bar{\lambda}_w$ in Eqs.(31-31'). While $\bar{\lambda}_z$ is computed considering the area A and the moment of inertia I_z of the whole cross section, the area and the moment of inertia of a conventional cross section (consisting of the flange and 1/6 of the web depth) should be taken into account when computing $\bar{\lambda}_w$.

As for the pure (St.Venant) torsional stiffness, it was concluded by Lindner (1971) and Ackermann (1981) that assuming it to be purely elastic does not lead to significant errors.

3. Conclusions

The above procedure can be subject to further improvement, but it seems to be more accurate than the equivalent geometrical imperfection concept whenever the deformation from primary loads includes the fundamental buckling shape (which is the usual case by frames). The described method for computing equivalent stiffnesses can easily be incorporated into any of the available com-

(8)
puter programs for second-order analysis of plane frames. Since stiffnesses depend on the member forces (N, M) and on their effective lengths, which are not known beforehand, the process is more complex than in the equivalent imperfection alternative, because their determination requires an iterative analysis. Taking into account the approximate character of this method and in order to spare computer time, it may be suggested to estimate them by some simplified procedures.

Besides geometrical and mechanical imperfections, the stability of statically indeterminate structures is also influenced by the initial state of stresses due to lack of fit by erection. This aspect is, however, beyond the scope of the present paper.

References

/1/Ackermann, Th. (1981): Traglastberechnung räumlicher Rahmen aus Stahl-oder Leichtmetallprofilen mit dünnwandigen offenen Querschnitten. Dissertation, Karlsruhe.

/2/Bălut, N. (1988): A Possible Alternative to the Equivalent Geometrical Imperfection Concept. 5th Conference on Metal Structures, Timişoara, Romania, Sept. 22-24, Vol.1, p.132.

/3/Beer, H., Schulz, G. (1969): Die Traglast des planmässig mittig gedrückten Stabs mit Imperfektionen. VDI Zeitschrift (111), 1969/21, p.1537; 1969/23, p.1683; 1969/24, p.1767.

/4/Boraeve, Ph., Maquoi, R., Rondal, J. (1983): Influence des caractéristiques effectives des profils sur le niveau des courbes de flambement. Stabilité des structures métalliques. Troisième Colloque International, Paris, 16-17 nov. Rapport préliminaire.

/5/Chen, W.F. (1971): Further Studies on Inelastic Beam-Column Problem. Journal of the Structural Division, ST2, February, p.529.

/6/Costa Ferreira, C.M., Rondal, J. (1987): Effet des imperfections sur les phénomènes d'instabilité des structures en acier. Annales de l'Institut Technique du Bâtiment et des Travaux Publics, No.451-janvier. Série: Théorie et Méthodes de Calcul 287, p.79.

/7/Kindmann,R. (1984): Zum Tragverhalten ebener Rahmen aus Baustahl. Institut für konstruktiven Ingenieurbau, Ruhr-Universität Bochum. Festschrift Roik, Mitteilung Nr.84-3, p.200.

/8/Lindner, J. (1971): Näherungsweise Ermittlung der Traglasten von auf Biegung und Torsion beanspruchten Trägern. Die Bautechnik, Nr.5, p.160.

/9/Maquoi, R., Rondal, J. (1978): Mise en équation des nouvelles courbes européennes de flambement. Construction Métallique, No.1, p.17.

/10/Rondal, J., Maquoi, R. (1979): Formulations d'Ayrton-Perry sur le flambement des barres métalliques. Construction Métallique, No.4,p.41.

/11/Vinnakota, S. (1973): Design of Columns in Planar Frames - A Few Comments. Paper presented at the National Conference on Tall Buildings held at New Delhi from 22nd to 24th January.

/12/Vogel, U. (1986): On the Reliability and Sense of the Effective Length Concept for the Stability Check of Steel Frames. Second Regional Colloquium on Stability of Steel Structures, Hungary, Sept.25-26, Vol.1/2, p.1/359.

BOGACZ, Roman (1)
IMIEŁOWSKI, Szymon (2)

ON THE DISCONTINOUS CHANGES OF CRITICAL FORCE FOR COLUMNS WITH TRANSVERSE-SLIDABLE JOINT UNDER FOLLOWER LOAD

INTERNATIONAL COLLOQUIUM
STABILITY OF STEEL STRUCTURES
BUDAPEST, HUNGARY, 1990
PRELIMINARY REPORT

Summary: The column, consisting of segments connected by elastic or viscoelastic transverse-slidable joint, subjected to circulatory load is considered. Analitical solution to the problem was found by the transfer matrix method. In the case of viscoelastic structure the generalized Mikhailov stability criterion was applied. It was shown that the value of critical force of such a structure depends of joint position and in the case of elastic structure of joint flexibility too. Near twofold increase in critical force is possible when discontinuity modeled elastically is localized in the centre of column. However when viscoelastic joint is taken into account the critical load is never higher than in the case of uniform column. For selected values of joint parameters the effect of discontinous changes of critical force caused by qualitative differences of characteristic curves shape on frequency-load plane was observed.

1. Introduction

The problem of stability of structures subjected to nonconservative load find many aplications in egineering practice, particulary problems connected with columns subjected to circulatory loading. A wide review of literature related to this theme is given in [1]. Present paper is the continuation of earlier investigations concerning the influence of localized loss of stiffness on value of critical load, which were began by the Authors of [2]. Results of investigations related to the column with elastic and viscoelastic hinge-joint are to find in [3],[4], and to the column with transverse-slidable joint in [5],[6]. Effects of stabilization or destabilization of column were observed. Above fourfold increase of critical force is possible when hinge-joint modeled elastically is localize in the centre of column [3].

Present paper is devoted to the generalization of the results related to the Beck-Reut column with localized loss of shear rigidity, modeled as elastic or viscoelastic joint. The problem is solved by using the transfer matrix technique.

2. Formulation of the problem

2.1. Case of elastic structure

The structure shown schematically in Fig.1, will be considered. It consist of segments connected by elastic transverse-slidable joint, Fig.1b), placed at position x_1 and characterized by the stiffness parameter κ_{ej} or flexibility parameter $\gamma_{ej} = \frac{1}{\kappa_{ej}}$ sometimes more convenient in calculations.

Analitical solution of the problem was found by the transfer matrix technique .The equation of motion for a segment of column is assumed as:

---

(1) Professor of Mechanics, IFTR Polish Academy of Sciences
(2) Assistant Professor, IFTR Polish Academy of Sciences

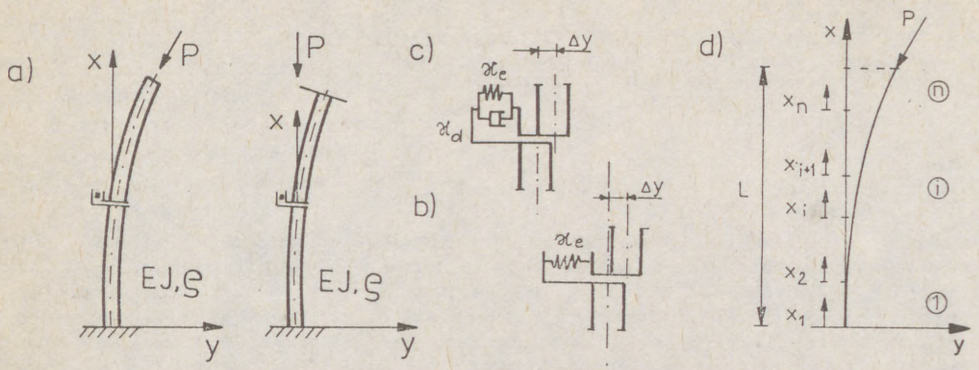

Fig.1.a)Beck-Reut column with localzed discontinuity of displacement b)Elastic model of transverse-slidable joint c)Kelvin-Voigt model of joint d)Segmentation of column

$$(1) \qquad \frac{\partial^2}{\partial x^2}\left(EJ\frac{\partial^2 y}{\partial x^2}\right) + P\frac{\partial^2 y}{\partial x^2} + \rho A\frac{\partial^2 y}{\partial x^2} = 0 \quad .$$

The boundary conditions for column (Beck problem)

$$(2) \qquad x = 0 \qquad y = 0 \quad , \quad \frac{\partial y}{\partial x} = 0 \quad ,$$

$$(3) \qquad x = L \qquad \frac{\partial^2 y}{\partial x^2} = 0 \quad , \quad \frac{\partial}{\partial x}\left(EJ\frac{\partial^2 y}{\partial x^2}\right) = 0 \quad .$$

The exact solution of Eq.(1) i.e. for the segment of constant mass and stiffness distribution has the form

$$(4) \qquad y(x,t) = e^{i\omega t}(A_1 sh\lambda_1 x + A_2 ch\lambda_1 x + A_3 sin\lambda_2 x + A_4 cos\lambda_2 x) \quad ,$$

where

$$(5) \qquad \lambda_{1/2} = \left\{ \pm \frac{P}{2EJ} + \sqrt{\left(\frac{P}{2EJ}\right)^2 + \frac{\rho A \omega^2}{EJ}} \right\}^{1/2} \quad .$$

All dependent variables y , ϕ , M , Q , have a similar constitutive form and they are closed in state vector $\underline{G}$ defined as

$$(6) \qquad \underline{G} = [\, y, \phi, M, Q \,] = [\, y, y', -EJy'', -EJy''' \,]^T \quad .$$

Two states vectors on both ends of i-th segment are connected by the partial trasfer matrix $\underline{T}_i$

$$(7) \qquad \underline{G}^o_{i+1} = \underline{T}_i \, \underline{G}^o_i \quad ,$$

$$(8) \qquad \underline{G}^o_i = \underline{G}\,(x_i = 0) \quad \text{and} \quad \underline{G}^o_{i+1} = \underline{G}\,(x_{i+1} = 0) \quad .$$

For the complete structure we have

$$\underline{G}^{o}_{n+1} = \underline{T}_{n} \cdot \ldots \cdot \underline{T}_{2}\, \underline{T}_{1}\, \underline{G}^{o}_{1} = \underline{T}\, \underline{G}^{o}_{1} \quad . \tag{9}$$

The partial transfer matrix for the segment can be found using the solution (4) of Eq. (1) and is given * in [7]* . For the transverse-slidable joint, characterized by a parameter κ_j or γ_j we have

$$\Delta y\,(\kappa^{*}_{ej}) = \frac{1}{\kappa^{*}_{ej}}\, Q(x_j) = \gamma^{*}_{ej}\, Q(x_j) \quad , \tag{10}$$

where $\kappa^{*}_{ej} = \kappa_{ej} l^3/EJ$ is the nondimensional stiffness and $\gamma^{*}_{ej} = \gamma_{ej}\, EJ/l^3$ the nondimensional flexibility of joint in the shear force direction .

According to (10) nonzero elements of the transfer matrix for such a joint are :

$$t_{ii} = 1 \quad , \quad t_{14} = \kappa^{*}_{ej} \quad . \tag{11}$$

Satysfying the boundary coditions (2) , (3) , we get a characteristic equation as the relation betweem force and frequency

$$\begin{vmatrix} t_{33} & t_{34} \\ t_{43} & t_{44} \end{vmatrix} = G\,(P,\omega) = 0 \quad . \tag{12}$$

2.2. The structure with viscoelastic joint

In the case of viscoelastic joint , Fig.1 c),the Kelvin-Voigt model is assumed

$$\sigma = \varepsilon\, \kappa_e + \frac{d\varepsilon}{dt}\, \kappa_d \quad , \tag{13}$$

where ε means strain, κ_e elastic stiffness and κ_d damping coefficient. Because the solution (4) of Eq. (1) is of harmonic form $\varepsilon = \varepsilon_o\, e^{i\omega t}$, in which ε_o is amplitude and ω frequency of vibrations we can write Eq. (13) as

$$\sigma = \varepsilon_o\, e^{i\omega t}\, \kappa = \varepsilon\, \kappa \quad , \tag{14}$$

where stiffness of joint is written as a sum

$$\kappa = \kappa_e + i\, \omega\, \kappa_d \quad . \tag{15}$$

In the case of weightless elastic joint, Fig.1 c), $\kappa = \kappa_e$ and for viscous only joint $\kappa = i\, \omega\, \kappa_d$.

The characteristic equation (13) for dissipative structure is of complex form

$$\Phi\,(P,\omega) = \Phi_{Re}(P,\omega) + i\, \Phi_{Im}(P\, w) \quad . \tag{16}$$

In order to get critical values of $P^{*} = P^{*}_{cr}$, $P^{*} = P\, l^2/EJ$, the generalized Mikhajlov stability criterion is used. A typical configuration in the force-frequency plane corresponding to (16) is shown in Fig.2. The full and dashed lines represent the real and imaginary parts of the characteristic equations respectively. The point of intersection determines

(4)

the critical value $P^*_{cr} = P_{II}$ as illustrated on the right-hand side of Fig.2. For $P^* = P_I$ the column is stable and the shape of Re Φ, Im ϕ - plane for $P^* = P_{III}$ is typical for unstable case.

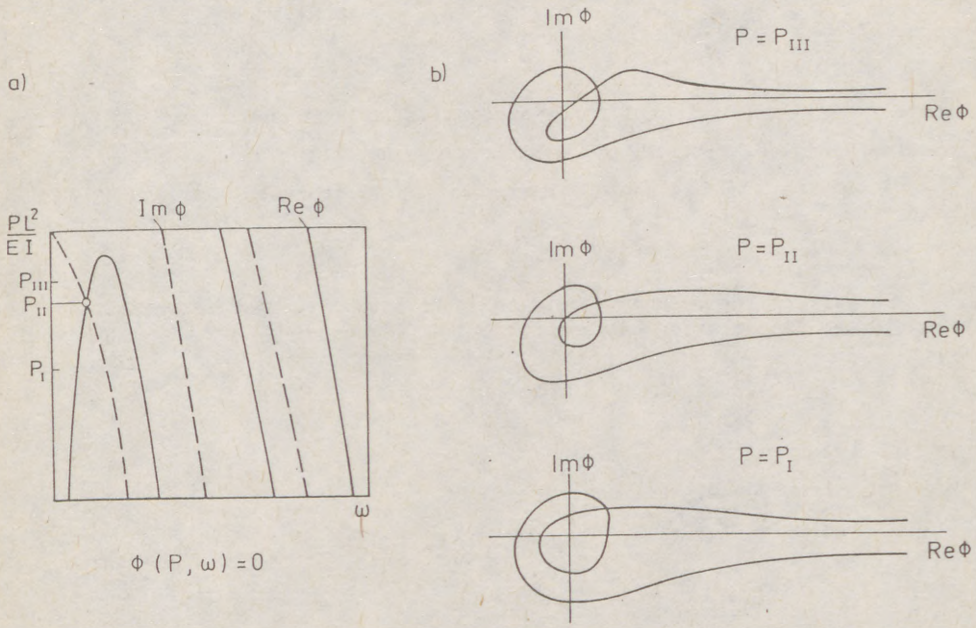

Fig.2. Force-frequency plane and shapes of Mikhailov curves for the stable (P_I), critical (P_{II}) and unstable (P_{III}) case of the column

3. Results of numerical calculations - elastic structure

A typical configuration of curves on the frequency - load plane for Beck-Reut column is given in Fig.6 (dotted line). Appearence of displacement discontinuity causes qualitative and quantitative changes of the shape of characteristic curves and is connected with continous and discontinous changes of critical load.

The nondimensional critical force $P^*_{cr} = P_{cr} l^2/EJ$ versus joint flexibility γ^*_e for various joint position x_1 and on the other hand, the relations $P^*_{cr} = P^*_{cr}(x_1)$ for diffrent γ^*_e are shown on graphs in Fig.3, Fig.4 .

It can be seen , Fig.3, that for $x_1 \in <0.0, 0.25)$ the critical force decrease with increasing of flexibility taking its minimum at $\gamma^*_e \approx 0.2$ for $x_1 = 0.0$. Further change of the joint position to the centre of column effects that this minimum grows up, relocating to higher value of γ^*_e simultaneusly .

(5)

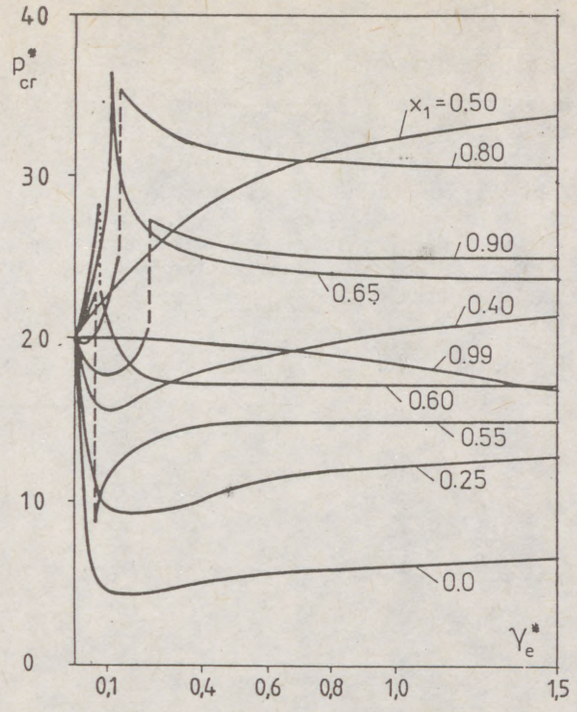

Fig. 3. Critical load versus a relative flexibility of elastic joint for various values of x

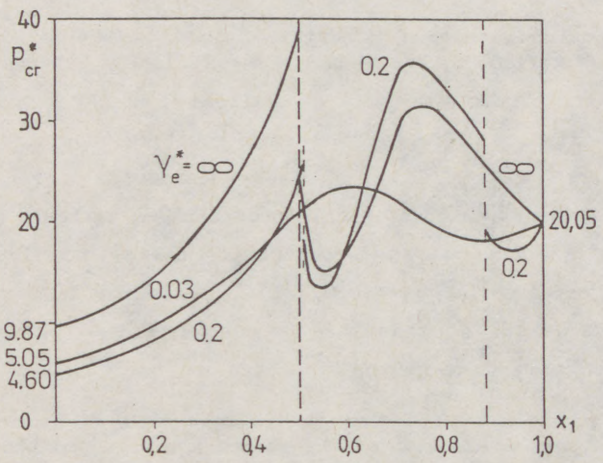

Fig. 4. Critical load versus joint location for various values of flexibility γ

For $x_1 = 0.5$ critical value of load increase monotonically taking for $\gamma_e^* = 2.0$ a value 34.4 EJ/l^2. For $\gamma_e^* \to \infty$ the value of critical force dropped from $P_{cr} = 39.3\ EJ/l^2$ to $P_{cr} = 27.25\ EJ/l^2$.

The effect of considerable reduction of critical load for a small values of joint flexibility, for $x_1 = 0$, and near twofold increase in critical force for a small values of joint stiffness, when $x_1 = 0.5$, are well seen in Fig.4. For each localization of joint above the center of

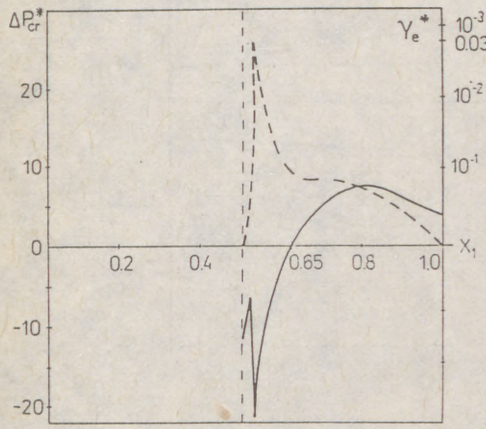

Fig.5. "Jump" of critical load (ΔP^*) and its flexibility (γ_e^*) versus joint location.

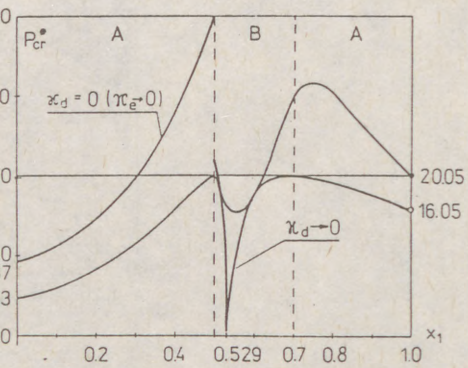

Fig.7. Critical load versus joint location for elastic ($\kappa = 0$) and viscoelastic ($\kappa \neq 0$) properties of joint

column a discontinous changes of critical load is noticed. When joint is located in $0.5 < x_1 < 0.65$, and when its flexibility γ_e^* changes from 0 to ∞, we observed discontinous decrease of critical load value, ΔP_{cr}^* in Fig.5, which appears with γ_e^* different for each position of joint plotted with dashed line. For $x_1 > 0.65$ a "jump" of P_{cr}^* causes an increase of critical force. At last, when $x_1 = 0.65$ critical force changes without "jump' in whole range of γ_e^*, Fig.5. It is important to notice that this discontinous changes of P_{cr}^* appears for $\gamma_e > 0.038\ EJ/l^2$ only. How it is seen in Fig.4, Fig.5, each value of γ_e^* from this range causes two "jumps" in diffrent cross-sections placed above centre of column.

The configuration of the characteristic curves in the P^*, ω^* - plane, Fig.6, enables the explanation of the phenomenon of discontinous changes of critical force. It is caused by gualitative change of the shape of characteristic curves.

Parameters γ_{ep}^*, x_{jp} characterize the discontinues changes on P^*, ω^*

chart. For the value of parameters γ_e^* γ_{ep}^{*-} ,Fig.6a) or x_j x_{jp}^- ,Fig.6b), instability occurs with the first and the second natural form while for γ_e^* γ_{ep}^{*+} or x_j x_{jp}^+ the column loses its stability oscillating with the second and the third mode. This skip of critical force is connected together with a discontinous increase of critical frequency.

The configurations of characteristic curves connected with increase of P_{cr} for $x_1 = 0.75$ ($\gamma_e^* = 0.12$, $\gamma_e^* = 0.125$) and with decrease of P_{cr}^* for $\gamma_e^* \to \infty$ ($x_1 = 0.495, 0.5, 0.502$) are shown in Fig.6a) and Fig.6b) respectively. For $x_{1p} = 0.5$,Fig.6b) we observe an intersection of the characteristic curves for second and third modes and a skip of the critical force and critical frequency cosequently .

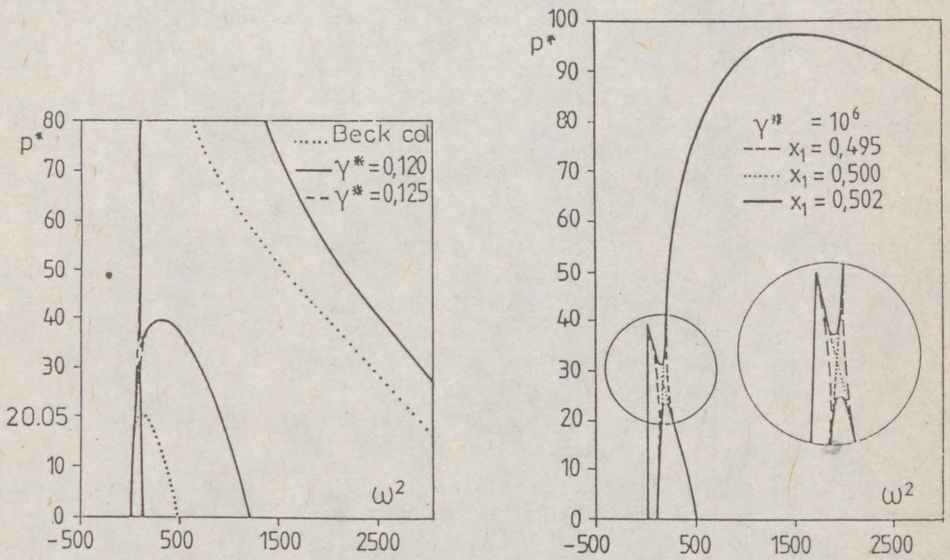

Fig.6. Switch-over of characteristic curves curves. a)Case of increase of P_{cr}^* b)Case of decrease of P_{cr}

4. Results of numerical calculations - case of viscoelastic joint

The computational results , Fig.7, have shown that in case of single viscoelastic or viscous only joint the critical force as well as critical frequency are independent of damping coefficient and elastic stiffnes of joint. Its depends only on the joint location. The results for $\kappa_d \to 0$ and $\kappa_d = 0$ are different , similar as in [4], [6] .

Viscosity at the joint causes destabilization of the column. A skip of critical force bring about viscoelasticity is largest , when elastic stiffness of joint κ_e tends to zero, Fig.7 .The critical force of such a structure is never higher than for the uniform column and reach its minimum value $P_{cr} = 0.11\ EJ/l^2$ for $x_1 = 0.529$.

The critical force of the column with joint placed near free end $x_2 \cong 0$,

$x_2 \neq 0$, tends to $P_{cr}=16.05\ EJ/l^2$. However for $x_2= 0$ its value changes to $P_{cr}= 20.05\ EJ/l^2$ as in the case of Beck-Reut column. The skip of P_{cr} is observed. More details related to the column with localized discontinuity of displacement modeled by viscoelestic joint is presented in [6].

5. Conclusion

The result obtained in this paper shows that local loss of shear rigidity of column subjected to the circulatory load may stabilize or destabilize the structure. In the case when elastically modeled discontinuity of displacement is localized near clamped end of column the critical load diminishes considerably. When this discontinuity is placed in the centre of column for small value of elastic stiffness near twofold increase in critical load is possible .

However, when a viscoelastic joint is taken into account the value of critical force is never higher than in uniform column. How it is shown in [8],[9] and similarly in [3] for the case of viscous supports, infinitesimally small external damping can complete eliminate destabilizing effect. The question of destabilizing effect of nonconservatively loaded structure were considered in [10], [11] lately. It seems to be interesting to take into account external damping relative to the structure considered in this paper. This problem will be investigate.

References

1. Богач Р., Янишевский Р., 1985, Анализ и синтез колонн , нагруженных следящими силами с точки зрения устойчивости, Успехи Механики, Vol.3

2. ANIFANTIS N., DIMAROGONAS A., 1983, Stability of columns with a single crack subjected to follower and vertical loads, International Journal of Solids Structures, Vol.19, No.4, 281-291

3. BOGACZ R., MAHRENHOLTZ O., 1986, On stability of column under circulatory load, Archives of Mechanics, Vol.3, 281-287 .

4. BOGACZ R., NIESPODZIANA A., 1987, On stability of continous Beck column with localized loss of rigidity, IFTR Reports, Vol.27 (in Polish)

5. BOGACZ R., IMIEŁOWSKI Sz., 1986, Stability of column with localized discontinuity of displacement loaded by follower forces, IFTR Reports, Vol.6, (in Polish)

7. IMIEŁOWSKI Sz., 1989 , Influence of localized internal damping on stability of column subjected to circulatiry load, Ingineering Transactions (in print

6. PESTEL E.C., LECKIE F.A., 1963, Matrix Methods in Elastomechanics Mc. Graw-Hill Book Company, New York

8. GAJEWSKI A., 1972, On the destabilizing effect in a non-conservative system with slight internal and external damping, Proceedings of Vibrating Problems, Vol.13, No.2, 187-190

9. GAJEWSKI A., ZYCZKOWSKI, 1972, Influence of simultaneus non-homogeneus external and internal damping upon the stability of non-conservative systems, Theoretical and Applied Mechanics, Vol.10, No.1, 127-142

10. СЕЙРАНИЯН А.П., 1987, Парадокс дестабилизации и критерии колебательной устойчивости, Инст. Пробл. Мех. АН СССП, Препринт Но.301

11. БАНИЧУК Н.В., БРАТУСЬ А.С., МЫШКИС А.Д., 1987, Анализ стабилизирующих эфектов малого демпфирования в неконсервативных системах с конечным чицлом степеней свободы, Инст. Пробл. Мех. АН СССП, Препринт Но.312

(1)
CARABA, Ioan (1)
DRUZENCO, Valentin (2)

OPTIMIZATION OF BEHAVIOUR AT STABILITY OF WELDED STEEL BARS SUBJECTED TO ECCENTRICAL COMPRESSION

INTERNATIONAL COLLOQUIUM
STABILITY OF STEEL STRUCTURES
BUDAPEST, HUNGARY, 1990
PRELIMINARY REPORT

Summary: This paper studies the behaviour at stability of electric welded steel bars, subjected to eccentrical compression when voltage (U), intensity (I) and welding speed (v) vary.

The behaviour at stability of eccentrical compressed welded bars can be optimized using the precalculated variation of the U, I, v parameters.

The differentiated choise of U, I, v parameters in terms of the seams induces in the structure a state of initial stresses opposing to the state of stresses induced in service by external forces.

The results obtained by theoretical investigations are compared with laboratory tests on physical models.

§1. The physical model of the extended bar. If a bar with an initial length l is extended under the force F we detect the elongation par unit length ε_l and a transversal deformation $\varepsilon_t = -\mu \cdot \varepsilon_l$ where μ is Poisson's coefficient.

If two bars of figure 1.a are extended with the help of the forces in equipartition on the two ends (see figure 1.b) are completely elastic braced on the parts of the plane p_1, p_2 with the same material m or with another material m^* (but completely elastic, $E_{m^*} = E_m$) (see figure 1.c), we detect the variation of Δl after we remove the force F (see figure

(1) Associate Professor, dr.eng. "Traian Vuia" Polytechnic Institute, Timişoara
(2) Eng. "Traian Vuia" Polytechnic Institute, Timişoara

(2)
1.d and figure 2.a).

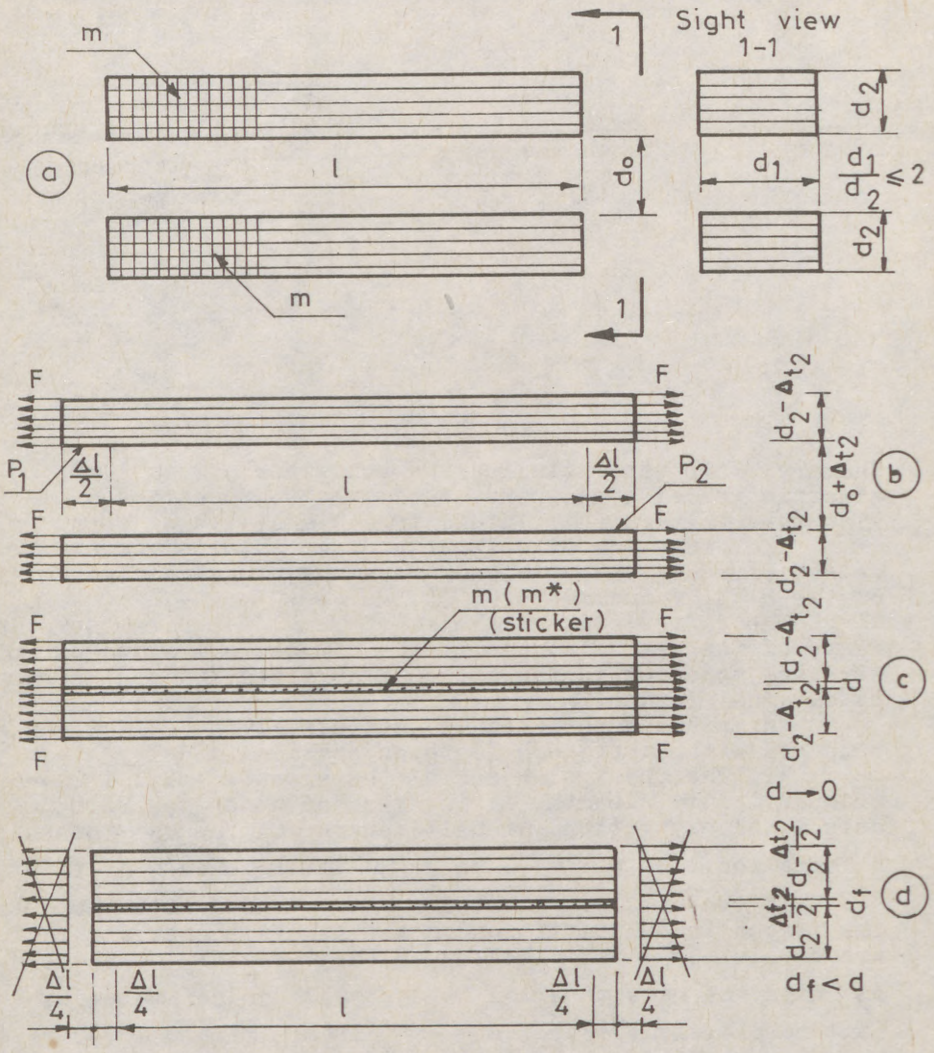

FIG. 1.

If two extended bars of elastic polymer are braced with the help of the sticker (figure 1.c), after we remove the forces F, the variation of Δl is represented by the

(3)

figure 2. If m^{*} is a elastic material and $E_{m^{*}} = E_m$, see a variation of Δl in figure 2.a; the parallel lines are parallel after we remove the force F (figure 1). If the sticker is a viscid material m_v $(0 < E_{m_v} < E_m)$, see a variation of Δl in figure 2.b.

If we kill the liaison m_v of the semi-bars of figure 2.c, we obtain two distorded semi-bars (figure 2.d). The tranverse bending resilience is induced by the flexural rigidity in excess on the parts of the plane p_1, p_2.

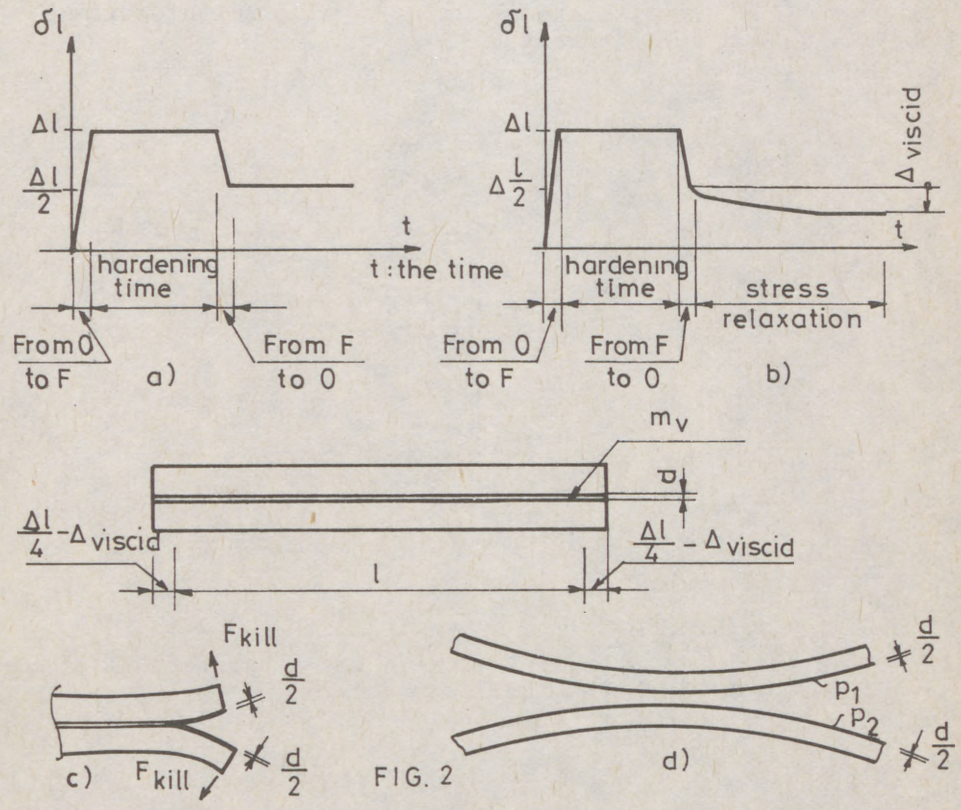

FIG. 2

2. Studies on the electrically welded metalic bars.

For the bar 2U8 of OL 37 with a transversal section double connected we chose the parameters of the welding seams which induce in all points of the bar a temperature $T \geqslant 100^{\circ}C$, so that the incompletely annealed bar should approximate the physical model of §1 (figure 1 and 2.a).

(4)

At temperatures T higher than $100^{o}C$ when the element of the metal is free to deform, the rate of strain is $\varepsilon_1 = \frac{\Delta l}{l} = \alpha . T = 1,2.10^{-5}.100 = 0,12\ \%$.

For the metal plates of figure 3 (where b:t > 25), the overall width, c, of the metal plate where there are tensile stress R_c doesn't depend on b and $c = \eta_1 t_1 = \eta_2 t_2 = \ldots = \eta_i t_i = \frac{96\ QE}{vR_c \sum_i t_i}$, $Q = \varrho UI$ where:

ϱ : efficiency of electric arc; E: modulus of elasticity (daN/mm^2); v: rate of welding (mm/s); R_c: flow resistance (daN/mm^2); t: plate thickness (mm); U: alternating voltage (V); I: intensity of curent (A).

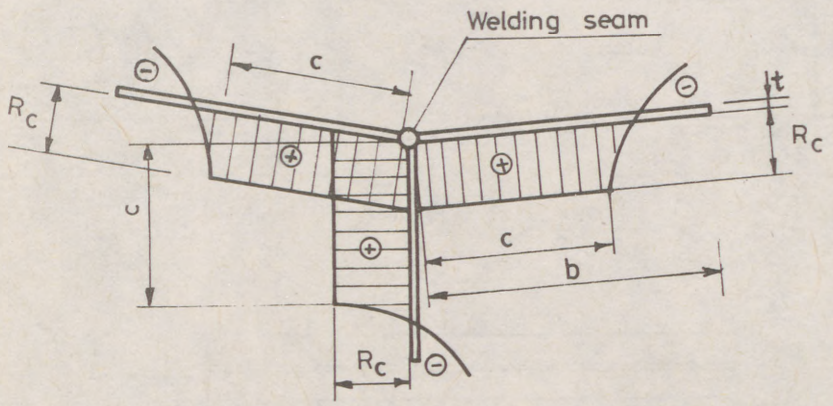

FIG. 3

In computation table 1 we give the parameters of electric welding for the bars of 2U8 (figure 4).

$$t_{U8}^{medium} = \frac{A_{U8}}{2b+h} = \frac{11}{4,5.2 + 8} = 0,647\ cm\ ;$$

$$\frac{2b + h}{t_{U8}^{medium}} = 26,27\ cm > 25\ cm$$

In figure 5 we render the elastic behaviour of the bar, after the electric welding.

(5)

Computation table 1

Welding seam characteristics / Denomination of the welding seam	Welding electrode: Electrode paste	Welding electrode: Electrode diamet. (mm)	ϱ	U (V)	I (A)	v (mm/s)	The general executing sequence of the welding seams	c (C_1) c (C_2) (mm)
C_1	Acid	4	0,7	25...35	160	2,5...3,125	1	87...97
C_2	Basic	2,5	1	22...28	110	1,835..2,11	2	102...112

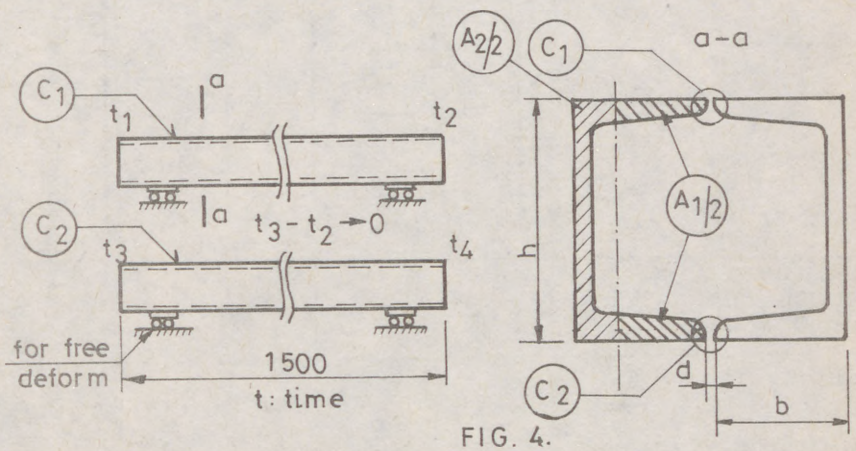

FIG. 4.

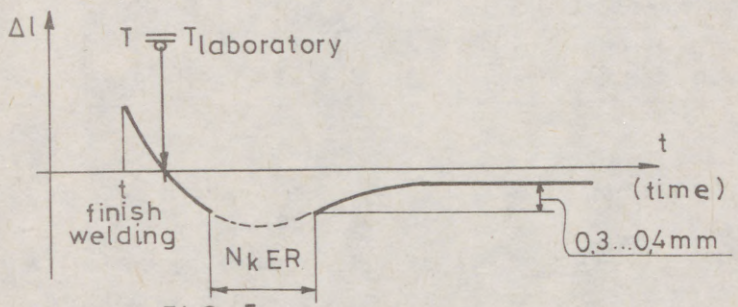

FIG. 5.

(6)

NkER represents a non-known electric range between two geometrical levelling (0,05 mm measuring accuracy).

In computation table 2 we render the small-scale tests.

§ 3. Calculus of the bar extended by the electric welding, subjected to eccentrical compression.

Theoretical considerations

th 1). In the calculus domain we consider the bar with a double cpnnected a double symmetrical transversal section built up two congruent parts connected by two parallel arc-welding seams.

th 2). The distance between the congruent parts is "d"

Computation table 2

Static scheme / Performances	The 1st bar	The 2nd bar	The 3rd bar
	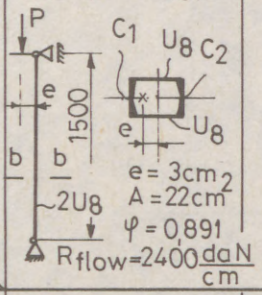	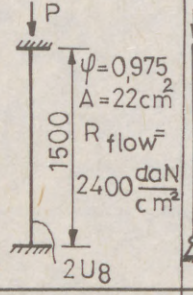	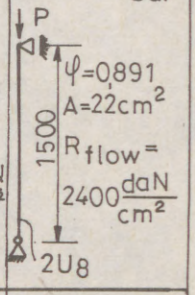
P calculus capable, flow (daN) (without electric welding)	22 301	51480	47 045
P employeis flow (daN) (with electric welding)	31 000	75000	65 000
P calculus with formulas capable flow (see § 3) (with electric welding)	30 958	71683	65 306
Executing seqwence of the welding seams	C_1, C_2	C_1, C_2	C_2, C_1

(see figure 4) and $d > 2 \cdot \mu \cdot \varepsilon_{1,flow} \cdot b$ before executing the electric welding.

th 3). $C(C_1) + C(C_2) \geqslant 2b + h$ (see figure 4). After the execution of the first welding seam C_1, $Q(C_1) > Q(C_2)$, the second welding seams must be executed immediately, so that the temperature T_i in all points i of the bar shouldn't be less than $100^{\circ}C$, before the pass of the electrode.

(7)

th 4). For the extended bar there are two neutral plans n_1, n_2 for ε_{t_1}, ε_{t_2}. For the semi-bar 1 there are two neutral plans n_1^1, n_2^1 for ε_{t_1}, ε_{t_2}; for the semi-bar 2 there are two neutral plans n_1^2, n_2^2 for ε_{t_1}, ε_{t_2}.

Than $n_1 \parallel n_1^1 \parallel n_1^2$ and $n_2 = n_2^1 = n_2^2$ (see figure 6 and figure 1).

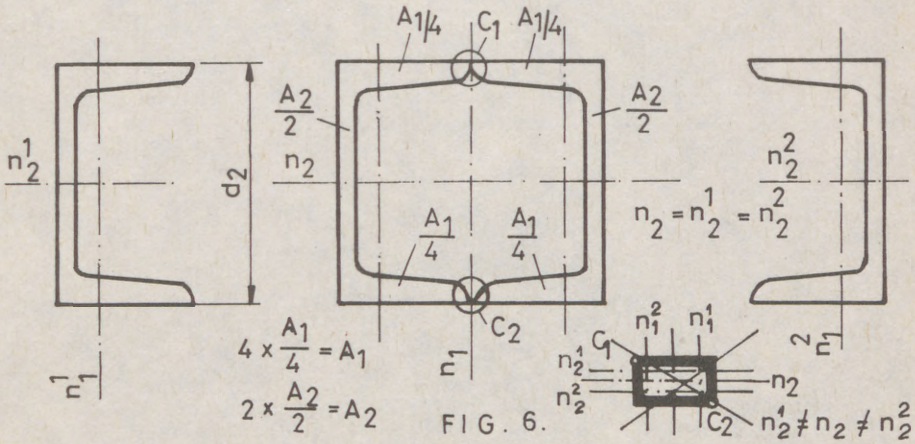

FIG. 6.

The neutral plan n_1 is determined by two parallel lines represented by the welding seams.

th 5). We accept the theoretical affirmations of § 1. After the cooling of the bar, the welding seams should not permit the slackening of the deformations more than

$$\varepsilon_{1,\text{slackening}} = \frac{A_2}{A_1+A_2} \cdot \varepsilon_{1,\text{flow}} ;$$

$$\varepsilon_{1,\text{remanent}} = \frac{A_1}{A_1+A_2} \cdot \varepsilon_{1,\text{flow}} = \frac{A_1}{A_1+A_2} \cdot \frac{R_{\text{flow}}}{E}$$

in all the points of the transversal section.

th 6). th 1)...th 5) result in calculus formulas (see

(8)

computation table 3).

Computation table 3

Denomination of stress	Centrical compression	Eccentrical compression
Value of calculus $P_{flow,capable}$	$(2A_1+A_2)R_{flow}$	$\frac{(2A_1+A_2)R_{flow}}{W + e.\ (A_1+A_2)}$

Of

$$\varepsilon_{1,remanent} = \frac{\sigma_{remanent}}{E} = \frac{A_1}{A_1+A_2}\,\frac{R_{flow}}{E},$$

$$\sigma_{remanent} + R_{flow} = \frac{2A_1+A_2}{A_1+A_2}\,R_{flow}$$

and

$$\frac{P}{\varphi(A_1+A_2)} = \sigma_{remanent} + R_{flow}$$

$$\frac{P}{(A_1+A_2)} + \frac{Pe}{W} = \sigma_{remanent} + R_{flow}$$

we obtain the formulas of table 3 and $P^{calculus}_{flow,capable}$ for the bars of 2U8 (see table 2).

Conclusions. The electric welding can improve the stability behaviour of the bar subjected to centrical or eccentrical compression within the form of the physical model of the extended bar achievable with the help of U, I, v parameters.

REFERENCES

1. Dwight, I.B., Moxham, K.E., Welded steel plates in compression. The Structural Engineer, vol.47, No.2, 1969.

2. Kim Rasmussen, Electric-Plastic Buckling of Long Plates in Compression, Dep.of Structural Eng.Technical University of Denmark, No.199, 1985.

(1)
CHRISTOV, Christo T. (1)

ON THE OVERALL STATIC STABILITY OF HIGH ELASTIC STEEL TOWERS

INTERNATIONAL COLLOQUIUM
STABILITY OF STEEL STRUCTURES
BUDAPEST, HUNGARY, 1990
PRELIMINARY REPORT

SUMMARY

In this paper a computer-aided technique for a static overall stability practical analysis of high elastic steel towers (water towers, television- and radio towers, industrial chimneys, silos etc.) is presented. The Euler's safety factor against overall buckling is determined and the external higher order bending moments on the deformed geometric scheme of a plane cantiliever beam-column discrete model are computed when small displacements are assumed (a geometrical non-linearity according to the second order theory). A simple semi-analytical version of the iterative Vianello-Dischinger method and the modified finite element method (FEM) are used for a coupled stability and static analysis of the model with a variable cross-section under arbitrary compressive axial, bending and shear loads.

1. INTRODUCTION

The steel towers are usually composed from thin shells of revolution and thin-walled circular rings. These ground-based high structures with an arbitrary axisymmetric shape are subjected to general static and dynamic external loads.

---

(1) Senior Research Scientist, Computer Centre in Construction and Technology, Sofia, Bulgaria.

(2)

At present, the overall stability and static analysis of such structures is practically studied approximately on the basis of a plane elastic slightly-deformed bar model under large static and quasi-static axial and transverse loads. Modified versions of the classic analytical and numerical methods for a linear static analysis and specific iterative approaches for a stability analysis are traditionally applied for solving this simplified coupled problem for elastic bar structures with a large number of degrees-of-freedom. In the usual cases the internal compressive normal forces, from which the displacements and the internal forces in the bars are dependent, are not previously known and their effect is normally expressed by various trigonometric correction functions, given by Livesley R. K. (1975), Tankov N. G. and Bobev T. B. (1981), Smirnov A. F. and co-workers (1984), and others.

The common iterative methods for an interactive stability and static analysis of the strong-non-linear structures are not sufficiently effective when the slightly-non-linear stuctures are computed by the second range theory. The separate calculations of these two problems are also uneffective. The conventional analytic methods (the initial parameters method, the displacements method, the forces method etc.) are effective rarely in the second order non-linear coupled stability and static analysis of the real bar structures. The numerical methods, and first of all the FEM, are often used then.

The iterative Vianello-Dischinger method (the sequential approximation method), presented by Dischinger F. (1937) and discussed by Miltchev E. M. (1976), is effective for a coupled stability and static analysis of the static-definable elastic plane bar structures under combined loading by the deformed geometrical scheme. This method is used by Miltchev E. and co-authors (1979) for a similar analysis of high reinforced concrete structures with a slightly-variable geometry (industrial chimneys etc.) by the forces method and a plane cantilever beam model, resting on elastic supports. The shear and axial strains are neglected. An effective iterative method is presented by Miltchev E. M. (1976) for a static and stability

(3)

analysis of arbitrary elastic plane bar structures according to the deformed scheme using available computer programms for a static analysis by the FEM.

The generalized stiffness matrix of a two-nodal plane straight bar finite element with six degrees-of-freedom, a cubic shear displacement and a linear axial displacement is derived by many authors using various correction functions for the axial compressive forces effect. This effect is separated by Livesley R.K. (1975) as an explicit form in a particular "geometric" matrix. The traditional element stiffness matrix is refined by Ganev T. and Levy I. (1985) with the shear deformations effect.

The safety factor against linear buckling of the bar structures, due to a given loading, can be computed by ICES STRUDL-II (1971) using the iterative Stodola-Vianello method and FEM. The minimum eigenvalue and the adequate buckling mode are calculated into each cycle for the relevant achieved level of the incremental load. The static solution and minimum critical buckling force for each loading combination of plane metal inelastic frames with small displacements under incremental axial forces are determined by Gotchev V. A. (1987) using FEM with a variable stiffness matrix. The displacements are very increased under constant buckling loads.

2. DISCRETE MODEL AND TECHNIQUE FOR STABILITY ANALYSIS

A refined discrete plane model of a vertical elastic cantiliever beam-column with an undeformable variable thin-walled usually tubular cross-section (Fig. 1) is applied for a coupled stability and static analysis of the high steel towers. Factors taken into account are: three degrees-of-freedom (the horizontal displacement v, the rotation φ and the vertical displacement u) at each node of the axe Ox; the effect of the compressive internal normal forces; the elastic supports of the lower end in the three directions; the distributed and concentrated large external axial forces, transverse forces and bending moments; the flexural, shear and axial deformations; small displacements; homogeneous, isotropic and linearly-elastic materials. The internal normal forces are known and they remains constants.

(4)

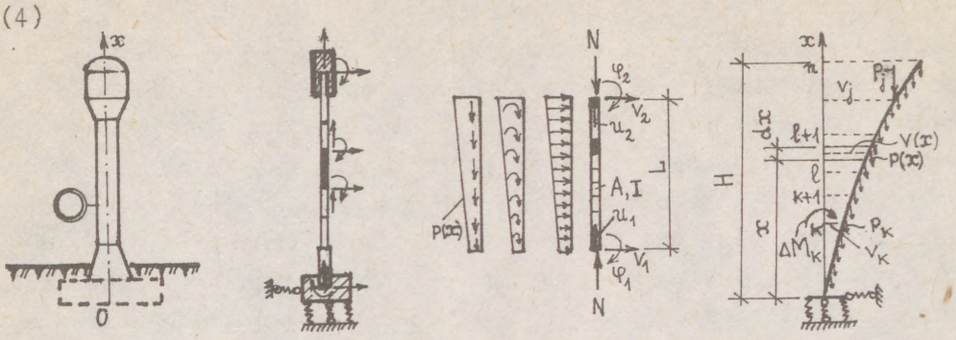

a) Sample tower b) Bar model c) Finite element d) Deformed axe

Fig. 1. Beam-column model for stability analysis of high towers

An overall stability analysis for each specified loading combination of the axial and transverse external loads is accomplished by a vertion of the iterative Vianello-Dischinger method using additional external bending moments. The problem is static definable. But the analytical solution is uneffective because of the large elements number. Therefore, the static analysis is implemented by the FEM.

A two-nodal straight uniform beam-column finite element (Fig. 1) is used. This element has six degrees-of-freedom, partially-dependent cubic polynomial trial functions for the transverse and angular displacements, but a conventional linear function of the axial displacement.

The generalized element stiffness matrix, given by the above-mentioned authors, with the symbols in Fig. 1 is as

$$[\kappa]^e = \begin{bmatrix} EA/L & 0 & 0 & -EA/L & 0 & 0 \\ 0 & 12c & 6Lc & 0 & -12c & 6Lc \\ 0 & 6Lc & (4+\mu)L^2c & 0 & -6Lc & (2-\mu)L^2c \\ -EA/L & 0 & 0 & EA/L & 0 & 0 \\ 0 & -12c & -6Lc & 0 & 12c & -6Lc \\ 0 & 6Lc & (2-\mu)L^2c & 0 & -6Lc & (4+\mu)L^2c \end{bmatrix} - \frac{N}{30L} \begin{bmatrix} 0 & 0 & 0 & 0 & 0 & 0 \\ 0 & 36 & 3L & 0 & -36 & 3L \\ 0 & 3L & 4L^2 & 0 & -3L & -L^2 \\ 0 & 0 & 0 & 0 & 0 & 0 \\ 0 & -36 & -3L & 0 & 36 & -3L \\ 0 & 3L & -L^2 & 0 & -3L & 4L^2 \end{bmatrix} \quad (1)$$

where L is a element length; E - a Young's modulus; G - a shear strains modulus; N - a constant compressive (positive) normal force in the element; A, I - an area and an inertial moment of the cross-section; μ - a coefficient for the ununiformly-distributed tangential stresses into the cross-section; $c = 12EI\mu/L^2GA$. The matrix $[\kappa]^e$ is also used for a preceding linear dynamic analysis of the same beam-column model. Then the quasi-static

(5)

seismic and wind loads are computed by the spectral method.

The finite element is subjected to the linearly-distributed external loads (Fig. 1). The equivalent nodal loads at the element ends are obtained by the modified initial parameters method and then the bending and shear deformations and the internal normal force are considered. The superposition principle can not be used for the axial forces in the second order geometrically non-linear analysis. Each modal loading combination may includes static loads and quasi-static loads also but for one vibration mode only. If transverse loads are really missing the small ficticious ones must be added then.

A static analysis into each cycle is carried out with the initial undeformed geometric axe of the compressed-bended bar. Into the first cycle the solution is performed for the given external axial and transverse loads. In the following cycles the analysis is achieved for the external higher order bending moments only, derived into the last cycle by the initial external axial forces on the deformed axe. In view of the constant internal normal forces for each partial loading combination, the model stiffness matrix remains constant in the cycles, but the load vector changes.

The concentrated higher order bending moment at any section, due to an external above-applied vertical force into each cycle, is equal to the multiplication of this force and the difference between the horizontal displacements of these two sections. Thus, the additional bending moment ΔM_{Ki} at any node K (K=1, 2,..., n), caused from above-applied external distributed vertical forces P(x) and from the concentrated vertical forces P_j into the i-th cycle, is computed by the following evident formula (Fig. 2, 1):

$$\Delta M_{Ki}=\int_{x_K}^{H}P(x)(V_i-V_{Ki})dx+\sum_{j=K+1}^{n}P_j(V_{ji}-V_{Ki})=\sum_{\ell=K}^{n-1}\int_{x_\ell}^{x_{\ell+1}}P(x)(V_i-V_{Ki})dx+\sum_{j=K+1}^{n}P_j(V_{ji}-V_{Ki}), \qquad (2)$$

where n is the number of all nodes; $\ell=K, K+1,\ldots, n-1$ - numbers of the finite elements, placed above joint K; $j=K+1, K+2, \ldots, n$ - numbers of the above-placed nodes; x, x_K, x_ℓ, $x_{\ell+1}$ - abscissae (heights) of the current section and of the nodes K, ℓ, $\ell+1$ respectively; V_i, V_{Ki}, V_{ji} - horizontal (transverse)

(6)

displacements of the current section, of sections κ and j respectively. The numerical integration by the trapezia rule leads to the next recurrent formula:

$$\Delta M_{\kappa i} = \sum_{\ell=\kappa}^{n-1} \frac{1}{2L_\ell}\left[P_\ell (V_{\ell i} - V_{\kappa i}) + P_{\ell+1}(V_{\ell+1,i} - V_{\kappa i})\right] + \sum_{j=\kappa+1}^{n}\left[P_j (V_{ji} - V_{\kappa i})\right], \quad (3)$$

where L_ℓ is a length of the ℓ-th finite element; P_ℓ, $P_{\ell+1}$ - values of the external axial forces $P(x)$ at the ends ℓ and $\ell+1$ of this element respectively; $V_{\ell i}$, $V_{\ell+1,i}$ - the relevant horizontal displacements of these joints into the i-th cycle. The nodal moments $\Delta M_{\kappa i}$, treated as external loads, can be resolved approximately into equivalent external linearly-distributed bending moments for each finite element and the ends values are calculated. Evidently, the values of the moments $\Delta M_{\kappa i}$ decreases.

The Euler's safety factors against overall (total) buckling $\lambda_{\kappa i}$ are computed as a ratio of any bending or shear magnitude values Z (an internal force, a displacement) at any node κ for two sequential cycles $i-1$, i, namely

$$\lambda_{\kappa i} = Z_{\kappa,i-1} / Z_{\kappa i}, \qquad (\kappa = 1, 2, \ldots, n). \quad (4)$$

According to the recommendation, given by Miltchev M. (1976) in view of the accuracy, the final modal safety factor value λ_{cr} for any modal loading combination is determined by means of the transverse displacements V or by the internal bending moments M at the node κ, where the absolute values of these magnitudes are maximum, i.e.,

$$\lambda_{cr} = |V_{\kappa,m-1}| / \max|V_{\kappa m}| \quad \cup \quad \lambda_{cr} = |M_{\kappa,m-1}| / \max|M_{\kappa m}| \quad (5)$$

where m is the cycles number. The iterative process for any loading combination is finished when the safety factors, computed in two sequential cycles are differed up to 3 %. The maximum cycles number is also limited up to 5.

The final value of any magnitude Z_κ (an internal force, a displacement), including the higher order bending moments, at any cross-section κ are computed as an algebraic sum of their relevant values $Z_{\kappa i}$ from all cycles, so that

$$Z_\kappa = \sum_{i=1}^{m} Z_{\kappa i}, \qquad (i = 1, 2, \ldots, m), \quad (\kappa = 1, 2, \ldots, n). \quad (6)$$

(7)

3. COMPUTER PROGRAM

The computer program ROKU, given by Christov C. T. (1987), is written in the FORTRAN IV language for IBM 370/148. This program is used for a stability and static analysis and for computer-aided design of high tower-type structures of revolution when the structural geometry, materials, supports and static loads are given. An usual precision is used. The quasi-static loads are determined; the safety factors against buckling, the higher order bending moments, the internal forces, the stresses and strains of the beam-column model are computed.

4. CONCLUSIONS

For high steel towers the internal normal forces N in the beam-column model are usually less than about 80 % of their Euler's critical buckling values N_{cr} ($N \leq 0,8 N_{cr}$). Then the stability and static analysis, based on the second order geometrically non-linear theory, on the described model and on the presented vertion of the Vianello-Dischinger method and FEM, is effective. The mentioned theory is unreliable for a post-buckling analysis since large displacements are established. This version of the Vianello-Dischinger method is uneffective for solving the arbitrary static undefinable frames.

The accepted convergence tolerance is normally achieved for 2-4 cycles. For structures with a comparatively small safety factor against buckling ($2,5 \leq \lambda_{cr} \leq 15$) the needed cycles number is up to 4 ($m \leq 4$) and the static analysis is to be performed by the deformed geometric scheme. The design standards need to be added and refined towards the safety factors.

The effect of the higher order bending moments onto the stresses and strains is relatively small than the influence of the initial external loads. Moreover, the main contribution is caused by the loads according to the lowest free vibrations mode. Then the relevant safety factors values are usually minimum and the higher order bending moments values are maximum since the horizontal displacement of all cross-sections and all additional moments are unidirectional. The reliable safety factor value is minimum from all modal safety factors values.

(8)

The model stiffness matrix remains constant for all loading combinations with equal external axial forces. The relevant modal safety factors values for this group are commonly slightly-different, but the additional moments values can be very different. If the modal interaction is considered, the resulting values of any magnitude may be computed by mode superposition.

The external seismic vertical forces and bending moments should be taken into account since they increases the higher order bending moments but reduces the safety factors values.

REFERENCES

1. Christov C. T., 1987, CAD of High Towers of Revolution, Report No 108, CESSI, Sofia, Buigaria, p 214, (in bulg.).
2. Dischinger F., 1937, Untrsuchungen uber die Knicksicherheit, die elastische Verformung und das Kriechen des Betons bei Bogenbrucken, Der Bauingenieur, H 33/34 35/36 39/40.
3. Ganev T. and Levy I., 1985, Effect of Some Factors on the Dynamic Characteristics of High Towers, J. Building, Sofia, Bulgaria, No 3-4, pp 25-27, (in bulg.).
4. Gotchev V. A., 1987, Optimal Design of One-storey Metal Frames in Non-linear Setting, Ph. D. Thesis, Sofia, p 275.
5. Integrated Civil Engineering System (ICES). The Structural Design Language - II (STRUDL-II), 1971, Handbook, MIT, School of Engng, Cambridge, Massachusetts, USA, Vol I.
6. Livesley R. K., 1975, Matrix Methods of Structural Analysis, Pergamon Press, Oxford-New York-Toronto-Sydney, p 224.
7. Miltchev E. M., 1976, On a Method for Static Analysis of Geometrically Non-linear Elastic Bar Structures and Their Security against Buckling, Ph. D. Thesis, Sofia, p 126.
8. Miltchev E., Dolaptchiev I. and Vaseva E., 1979, Computer-Aided Analysis of High Concrete Reinforced Industrial Chimneys and Towers, J. Building, Sofia, No 5, pp 23-26.
9. Smirnov A. F., Aleksandrov A. V., Laschenikov B. Y. and Schaposchnikov N. N., 1984, Structural Mechanics (Dynamics and Stability of Structures), Stroyizdat, Moscow, p 416.
10. Tankov N. G. and Bobev T. B., 1981, Beams and Frames. Analysis by Deformed Scheme, Publ. Technica, Sofia, p 176.

(1)
DĄBROWSKI, Ryszard (1)

TWO EXAMPIES OF INSTABILITY UNDER FOLLOWER LOAD

INTERNATIONAL COLLOQUIUM
STABILITY OF STEEL STRUCTURES
BUDAPEST, HUNGARY, 1990
PRELIMINARY REPORT

Summary - Introduction: Two rather simple and loosely interrelated, but at the same time intriguing, examples of instability of a beam or a column under follower load are examined: (1) a beam-cantilever acted on by a so-called quasitangential or semitangential bending moment at the free end, and (2) a free-standing column loaded, at the free end, by a semitangential follower force accompanied by displacement-dependent bending moment.

The first topic - even if in a straightforward form very well known - serves herein as an introductory example to the intricacies of a consistent large-displacement analysis of flexible space frames with inherently rigid connections at the joints, which is dealt with in referenced literature. The second example offers an opportunity to demonstrate how a smooth equilibrium path of divergence can drastically be cut off by bifurcation of equilibrium.

1 A SLENDER BEAM ACTED ON BY END MOMENTS

Instability by flexure and torsion of a simply supported beam loaded by equal end moments is a classical problem solved by L.Prandtl in 1899 - a problem subsequently extended by S.P. Timoshenko (1961) on a thin-walled beam with a double-tee cross-section. However, the mode of load application is of importance here and deserves scrutiny.

1.1 Quasitangential end moment

Two types of a quasitangential end moment acting on a beam cantilever of span l are shown in Fig.1a,b. A quasitangential bending moment M is formed by a couple of forces, in which each force during deformation remains parallel to its original line of action. In the case of Fig.1a the moment vector rotates with end section in the yz-plane while remaining perpendicular to the longitudinal x-axis. In this case the problem of insta-

(1) Professor of Eng.Mechanics, Technical University Gdańsk.

(2)

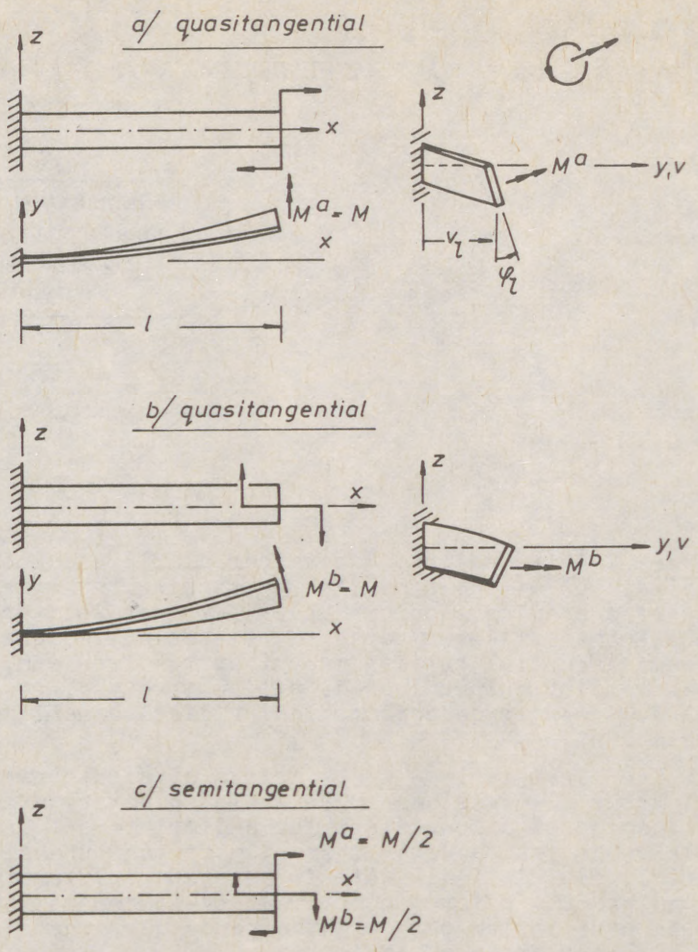

Fig.1

bility is equivalent to the original Prandtl problem of a beam of span 2l. It takes only to imagine that the diagram on the right-hand side in Fig.1a has been rotated clockwise so that end section turns out vertical; in a beam of span 2l bend by end moments causing tension at the top edge, the midsection is displaced and twisted in such a way that the lower compressed edge displaces more outwardly than the upper one. The critical bending moment is equal to, Timoshenko (1961), p.158,

$$M_{cr} = \frac{\pi}{2l}\sqrt{EJ_z GJ_T} \qquad (1)$$

in which EJ_z and GJ_T are the bending and torsional stiffness, respectively.

In the case shown in Fig.1b the moment vector rotates in the xy-plane remaining normal to the z-axis. The critical value is given again by Eq.(1), see e.g. DIN 4114 (1953). This type of instability is illustrated qualitatively by a model of a

(3)
cantilever under gravity force concentrated at the free end. (An impressive model photograph can be found e.g. in a book by N.S.Trahair (1977) on p.179.)

1.2 Semitangential end moment

A semitangential end moment M is formed by two pairs of forces, each pair of which is equal to M/2 and corresponds to scheme a and b, respectively (Fig.1c).

Two equilibrium equations at bifurcation, with respect to transverse displacement v and cross-sectional rotation φ, assume the form

$$\begin{aligned} EJ_z v'' &= M^a(\varphi_1 - \varphi) - M^b\varphi \\ GJ_T \varphi' &= M^a v' - M^b(v_1' - v') \end{aligned} \qquad (2)$$

Where $M^a = M^b = M/2$, and φ_1 and v_1 are the angle of rotation and transverse displacement at beam end, respectively.

From inspection of right-hand side of equation (2) it follows that the load components M^a and M^b counteract each other, thus escalating the critical moment value (attention is drawn to opposite end rotations at bifurcation for the schemes a and b in Fig.1a,b). The critical value given by H.J. Argyris et al. (1978) amounts to double the value of Eq.(1):

$$M_{cr} = \frac{\pi}{l}\sqrt{EJ_z GJ_T} \qquad (3)$$

On far reaching consequences of the concept of semitangential end moments attention has been drawn by H.J.Argyris et al, (1978). In the analysis of large deformations of space frames with rigid joints certain difficulties are encountered in satisfying equilibrium conditions of moments at nodal points. A quotation from Argyris et al. (1978) might be appropriate at this place:

"The matrix displacement analysis of geometrically nonlinear structures becomes an intricate task as soon as finite elements in space with rotational degrees of freedom are considered. The fundamental reason for these difficulties lies in the non-commutativity of successive finite rotations about fixed axes with different direction. In order to circumvent this difficulty, a new definition of rotation - the so-called semitangential rotation - is intruduced ... These semitangential rotations which correspond to the semitangential torques of Ziegler (1968) possess the most important property of being commutative."

Details of an appropriate stiffness matrix for a thin-walled beam element were given by Y.B.Yang and W.McGuire (1986). A warping degree of freedom has been incorporated at each end of element in addition to conventional six degrees of freedom (the torque can be either quasitangential or semitangential, depending on type of the cross-section).

An analysis of three-dimensional space structures which are of low mass and very high flexibility has been dealt with by K.Kondoh et al. (1986). A geometrically nonlinear static analysis of a (156 element) shallow geodetic dome with rigid

(4)
joints has been presented by J.L.Meek and S.Loganathan (1989). A "joint oriantation matrix" was employed to update the rotational displacement of joints in an incremental analysis.

2 STABILITY OF A FREE-STANDING COLUMN LOADED THROUGH A ROLLER BEARING

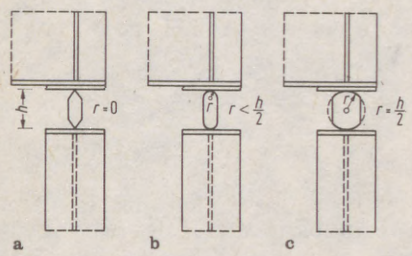

Fig.2

A column fixed at the base supporting a transversally stabilized structure (a beam for example) is loaded through a roller bearing (Fig.2c). A roller is a special type of rocker bearing (Fig.2a,b) in which the rocker height h is equal to roller diameter (h = 2r). (A freestanding column loaded through a true rocker bearing can loose stability under a fracture of that gravity load that, if directly acting, this column should safely support.)

Is is assumed that a vertical load P is acting through roller on the column on initial eccentricity e with respect to column axis. Initial and deformed configurations of the system are shown in Fig.3, see R.Dąbrowski (1984) for details.

The roller as a free-body is in equilibrium which is secured by the presence of a horizontal component to the load P, equal to $Pu_o'/2$, u_o' denoting the angle of rotation of the end section. The resulting column load is inclined to the vertical by the angle $u_o'/2$ and constitutes a semitangential follower force $\sim P$. This force is accompanied by a displacement-dependent bending moment equal to $-Pu_o/2$ with u_o being the column end displacement. (Initial end moment Pe remains acting during deformation.)

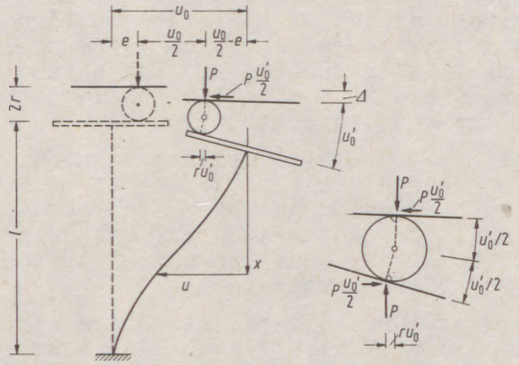

Fig.3

(5)

The equilibrium between the section bending moment and the resultant of axternal forces is expressed by the Eularian equation in travelling coordinates x,u (Fig.3) :

$$EIu'' + Pu = P(u_0/2 - e + \underline{u_0' r} + u_0' x/2). \tag{4}$$

The final form of displacement function u reads

$$u = \frac{2e}{\alpha l(1 - \cos \alpha l) + 2 \sin \alpha l} [(1 - \cos \alpha l)(\sin \alpha x + \alpha x) - \sin \alpha l(1 - \cos \alpha x)]. \tag{5}$$

with

$$\alpha = \sqrt{P/EI}, \tag{6}$$

(underlined term in Eq.(4) can in principle be neglected). The end displacement u_o which is equal to u at x=l in travelling coordinates is given by

$$\frac{u_0}{2e} = \frac{\alpha l(1 - \cos \alpha l)}{\alpha l(1 - \cos \alpha l) + 2 \sin \alpha l} = \frac{1}{1 + \left(\frac{\alpha l}{2} \operatorname{tg} \frac{\alpha l}{2}\right)^{-1}}. \tag{7}$$

and the end rotation, u_o' , reads simply

$$u_0' = \frac{2u_0}{l}. \tag{8}$$

The diagram of displacement u_o versus P is shown in Fig.4 (Case 2, curve 2) . Case 1 belongs to an initially cen-

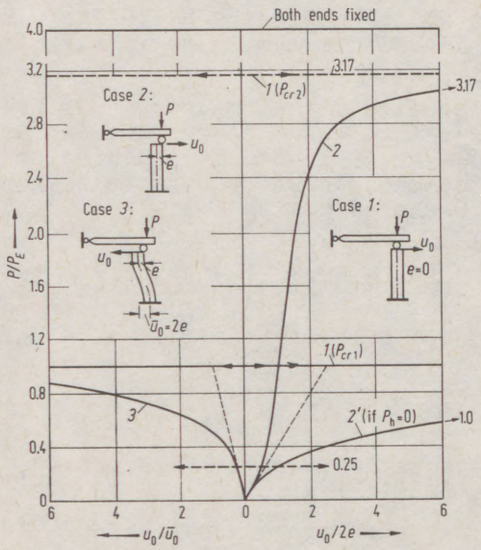

Fig.4

(6)
tral loading and Case 3 to an S-shaped initial stress-free deformation. In case of central loading two lowest critical loads of bifurcation are determined: $P_{cr1} = P_E$ and $P_{cr2} = 3{,}17\ P_E$ where $P_E = \pi^2 EJ/l^2$.

The equilibrium path 2 forms a smooth curve of divergence tending to infinity at $P = 3{,}1738\ P_E$. For a free-standing cantilever the critical conservative load acting at the free end is equal $P_E/4$. It is worth noticing that P_E forms a limit of divergence of a rapidly growing curve 2′ for eccentrically roller-loaded cantilever column if stabilizing horizontal component $P_h = Pu_o'/2$ is being neglected (Fig.4).

The high disparity of divergence loads for Cases 2 and 2′ is intriguing. It turns out that equilibrium path 2 in Fig.4 is unstable beyond $P = P_E$. This fact has been pointet out by W.T.Koiter in his deferred discussion on author's paper (1984).

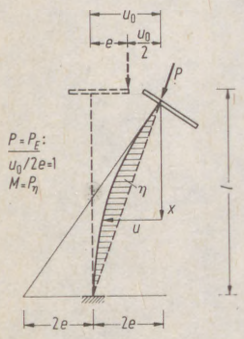

Fig.5

Kinematics of bifurcation of equilibrium at P_E ought to be considered here in some detail. The shape of equilibrium at that load is seen from Fig. 5. End displacement u_o is equal twice the initial eccentricity e ; the roller displacement is, as usual in this problem, equal half this value. Point of load application in deformed position coincides with the column-end center. Displacement function u is given in form

$$u = u_o\left(\frac{x}{l} + \frac{1}{\pi}\sin\frac{\pi x}{l}\right) = u_o\frac{x}{l} + \eta(x) \qquad (9)$$

and its shape is an inclined sine half-wave with amplitude $2e/\pi$. Thus the dashed diagram in Fig.5 signifies the bending moment $-EJu'' = M = P_E\eta$.

One observes, first, that because of kinematic restraint this symmetric sine half-wave cannot grow unless the load is increased as well (as indicated by equilibrium path 2 in Fig. 4). Secondly, a compatible shape of displacement variation at $P = P_E$ forms an S-shaped cosins half-wave (Fig.6) written in form

$$\delta u = \frac{\delta u_o}{2}\left(1 - \cos\frac{\pi x}{l}\right) = \frac{\delta u_o}{2} + \delta\eta(x) \qquad (10)$$

And this leads to the required equation of equilibrium at bifurcation:

$$-EJ\,\delta u'' = \delta M = P_E\,\delta\eta \qquad (11)$$

in supplement to equation, written previously, for the initial state just prior to bifurcation.

Herewith it has been proved that bifurcation characterized by δu at $P = P_E$ is statically admissible, also kinematically possible, and thus inevitable. The following observation

(7)

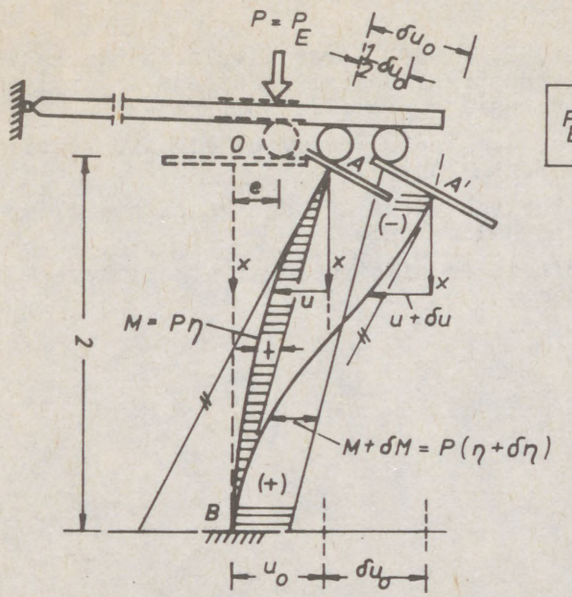

$$P_E = \frac{\pi^2 EJ}{l^2}$$

Fig.6

would be helpful in assessing the situation. The displacement variation δu , Eq.(10), means that the center of free-end section A moves perpendicularly to the straight line AB, connecting both column ends, to a new position A´ (see Fig.6). Point A´ is lowered with respect to point A by the vertical displacement component equal to $\delta u_0 (u_0/l)$. At the same time the roller moves upward and to the left with respect to point A´ remaining on the initial level. Within the framework of second order theory the equilibrium is indifferent.

References

Argyris, H.J. et al. (1978) On large displacement-small strain analysis of structures with rotational degrees of freedom. Computer Methods in Applied Mechanics and Engineering. Vol.14, 401-451; Vol.15, 99-135.

Dabrowski, R. (1984) Stability of a free-standing column loaded through a roller bearing. Ingenieur-Archiv. Vol.54, No 1, 16-24; correction Vol.54, No 5, p.400.

DIN 4114 (1953) Stabilitätsfälle - Knickung, Kippung, Beulung. Richtlinie 15.13.

Yang, Y.B., Mc Guire, W. (1986) Stiffness matrix for geometric nonlinear analysis. Journal of Structural Engineering. Vol.112, No 4, 853-877. Also: Joint rotation and geometric nonlinear analysis. Ibid. Vol.112, No 4, 879-905.

Kondoh, K., Tanaka K., Atluri, S.N. (1986) An explicit expression for tangent-stiffness of a finitely deformed 3-d beam and its use in the analysis of space frames. Computers and Structures, Vol.24, No 2, 253-271.

(8)

Meek, J.L., Loganathan, S. (1989) Large displacement analysis of space-frame structures. Computer Methods in Applied Mechanics and Engineering. Vol.72, No 1, 57-75

Timoshenko, S.P., Gere, J. (1961) Theory of elastic stability. McGraw-Hill, New York (2nd ed.).

Trahair, N.S. (1977) The behaviour and design of steel structures. Chapman and Hall, London.

Ziegler, H. (1968) Principles of structural stability. Blaisdell, Waltham.

(1)

GOSOWSKI, Bronisław (1)

STABILITY OF MONOSYMMETRICAL THIN-WALLED MEMBERS WITH LOCAL LATERAL RESTRAINTS

INTERNATIONAL COLLOQUIUM
STABILITY OF STEEL STRUCTURES
BUDAPEST, HUNGARY, 1990
PRELIMINARY REPORT

Summary: The paper presents an algorithm of determining the critical load of elastic spatial buckling for monosymmetrical thin-walled members derived from the general solution of distributional differential stability equations. A prismatic members considered have an open cross-section with elastic point constraints due to lateral bending and torsion over the length and are loaded by a both constant axial load and bending moment. The practical advantages of the presented solution were depicted by computed critical loads of lateral buckling and flexural-torsional buckling of steel beams and columns. The theoretical solution was verified experimentally on I steel members with lateral restraints.

1. Introduction

The correct assesment of load bearing capacity of metal members of open cross-section belonging to a skeleton (columns, frame spandrel beams, beams) should be based upon the stability analysis with a respect to the structural members (wall beams,

(1) Assistant Professor of Civil Engineering, Technical University of Wrocław, Poland

purlins, bracings, stiffeners, etc.) connected with main members along their length in the plane of minor flexural rigidity. An analytical model in a general case is built up of arbitrary supported on both ends thin-walled member of open cross-section with point elastic constraints due to lateral displacement and rotation placed arbitrary along the member length and his axis.

The spatial stability of different kinds of thin-walled elements (beams in majority) which performs a special case of mentioned above model has been approached by more than twenty authors. Owing to the limitations of pages the articles strictly associated have been refered only.

This paper presents a general solution of the spatial stability for monosymmetrical member arbitrary supported on both ends and some intermediate points placed out of the plane of symmetry. This thin-walled member of constant open cross-section works as a beam-column. The paper performs a generalization of appropriate solutions presented previously by the author (1981) for mono and bisymmetrical bars under axial compression which gave the basis for the stability analysis of steel I columns with constant and changing cross-section, Gosowski (1988).

2. Formulating and solution of spatial stability problem

Let us consider an arbitrary supported on both ends member of a constant, open, monosymmetrical cross-section with arbitrary number m of point elastic constraints characterized by the compliance $\mathcal{E}_{xi}$ and $\mathcal{E}_{\varphi i}$ respectively due to lateral deflection and torsion of the member to which a constant axial force P and constant bending moment M_x acting in the plane of symmetry are applied. The scheme of the member considered complete with the coefficients of compliance elastic constraints characterizing its supports on the ends and at the span is shown in Fig. 1.

The differential equations of the torsional-flexural buckling of the member considered out of the symmetry plane of his cross-section (Fig. 1) can be presented in the distribu-

(3)

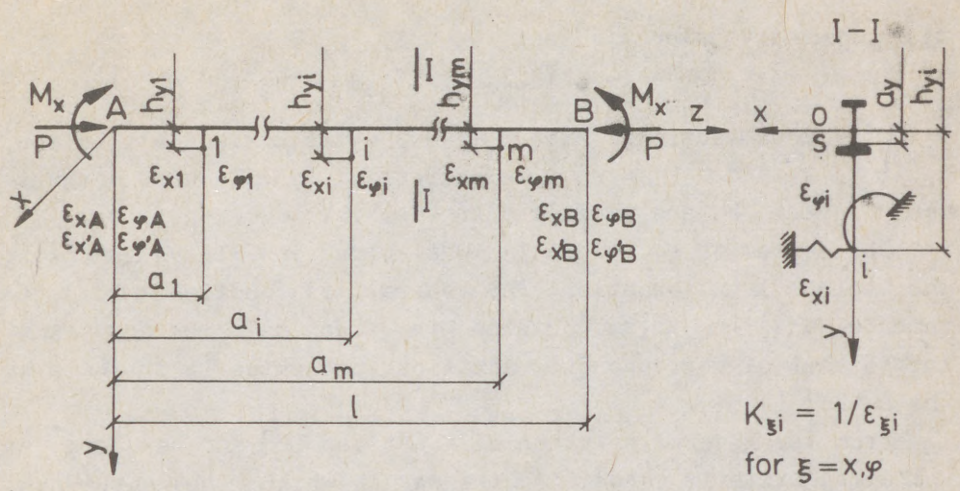

Fig. 1

tional form:

$$EI_y u^{(4)} + Pu^{(2)} + (Pa_y + M_x)\varphi^{(2)} + \sum_{i=1}^{m} R_x(a_i)\,\delta(z-a_i) = 0 , \quad (1a)$$

$$EI_\omega \varphi^{(4)} + \left[P(i_o^2 + a_y^2) - GI_d - (r_x - 2a_y)M_x\right]\varphi^{(2)} + (Pa_y + M_x)u^{(2)} + \sum_{i=1}^{m} M_z(a_i)\,\delta(z-a_i) = 0 , \quad (1b)$$

where: $u(z)$ - the line of lateral deflection of the axis of members shear centers S , $\varphi(z)$ - the angle of torsion of its cross sections respectively this axis, $R_x(a_i)$ and $M_z(a_i)$ - the component of the load caused by reactions at the points of elastic restraints determined by equations:

$$R_x(a_i) = K_{xi}\left[u(a_i) + (a_y - h_{yi})\varphi(a_i)\right] , \quad (2a)$$

$$M_z(a_i) = K_{\varphi i}\,\varphi(a_i) + (a_y - h_{yi})R_x(a_i) , \quad (2b)$$

E, G - the elastic modulus and shear modulus respectively, I_x , I_y , I_d , I_ω - the moments of inertia of the cross-section in respect to x , y axes, the St. Venant's torsional and warping moment of inertia respectively, i_o - the polar radius of gyration with respect to centroid O , r_x - the arm of the cross-sec-

(4)

tion asymmetry calculated as:

$$r_x = \int_F y(x^2 + y^2)dF / I_x ,$$

F - the cross-sectional area, $\delta(z-a_i)$ - the Dirac distribution, $\zeta^{(k)} = d^k\zeta(z)/dz^k$ ($\zeta = u, \varphi$). The rest of symbols used in equations (1) and (2) are explained in Fig. 1.

The system of equations (1) was solved in a closed form using the Laplace transformation. The generalized functions of displacements $u(z)$ and $\varphi(z)$ obtained in effect have the form similar to that of corresponding functions presented in the work by the author (1981).

From the general solution of equations (1) and assuming the following criteria concerning the way in which the member considered is supported (cf. Fig. 1):

- on ends

$$u(0)=\varepsilon_{xA}R_{xA},\ u^{(1)}(0)=\varepsilon_{x'A}M_{yA},\ \varphi(0)=\varepsilon_{\varphi A}M_{zA},\ \varphi^{(1)}(0)=\varepsilon_{\varphi'A}B_A,$$
$$u(1)=\varepsilon_{xB}R_{xB},\ u^{(1)}(1)=\varepsilon_{x'B}M_{yB},\ \varphi(1)=\varepsilon_{\varphi B}M_{zB},\ \varphi^{(1)}(1)=\varepsilon_{\varphi'B}B_B,$$

- in span

$$u(a_i) + (a_y - h_{yi})\varphi(a_i) = \varepsilon_{xi}R_x(a_i) \quad \text{for } i = 1,2,\ldots,m ,$$
$$\varphi(a_i) + \varepsilon_{\varphi i}(a_y - h_{yi})R_x(a_i) = \varepsilon_{\varphi i}M_z(a_i) \quad \text{for } i = 1,2,\ldots,m ,$$

similar to the work by author (1989) the criterion of buckling has been derived in a form:

$$\det\left[B_{\varphi y}\right] = 0 , \qquad (3)$$

where: $\left[B_{\varphi y}\right]$ - the square matrix of $2r$ ($r = 4 + m$) degree.

The general solution of the problem of spatial stability (3) was reduced to the problem of eigenvalues $P = P_{\varphi ycr}$ (flexural--torsional buckling) or $M_x = M_{xcr}$ (lateral buckling). The smallest positive eigenvalues will be of practical importance.

The numerical determination of the critical load of the spatial stability of the thin-walled members considered (Fig. 1), according to the algorithm presented, is made possible for the flexural-torsional buckling by program WGSPCZP and for lateral buckling by program ZPCZSM . These program were written in FOR-

(5)

TRAN and were intended for ODRA 1300 digital computers. At present the programs were adjusted for IBM PC computers.

3. Numerical examples

A steel elements with length $l = 6,0$ m pivoted on both ends ($\varepsilon_{xA} = \varepsilon_{xB} = \varepsilon_{\varphi A} = \varepsilon_{\varphi B} = 0$, $\varepsilon_{x'A} = \varepsilon_{x'B} = \varepsilon_{\varphi'A} = \varepsilon_{\varphi'B} = \infty$), with determined number m of intermediate lateral restraints having the same characteristic $\varepsilon_{xi} = \varepsilon_x = 0$, $\varepsilon_{\varphi i} = \varepsilon_\varphi = \infty$ have been analyzed. The bisymmetrical beam was made of rolled I section IPE 400, the column was made of welded plates as follows (cf. Fig. 1): the upper flange - 15x160 mm, the web - 10x400 mm, the bottom flange - 20x200 mm. The characteristics of the members considered are presented in Table 1. The Young's modulus and shear modulus of elasticity have been taken as $E = 205$ GPa, $G = 80$ GPa.

Table 1. Characteristics of sections of the members

Member	F	I_x	I_y	I_ω	I_d	i_o	a_y	$-r_x$
	$10^{-4}m^2$	$10^{-8}m^4$		$10^{-12}m^6$	$10^{-8}m^4$	$10^{-2}m$		
Beam	84,5	23130	1320,0	490000	52,40	17,01	0,000	0,000
Column	104,0	32200	1848,7	644830	84,67	18,09	6,117	4,927

First the effect of a single transversal brace ($m = 1$) placed arbitrary with respect to both axis ($h_{y1} = h_y$) and length ($a_1 = a$) on the critical load of the lateral buckling of the rolled beam under pure bending has been studied. The results obtained are presented in Fig. 2.

Second the effect of the number m of lateral restraints spaced equally over the length, at a distance $h_{yi} = h_y$ from the axis, on the critical load of the flexural-torsional buckling of the monosymmetrical, welded column subjected to compression and bending has been analyzed. The results have been listed in Table 2.

(6)

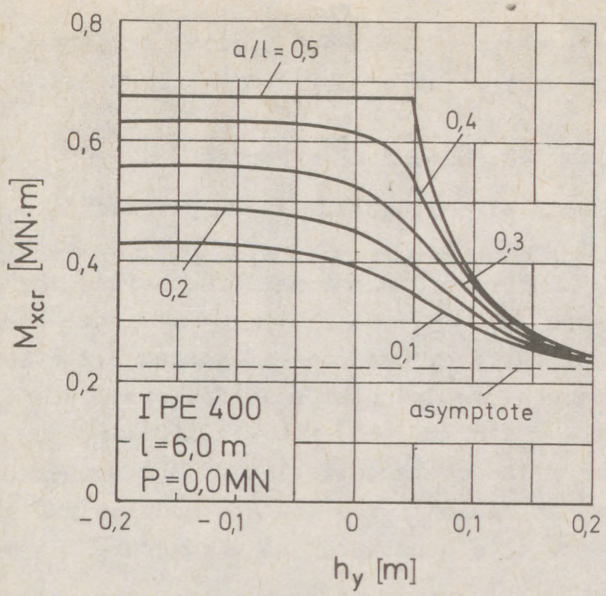

Fig. 2

Table 2. The critical force of elastic spatial buckling for monosymmetrical welded columns

Distance h_y [m]	Number of intermediate supports m	$P_{\varphi ycr}$ [kN] for columns loaded by compressive force P and constant bending moment M_x [kN·m]		
		-200,0	0,0	+200,0
—	0	833,2	985,6	262,2
0,187	1	3006,5	1765,3	520,6
	2	3026,2	1776,7	527,1
	∞	3028,9	1778,6	528,3
0,06117	1	3790,3	2833,2	1860,2
	2	3790,9	2848,2	1903,2
	∞	3790,9	2850,1	1909,3
0,000	1	3581,3	3291,3	2605,7
	2	3594,1	3294,3	2987,3
	∞	3595,6	3294,6	2993,6
-0,248	1	1193,8	2127,0	2605,7
	2	1206,5	2153,1	3099,1
	∞	1209,0	2157,1	3105,1

(7)

4. Verification on models

Within an extensive scope of experiments on the spatial stability of thin-walled steel members with structural stiffeners which were executed in the Institute of Building Engineering of Wrocław Technical University in 1986 - 1988, the critical load of elastic, flexural-torsional buckling of IPE 100 columns ($l = 2{,}64$ m) was studied. The columns were free supported on both ends and on two other identical supports with characteristics $\varepsilon_x = 0$, $\varepsilon_\varphi = \infty$ located each 0,88 m over the length in the plane of the minor flexural rigidity, at a distance $h_y = 0{,}15$ m from the axis. The models 1.1 and 1.2 were compressed by forces P acting axially ($M_x = 0$), whereas models 2.1, 2.2, 2.5 and 2.6 by forces P applied eccentrically $e_y = -0{,}01$ m ($M_x = -P \cdot e_y$).

The comparison of the critical forces of elastic, flexural-torsional buckling obtained experimentally - $P^e_{\varphi ycr}$, with that determined theoretically (3) - $P^t_{\varphi ycr}$ was presented in the Table 3. The experimental critical forces were obtained by Southwell method basing on the angle of twist of the column at the half of the length. The theoretical critical forces were calculated for nominal sizes of IPE 100. Other details and the comparison of the critical moments of lateral buckling obtained experimentally by Milner (1977) with that determined theoretically according to (3) shall be given during the Conference.

Table 3. The comparison of critical forces of flexural-torsional buckling obtained experimentally and theoretically

Model	$P^e_{\varphi ycr}$ [kN]	$P^t_{\varphi ycr}$ [kN]	Model	$P^e_{\varphi ycr}$ [kN]	$P^t_{\varphi ycr}$ [kN]
1.1	103,29	85,76	1.2	99,24	85,76
2.1	77,17	76,46	2.2	79,77	76,46
2.5	82,96	76,46	2.6	77,09	76,46

(8)

5. Conclusions

The computer programs based on the general solution of the spatial stability problem, for the case shown in Fig. 1 , give the possibility of the stability analysis during dimensioning procedure for a big variety of thin-walled members appearing in steel structures.

The experimental verification of the mentioned above theoretical solution proves the correctness of the assumed numerical model in the considered problem of the spatial stability.

References

Gosowski, B. (1981), Buckling of axially loaded thin-walled bars with concentrated elastic constraints (in Polish). Archiwum Inżynierii Lądowej, 27, 635-652.

Gosowski, B. (1988), Zur Stabilitätsanalyse der axial belasteten Stahlbaustützen mit I-Querschnitt. Bauingenieur, 63, 229-237.

Gosowski, B. (1989), Spatial buckling of eccentric compressed I-columns braced in plane of minor rigidity (in Polish). VIII-th International Scientific Technical Conference "Metal Structures", Gdańsk, Volume 2, 63-70.

Milner, H.R. (1977), Tests on equal flanged beams braced against twisting on the tension flange. Civil Engineering Transactions, The Institution of Engineers, Australia, CE19, 92--100 .

(1)
SCHOLZ, Hans (1)

BEAM-COLUMNS IN DESIGN SPECIFICATIONS AND A NOVEL APPROACH

INTERNATIONAL COLLOQUIUM
STABILITY OF STEEL STRUCTURES
BUDAPEST, HUNGARY, 1990
PRELIMINARY REPORT

SUMMARY

In this paper a comparison of specified beam-column design equations is provided. A number of subassemblages are evaluated for this purpose. A rigorous and a new technique are also applied to the same subassemblages. The comparisons show that specification results for beam-columns differ widely due to the difference in the used column curves and the variations in the presentation of the moment magnification factors. The aspect of lateral buckling is excluded from this study.

INTRODUCTION

In-plane beam-column design in steel specifications is typically based on interaction equations involving the applied and allowable axial forces and bending moments respectively. The following aspects of in-plane stability should be properly covered:

a) Column buckling under conditions approaching pure axial load.

b) Frame instability in a sway mode of the unbraced frame subjected to pure gravity load.

c) For braced and unbraced columns, recognition of possible hinge formation at a critical section between member ends.

d) Additional column end moments should be included in the design of adjoining beams.

e) Cases between fully braced and completely free to sway should be covered.

---

(1) Associate Professor of Civil Engineering, University of the Witwatersrand, Johannesburg

(2)

It will be seen from the following comparative study that many of the existing design specifications are not adequately addressing the above points.

AISC LOAD AND RESISTANCE FACTOR SPECIFICATIONS (1986)

For elastic analysis and singly and doubly symmetric members in uniaxial flexure and compression, the following interaction equation is to be satisfied for members within the allowable slenderness range.

$$\frac{P}{0.85P_u} + \frac{8}{9}\frac{M}{0.9M_P} \leq 1 \qquad (1)$$

where M_P is the fully-plastic moment capacity of the section and P_u the axial force capacity in the absence of bending, based on the relevant column curves and effective member length. The coefficients 0.85 and 0.9 are member performance factors, allocated to the limit states of column and beam failure respectively. The terms P and M are the design axial force and bending moment. The axial force, P, follows directly from a conventional analysis. However, the design bending moment is determined as follows:

$$M = B_1 M_V + B_2 M_H \qquad (2)$$

where M_V is the bending moment due to gravity load and M_H is the bending moment due to lateral load. The magnification factors B_1 and B_2 are defined as

$$B_1 = \frac{C_m}{1 - \frac{P}{P_c}} \geq 1 \qquad (3)$$

$$B_2 = \frac{1}{1 - \frac{\Sigma P}{\Sigma P_c}} \qquad (4)$$

where P_c is the elastic column buckling load and ΣP_c the elastic storey buckling load. The factor C_m equals $0.6 \mp 0.4 M_1/M_2$; with M_1/M_2 the ratio of the smaller to larger gravity end moment, when no lateral loads are applied between the column ends. If the axial load is less than $0.85 \times 0.2 P_u$, Eq 1 is replaced by

$$\frac{P}{1.7P_u} + \frac{M}{0.9M_P} \leq 1 \qquad (5)$$

The AISC LRFD specification thus magnifies the sway moments by way of B_2 and recognises the possibility of hinge formation between member ends by the factor B_1. If B_1 is less than 1, hinge

(3)

formation between ends is not critical. If B_1 exceeds 1, the total design moment, M, is obtained as the direct summation of the magnified moments M_V and M_H. This is conservative, since these will not occur at the same section. Column buckling is introduced in Eqs 1 and 5 by using the term P_u.

SSRC (1976), AISC (1978), SABS (1984)

Beam-columns in the above specifications are checked against instability with an equation of the following format

$$\frac{P}{P_u} + \frac{C_m M}{(1 - \frac{P}{P_c}) M_P} \leq 1 \qquad (6)$$

The factor $C_m = 0.6 + 0.4 M_1/M_2 \geq 0.4$ for the braced column. For the unbraced column $C_m = 0.85$ is suggested and the moment, M, in Eq 6 represents the total moment from a first-order elastic analysis. Thus for the unbraced member, $M_H + M_V$, will be magnified by $0.85/(1-P/P_c)$. The strength interaction equations for zero slenderness of all these specifications are very similar. The results of the above specifications will only differ on account of the parameter P_u, which represents the axial column capacity as a function of the slenderness ratio. SSRC and AISC 1978 use the CRC column curve (SSRC, 1976), whereas SABS (1984) is based on the well-known Perry-Robertson equation. For braced columns, $C_m/(1-P/P_c) \geq 1$ is not a requirement.

ECCS (1976)

The European Convention for Constructional Steelwork (ECCS) uses the following formula for in-plane failure of uni-axially bent beam-columns

$$\frac{P}{P_{SQ}} + \frac{C_m (M + Pe)}{(1 - \frac{P}{P_c}) M_P} \leq 1 \qquad (7)$$

Two differences exist compared with the previously discussed codes. First, the axial force ratio is based on the squash load, P_{SQ}, ie area times yield stress; and second, a compulsory minimum moment of applied force P times an eccentricity, e, is incorporated into the interaction equation. $C_m/(1-P/P_c) \geq 1$ is not a requirement. For unbraced columns ECCS suggests to execute a second-order analysis to obtain the magnified design moment.

BS 5950 (1985)

The British steel design code gives a simplified as well as a more exact beam-column design approach. The more accurate buckling interaction equation for uniaxial bending is relevant for this comparative study

(4)

$$\frac{C_m M}{M_P \dfrac{1-\dfrac{P}{P_u}}{1-\dfrac{0.5P}{P_u}}} \leq 1 \qquad (8)$$

All parameters have the previous meaning, but the factor C_m is defined as $0.57+0.33M_1/M_2+0.1(M_1/M_2)^2 \geq 0.43$ for the braced and unbraced member. The denominator in Eq 8 represents the maximum buckling moment capacity about the major axis in the presence of axial load, P, but excluding lateral-torsional buckling failure.

For the unbraced case BS 5950 distinguishes between vertical and lateral load moments. For pure vertical loads Eq 8 is evaluated exactly as for the braced column. However, the application of a nominal lateral load is mandatory (one half percent of the factored dead and imposed loads). For combined vertical and lateral load moments, the end moments due to lateral loads are magnified by $1/(1-P/P_c)$ using the unbraced elastic buckling load P_c. Thereafter, Eq 8 including C_m is evaluated for the critical section between member ends using the physical member length when computing P_u. Also P/P_{SQ}+magnified $M/M_P \leq 1$ is evaluated at the ends of the member. The more critical result is relevant.

NOVEL METHOD (Scholz, 1987,1989)

The computation of the frame instability effect (P-Delta) and the member instability effect (column buckling and hinge formation between member ends) is accomplished by using the multi-curve diagram of Fig 1 below.

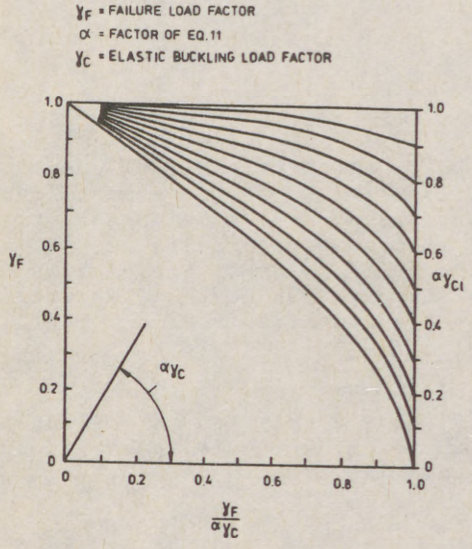

FIG 1: INTERACTION GRAPH

(5)

These empirical curves represent the approximate elastic-plastic failure loads of frames or columns with varying slenderness and different loadings. To use the curves of Fig 1, various parameters need to be established. The curves and the derivation of the input parameters were previously discussed by Scholz (1987) for sway structures and then extended to braced columns (1989). For unbraced columns the elastic sway buckling load of the storey is used and for braced columns the elastic buckling load of the braced case. The meaning of the used symbols remains unchanged.

$$\gamma_c = \frac{P_c}{P} = \frac{\text{elastic buckling load}}{\text{applied axial load}} \tag{10}$$

$$\alpha = \frac{0.4}{1 - 0.6\left(1 - \frac{0.05\gamma_c}{1 + \frac{M_V}{M_H}}\right)^3} \geq 0.4 \tag{11}$$

For members not subjected to sway moments the term α reduces to 1.0. Further parameters for use in Fig 1 are

$$\alpha\gamma_{c\ell} = \frac{\alpha\gamma_c}{\left\{\mu\left[\frac{1}{2} + \frac{1}{2}\sqrt{1 + \frac{\nu}{\mu^2}}\right]\right\}^{\omega}} \tag{12}$$

$$\mu = \frac{\alpha\gamma_c\left(\frac{M_H}{1-\alpha} + M_V\right)\varkappa}{0.7M_P} \tag{13}$$

$$\nu = \frac{4\alpha P_c}{0.7P_{SQ}} \tag{14}$$

$$\omega = \left(1 - \frac{\mu}{\nu}\right)^2 + 1 \quad \begin{matrix} \geq 1 \\ \leq 2 \end{matrix} \tag{15}$$

To cover the formation of a hinge between member ends, the following modification to Eq 13 is required; then μ^* replaces μ.

$$\mu^* = \mu(6 + 5M_1/M_2) \tag{16}$$

The term $6+5M_1/M_2$ magnifies the maximum end moment M_2.

The factor 0.7 in Eqs 13 and 14 allows for the commencement of non-linear sectional behaviour at about 70% of the fully-plastic condition (equivalent to a residual stress of 30% of the yield stress) and the term $\varkappa$ is the so-called shape factor in bending.

(6)

The input parameters for Eqs 10-15 are derived from the results of a conventional first-order elastic structural analysis (P, M_V, M_H), from the strength interaction curve at zero slenderness (M_P, P_{SQ}) and from an elastic buckling analysis, (P_c). Once $\alpha\gamma_c$ and $\alpha\gamma_{cl}$ are known, the relevant failure load as affected by instability can be found from Fig 1 in terms of the ratio γ_F. In design the novel beam-column approach thus assumes the following simplified format using the strength envelope of SSRC and AISC 1978 for instance.

$$\frac{\frac{P}{\gamma_F}}{P_{SQ}} + \frac{\frac{M}{\gamma_F}}{1.18M_P} \leq 1 \qquad (17)$$

$$\frac{\frac{M}{\gamma_F}}{M_P} \leq 1 \qquad (18)$$

APPLICATIONS

The various beam-column equations outlined in this paper have been applied to four substructures for comparison purposes. Two braced and two unbraced cases have been considered. For the AISC LRFD method the performance factors have been excluded. Where the results of a rigorous analysis are shown these are reproduced from Ketter (1961), Wood (1976) and in the case of pure gravity load acting on a sway subassemblage the method by Lu (1965) was emloyed.

BRACED SUBASSEMBLAGES (FIGS 2 AND 3)

A double curvature and a single curvature case has been examined.

For the braced column bent in double curvature, design specifications are typically conservative. Design codes vary widely in regard to their starting point on the axial load axis. The South African steel code and the AISC LRFD specifications (for low axial load) give the most conservative predictions. The novel method of beam-column design compares very well with a rigorous elastic-plastic analysis throughout the entire range of forces.

For the braced single curvature case all methods are relatively close together. ECCS and SABS are conservative, especially for low bending moment values. The best fit with a rigorous analysis is obtained by BS 5950 and the novel approach by Scholz. There is still a large variation in the treatment of cases approaching pure axial load, ie the column buckling case.

(7)

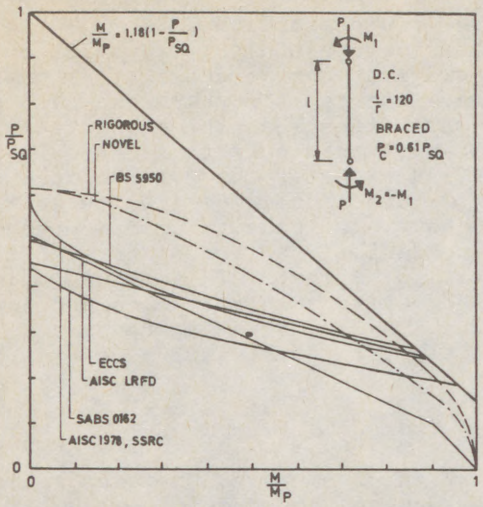

FIG 2: BRACED - DOUBLE CURVATURE

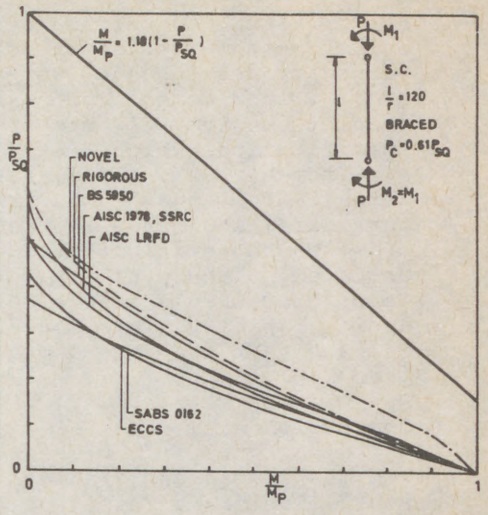

FIG 3: BRACED - SINGLE CURVATURE

UNBRACED SUBASSEMBLAGES (FIGS 4 AND 5)

A sway subassemblage subjected to lateral load only and another subjected to gravity load only has been evaluated.

For the lateral load case, code results are typically conservative, with the exception of the British steel code, which is slightly unconservative for low moment values. The results of the novel method compare closely with the rigorous results.

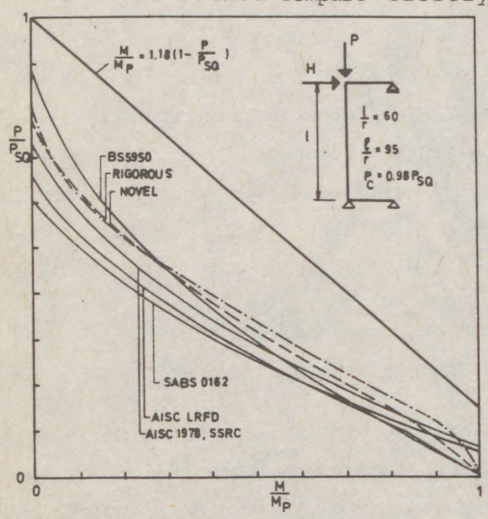

FIG 4: SWAY - LATERAL LOAD

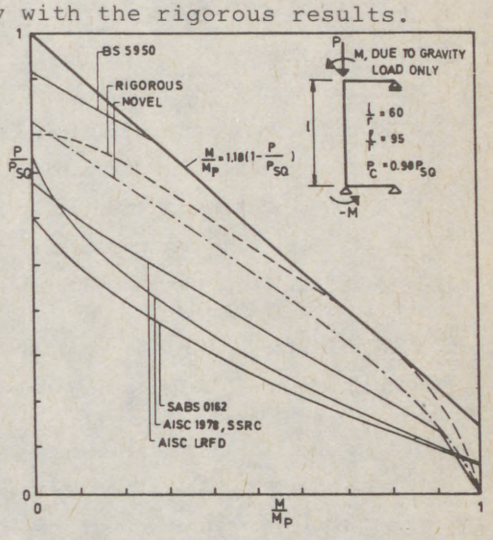

FIG 5: SWAY - GRAVITY LOAD

(8)

For gravity load only on a sway subassemblage, the novel beam-column method is closest to a rigorous analysis. Results obtained by design codes vary widely. Those codes that separate gravity load moments from sway moments (AISC LRFD and BS 5950) predict considerably higher capacities than the conservative specifications which treat gravity load moments identical to sway moments (AISC 1978, SSRC and SABS). The British code relates to the squash load or the braced column capacity as the pure axial load case is reached. This leads to an overprediction of strength as illustrated in Fig 5. If on the other hand the unbraced column capacity is taken as the limit for pure axial load (AISC LRFD), then a conservative result is obtained for the design capacity. This conservatism is further aggravated by requiring that the braced magnifier, B_1, must always be greater than 1.

CONCLUSION

The most important findings of this comparison between a rigorous solution, a novel approximation and beam-column equations of various design codes can be summarized as follows:

a) Although most design code results are conservative, widely differing column curves are incorporated into the allowable axial load term of the interaction equation.

b) The design code equations do not cover well the case of pure gravity load on a sway structure.

c) Hinging between member ends is not well covered in most specifications.

d) A novel beam-column method gives the most consistent correlation with a rigorous analysis.

REFERENCES

AISC 1978, American Institute of Steel Construction, Chicago

AISC LRFD.1986. American Institute of Steel Construction, Chicago

BS 5950.1985. British Standards Institution, London

ECCS.1976. European Convention for Constructional Steelwork, Int. Rep.,Liege

Lu, LW.1965. "Inelastic Buckling of Steel Frames", ASCE, 113, 10, 1953-1970

Ketter, RL.1961. "Further Studies of the Strength of Beam-Columns",ASCE, 87, 6, 135-152

SABS 0162.1984. South African Bureau of Standards, Pretoria

Scholz, H.1987. "P-Delta Effect in Elastic Analysis of Sway Frames", ASCE, 113, 3, 534-545

Scholz, H.1989. "Survey of Beam-Column Approaches and a New Method", unpubl.

SSRC Guide.1976."Stability Design Criteria for Metal Structures", N. York

Wood, BR.1976. "Further Aspects of Design by P-Delta Method", ASCE, 102, 3, 487-500

(1)
TAKANASHI, Koichi (1)
NAKASHIMA, Masayoshi (2)

DESIGN OF STEEL BEAM-COLUMNS SUBJECT TO SIDESWAY

INTERNATIONAL COLLOQUIUM
STABILITY OF STEEL STRUCTURES
BUDAPEST, HUNGARY, 1990
PRELIMINARY REPORT

SUMMARY
This paper presents the outline and major results of an experimental study conducted for steel beam-columns subject to sidesway. The strength obtained experimentally was compared with the strength assumed in the LRFD Specification. It was found that the experimental strength is larger (by 11 % on the average) than the assumed strength but this discrepancy is no worse than the differences given for beam-columns with loading and support conditions other than sidesway.

1. INTRODUCTION

Columns are no doubt one of the most critical structural members that control the structural performance of buildings. When a building is subjected to earthquakes, lateral forces are applied to the building, and, accordingly, the building is deflected in horizontal directions. In this condition, the top of each column deflects laterally relative to its bottom as shown in Fig.1(a), and this type of deflection called "sidesway". When a building is to be built in a seismically active area, large lateral forces are required in the design and, as a result, often control the dimensions of the columns; thus, to achieve good seismic design, the behavior of columns subject to sidesway should be evaluated accurately. Of course, seismic design codes acknowledge the importance and give provisions for designing such columns. A question to be addressed here is; are these provisions accurate, or has their accuracy been checked against experimental data? The answer seems rather no. For example, Chapter 8 of the Guide to Stability Design Criteria for Metal Structures (1988) presents a comprehensive survey on the experimental study conducted for steel beam-columns. Most of the tests referred in the literature, however, dealt with beam-columns without sidesway. More specifically, a majority of the tests were for beam-columns with uniform moment (Fig.1(b)). Japan is an earthquake-prone country, and the seismic lateral forces required by its seismic design code are one of the largest in the world. The second writer surveyed experimental studies conducted by Japanese researchers for the past 20 years with respect to the steel beam-column (Nakashima, et al.,

(1) Professor, Institute of Industrial Science, The University of Tokyo,
7-22-1, Roppongi, Minato-ku, Tokyo 106 JAPAN
(2) Associate Professor, Dept. of Environmental Planning, Faculty of Engineering,
Kobe University, Rokkodai, Nada, Kobe 657 JAPAN

(2)

(1989a). Out of the 286 test data collected in the survey, only 16 data were for beam-columns with sidesway.

A beam-column subject to sidesway is by no means a special column. As long as out-of-plane deflection is prevented, a beam-column bent in double curvature (whose moment ratio is 1.0) without sidesway (Fig.1(c)) provides the same moment distribution as a beam-column with sidesway. The only difference between the two is that additional P-Δ moment caused by the sidesway is included in the latter beam-column; so we should be able to estimate the behavior of a beam-column with sidesway from the behavior of the same beam-column but bent in double curvature. However, it is not always an easy task, because the deflections corresponding to the maximum moment resistance are not necessarily the same between the two beam-columns. A cantilever beam-column (Fig.1(d)) or a beam-column subjected to concentric transverse load at its mid-span (Fig.1(e)) also provides similar moment distribution to a beam-column with sidesway since all of the three beam-columns have a triangular unit in the moment distribution. Thus, data obtained for these three types of beam-columns should be interchangeable to one another if they undertake in-plane deflection only. Exactly speaking, however, these three beam-columns are not the same in behavior, because the cantilever beam-column and the beam-column with transverse load are statically determinate, and the moment distribution is uniquely defined, whereas, the beam-column with sidesway is indeterminate, which may lead to changes in moment distribution during the loading in accordance the material and sectional properties along the length. The difference may be very subtle, but, at least, we need to confirm it, say, by comparing the test results obtained for these three types of beam-columns.

Accounting for the importance of steel beam-columns subject to sidesway and the lack in experimental data on their behavior, the writers carried out tests for such beam-columns with a wide-flange cross section. This paper presents the outline and major results of the tests and discusses the accuracy of provisions stipulated for designing these beam-columns.

2. EXPERIMENT

Test Specimens: A total of 42 steel beam-columns were tested. Major test parameters selected in the test were: material, slenderness, and axial load. Table 1 shows the properties of four types of material employed in the test. All types of material are mild steel, having a significant yield plateau before experiencing strain hardening and a yield ratio (the yield stress divided by the maximum stress) of about 0.7. Two cross sections were selected in the test. They were 100 mm (flange width) by 100 mm(depth) and 125 mm by 125 mm, and identified by a number "10" and "12" respectively. The width-to-thickness ratio of the flange plates was 6.3 for "10" and 6.9 for "12". These values were so small that the sections were classified as "compact sections". The slenderness ratio about the strong axis ($=L/r_x$, with L and r_x as the length of the specimen and the radius of gyration about the strong axis of the section) ranged from 25 to 54, which are typical values for structural columns used in medium- to high-rise buildings constructed in seismically active regions. Each end of the specimen was welded to a steel plate with a thickness of 30 mm, but the specimen was not annealed afterward. The value

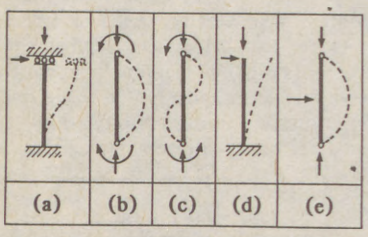

Fig.1 Type of Loading and Support Conditions

Table 1 Material Properties of Test Specimens

Notation	E	σy	σu	σy/σu
	(GN/m^2)	(MN/m^2)	(MN/m^2)	
S10	197.0	300	420	0.714
S12	197.3	301	421	0.715
M10	188.7	368	502	0.733
M12	212.2	377	518	0.728

(3)

Table 2 Designation and Values of Parameters Employed for Tests and Major Test Results

Notation	Material	Length (mm)	λ^*	P/Py	Max. First Order Moment Divided by Mp	Max. Second Order Moment Divided by Mp	Overstrength Ratio
S103200	S10	1040	0.316	0.0	1.42	----	1.42
S103203	S10	1040	0.316	0.3	0.886	1.14	1.12
S103206	S10	1040	0.316	0.6	0.442	0.552	1.05
S104402	S10	1440	0.437	0.2	0.954	1.05	1.10
S104404	S10	1440	0.437	0.4	0.705	0.845	1.11
S104406	S10	1440	0.437	0.6	0.435	0.560	1.09
S105602	S10	1840	0.558	0.2	0.924	1.04	1.09
S105604	S10	1840	0.558	0.4	0.631	0.769	1.09
S105606	S10	1840	0.558	0.6	0.334	0.454	1.06
S106802	S10	2240	0.680	0.2	0.781	0.910	1.00
S106804	S10	2240	0.680	0.4	0.568	0.770	1.09
S106806	S10	2240	0.680	0.6	0.384	0.575	1.19
S123200	S12	1340	0.319	0.0	1.27	----	1.27
S123203	S12	1340	0.319	0.3	0.830	1.07	1.07
S123206	S12	1340	0.319	0.6	0.461	0.565	1.06
S124402	S12	1840	0.439	0.2	0.931	1.02	1.07
S124404	S12	1840	0.439	0.4	0.608	0.719	1.01
S124406	S12	1840	0.439	0.6	0.360	0.456	1.01
S125602	S12	2340	0.559	0.2	0.858	0.981	1.02
S125604	S12	2340	0.559	0.4	0.566	0.709	1.02
S125606	S12	2340	0.559	0.6	0.323	0.468	1.03
M103600	M10	1040	0.359	0.0	1.36	----	1.36
M103603	M10	1040	0.359	0.3	0.829	1.12	1.10
M103606	M10	1040	0.359	0.6	0.427	0.559	1.10
M105002	M10	1440	0.498	0.2	0.956	1.09	1.12
M105004	M10	1440	0.498	0.4	0.713	0.892	1.17
M105006	M10	1440	0.498	0.6	0.450	0.623	1.18
M106402	M10	1840	0.636	0.2	0.928	1.08	1.13
M106404	M10	1840	0.636	0.4	0.598	0.820	1.12
M106406	M10	1840	0.636	0.6	0.427	0.626	1.23
M107802	M10	2240	0.775	0.2	0.851	1.03	1.11
M107804	M10	2240	0.775	0.4	0.616	0.912	1.25
M107806	M10	2240	0.775	0.6	0.251	0.482	1.18
M123500	M12	1340	0.348	0.0	1.27	----	1.27
M123503	M12	1340	0.348	0.3	0.846	1.07	1.08
M123506	M12	1340	0.348	0.6	0.437	0.549	1.04
M124802	M12	1840	0.478	0.2	0.846	0.978	1.00
M124804	M12	1840	0.478	0.4	0.495	0.733	1.01
M124806	M12	1840	0.478	0.6	0.338	0.468	1.00
M126102	M12	2340	0.607	0.2	0.821	0.947	1.01
M126104	M12	2340	0.607	0.4	0.552	0.727	1.02
M126106	M12	2340	0.607	0.6	0.361	0.514	1.08

λ^* = Slenderness Ratio about Strong Axis normalized by Yield Slenderness Ratio.
Py = 685 (kN) for S10; 930 (kN) for S12; 930 (kN) for M10; and 1175 (kN) for M12.
Mp = 26.1 (kNm) for S10; 46.0 (kNm) for S12; 33.9 (kNm) for M10; and 59.2 for M12.

(4)

of axial load (P) imposed were 0.0, 0.2, 0.3, 0.4, or 0.6 of the yield axial load (Py), which was computed using the measured material and geometrical properties. Table 2 summarizes the designation of 42 specimens and the values of major test parameters employed for individual specimens.

Loading: Figure 2 illustrates a view of the setup used in the test. The end plates of the specimen ("A" in the figure) were fastened securely by bolts to the top girder ("B") and base ("C") of the test apparatus and in the direction so that the specimen would be loaded in the plane of the web. Electro-hydraulic actuators ("D") and ("E") were used to apply axial and lateral forces to the top of the specimen. End rotations of the specimen were prevented in all three directions: i.e. in the strong and weak axes of the section and in the longitudinal direction of the specimen. The test apparatus whose top girder and base were connected by two pairs of parallelograms (one pair on each side of the specimen: "F" in Fig.2) was designed specially to achieve these end conditions. In each test, first, axial load was applied to the specimen up to the specified value and held constant throughout the loading; then, lateral force was applied quasi-statically to the top of the specimen with a successive incremental displacement until the specimen lost its lateral resistance completely.

3. RESULTS

Some of the lateral resistance versus lateral deflection relationships obtained from the test are shown in Fig.3. In this figure, Mp = the plastic moment computed using the measured material and sectional properties; M = the first-order end moment given as the lateral resistance (H) multiplied by the half length (L/2) of the specimen; Δy = the yield deflection defined as Mpc divided by the computed elastic stiffness, where Mpc = the reduced plastic moment considering the presence of axial force; and Δ = the lateral displacement at the top of the specimen, respectively. Symbol ▲ shows the point where flange local buckling was observed

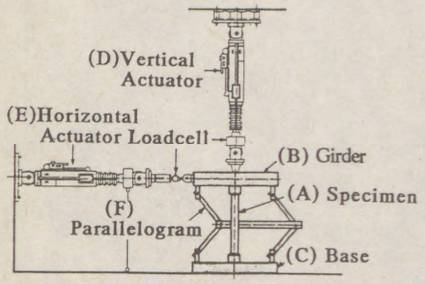

Fig.2 Test Specimen and Setup

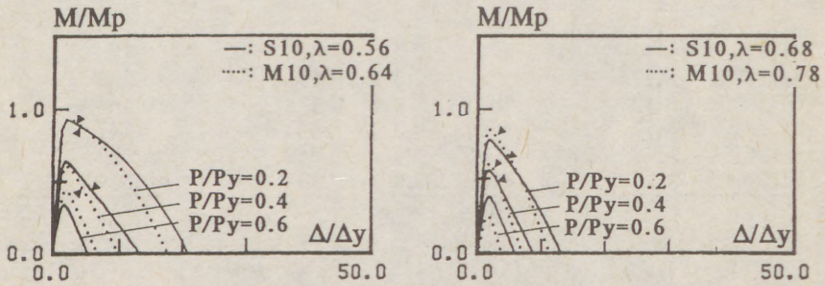

Fig.3 End Moment vs. Lateral Deflection Curves

(5)

for the first time. Table 2 summarizes the major test results. In this table, the maximum second-order end moment is the maximum moment applied to the end section and defined as the sum of the maximum first-order end moment and the P-Δ moment at that time: $P\Delta_b/2$ (the axial load multiplied by half the lateral displacement (Δ_b) corresponding to the maximum first-order end moment). The out-of-plane displacement and the angle of torsion were also measured at the mid-span of the specimen. The results indicated that the out-of-plane deflection was larger for a specimen with smaller values of axial load and slenderness ratio but still remained within a range of 1/500 of the length even in the large deflection range. Local buckling effect was also found secondary. In most specimens, the buckling was not observed before reaching the maximum first-order end moment, and, furthermore, did not reveal any conspicuous change in lateral resistance in all stages of loading. It was concluded from the test that the behavior of the specimens was essentially unaffected by either local buckling or out-of-plane deflection. Complete information on the test results can be found elsewhere (Nakashima, et al., 1989b).

4. CALIBRATION

Overstrength Ratio: Strength stipulated by the Load and Resistance Factor Design (LRFD) Specification of USA (1986) was calibrated against the results obtained from the test. The specification provides the following equations for the strength of steel beam-columns subject to uniaxial loading.

$$Pu/(\phi Pn) + (8/9)(B_1Mnt+B_2M/t)(\phi_bMn) = 1.0; \text{ for } Pu/Pn > 0.2 \quad (1)$$

$$Pu/(2\phi Pn) + (B_1Mnt+B_2M/t)/(\phi_bMn) = 1.0; \text{ for } Pu/Pn \leq 0.2 \quad (2)$$

By considering the loading and support conditions employed in the test, Pn was computed with the effective length factor of unity; Mn with the moment ratio of 1.0; Mnt = 0 (because no load was applied in the end-restraint condition); and

$$B_2 = 1/(1 - PL^2/12EIx)) \quad (3)$$

Where E and Ix are Young's Modulus and the moment of inertia of the section, with all computations made based on the measured material and geometrical properties. Further, resistance factors ϕ and ϕ_b were removed from the equation. The strength estimated by substituting these values into Eqs.(1) and (2) was considered to represent the mean of the strength that the specification assumes, and this strength, termed the assumed strength, was compared with the experimentally obtained maximum first-order moment. The difference between the assumed and experimental strengths was estimated using the procedure shown in Fig.4. In this figure, the chained line shows the axial load versus bending moment interaction that specifies the assumed strength, and point T the experimental strength mapped in this figure. Point D is the intersection of the line connecting point T and the origin with the interaction line. The ratio of distance OT to OD was defined as the overstrength ratio and taken as an index to quantify the difference between the two strengths. The overstrength ratios thus computed are tabulated in Table 2. First, the overstrength ratio is never less than unity, indicating that the experimental strength is always larger than the assumed strength; i.e. the assumed strength conservative. When the axial load imposed was large, the ratio fluctuated more significantly with respect to the slenderness ratio, but no strong correlation was found between the overstrength ratio and the axial load or the slenderness ratio. The average of the overstrength ratios was 1.11.

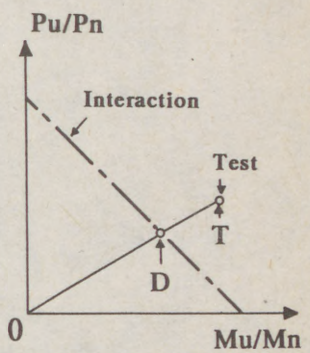

Fig.4 Procedure to Compute Overstrength Ratio

(6)

P-Δ Moment: In order to identify reasons that had caused the difference cited above, P-Δ moment applied to the specimen was examined. Figure 5 shows the ratio of the maximum second-order end moment to the maximum first-order end moment. The ratio was larger for specimens with a larger axial load and a larger slenderness ratio; the result was no surprise. This ratio was then compared with the moment amplification factor: B_2 (Eq.(3)) included in the design equations. Figure 6 shows the ratio of the experimental moment amplification (Fig.5) to B_2. The ratio is never below zero, which indicates that the amplification factor: B_2, underestimates the moment amplification caused by the P-Δ effect, but this ratio remains relatively constant with respect to both the axial load and slenderness ratio, with its average as 1.06.

Moment at End Section: The maximum second-order end moments were plotted in Figure 7. The solid lines in this figure present the interaction of the maximum moment sustained by a wide-flange cross section bent in its strong axis and defined as:

$$Mpc = 1.18(1 - P/Py) \leq Mp \qquad (4)$$

All experimental data are positioned on or outside the interaction, and this suggests that the end sections were already in the strain hardening region when the specimen reached its maximum resistance. From these observations, it was speculated that the second term of the left side of the design equations (Eqs.(1) and (2)), which stipulates the bending moment capacity, underestimates the effect of P-Δ moment but still gives conservative estimate for the capacity, because it neglects the effects of strain hardening, which indeed was significant for the specimens tested in this study.

Accuracy of Design Strength: This speculation, however, by no means leads to a conclusion that modifying B_2 (the moment amplification factor) and including the strain hardening effect in estimating Mn automatically make the design equations more accurate. We say so, because in

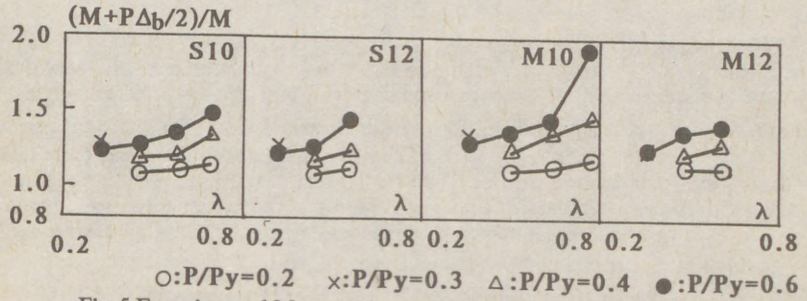

Fig.5 Experimental Moment Amplification at Maximum Resistance

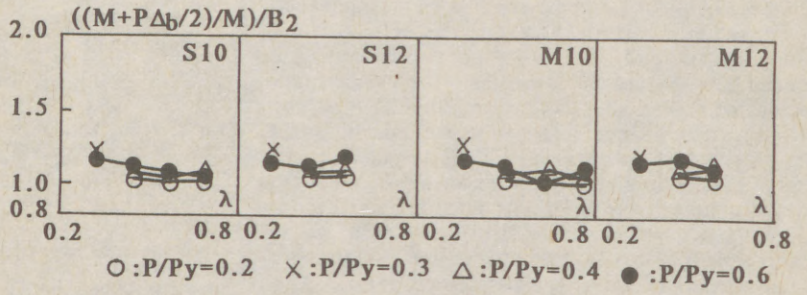

Fig.6 Experimental Moment Amplification to Design Amplification Factor (B_2)

(7)

the above observations, the first term of the left side: the term considering the effect of axial force, was treated as if this term involved no uncertainty, but, most likely, it is not the case. If we wish to develop a more accurate design equation, balance in accuracy between the two terms should be taken into account. Furthermore, before trying to develop a new equation, a more fundamental question need be answered: i.e., is an offset by 11 % on the average unacceptably large or not? It should be remembered that, from the beginning, we permit some error in the design equations in compensation for design simplicity.

Loading and Support Conditions: One way to judge the significance of this difference is to compare it with the differences lying for beam-columns having other loading and support conditions. For this purpose, the design equations (Eqs.(1) and (2)) were also calibrated against test data obtained for other conditions. A total of 237 test data surveyed by Nakashima et al. (1989a) were used in this calibration. The designation and the effective length factor and moment ratio used for computing Pn, Mn, and B_2 are shown in Fig.8 for respective loading and support conditions. In 214 out of 237 specimens calibrated, Mn equaled Mp, and, among them, 183 had a compact section. That is, most of the test data were for stocky beam-columns with a compact section. Note that, out of the 54 test data assigned for the beam-column subject to sidesway, 38 were those obtained in this study. All data are plotted in Fig.9, in which the chained line indicates the interaction of the assumed strength. Table 3 lists the mean (average) and coefficient of variation of the overstrength ratios obtained for respective loading and support conditions. This table leads us to several important observations. First, the mean for the beam-column bent in double curvature (DC) is the largest. Plausible interpretation is that this type of beam-columns sustain most significant strain-hardening, whereas its effects have been ignored in the design equations. On the other hand, the beam-column with uniform moment (UM) has the smallest mean. It is understandable, too, because, contrary to beam-columns bent in double curvature, this type of beam-columns have the least chance in falling into the strain hardening range and are possibly accompanied by lateral-torsional buckling. The beam-column with sidesway (SS) has the second smallest mean. The means given for the cantilever beam-column (CL) and the beam-column with transverse load (TL) are larger by 6 and 9 % than the mean for the beam-column with sidesway. Since the conditions to compute Pn, Mn, and B_2 were slightly different between the three types of beam-columns, the data assigned for the cantilever beam-column and beam-column with transverse load were recalibrated using the conditions employed for the beam-column with sidesway. The ratios thus obtained were 1.22 and 1.20, which are yet larger than the mean obtained for the beam-column with sidesway. Since the number of data is limited and different between the three

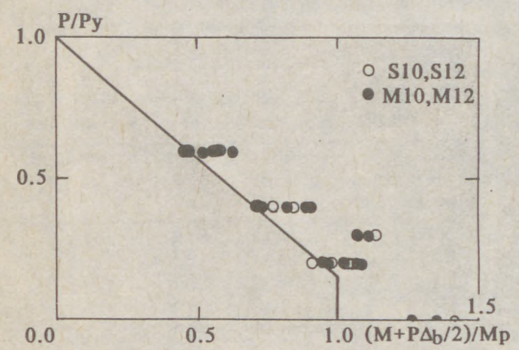

Fig.7 Moment at End Cross Section Corresponding to Maximum Resistance

Type of Loading	DC	UM	ME	CL	TL	SS
k	1.0	1.0	1.0	2.0	1.0	1.0
M_1/M_2	1.0	-1.0	0.0	0.0	1.0	1.0

k=Effective Length Factor
M_1/M_2=End Moment Ratio

Fig.8 Type of Loading and Support Conditions Classified in Calibration

types of beam-columns, it is too early to draw a conclusion, but, at least, the results suggest that the behavior of cantilever beam-columns or beam-columns with transverse load may not be transformed exactly to the behavior of beam-columns subject to sidesway.

5. CONCLUSION

This paper presented the results of an experimental study conducted for steel beam-columns subject to sidesway. A summary and major findings follow:

1. A total of 42 specimens were tested, and the results were evaluated with respect to the design equations stipulated by the LRFD Specification.
2. The experimental strength was never smaller than the strength assumed in the specification, indicating that the design provisions are conservative. The ratio of the experimental to assumed strength, defined as the overstrength ratio, was 1.11 on the average. The amplification factor stipulated in the design equations underestimated the experimental moment amplification, but this underestimate was overshadowed after all, because the equations neglect the effect of strain hardening.
3. Experimental data previously obtained for beam-columns having loading and support conditions other than sidesway was also compared with the strength assumed in the specification. The beam-column with uniform moment had the smallest overstrength ratio with 1.09, and the beam-column with sidesway was the next with the ratio of 1.12, whereas, the beam-column bent in double curvature had the largest ratio with 1.25.
4. It is a matter of debate whether or not the differences between the experimental and assumed strengths observed in this study is tolerable. No objective judgement can be made unless we have enough information on the accuracies of other design provisions as well as the relative importance of respective provisions to the overall design. A modest conclusion that can be drawn from this study is that the strength assumed in the specification is reasonably accurate for beam-columns subject to sidesway relative to for those having most of other loading and support conditions.

References:

Galambos, T. V. (Editor) (1988)."Guide to Stability Design Criteria for Metal Structures." John Wiley & Sons.

"Load & Resistance Factor Design, Specification for Structural Steel Buildings." (1986). American Society of Steel Construction, USA.

Nakashima, M., Morino, S., and Koba, S.(1989a)."Strength of Steel Beam-Columns With Wide Flange Cross Section." Annual Transactions of the Architectural Institute of Japan, Kinki Branch, pp.313-316 (in Japanese).

Nakashima, M., Takanashi, K., Kato, H., and Kim, J-M.(1989b)."Strength and Deformation of Steel Beam-Columns Subject to Sidesway." Annual Transactions of the Architectural Institute of Japan, Kinki Branch, pp.317-320 (in Japanese).

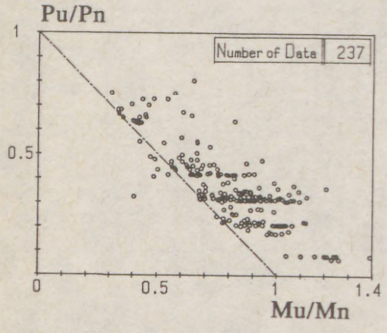

Fig.9 Experimental Maximum Resistance

Table 3 Designation and Number of Data Employed in Calibration, and Means and COV's Obtained

Type of Loading and Support Condition	Number of Data	Mean	Coefficient of Variation
All Data	237	1.16	0.10
DC	18	1.25	0.05
UM	33	1.09	0.13
ME	21	1.13	0.06
CL	25	1.22	0.10
TL	86	1.19	0.07
SS	54	1.12	0.12

TABLE OF CONTENTS

VOLUME I.

Session 1. "General Design Concepts"

Session 2. "Compression Members"

Session 3. "Built- Up Members"

Session 4. "Beams"

Session 5. "Beam-Columns"

VOLUME II.

Session 6. "Plate and Box Girders"

VOLUME III.

Session 8."Arches"

Session 9. "Triangulated Structures"

Session 10. "Tubular Structures"

Session 11. "Shells"

Session 12. "Cold Formed Members and Interactive Buckling"

VOLUME IV.

Session 13. "Composite Members"

Session 14. "Earthquake Engineering and Dynamic Behaviour"

Session 15. "Special Problems"


Insignia Liberæ Regiæ Me
ropolitanæ Civitatis Budensis

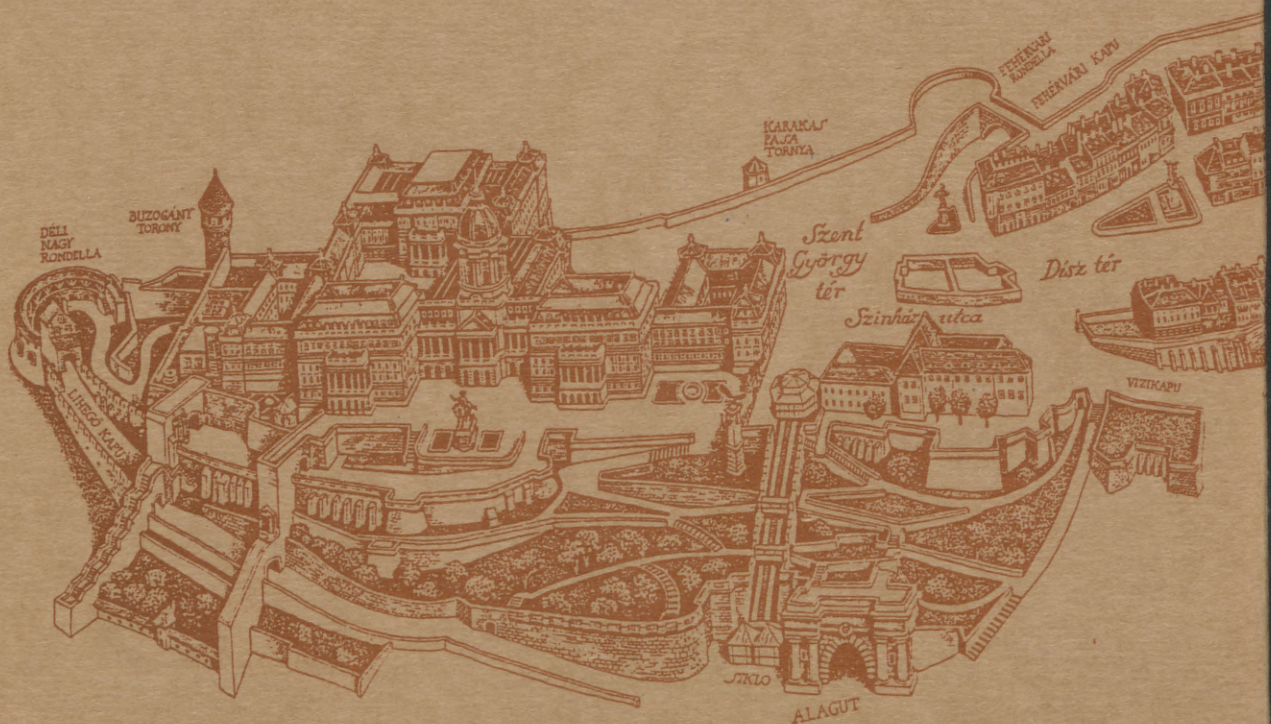
KARAKAS PASA TORNYA
FEHÉRVÁRI KAPU
DÉLI NAGY RONDELLA
BUZOGÁNY TORONY
Szent György tér
Dísz tér
Színház utca
VIZIKAPU
LIHEGŐ KAPU
SIKLÓ
ALAGUT